N73 10890

CR-128592

CONTRACT NAS9-12183

SPACECRAFT BOOST AND ABORT GUIDANCE AND CONTROL SYSTEMS REQUIREMENTS STUDY, BOOST DYNAMICS AND CONTROL ANALYSIS STUDY

EXHIBIT A

FINAL REPORT

BOOST DYNAMICS AND CONTROL ANALYSIS

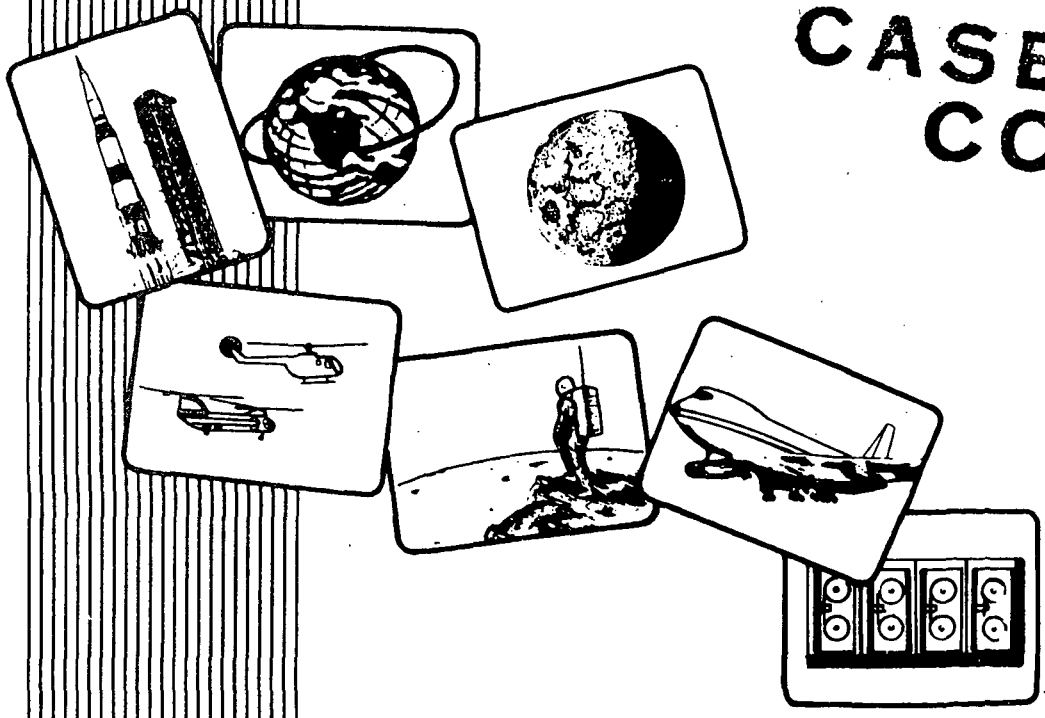

CASE FILE COPY

THE BOEING COMPANY
HOUSTON, TEXAS

SEPTEMBER 15, 1972

CONTRACT NAS9-12183

SPACECRAFT BOOST AND ABORT GUIDANCE AND CONTROL SYSTEMS REQUIREMENTS STUDY, BOOST DYNAMICS AND CONTROL ANALYSIS STUDY

EXHIBIT A FINAL REPORT

BOOST DYNAMICS AND CONTROL ANALYSIS

SEPTEMBER 15, 1972

Prepared by F. E. Williams

J. B. Price

R. S. Lemon

Approved by W. G. Ryals
Program Manager

ABSTRACT

This final report summarizes the work performed under Exhibit A of NASA Contract NAS9-12183. It includes the simulation developments for use in dynamics and control analysis during boost from liftoff to orbit insertion. It also includes wind response studies of the NR-GD 161B/B9T delta wing booster/delta wing orbiter configuration, the MSC 036B/280 inch solid rocket motor configuration, the MSC 040A/LOX-propane liquid injection TVC configuration, the MSC 040C/ dual solid rocket motor configuration, and the MSC 049/solid rocket motor configuration. All of the latest math models (rigid and flexible body) developed for the MSC/GD Space Shuttle Functional Simulator, are included in this report.

KEY WORDS

SPACE SHUTTLE VEHICLE

BOOST DYNAMICS

FLIGHT CONTROL SYSTEM

SIMULATION MODELS

LTG (LINEAR TANGENT GUIDANCE)

ORBITER

SRM (SOLID ROCKET MOTOR)

TVC (THRUST VECTOR CONTROL)

SSFS (SPACE SHUTTLE FUNCTIONAL SIMULATOR)

RIBBS (RIGID BODY BOOST SIMULATION)

TABLE OF CONTENTS

TABLE OF CONTENTS (CONTINUED)

LIST OF FIGURES

LIST OF FIGURES (CONTINUED)

LIST OF FIGURES (CONTINUED)

LIST OF FIGURES (CONTINUED)

LIST OF TABLES

NOMENCLATURE

AERO	Aerodynamics Subroutine
ATMOS	Atmosphere Subroutine
ATTUDE	Boost Polynomial Guidance Subroutine
AVEH	Equations of Motion (6 DOF) Subroutine
BLCONT	Flight Control Subroutine
CCW	Counter Clockwise
CG	Center of Gravity
CGAINS	Control Gains Calculation Subroutine
CW	Clockwise, Crosswind
DOF	Degrees of Freedom
DRD	Data Requirement Description
EOM	Equations of Motion
GCD	Guidance and Control Division
GUIDE	Active Guidance Subroutine
HINGE	Rudder Hinge Moment Subroutine
LEC	Lockheed Electronics Corporation
LOX	Liquid Oxygen
MASPRO	Mass Properties Subroutine
MAXMIN	Maximum, Minimum Values Subroutine
MDELTA	Matrix Differential Equation Linear Transformation Analyzer
MSC	Manned Spacecraft Center
NASA	National Aeronautics and Space Administration
NR-GD	North American Rockwell - General Dynamics

NOMENCLATURE (Continued)

ORBIT 1	Orbital Parmeters Subroutine
ORBTAR	Equations of Motion (3 DOF) Subroutine
$q\alpha$	Dynamic Pressure x Angle of Attack
$q\beta$	Dynamic Pressure x Sideslip Angle
RCS	Reaction Control System
RIBBS	Rigid Body Boost Simulation
RMS	Root Mean Square
SRM	Solid Rocket Motor
SSFS	Space Shuttle Functional Simulator
SSV	Space Shuttle Vehicle
THRUST	Thrust Subroutine
TSHAPE	Trajectory Shaping Subroutine
TVC	Thrust Vector Control
δ	Engine Deflection Angle
ζ	Damping Ratio
θ	Inertial Pitch Attitude
ϕ	Inertial Roll Attitude
ψ	Inertial Yaw Attitude
ω	Natural Frequency

NOTE: Nomenclature and symbols for the various math models are listed in the respective section of the report that gives the equations and discussion of the particular math model.

1.0 SUMMARY

This final report is submitted to the NASA MSC Guidance and Control Division as required by MSC DRD SE-272T of Exhibit A of Contract NAS9-12183. This report covers the work performed from contract go-ahead to contract completion on 15 September 1972. Under the terms of the contract, analysis programs were to be updated (Task I), rigid body dynamic and control analyses were to be performed (Task II), and flexible body stability and control analyses were to be performed (Task III). A brief summary of these studies, which have been reported to MSC/GCD in 49 interim reports (listed in the references) is given in the following paragraphs.

Task I Summary - Update of Analysis Programs

Initially, mathematical models were developed for the MSC Space Shuttle Functional Simulator to provide a launch phase boost to staging simulation equivalent to the Boeing-developed Rigid Body Boost Simulation (RIBBS). These models were programmed by MSC C&AD into the Space Shuttle Functional Simulator (SSFS) developed by the Guidance and Control Division. The SSFS first stage simulation was checked out jointly by MSC and Boeing personnel.

In order to provide analysis capability from liftoff through orbit insertion, several additional models not already in RIBBS were developed for SSFS. These models were: targeting to orbit; active guidance; a three degree of freedom upper stage to orbit; and calculation of orbital parameters. During the course of the model development, programming, and checkout of SSFS, numerous modifications were made to the RIBBS program as a result of updated analysis requirements in Task II. SSFS was then updated to meet these additional analysis capability requirements by adding: trajectory shaping and control gain calculations; baseline control system, multistage guidance; and liftoff state vector calculations.

Point time stability analysis equations were also developed during Task I and programmed into the M DELTA Program.

All of the math models which were developed for the SSFS have been updated and are included in this final report.

Task II Summary - Rigid Body Dynamics and Control Analysis

The NR/GD 161B/B9T delta wing booster/delta wing orbiter configuration was extensively analyzed during the first half of the contract. Brief studies were performed on the 036B/280 inch solid rocket motor series burn configuration and the 040A/LOX propane series burn configuration using liquid injection thrust vector control. In February 1972 studies were initiated on parallel burn dual solid rocket motor (SRM) configurations.

Liftoff studies of the 040C/SRM configuration revealed that 0.25° SRM misalignments and ground winds were satisfactorily controllable. However, 0.5° misalignments caused thrust torques exceeding the TVC roll control authority. Orbiter engine out analysis demonstrated that the SRMS must be oriented to thrust nearly through the liftoff cg or the vehicle would be uncontrollable in event of an orbiter engine failure. Inflight analysis of the 040C/SRM showed that the available roll torque was insufficient to maintain a fixed roll attitude in crosswinds, so studies of active roll control to minimize sideslip were conducted.

The configuration was changed to the MSC049 Model and control system development was continued. The resulting control system is based on a gravity turn trajectory so the vehicle can roll and keep trajectory dispersions to a minimum. The roll control problem is minimized by sensing sideslip and actively rolling its tail into the wind. Results of several hundred simulated flights to orbit indicated that this control system can handle any wind conditions as long as SRM misalignments are constrained within 0.25 degrees. Aerodynamic loads were automatically minimized without load relief techniques, and weight to orbit was maintained within a few thousand pounds of the nominal no-wind value for all cases.

Because of the 0.25 degree alignment constraint studies of trim gimballing of the SRMS were also performed. It was determined that gimballing the SRMS $\pm$ two degrees at a rate limited to 0.3 degrees/second not only permitted misalignments greater than one degree but also improved wind response of the vehicle.

Task III Summary - Flexible Body Stability and Control Analysis

Flexible body models were developed and programmed into the space shuttle functional simulator so that flexible body analysis can be initiated as soon as bending data becomes available. The flexible body program uses a generalized modal approach to bending which represents the elastic response by standard normal modal equations with viscous damping. Included are models for distributed aerodynamic forces and moments, and thrust forces and moments to account for bending effects as well as the tail wags dog contribution to bending. The vibration model sums all the forces and moments acting on each of the equivalent mass points and for a given mode numerically integrates the sum with a second order differential equation in modal displacement.

2.0 Task I - Update of Analysis Programs

The three major programs which were included as part of the updating procedure of this task were the Space Shuttle Functional Simulator (SSFS), Rigid Body Boost Simulation (RIBBS), and Matrix Differential Equation Linear Transform Analysis (MDELTA). SSFS was updated with mathematical models to provide a launch phase simulation for the MSC Guidance and Control Division. All of the models which were developed during this contract period have been updated to the current configuration and are presented in Section 2.1. The Boeing RIBBS program was used for analysis of shuttle during the development of SSFS. RIBBS was also updated with a new guidance model and other modifications as explained in Section 2.2. The Boeing MDELTA program was modified for use in point time stability analysis. This is mentioned in Section 2.3. Also included in Section 2.4 is a discussion of the development of the boost Linear Tangent Guidance (LTG) equations.

2.1 Space Shuttle Functional Simulator (SSFS) Math Models

Rigid body mathematical models were prepared and delivered to MSC Guidance and Control Division to provide the Space Shuttle Functional Simulator (SSFS) with the same capability as the Boeing Rigid Body Boost Simulation (RIBBS). These models which were originally presented in References 1 and 2 include: boost polynomial guidance; mass properties thrust; thrust vector control; rigid body 6 DOF equations of motion; aerodynamics; RCS; and atmosphere models. These models were programmed by Lockheed Electronics Corporation (LEC) and jointly checked out by LEC and Boeing by making comparison runs on RIBBS and SSFS. References 3 and 4 describe the comparison results. Slight differences were observed due to some fundamental program structure differences and updated gravity and atmosphere models in SSFS. The final checkout used design shear and gust winds to verify the short period dynamics and included detailed examination of the computer programming to assure that the differences that remained after debugging were not the result of coding errors. Additional confidence was gained by duplicating some of the more complex transformations and equation sets on the Boeing computers (using the Boeing computer service remote terminals) and verifying them using known input-output data sets.

Several additional new models were also developed and delivered to MSC. These include orbit insertion targeting, active guidance, three degree of freedom upper stage to orbit equations of motion, orbital parameters, initial state vector, hinge moment calculations, control gains calculations, and trajectory shaping. These models were detailed in References 5 - 11. These models were also programmed by LEC and comparisons of results with existing simulation data was favorable. The control gains and trajectory shaping equations were verified, as shown in References 12 and 13, by comparison with similar equations programmed into the RIBBS program.

The following subsections give a complete description of the current math models developed during this contract and incorporated in the Space Shuttle Function Simulator. The baseline control system of Reference 14 that was accepted for inclusion in the MSC Guidance and Control Equations Document "MSC-04217 Revision B" has since been updated to include sideslip feedback and gimballed solid rocket motors as presented in paragraph 2.1.5.

2.1.1 AERO (Aerodynamics)

2.1.1.1 DESCRIPTION

This model calculates the latitude and longitude of the vehicle position, the contribution to velocity due to wind speed and direction, flight path angle, Mach number, dynamic pressure, angle of attack and angle of sideslip. The vehicle forces and moments due to the air and control surface deflections are calculated and summed.

2.1.1 AERO (Continued)

2.1.1.2 MATH MODEL

$$\begin{bmatrix} X_F \\ Y_F \\ Z_F \end{bmatrix} = [A]^T \begin{bmatrix} X_P \\ Y_P \\ Z_P \end{bmatrix}$$

$$\lambda_V = \sin^{-1}(Z_F/R_V)$$

$$\phi = \tan^{-1}\left(\frac{Y_F}{X_F}\right) - \omega_e (t_L + t)$$

$$V_{EARTH_X} = -W_e Y_F$$

$$V_{EARTH_Y} = W_e X_F$$

$$\begin{bmatrix} V_{R_{X_P}} \\ V_{R_{Y_P}} \\ V_{R_{Z_P}} \end{bmatrix} = \begin{bmatrix} \dot{X}_P \\ \dot{Y}_P \\ \dot{Z}_P \end{bmatrix} - [A] \begin{bmatrix} V_{EARTH_X} \\ V_{EARTH_Y} \\ 0 \end{bmatrix}$$

$$V_{R_P} = \left(V_{R_{X_P}}^2 + V_{R_{Y_P}}^2 + V_{R_{Z_P}}^2\right)^{1/2}$$

$$\begin{bmatrix} V_{X_{LV}} \\ V_{Y_{LV}} \\ V_{Z_{LV}} \end{bmatrix} = [D]^T [A]^T \begin{bmatrix} V_{R_{XP}} \\ V_{R_{YP}} \\ V_{R_{ZP}} \end{bmatrix}$$

$$\gamma = \sin^{-1}(V_{X_{LV}}/V_{R_P})$$

2.1.1 AERO (Continued)

$$V_W = \text{table lookup} \sim f(\text{altitude})$$

$$AZ_W = \text{table lookup} \sim f(\text{altitude})$$

$$\begin{bmatrix} V_{W_{XP}} \\ V_{W_{YP}} \\ V_{W_{ZP}} \end{bmatrix} = \begin{bmatrix} A \end{bmatrix} \begin{bmatrix} D \end{bmatrix} \begin{bmatrix} 0 \\ -V_W \sin AZ_W \\ -V_W \cos AZ_W \end{bmatrix}$$

$$\begin{bmatrix} V_{R_{X_B}} \\ V_{R_{Y_B}} \\ V_{R_{X_B}} \end{bmatrix} = \begin{bmatrix} B \end{bmatrix} \begin{bmatrix} V_{R_{X_P}} - V_{W_{X_P}} \\ V_{R_{Y_P}} - V_{W_{Y_P}} \\ V_{R_{Z_P}} - V_{W_{Z_P}} \end{bmatrix}$$

$$V_B = \left(V_{R_{X_B}}^2 + V_{R_{Y_B}}^2 + V_{R_{Z_B}}^2 \right)^{\frac{1}{2}}$$

$$\beta = \sin^{-1} \left(V_{R_{Y_B}} / V_B \right)$$

$$\alpha = \tan^{-1} \left(V_{R_{Z_B}} / V_{R_{X_B}} \right)$$

Obtain from ATMØS

1) $\rho = f$ (altitude)
2) $a = f$ (altitude)
3) $P = f$ (altitude)

2.1.1 AERO (Continued)

$$M = V_B/a$$

$$q = \tfrac{1}{2} \rho V_B^2$$

The following aerodynamic coefficients are looked up in tables:

$$C_{Z_0} = f(M)$$

$$C_{Z_\alpha} = f(M, \alpha)$$

$$C_{M_0} = f(M)$$

$$C_{M_\alpha} = f(M, \alpha)$$

$$C_{X_0} = f(M)$$

$$C_{X_\alpha} = f(M, \alpha)$$

$$C_{Y_\beta} = f(M)$$

$$C_{l_\beta} = f(M)$$

$$C_{n_\beta} = f(M)$$

$$C_{n_p} = f(M)$$

$$C_{l_p} = f(M)$$

$$C_{l_r} = f(M)$$

$$C_{m_q} = f(M)$$

$$C_{Z_{\delta e}} = f(M)$$

$$C_{M_{\delta e}} = f(M)$$

$$C_{Y_{\delta r}} = f(M)$$

2.1.1 AERO (Continued)

$$C_{l_{\delta r}} = f(M)$$

$$C_{n_{\delta r}} = f(M)$$

$$C_{l_{\delta a}} = f(M)$$

$$C_{n_{\delta a}} = f(M)$$

$$F_{A_X} = qS\,(C_{X_0} + C_{X_\alpha}\,\alpha)$$

$$F_{A_Y} = qS\,C_{Y_\beta}\,\beta + \frac{q\,S\,b}{2\,V_{R_{X_B}}}\,C_{Y_p}\,P + q\,S\,C_{Y_{\delta r}}\,\delta r$$

$$F_{A_Z} = qS\,(C_{Z_0} + C_{Z_\alpha}\,\alpha) + q\,S\,C_{Z_{\delta e}}\,\delta e$$

$$M_{A_X} = F_{A_Y}\,(Z_{CG} - Z_{A_R}) - F_{A_Z}\,(Y_{CG} - Y_{A_R}) + q\,S\,b\,(C_{l_\beta}\,\beta + C_{l_{\delta a}}\,\delta a + C_{l_{\delta r}}\,\delta r) + \frac{q\,S\,b^2}{2V_{R_{X_B}}}\,(C_{l_p}\,P + C_{l_r}\,R)$$

$$M_{A_Y} = q\,S\,\bar{c}\,(C_{m_0} + C_{m_\alpha}\,\alpha) + F_{A_Z}\,(X_{CG} - X_{A_R}) - F_{A_X}\,(Z_{CG} - Z_{A_R}) + q\,S\,\bar{c}\,C_{m_{\delta e}}\,\delta e + C_{m_q}\,Q$$

$$M_{A_Z} = q\,S\,b\,C_{n_\beta}\,\beta - F_{A_Y}\,(X_{CG} - X_{A_R}) + F_{A_X}\,(Y_{CG} - Y_{A_R}) + \frac{q\,S\,b^2}{2\,V_{R_{X_B}}}\,C_{n_p}\,P + q\,S\,\bar{c}\,(C_{n_{\delta a}}\,\delta a + C_{n_{\delta r}}\,\delta r)$$

2.1.1 AERO (Continued)

Where:

X_F, Y_F, Z_F = vehicle position in inertial polar-equatorial coordinates

X_P, Y_P, Z_P = vehicle position in inertial plumbline coordinates

$[A]$ = transformation matrix from inertial polar-equatorial to plumbline coordinates

λ_v = latitude of present position of vehicle

ϕ = East longitude of present position of vehicle corrected for earth's rotation

t_L = time of launch (from epoch)

C_1 = radians to degrees conversion constant

W_e = angular rate of earth

t = elapsed time from liftoff

R_V = distance from the center of the earth to the vehicle

V_{EARTH_X}, V_{EARTH_Y} = components of earth's velocity in inertial polar-equatorial coordinates

$V_{R_{X_P}}$, $V_{R_{Y_P}}$, $V_{R_{Z_P}}$ = components of vehicle relative velocity in plumbline coordinates

$\dot{X}_P$, $\dot{Y}_P$, $\dot{Z}_P$ = components of vehicle velocity in plumbline coordinates

V_{R_P} = total vehicle relative velocity in plumbline coordinates

$V_{X_{LV}}$, $V_{Y_{LV}}$, $V_{Z_{LV}}$ = components of relative velocity in local vertical coordinates

$[D]$ = transformation matrix from local vertical to inertial polar-equatorial coordinates

γ = vehicle flight path angle with respect to local horizontal

2.1.1 AERO (Continued)

V_W = horizontal wind speed in local vertical coordinates

AZ_W = wind azimuth (North = 0^o)

$V_{W_{X_P}}$, $V_{W_{Y_P}}$, $V_{W_{Z_P}}$ = components of wind velocity in plumbline coordinates

$V_{R_{X_B}}$, $V_{R_{Y_B}}$, $V_{R_{Z_B}}$ = vehicle velocity with respect to air in body coordinates

$[B]$ = transformation matrix from body to plumbline coordinates

V_B = total vehicle velocity with respect to air in body coordinates

α = vehicle angle of attack

β = vehicle sideslip angle

ρ = local air mass density

a = local speed of sound

p = local air pressure

M = Mach number

q = dynamic pressure

F_{A_X}, F_{A_Y}, F_{A_Z} = components of aerodynamic force in body coordinates

S = vehicle aerodynamic reference area

$\bar{c}$ = vehicle mean aerodynamic chord

b = vehicle reference span

δ_a = aileron deflection

δ_e = elevator deflection

2.1.1 AERO (Continued)

δ_r = rudder deflection

P = vehicle roll rate

Q = vehicle pitch rate

R = vehicle yaw rate

M_{A_X}, M_{A_Y}, M_{A_Z} = Aerodynamic moments about the X, Y, and Z body axes, respectively

2.1.1.3 INPUT/OUTPUT ††

Input from routines:

X_P, Y_P, Z_P	vehicle position in inertial plumbline coordinates from EOM
$\dot{X}_P$, $\dot{Y}_P$, $\dot{Z}_P$	vehicle velocity in inertial plumbline coordinates from EOM
V_W	wind velocity from tables
AZ_W	wind azimuth from tables
ρ, a, p	current air density, speed of sound and air pressure from ATMOS
X_{CG}, Y_{CG}, Z_{CG}	current location of vehicle center of gravity from MASPRO
t	elapsed time from liftoff from flight sequencer
R_V	distance from center of the earth to the vehicle from EØM
δ_a,δ_e,δ_R	aerodynamic control surface deflections from flight software commands
P, Q, R	vehicle roll, pitch and yaw rates from EØM

All aerodynamic coefficients are input from tables.

Input from cards for initialization:

t_L	time of launch (from epoch)
C_1	radians to degrees conversion constant
W_e	angular rate of earth
S	vehicle aerodynamic reference area
$\bar{c}$	vehicle mean aerodynamic chord
b	vehicle reference span
X_{A_R}, Y_{A_R}, Z_{A_R}	aerodynamic reference location in body coordinates

2.1.1 AERO (Continued)

Output to routines:

p	current air pressure to THRUST
F_{A_X}, F_{A_Y}, F_{A_Z}	components of aerodynamic forces to the EØM
M_{A_X}, M_{A_Y}, M_{A_Z}	moments due to aerodynamic forces to EØM

Output to printer:

λ_V	latitude of vehicle's position
ϕ	longitude of vehicle's position
$V_{X_{LV}}$	rate of climb
γ	flight path angle
V_W	wind speed
AZ_W	wind azimuth
V_B	vehicle velocity with respect to air
α	angle of attack
β	angle of sideslip
ρ	local air mass density
a	local speed of sound
p	local air pressure
M	Mach number
q	dynamic pressure
δ_e, δ_r, δ_a	aerodynamic control surface deflections

2.1.2 ATMOS (Atmosphere Model)

2.1.2.1 PROGRAM DESCRIPTION

This program calculates the speed of sound, pressure and air density from an altitude input.

2.1.2.2 MATH MODEL

Use the Cape Kennedy Reference Atmosphere (TM-X-53872, PARAGRAPH 14.7 - MSFC "COMPUTER SUBROUTINE PRA-63") as specified for SSV design studies.

2.1.2.3 INPUT/OUTPUT

The altitude above the mean earth surface must be supplied to the model which returns the speed of sound, pressure, and atmospheric density.

2.1.3 ATTUDE (Boost Polynomial Guidance)

2.1.3.1 PROGRAM DESCRIPTION

This program is used in the flight software to guide the vehicle during atmospheric flight or until active guidance is commanded to take over the guidance function. The yaw and roll commands are set to zero and the pitch command is taken from a pitch table look-up. The pitch table is derived by shaping the desired trajectory (using T_{SHAPE}), and using the pitch angles from this trajectory as the commands for the Boost Polynomial Guidance.

2.1.3.2 MATH MODEL

The pitch commands (TA) and their corresponding time (T) are taken from a desired trajectory and entered into a table of commands and times. The following logic is then used to derive the commanded vehicle attitude during this part of the flight.

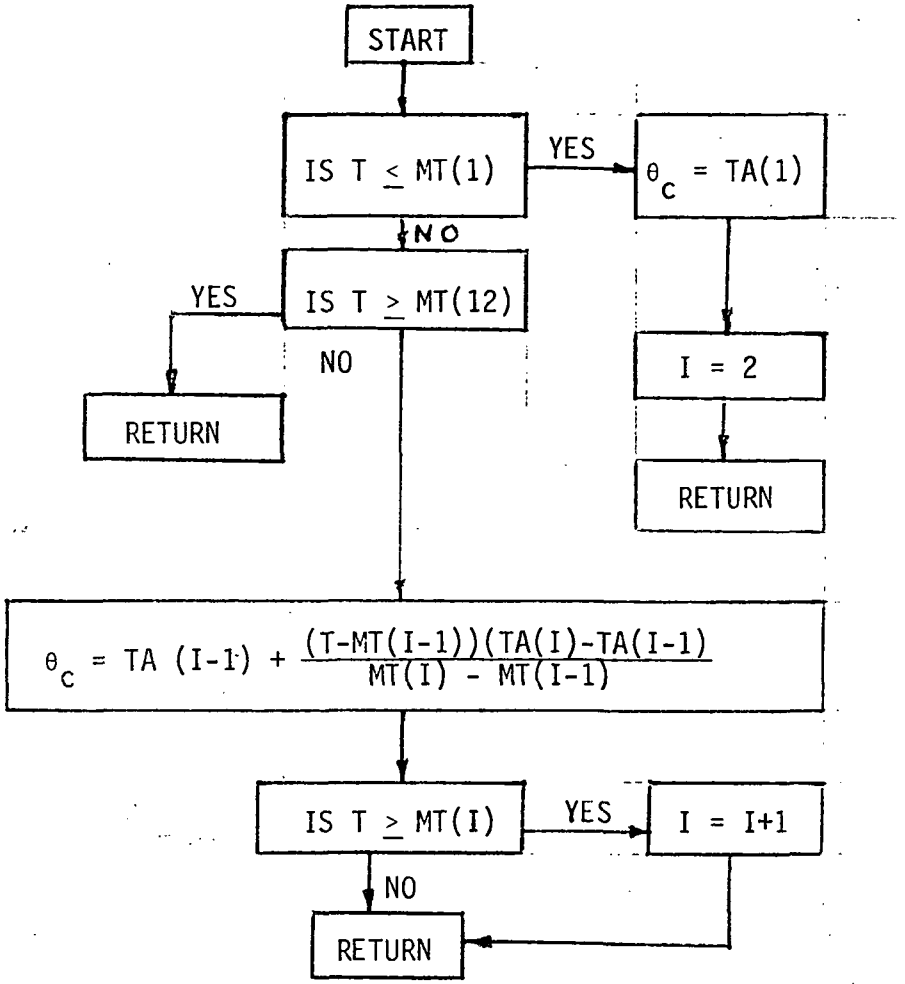

where T = time after launch, seconds

θ_c = commanded pitch angle

ψ_c = 0. = commanded yaw angle

ϕ_c = 0. = commanded roll angle

The coordinate systems used in this model are the platform systems and the body systems which will be described in section IV.

2.1.3.3 INPUT/OUTPUT

This model requires time after launch as an input and it calculates the roll, pitch, and yaw attitude angles. The program requires no software command, calling arguments, or other subroutine. It should be called about every two seconds.

2.1.3.4 COORDINATE SYSTEMS

The angles calculated by this model relate the body coordinate system to the platform coordinate system. The body system is fixed with respect to the vehicle with the X axis forward thru the main propellant tank centerline, the Z axis in the engine gimbal pivot plane and pointing down, and the Y axis points toward the pilot's right forming the right handed triad. The platform system origin is at the earth's center of mass and is fixed in inertial space at the time of launch. The X axis is parallel but opposite in sense to the launch pad gravity vector, the Z axis points downrange in the launch plane and the Y axis points toward the pilot's right completing the right handed triad.

$$[\theta] = \begin{bmatrix} \cos\theta & 0 & \sin\theta \\ 0 & 1 & 0 \\ -\sin\theta & 0 & \cos\theta \end{bmatrix} \qquad (1)$$

$$[\psi] = \begin{bmatrix} \cos\psi & -\sin\psi & 0 \\ \sin\psi & \cos\psi & 0 \\ 0 & 0 & 1 \end{bmatrix} \qquad (2)$$

2.1.3 ATTUDE (Continued)

$$[\phi] = \begin{bmatrix} 1 & 0 & 0 \\ 0 & \cos\phi & -\sin\phi \\ 0 & \sin\phi & \cos\phi \end{bmatrix} \quad (3)$$

$$\begin{bmatrix} X_P \\ Y_P \\ Z_P \end{bmatrix} = [\theta]\ [\psi]\ [\phi] \begin{bmatrix} X_B \\ Y_B \\ Z_B \end{bmatrix} \quad (4)$$

where: X_P, Y_P, Z_P = platform coordinate vector

X_B, Y_B, Z_B = body coordinate vector

2.1.4 AVEH (6 DOF Equations of Motion)

2.1.4.1 DESCRIPTION

AVEH defines the motions of the center of gravity of the vehicle. For convenience it is separated into three parts; 1) translation equations, 2) rotation equations, and 3) euler angles.

These equations should be solved at least once each second during powered flight. In the vicinity of environmental discontinuities more frequent solution is required; for instance, the vehicle can fly completely through a wind gust at maximum dynamic pressure within 0.1 second. Other discontinuities include: staging, start of closed loop guidance, and engine or actuator failures. As a rule of thumb, the integration rate during transients can be ½ x rotational acceleration (in degrees/sec^2).

2.1.4.1.1 TRANSLATION EQUATIONS

DESCRIPTION

This model defines the linear accelerations of the rigid body.

MATH MODEL

$$\begin{bmatrix} \Sigma F_{X_P} \\ \Sigma F_{Y_P} \\ \Sigma F_{Z_P} \end{bmatrix} = [\beta] \begin{bmatrix} \Sigma F_{X_B} \\ \Sigma F_{Y_B} \\ \Sigma F_{Z_B} \end{bmatrix}$$

$$\begin{bmatrix} g_{X_P} \\ g_{Y_P} \\ g_{Z_P} \end{bmatrix} = [\alpha] \begin{bmatrix} g_{X_I} \\ g_{Y_I} \\ g_{Z_I} \end{bmatrix}$$

$$\ddot{X}_P = g_{X_P} + \Sigma F_{X_P}/m \qquad \dot{X}_P = \int_{t_1}^{t_2} \ddot{X}dt + \dot{X}_{P_o} \qquad X_P = \int_{t_1}^{t_2} \dot{X}dt + X_{P_o}$$

$$\ddot{Y}_P = g_{Y_P} + \Sigma F_{Y_P}/m \qquad \dot{Y}_P = \int_{t_i}^{t_2} \ddot{Y}dt + \dot{Y}_{P_o} \qquad Y_P = \int_{t_1}^{t_2} \dot{X}dt + Y_{P_o}$$

$$\ddot{Z}_P = g_{Z_P} + \Sigma F_{Z_P}/m \qquad \dot{Z}_P = \int_{t_1}^{t_2} \ddot{Z}dt + \dot{Z}_{P_o} \qquad Z_P = \int_{t_1}^{t_2} \dot{Z}dt + Z_{P_o}$$

ΣF_{X_B}, ΣF_{Y_B}, ΣF_{Z_B} = sum of forces in the X, Y, Z body axis directions.

ΣF_{X_P}, ΣF_{Y_P}, ΣF_{Z_P} = sum of forces in the X, Y, Z inertial plumbline axis directions.

$[\beta]$ = transformation matrix from body to inertial plumbline.

ΣF = aero forces + thrust forces + RCS forces + engine deflection forces + slosh forces.

g_{X_I}, g_{Y_I}, g_{Z_I} = gravitational acceleration components in inertial polar-equatorial axis directions.

g_{X_P}, g_{Y_P}, g_{Z_P} = gravitational acceleration components in inertial plumbline axis directions.

$[\alpha]$ = transformation matrix from inertial polar - equatorial to inertial plumbline.

X_P, Y_P, Z_P = accelerations in inertial plumbline axis directions

m = total vehicle mass

$$\begin{bmatrix} g_{X_P} \\ g_{Y_P} \\ g_{Z_P} \end{bmatrix} = [\alpha] \begin{bmatrix} g_{X_I} \\ g_{Y_I} \\ g_{Z_I} \end{bmatrix}$$

$$\ddot{X}_P = g_{X_P} + \Sigma F_{X_P}/m \qquad \dot{X}_P = \int_{t_1}^{t_2} \ddot{X}dt + \dot{X}_{P_o} \qquad X_P = \int_{t_1}^{t_2} \dot{X}dt + X_{P_o}$$

$$\ddot{Y}_P = g_{Y_P} + \Sigma F_{Y_P}/m \qquad \dot{Y}_P = \int_{t_i}^{t_2} \ddot{Y}dt + \dot{Y}_{P_o} \qquad Y_P = \int_{t_1}^{t_2} \dot{X}dt + Y_{P_o}$$

$$\ddot{Z}_P = g_{Z_P} + \Sigma F_{Z_P}/m \qquad \dot{Z}_P = \int_{t_1}^{t_2} \ddot{Z}dt + \dot{Z}_{P_o} \qquad Z_P = \int_{t_1}^{t_2} \dot{Z}dt + Z_{P_o}$$

ΣF_{X_B}, ΣF_{Y_B}, ΣF_{Z_B} = sum of forces in the X, Y, Z body axis directions.

ΣF_{X_P}, ΣF_{Y_P}, ΣF_{Z_P} = sum of forces in the X, Y, Z inertial plumbline axis directions.

$[\beta]$ = transformation matrix from body to inertial plumbline.

ΣF = aero forces + thrust forces + RCS forces + engine deflection forces + slosh forces.

g_{X_I}, g_{Y_I}, g_{Z_I} = gravitational acceleration components in inertial polar-equatorial axis directions.

g_{X_P}, g_{Y_P}, g_{Z_P} = gravitational acceleration components in inertial plumbline axis directions.

$[\alpha]$ = transformation matrix from inertial polar - equatorial to inertial plumbline.

X_P, Y_P, Z_P = accelerations in inertial plumbline axis directions

m = total vehicle mass

INPUT/OUTPUT

The translation equations require as inputs:

Aerodynamic forces
Thrust forces
RCS forces
Engine deflection forces
Slosh forces
$[\alpha]$ and $[\beta]$ matrices
Gravitational acceleration components
Vehicle mass
Initial conditions on $\dot{X}_p$, $\dot{Y}_p$, $\dot{Z}_p$, X_p, Y_p, Z_p

The outputs from the translation equations are:

ΣF_{X_B}, ΣF_{Y_B}, ΣF_{Z_B} and the inertial plumbline position, velocity and acceleration components.

The translation equations require the presence of subroutines: RCS, THRUST, AERO,TVC, SLOSH AND GRAVITY.

COORDINATE SYSTEMS

Body axes - Orthogonal system with origin at engine gimbal pivot plane - X axis positive toward nose of vehicle; Z axis positive "down", and Y axis positive toward the right wing.

Inertial plumbline - Orthogonal system with origin at center of the earth - X axis parallel to the launch site gravity vector and positive in the direction opposite to gravitational acceleration.

Transformation matrix from body to inertial plumbline:

$$[\beta] = \begin{bmatrix} b_{11} & b_{12} & b_{13} \\ b_{21} & b_{22} & b_{23} \\ b_{31} & b_{32} & b_{33} \end{bmatrix}$$

2.1.4 AVEH (Continued)

b_{11} = Cos θ Cos ψ

b_{12} = Sin θ Sin φ -Cos θ Sin ψ Cos φ

b_{13} = Sin θ Cos φ + Cos θ Sin ψ Sin φ

b_{21} = Sin ψ

b_{22} = Cos ψ Cos φ

b_{23} = -Cos ψ Sin φ

b_{31} = -Sin θ Cos ψ

b_{32} = Cos θ Sin φ + Sin θ Sin ψ Cos φ

b_{33} = Cos θ Cos φ - Sin θ Sin ψ Sin φ

(See Euler Angles below for calculation of θ, ψ,φ)

Inertial polar - equatorial - orthogonal system with origin at the center of the earth - X axis is in equatorial plane, positive through a reference meridian at time of liftoff; the reference direction is defined by the time of liftoff and the coordinate system used for gravity calculations. The Z axis is positive through the North Pole.

Transformation matrix from polar - equatorial to plumbline

$$[\alpha] = \begin{bmatrix} a_{11} & a_{12} & a_{13} \\ a_{21} & a_{22} & a_{23} \\ a_{31} & a_{32} & a_{33} \end{bmatrix}$$

a_{11} = Cos λ_L^* Cos $(\phi_L + W_e t_L)$

a_{12} = Cos λ_L^* Sin $(\phi_L + W_e t_L)$

$$a_{13} = \text{Sin } \lambda_L^*$$

$$a_{21} = \text{Sin Al Sin}\lambda_L^* \text{ Cos } (W_e t_L + \phi_L) - \text{Cos Al Sin } (W_e t_L + \phi_L)$$

$$a_{22} = \text{Sin Al Sin}\lambda_L^* \text{ Sin } (W_e t_L + \phi_L) + \text{Cos Al Cos } (W_e t_L + \phi_L)$$

$$a_{23} = -\text{Sin Al Cos } \lambda_L^*$$

$$a_{31} = -\text{Cos Al Sin}\lambda_L^* \text{ Cos } (W_e t_L + \phi_L) - \text{Sin Al Sin } (W_e t_L + \phi_L)$$

$$a_{32} = -\text{Cos Al Sin}\lambda_L^* \text{ Sin } (W_e t_L + \phi_L) + \text{Sin Al Cos } (W_e t_L + \phi_L)$$

$$a_{33} = \text{Cos Al Cos } \lambda_L^*$$

Where:

λ_L^* = Geodetic latitude of launch site

ϕ_L = Longitude of launch site

W_e = Angular rate of the earth

t_L = Time of launch (from epoch)

A_L = Launch azimuth

2.1.4.1.2 ROTATION EQUATIONS

DESCRIPTION

This model defines the angular accelerations of the rigid body assuming that the center of mass lies in the X-Z plane ($I_{YZ} = I_{XY} = 0$).

MATH MODEL

1. Equations

$$\dot{q} = \frac{1}{I_{YY}} \quad \Sigma M_{Y_B} + pr\,(I_{ZZ} - I_{XX}) + (r^2 - p^2)\,I_{XZ}$$

$$\dot{p} = (a\,I_{ZZ} + b\,I_{XZ})/C$$

$$\dot{r} = (a\,I_{XZ} + b\,I_{XX})/C$$

$$a = \Sigma M_{X_B} + qr\,(I_{YY} - I_{ZZ}) + pq\,I_{XZ}$$

$$b = \Sigma M_{Z_B} + pq\,(I_{XX} - I_{YY}) - qr\,I_{XZ}$$

$$c = I_{XX}\,I_{ZZ} - I_{XZ}^2$$

2. Definition of Symbols

$\dot{q}$ = Angular acceleration about the Y body axis

$\dot{p}$ = Angular acceleration about the X body axis

$\dot{r}$ = Angular acceleration about the Z body axis

I_{XX}, I_{YY}, I_{ZZ} = Moment of inertia about X, Y, Z body axis respectively.

I_{XZ} = X - Z Cross product moments of inertia

p, q, r = Integral of $\dot{p}, \dot{q}, \dot{r}$ (Body rates)

$\Sigma M_{X_B}, \Sigma M_{Y_B}, \Sigma M_{Z_B}$ = Sum of moments about X, Y, Z body axes

= Aero moments + thrust moments + RCS moments + engine deflection moments + slosh moments

INPUT/OUTPUT

Inputs: From THRUST, AERO, RCS, TVC and SLOSH

Moments (about body axes) due to aerodynamics, main propulsion, reaction control, engine accelerations and slosh.

Outputs - $\dot{P}, \dot{Q}, \dot{R}$, P Q, R to IMU, Aero and Euler Angles

IV. COORDINATE SYSTEMS

Body axes - See translation equations for definiton.

2.1.4 AVEH (Continued)

2.1.4.1.3 EULER ANGLES

I. This model defines the rate of change of the euler angles describing the attitude of the vehicle in inertial space.

II. Math Model

$$\dot{\theta} = (q \cos \phi - r \sin \phi)/\cos \psi$$

$$\dot{\psi} = q \sin \phi + r \cos \phi$$

$$\dot{\phi} = p = \tan \psi \, (q \cos \phi + r \sin \phi)$$

Where:

$\dot{\theta}$, $\dot{\psi}$, $\dot{\phi}$ = Euler angle rates (1st, 2nd, and 3rd rotations, respectively)

θ, ψ, ϕ = Integral of $\dot{\theta}$, $\dot{\psi}$, $\dot{\phi}$

III. Input/Output

Inputs p, q, r from rotation equations

Outputs θ, ψ, ϕ to [B] and to IMU

2.1.5 BLCONT (Baseline Control System)

2.1.5.1 PROGRAM DESCRIPTION

This model issues commands to the engine gimbals such that the actual attitude is made to follow the attitude required by the guidance model.

2.1.5.2 MATH MODEL

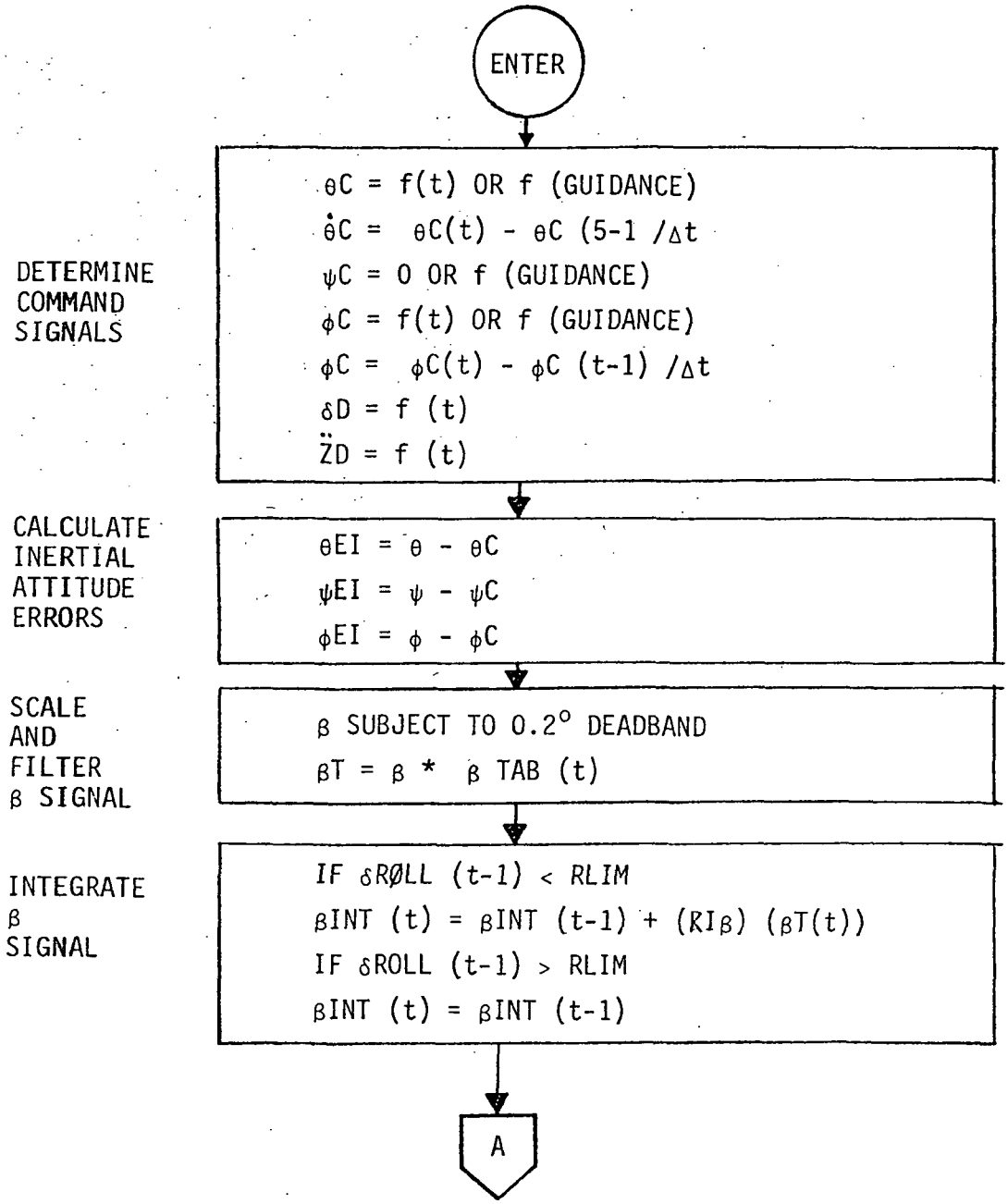

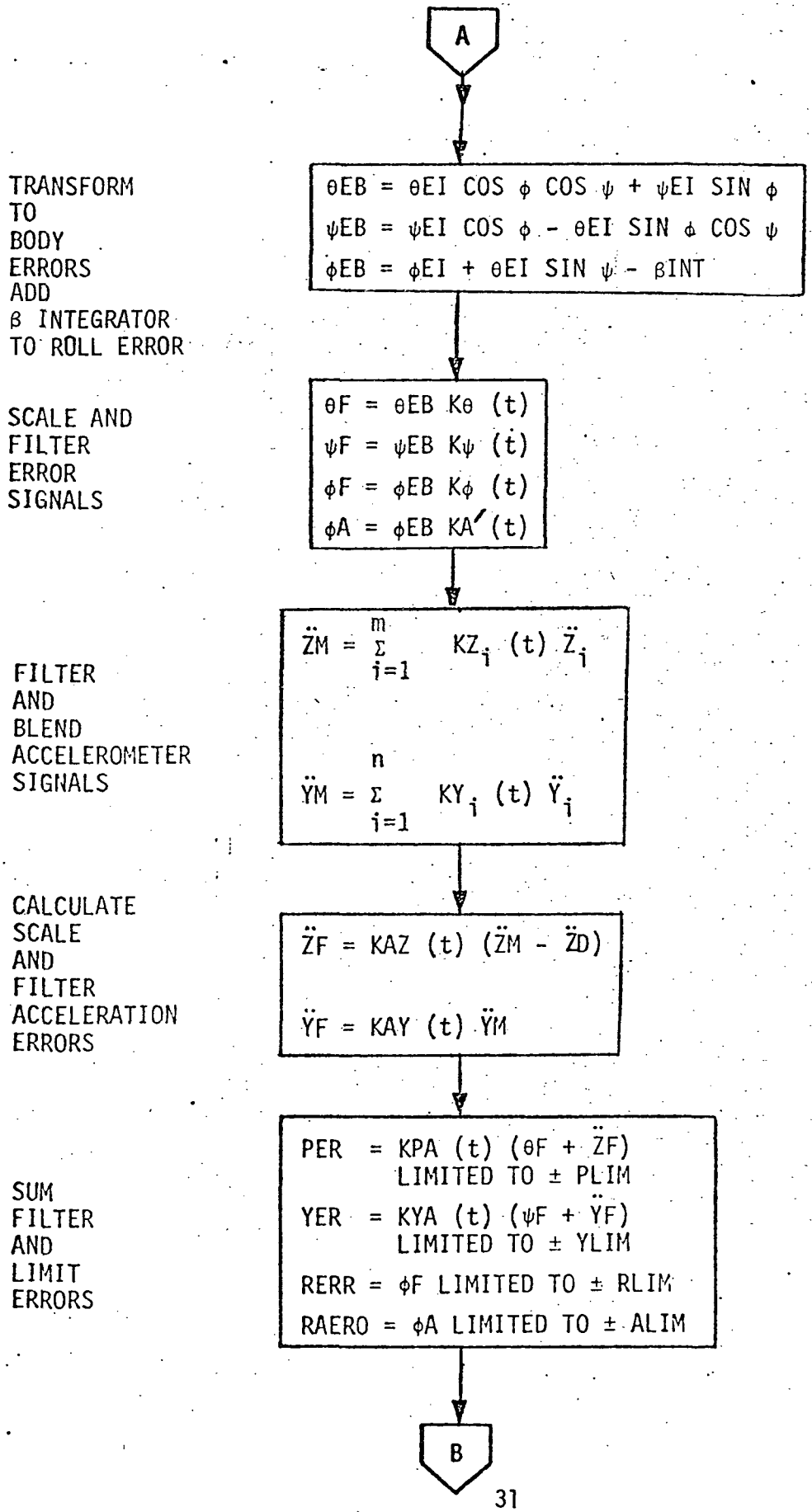
A
TRANSFORM TO BODY ERRORS ADD β INTEGRATOR TO ROLL ERROR
θEB = θEI COS φ COS ψ + ψEI SIN φ
ψEB = ψEI COS φ - θEI SIN φ COS ψ
φEB = φEI + θEI SIN ψ - βINT
SCALE AND FILTER ERROR SIGNALS
θF = θEB Kθ (t)
ψF = ψEB Kψ (t)
φF = φEB Kφ (t)
φA = φEB KA (t)
FILTER AND BLEND ACCELEROMETER SIGNALS
$\ddot{Z}M = \sum_{i=1}^{m} KZ_i(t)\,\ddot{Z}_i$
$\ddot{Y}M = \sum_{i=1}^{n} KY_i(t)\,\ddot{Y}_i$
CALCULATE SCALE AND FILTER ACCELERATION ERRORS
$\ddot{Z}F = KAZ(t)\,(\ddot{Z}M - \ddot{Z}D)$
$\ddot{Y}F = KAY(t)\,\ddot{Y}M$
SUM FILTER AND LIMIT ERRORS
PER = KPA (t) (θF + $\ddot{Z}$F) LIMITED TO ± PLIM
YER = KYA (t) (ψF + $\ddot{Y}$F) LIMITED TO ± YLIM
RERR = φF LIMITED TO ± RLIM
RAERO = φA LIMITED TO ± ALIM
B

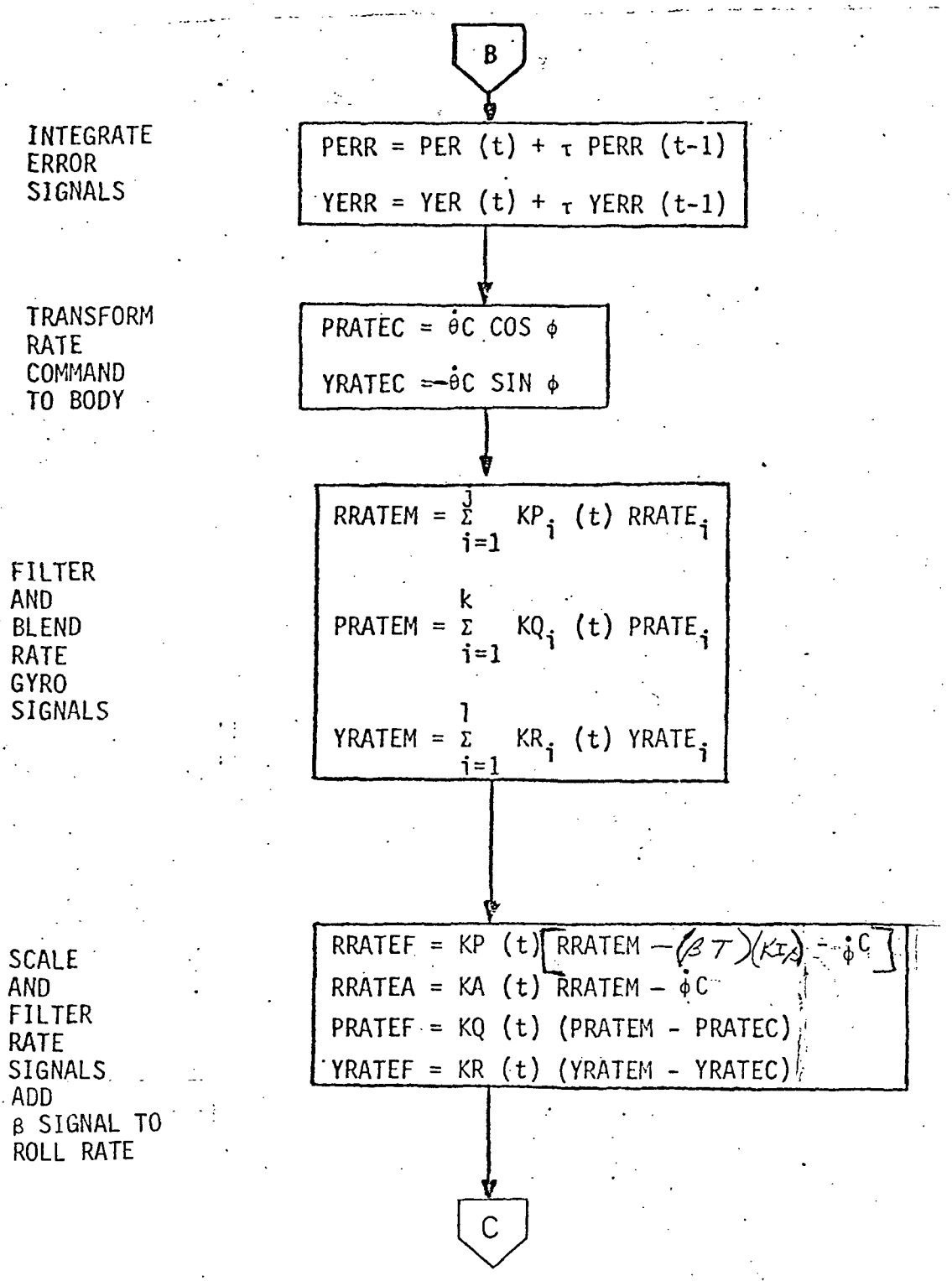
B
INTEGRATE ERROR SIGNALS
PERR = PER (t) + τ PERR (t-1)
YERR = YER (t) + τ YERR (t-1)
TRANSFORM RATE COMMAND TO BODY
PRATEC = θ̇C COS φ
YRATEC = −θ̇C SIN φ
FILTER AND BLEND RATE GYRO SIGNALS
RRATEM = Σ (i=1 to j) KP_i (t) RRATE_i
PRATEM = Σ (i=1 to k) KQ_i (t) PRATE_i
YRATEM = Σ (i=1 to l) KR_i (t) YRATE_i
SCALE AND FILTER RATE SIGNALS ADD β SIGNAL TO ROLL RATE
RRATEF = KP (t) [RRATEM − (βT)(KIA) − φ̇C]
RRATEA = KA (t) RRATEM − φ̇C
PRATEF = KQ (t) (PRATEM - PRATEC)
YRATEF = KR (t) (YRATEM - YRATEC)
C

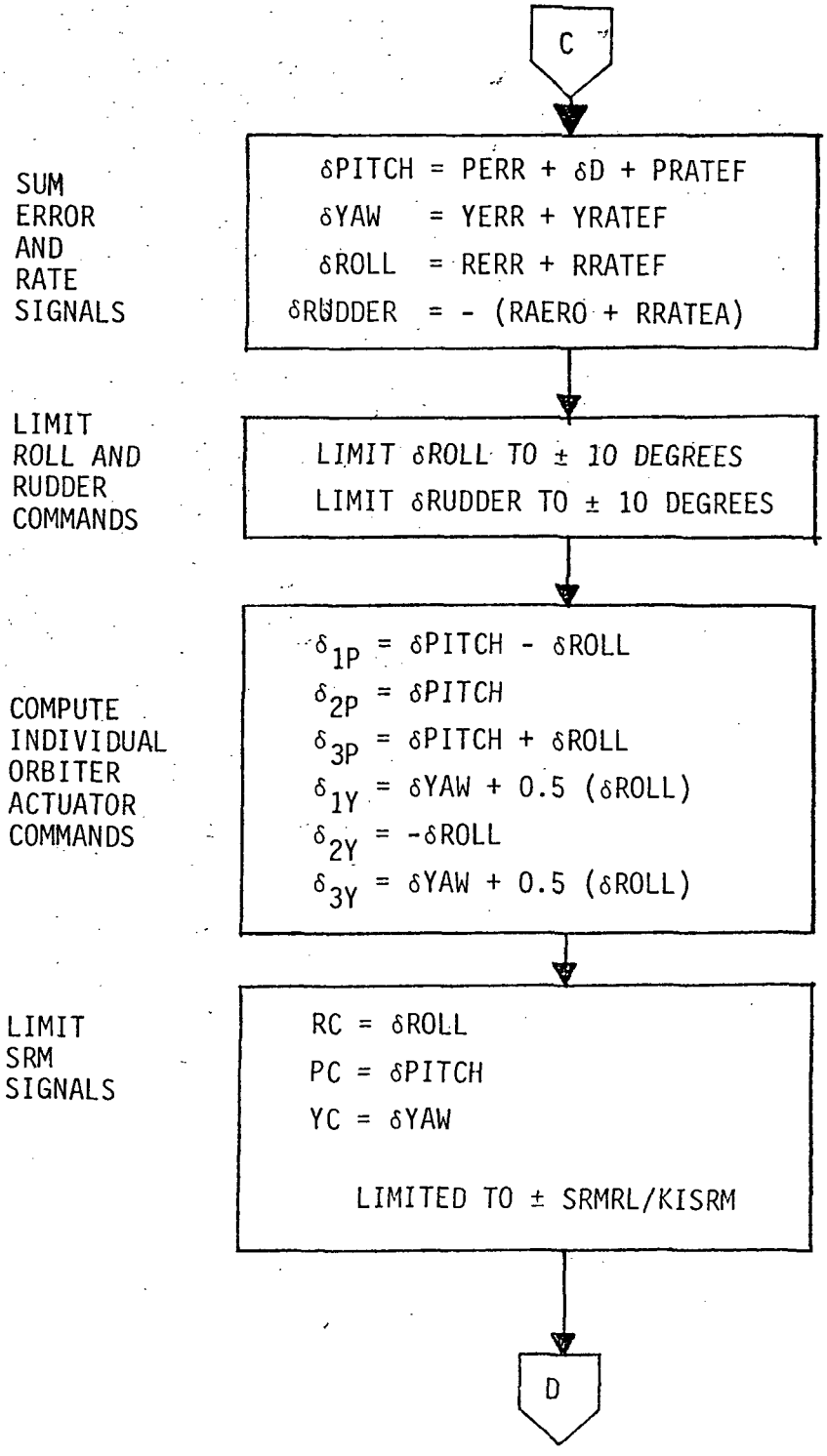
C
SUM ERROR AND RATE SIGNALS
δPITCH = PERR + δD + PRATEF
δYAW = YERR + YRATEF
δROLL = RERR + RRATEF
δRUDDER = - (RAERO + RRATEA)
LIMIT ROLL AND RUDDER COMMANDS
LIMIT δROLL TO ± 10 DEGREES
LIMIT δRUDDER TO ± 10 DEGREES
COMPUTE INDIVIDUAL ORBITER ACTUATOR COMMANDS
δ1P = δPITCH - δROLL
δ2P = δPITCH
δ3P = δPITCH + δROLL
δ1Y = δYAW + 0.5 (δROLL)
δ2Y = -δROLL
δ3Y = δYAW + 0.5 (δROLL)
LIMIT SRM SIGNALS
RC = δROLL
PC = δPITCH
YC = δYAW
LIMITED TO ± SRMRL/KISRM
D

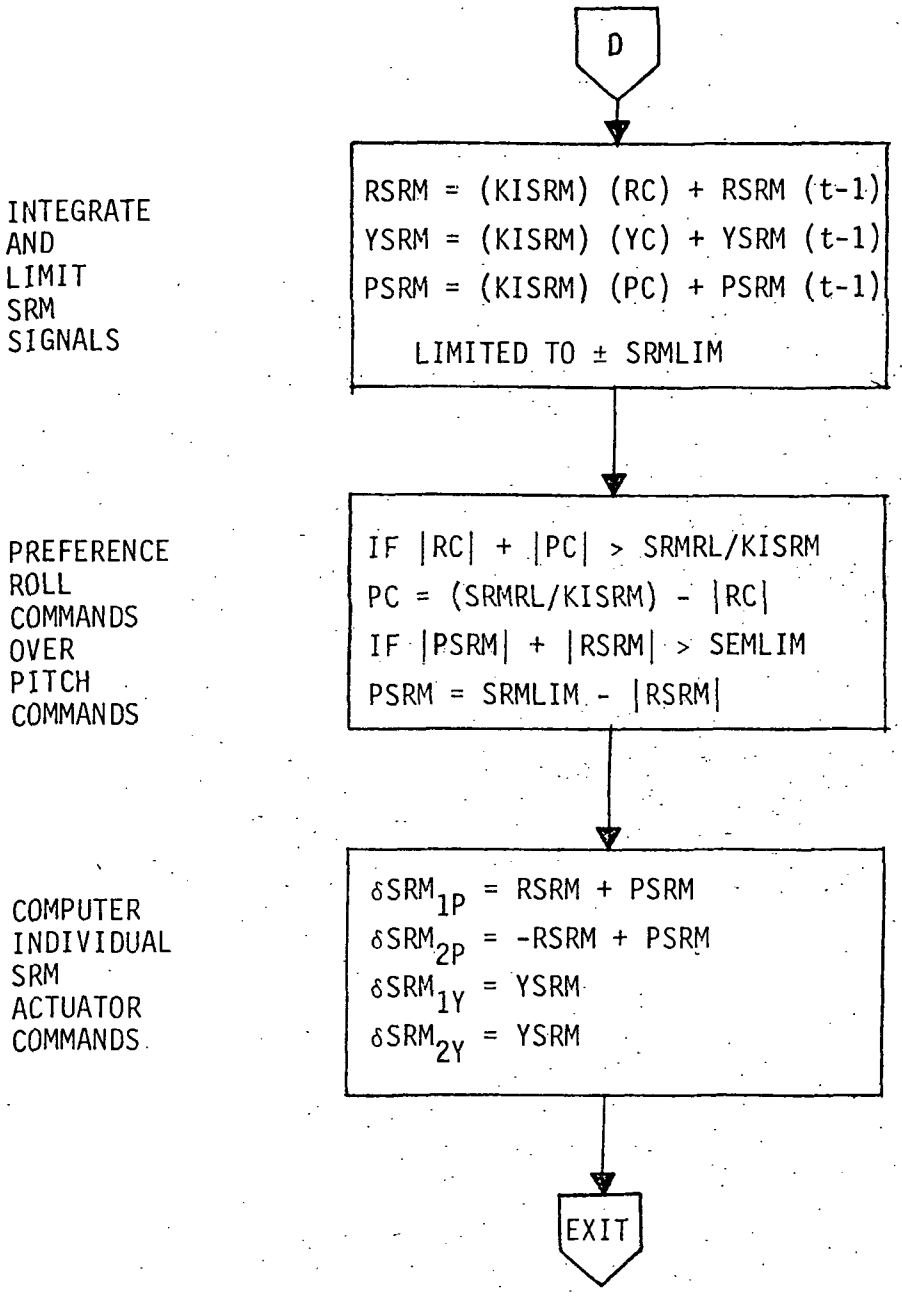
D
INTEGRATE AND LIMIT SRM SIGNALS
RSRM = (KISRM) (RC) + RSRM (t-1)
YSRM = (KISRM) (YC) + YSRM (t-1)
PSRM = (KISRM) (PC) + PSRM (t-1)
LIMITED TO ± SRMLIM
PREFERENCE ROLL COMMANDS OVER PITCH COMMANDS
IF |RC| + |PC| > SRMRL/KISRM
PC = (SRMRL/KISRM) - |RC|
IF |PSRM| + |RSRM| > SEMLIM
PSRM = SRMLIM - |RSRM|
COMPUTER INDIVIDUAL SRM ACTUATOR COMMANDS
δSRM1P = RSRM + PSRM
δSRM2P = -RSRM + PSRM
δSRM1Y = YSRM
δSRM2Y = YSRM
EXIT

2.1.5.3 SYMBOL DEFINITIONS

ALIM	Aero Error Software Limit
KA (t)	Aileron Roll Rate Gain
KA' (t)	Aileron Roll Error Gain
KAY (t)	Y Acceleration Gain
KAZ (t)	Z Acceleration Gain
KI_β	Sideslip Feedback Integrator Constant
KISRM	SRM Integrator Constant
KP (t)	TVC Roll Rate Gain
KP_i (t)	Individual Roll Rate Gyro Gain
KPA (t)	Pitch Channel Error Gain
KQ (t)	Pitch Rate Gain
KQ_i (t)	Individual Pitch Rate Gyro Gain
KR (t)	Yaw Rate Gain
KR_i (t)	Individual Yaw Rate Gyro Gain
KY_i (t)	Individual Y Accelerometer Gain
KYA (t)	Yaw Channel Error Gain
KZ_i (t)	Individual Z Accelerometer Gain
$K\theta$	Pitch Error Gain
$K\phi$	Roll Error Gain
$K\psi$	Yaw Error Gain
PC	SRM Pitch Error Signal
PER	Limited Pitch Channel Error
PERR	Integrated Pitch Channel Error
PLIM	Pitch Error Software Limit

2.1.5.3 SYMBOL DEFINITIONS (Continued)

$PRATE_i$	Individual Pitch Rate Gyro Signal
PRATEC	Pitch Rate Command
PRATEF	Scaled Pitch Rate Error
PRATEM	Blended Pitch Rate
PSRM	SRM Pitch Integrator
RAERO	Limited Roll Error for Aileron
RC	SRM Roll Error Signal
RERR	Limited Roll Error for TVC
RLIM	Roll Error Software Limit
$RRATE_i$	Individual Roll Rate Gyro Signal
RRATEA	Scaled Roll Rate for Ailerons
RRATEF	Scaled Roll Rate for TVC
RRATEM	Blended Roll Rate Signals
RSRM	SRM Roll Integrator
SRMLIM	SRM Integrator Limit
SRMRL	SRM Error Signal Rate Limit
$\ddot{Y}_i$	Individual Y Accelerometer Signal
YC	SRM Yaw Error Error Signal
$\ddot{Y}F$	Scaled Y Acceleration Error
YLIM	Yaw Error Software Limit
YM	Blended Y Accelerometer Signals
YER	Limited Yaw Channel Error
YERR	Integrated Yaw Channel Error
$YRATE_i$	Individual Yaw Rate Gyro Signal
YRATEC	Yaw Rate Command

YRATEF	Scaled Yaw Rate Error
YRATEM	Blended Rate Gyro Signals
YSRM	SRM Yaw Integrator
$\ddot{Z}_i$	Individual Z Accelerometer Signal
$\ddot{Z}D$	Z Acceleration Command
$\ddot{Z}F$	Scaled Z Acceleration Error
$\ddot{Z}M$	Blended Z Accelerometer Signals
$\dot{\beta}$	Vehicle Sideslip Angle
βINT	Sideslip Feedback Integrator Signal
βT	Scaled and Filtered Sideslip Signal
δ_{ip}, δ_{iy}	Individual Pitch and Yaw Engine Deflection Commands
δD	Prestored Engine Deflection Command
$\delta PITCH$	Total Pitch Channel Engine Deflection Command
$\delta ROLL$	Total Roll Channel Orbiter Engine Deflection Command
$\delta RUDDER$	Rudder Deflection Commands
δSRM_{ip}, δSRM_{iy}	Individual Pitch and Yaw SRM Engine Deflection Commands
δYAW	Total Yaw Channel Orbiter Engine Deflection Command
θ	Platform Inner Gimbal Angle
θc	Platform Inner Gimbal Angle Command
$\dot{\theta}c$	Platform Inner Gimbal Rate Command
θEB	Body Pitch Attitude Error
θEI	Platform Inner Gimbal Angle Error
θF	Scaled Pitch Error
τ	Integrator Gain
ϕ	Platform Outer Gimbal Angle

2.1.5.3 SYMBOL DEFINITIONS (Continued)

$\dot{\phi}C$	Platform Outer Gimbal Rate Command
ϕA	Scaled Roll Error for Ailerons
ϕC	Platform Outer Gimbal Angle Command
ϕEB	Body Roll Attitude Error
ϕEI	Platform Outer Gimbal Angle Error
ϕF	Scaled Roll Error
ψ	Platform Middle Gimbal Angle
ψC	Platform Middle Gimbal Angle Command
ψEB	Body Yaw Attitude Error
ψEI	Platform Middle Gimbal Angle Error
ψF	Scaled Yaw Error

2.1.5.4 INPUT/OUTPUT

Required inputs to this model are:

- Inertial attitude angles
- Body rotational rates
- Y & Z translational accelerations
- Prestored engine deflection commands
- Prestored accelerations commands
- Attitude commands from guidance system
- Vehicle sideslip angle

The system outputs are:

- Deflection commands to orbiter engines
- Deflection commands to SRM engines
- Deflection commands to aerosurfaces (rudder)

2.1.6 CGAINS (Control Gains Equations)

2.1.6.1 PROGRAM DESCRIPTION

The CGAINS program is used to calculate the control gains necessary for a desired type of control during the Shuttle boost. There are several options for the control gains that are calculated: load minimum, drift minimum, or attitude control for the pitch and yaw gains; and thrust vector control or aileron control for the roll gains. The following model presents the equations necessary to calculate these gains.

2.1.6.2 MATH MODEL

The following quantities must be calculated each time the control gains are needed. The symbols used in these equations are defined in Table 1.

$$l_0 = \bar{c}\,(C_{m0}/C_{z0}) + X_{cg} - X_R$$

$$l_{1p} = \bar{c}\,(C_{m\alpha}/C_{z\alpha}) + X_{cg} - X_R$$

$$l_{1y} = -\,(b\,C_{n\beta}/C_{y\beta}) + X_{cg} - X_R$$

$$N'_p = q\,S\,C_{z\alpha}$$

$$N'_y = q\,S\,C_{y\beta}$$

$$N_0 = q\,S\,C_{z0}$$

$$l_{ap} = -l_{ap}$$

$$l_{ay} = -l_{ap}$$

$$F_{AX} = q\,S\,C_{x0}$$

2.1.6 CGAINS (Continued)

$$K_{1p} = (F_0 \cos \delta_{CO} + F_B \cos \delta_{CB} + F_A)/m$$

$$K_{2p} = N'_p/m$$

$$K_{3p} = -F_0 \cos \delta_{CO}/m$$

$$K_{1y} = -K_{1p}$$

$$K_{2y} = -N'_y/m$$

$$K_{3y} = 2/3K_{3p}$$

$$\ddot{Z}_0 = N_0/m$$

$$l_x = X_{cg} - X_0$$

$$l_z = Z_{cg} - Z_0$$

$$l_g = (l_x^2 + l_z^2)^{\frac{1}{2}}$$

$$\ddot{\theta}_0 = (l_0 N_0 - F_{AX} l_z)/I_p$$

$$\delta_{CGO} = \tan^{-1} \frac{-l_z}{l_x}$$

$$C_{2p} = l_g F_o \cos (\delta_{CO} - \delta_{CGO})/I_p$$

$$\Delta_p = C_{2p} K_{2p} - C_{1p} K_{3p}$$

$$C_{1y} = -1_{1y} N'_y / I_y$$

$$C_{2y} = (2/31x)\ F/I_y$$

$$\Delta_y = C_{2y} K_{2y} - C_{1y} K_{3y}$$

2.1.6.2.1 PITCH AND YAW CONTROL GAINS FOR LOAD MINIMUM OPTION

$$a_{0p} = 0.$$

$$g_{2p} = \frac{\omega_y^2 - C_{1p}}{\Delta_p + \omega_y^2 (K_{3p} + 1_{ap} C_{2p})}$$

$$a_{1p} = \frac{2 \zeta_p \omega_y}{C_{2p}} \left[1 - g_{2p} (K_{3p} + 1_{ap} C_{2p})\right]$$

$$a_{0y} = 0.$$

$$g_{2y} = \frac{\omega_z^2 - C_{1y}}{\Delta_y + \omega_z^2 (K_{3y} + 1_{ay} C_{2y})}$$

$$a_{1y} = \frac{2 \zeta_y \omega_z}{C_{2y}} \left[1 - g_{2y} (K_{3y} + 1_{ay} C_{2y})\right]$$

2.1.6.2.2 PITCH AND YAW CONTROL GAINS FOR DRIFT MINIMUM OPTION

$$g_{2p} = \frac{\omega_y^2 - (1 + C_{2p} K_{1p}/\Delta_p) C_{1p}}{C_{2p} K_{1p} + \Delta_p + \omega_y^2 (K_{3p} + l_{ap} C_{2p})}$$

$$a_{0p} = g_{2p} K_{1p} + C_{1p} K_{1p}/\Delta_p$$

$$a_{1p} = \frac{2 \zeta_p \omega_y}{C_{2p}} \left[1 - g_{2p} (K_{3p} + l_{ap} C_{2p})\right]$$

$$g_{2y} = \frac{\omega_z^2 - (1 + C_{2y} K_{1y}/\Delta_y) C_{1y}}{C_{2y} K_{1y} + \Delta_y + \omega_z^2 (K_{3y} + l_{ay} C_{2y})}$$

$$a_{0y} = g_{2y} K_{1y} + C_{1y} K_{1y}/\Delta_y$$

$$a_{1y} = \frac{2 \zeta_y \omega_z}{C_{2y}} \left[1 - g_{2y} (K_{3y} + l_{ay} C_{2y})\right]$$

2.1.6.2.3 PITCH AND YAW CONTROL GAINS FOR ATTITUDE CONTROL

$$g_{2p} = 0$$

$$a_{0p} = \frac{\omega_y^2 - C_{1p}}{C_{2p}}$$

$$a_{1p} = \frac{2\,\zeta_p\,\omega_y}{C_{2p}}$$

$$g_{2y} = 0$$

$$a_{0y} = \frac{\omega_z^2 - C_{1y}}{C_{2y}}$$

$$a_{1y} = \frac{2\,\zeta_y\,\omega_z}{C_{2y}}$$

2.1.6 CGAINS (Continued)

2.1.6.2.4 ROLL CONTROL GAIN EQUATIONS

2.1.6.2.4.1 Thrust Vector Control

$$C_{2r} = \sqrt{Y_o^2 + Z_o^2}\ F/I_r$$

$$a_{0r} = \frac{\omega_x^2}{C_{2r}}$$

$$a_{1r} = \frac{2\ \zeta_r\ \omega_x}{C_{2r}}$$

2.1.6.2.4.2 Aileron Control

$$C_{2r} = \frac{q\ S\ b\ C_{l_{\delta_a}}}{I_r}$$

$$a_{0r} = \frac{\omega_x^2}{C_{2r}}$$

$$a_{1r} = \frac{2\ \zeta_r\ \omega_x}{C_{2r}}$$

2.1.6.2.4.3 TVC and Aileron Control

$$C_{2r} = \frac{\sqrt{Y_o^2 + Z_o^2}\ F + q\ S\ b\ C_{l_{\delta_a}}}{I_r}$$

a_{0r} and a_{1r} same as above

2.1.6.3 DEFINITION OF SYMBOLS

VARIABLE	DEFINITION
a_{op}	Pitch attitude gain
a_{oy}	Yaw attitude gain
a_{1p}	Pitch attitude rate gain
a_{1y}	Yaw attitude rate gain
b	Wing span
C	Coefficients for calculation of gains
$\bar{c}$	Mean aerodynamic chord
C_{mo}, C_m	Aero. moment coefficients
C_{zo}, $C_{z\alpha}$	Aero. normal force coefficients (pitch)
$C_{y\beta}$	Aero. normal force coefficients (yaw)
$C_{n\beta}$	Aero. moment coeff. (yaw)
$C_{l\delta_a}$	Coeff. of roll moment with aileron
C_{xo}	Aero. axial force coeff.
F_o	Total orbiter thrust
F_B	Total booster thrust
F_{AX}	Aero. axial force
g_{2p}	Pitch acceleration gain
g_{2y}	Yaw acceleration gain
I	Moments of inertia
K	Coefficients for calculation of gains
l	Moment arms
m	Mass
N_o	Normal force at zero angle-of-attack
N'	Partial of normal force
q	Dynamic pressure
S	Aerodynamic reference area

2.1.6 CGAINS (Continued)

VARIABLE	DEFINITION
X_o, Y_o, Z_o	Average location of orbiter engines
X_{CG}, Y_{CG}	Location of center of gravity
$\ddot{Z}_o$	Translational acceleration at zero angle-of-attack
Δ_p, Δ_y	Temporary variable
ζ	Damping ratio
$\ddot{\theta}$	Rotational acceleration at zero angle-of-attack
ω	Natural frequency

2.1.6.4 PROGRAM FORMAT, INPUT-OUTPUT

The control gains routine calculates the attitude gains, attitude rate gains and accelerometer gains for each of the desired conditions which have been previously mentioned. These gains are also calculated for a range of natural frequencies (ω). These results are output on a scratch tape or FASTRAND file for processing by a plotting program.

2.1.7 ACTIVE GUIDANCE

2.1.7.1 PROGRAM DESCRIPTION

Active guidance is used to provide inertial steering commands during the boost to orbit insertion. Described in this section are two active guidance schemes which are incorporated in the SSFS. These two guidance schemes are the Apollo Lunar Ascent Guidance or 'E' Guidance (program name - BACTGD);and Linear Tangent Guidance (program name - GUIDE).

2.1.7.2 BACTGD

The 'E' guidance method is baselined in Revision B of "MSC Space Shuttle GN&C Design Equations Document". The math model for this method is described as follows:

Preliminary Calculations

$$R_p(4) = (R_p(1)^2 + R_p(2)^2 + R_p(3)^2)^{\frac{1}{2}}$$

$$G(1,1) = R_p(1)/R_p(4)$$
$$G(1,2) = R_p(2)/R_p(4)$$
$$G(1,3) = R_p(3)/R_p(4)$$
$$G(3,1) = G(1,2)\ U_Q(3) - G(1,3)\ U_Q(2)$$
$$G(3,2) = G(1,3)\ U_Q(1) - G(1,1)\ U_Q(3)$$
$$G(3,3) = G(1,1)\ U_Q(2) - G(1,2)\ U_Q(1)$$
$$G(2,1) = G(3,2)\ G(1,3) - G(3,3)\ G(1,2)$$
$$G(2,2) = G(3,3)\ G(1,1) - G(3,1)\ G(1,3)$$
$$G(2,3) = G(3,1)\ G(1,2) - G(3,2)\ G(1,1)$$

2.1.7 GUIDANCE (Continued)

$$\begin{bmatrix} V_G(1) \\ V_G(2) \\ V_G(3) \end{bmatrix} = [G] \begin{bmatrix} V_P(1) \\ V_P(2) \\ V_P(3) \end{bmatrix}$$

$$V_{GD}(1) = \dot{R} - V_G(1)$$
$$V_{GD}(2) = \dot{Y} - V_G(2)$$
$$V_{GD}(3) = \dot{Z} - V_G(3)$$

$$\vec{V}_{PD} = [G]^T \vec{V}_{GD}$$

$$AM(1) = G(1,2)\, V_P(3) - G(1,3)\, V_P(2)$$
$$AM(2) = G(1,3)\, V_P(1) - G(1,1)\, V_P(3)$$
$$AM(3) = G(1,1)\, V_P(2) - G(1,2)\, V_P(1)$$

$$AM(4) = \sqrt{AM(1)^2 + AM(2)^2 + AM(3)^2}$$

$$A_{GRAV}(4) = \sqrt{A_{GRAV}(1)^2 + A_{GRAV}(2)^2 + A_{GRAV}(3)^2}$$

$$G_{EFF} = -A_{GRAV}(4) + AM(4)/R_P(4)$$

$$V_{PD}(1) = V_{PD}(1) - \tfrac{1}{2} T_{GO}\, G_{EFF}\, G(1,1)$$

$$V_{PD}(2) = V_{PD}(2) - \tfrac{1}{2} T_{GO}\, G_{EFF}\, G(1,2)$$

$$V_{PD}(3) = V_{PD}(3) - \tfrac{1}{2} T_{GO}\, G_{EFF}\, G(1,3)$$

$$V_{PD}(4) = \sqrt{V_{PD}(1)^2 + V_{PD}(2)^2 + V_{PD}(3)^2}$$

$$\tau = \frac{V_{EG}}{|A_T|}$$

NOTE: Prior to the end of Boost Polynomial Guidance the "Preliminary Calculations" portion of Active Guidance shall be cycled 5 times to establish an initial value of T_{GO} using the following equation:

$$T_{GO} = \left(1 - \ell^{-\frac{V_{PD}(4)}{V_{EG}}} \right)$$

CALCULATIONS FOR CONSTANT THRUST:

$$T_{TL} = \tau - \frac{V_{EG}}{A_{TL}}$$

$$Q_1 = \ln\left(1 - \frac{T_{TL}}{\tau}\right)$$

$$T_{GO} = T_{TL} + \frac{V_{PD}(4) + V_{EG}\, Q_1}{A_{TL}}$$

$$Q_2 = V_{EG}\, Q_1$$

$$Q_3 = T_{GO} - T_{TL}$$

$$A_{11} = -Q_2 + Q_3\, A_{TL}$$

$$Q_4 = \tau Q_2$$

$$Q_5 = V_{EG}\, T_{TL}$$

$$A_{12} = -Q_4 - Q_5 + \tfrac{1}{2} A_{TL}\,(T_{GO}^{\,2} - T_{TL}^{\,2})$$

$$A_{21} = Q_4 + Q_5 - Q_2 T_{GO} + \tfrac{1}{2} A_{TL} Q_3^{\,2}$$

$$A_{22} = \tau\,(Q_4 + Q_5 - T_{GO} Q_2) + Q_5\left(\frac{T_{TL}}{2} - T_{GO}\right) + \frac{A_{TL}}{6}\,(T_{GO}^{\,3} - 3T_{GO}\, T_{TL}^{\,2} + 2T_{TL}^{\,3})$$

CALCULATIONS FOR CONSTANT ACCELERATION:

$$T_{GO} = \frac{V_{PD}(4)}{A_{TL}}$$

$$A_{11} = A_{TL}\, T_{GO}$$

$$A_{12} = \tfrac{1}{2} A_{11}\, T_{GO}$$

$$A_{21} = A_{12}$$

$$A_{22} = 1/3\; A_{12}\, T_{GO}$$

FINAL CALCULATIONS:

$$\nabla = A_{11}\,A_{22} - A_{12}\,A_{21}$$

$$Q_2 = U_Q(1)\,R_P(1) + U_Q(2)\,R_P(2) + U_Q(3)\,R_P(3)$$

$$A = \frac{-A_{12}(R - R_P(4) - \dot{R}\,T_{GO}) + A_{22}\,V_G(1)}{\nabla}$$

$$B = \frac{A_{11}(R - R_P(4) - \dot{R}\,T_{GO}) - A_{21}\,V_G(1)}{\nabla}$$

$$C = \frac{-A_{12}(Y - Q_2 - \dot{Y}\,T_{GO}) + A_{22}\,V_G(2)}{\nabla}$$

$$D = \frac{A_{11}(Y - Q_2 - \dot{Y}\,T_{GO}) - A_{21}\,V_G(2)}{\nabla}$$

$$A_G(1) = |A_T|(A + B\delta\tau) - G_{EFF}$$

$$A_G(2) = |A_T|(C + D\delta\tau)$$

$$Q_6 = |A_T|^2 - A_G(1)^2 - A_G(2)^2$$

$$A_G(3) = \text{AMAX1}(0., \sqrt{Q_6})$$

$$Q_7 = \sqrt{A_G(3)^2 + A_G(1)^2}$$

$$\vec{A_P} = [G]^T\,\vec{A_G}$$

$$A_P(4) = \sqrt{A_P(1)^2 + A_P(2)^2 + A_P(3)^2}$$

2.1.7 GUIDANCE (Continued)

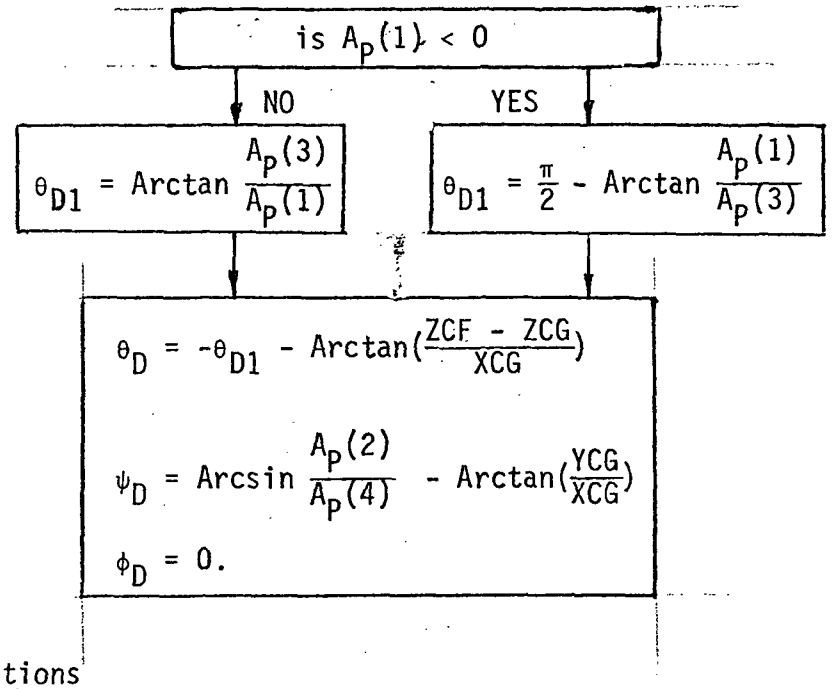

Symbol Definitions

$[G]$ = transformation from platform coordinates to guidance coordinates

$\vec{R_P}$ = current position vector in platform coordinates

$\vec{U_Q}$ = target unit vector normal to orbit plane in platform coordinates

$\vec{V_P}$ = current velocity vector in platform coordinates

$\vec{V_G}$ = current velocity vector in guidance coordinates

$\dot{R},\dot{Y},\dot{Z}$ = target velocity in guidance coordinates

$\vec{V_{GD}}$ = velocity to be gained in guidance coordinates

$\vec{V_{PD}}$ = velocity to be gained in platform coordinates

$\vec{AM}$ = angular momentum vector

$\vec{A_{GRAV}}$ = acceleration due to gravity in platform coordinates

G_{EFF} = effective gravity

T_{GO} = time to go until orbit insertion

V_{EG} = rocket exhaust gas velocity

$\vec{A_T}$ = acceleration due to thrust in platform coordinate = $\frac{\Sigma F}{M}$

τ = time required to burn up the vehicle's total mass

T_{TL} = time until thrust limiting

A_{TL} = vehicle acceleration at the acceleration limit

Q_1, Q_2, Q_3, Q_4, Q_5, Q_6, Q_7 = temporary variables

XCG, YCG, ZCG = coordinates of vehicle center of mass

ZCF = position of thrust centerline

A_{11}, A_{12}, A_{21}, A_{22} = parameters needed to compute linear control coefficients

∇ = temporaty variable

A, B. C. D = 1 linear control coefficients

$\delta\tau$ = time period between guidance calculations

$\vec{A}_G$ = desired acceleration in guidance coordinates

$\vec{A}_P$ = desired acceleration in platform coordinates

θ_{D1} = temporary variable

θ_D, ψ_D, ϕ_D = desired platform gimbal angles

R, Y = target position in guidance coordinates

2.1.7.3 GUIDE

The LTG guidance method is baselined in Revision C of "MSC Space Shuttle GN&C Design Equations Document", and also in NASA Internal Note MSC-IN-72-39. The LTG math model is as follows:

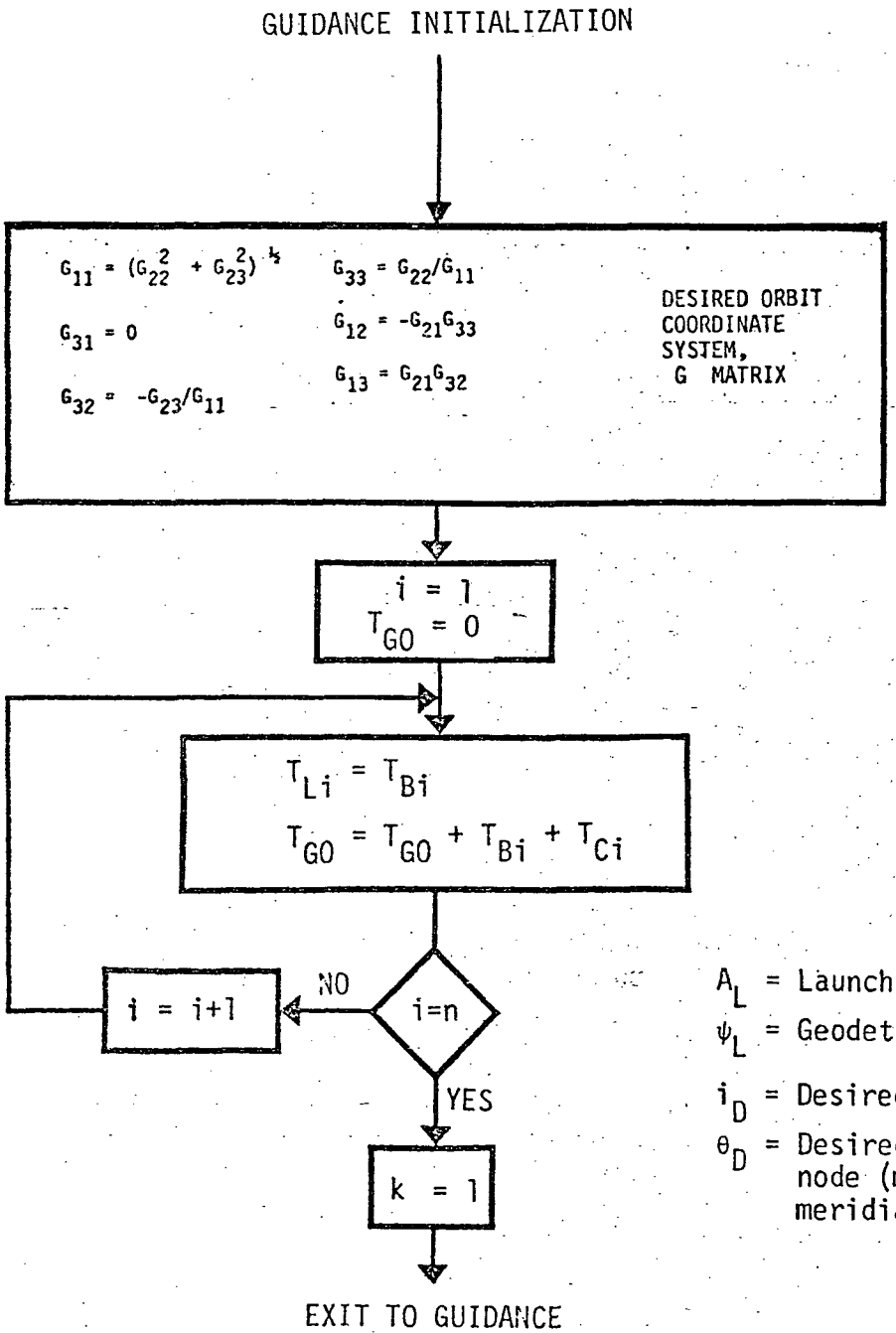

A_L = Launch Azimuth

ψ_L = Geodetic Launch Latitude

i_D = Desired orbit inclination

θ_D = Desired Longitude of descending node (measured from launch meridian)

ENTER GUIDANCE (MAJOR CYCLE LOOP)

$$\bar{R}_4 = [G]\,\bar{R}_p$$

$$\phi_o = \tan^{-1}(Z_4/X_4)$$

INITIAL RANGE ANGLE

$$\hat{U}_y = \begin{bmatrix} G_{21} \\ G_{22} \\ G_{23} \end{bmatrix}$$

$$\hat{U}_Z = \text{Unit}(\bar{R}_p \times \hat{U}_y)$$

$$\hat{U}_X = \hat{U}_y \times \hat{U}_Z$$

$$[E] = \begin{bmatrix} U_{X1} & U_{X2} & U_{X3} \\ U_{Y1} & U_{Y2} & U_{Y3} \\ U_{Z1} & U_{Z2} & U_{Z3} \end{bmatrix}$$

LOCAL GUIDANCE COORDINATE SYSTEM

$$\bar{R}_G = [E]\,\bar{R}_p$$

$$\bar{V}_G = [E]\,\bar{V}_p$$

RADIUS AND VELOCITY IN LOCAL GUIDANCE FRAME

$$a = \text{ABS}(\bar{a}_p)$$

MEASURED ACCELERATION MAGNITUDE

$$R = \text{ABS}(\bar{R}_p)$$

$$g_r = -(\bar{g}_p \cdot \bar{R}_p)/R$$

$$g_{AV} = .5g_r\left[1 + (R/R_D)^2\right]$$

AVERAGE RADIAL GRAVITY MAGNITUDE

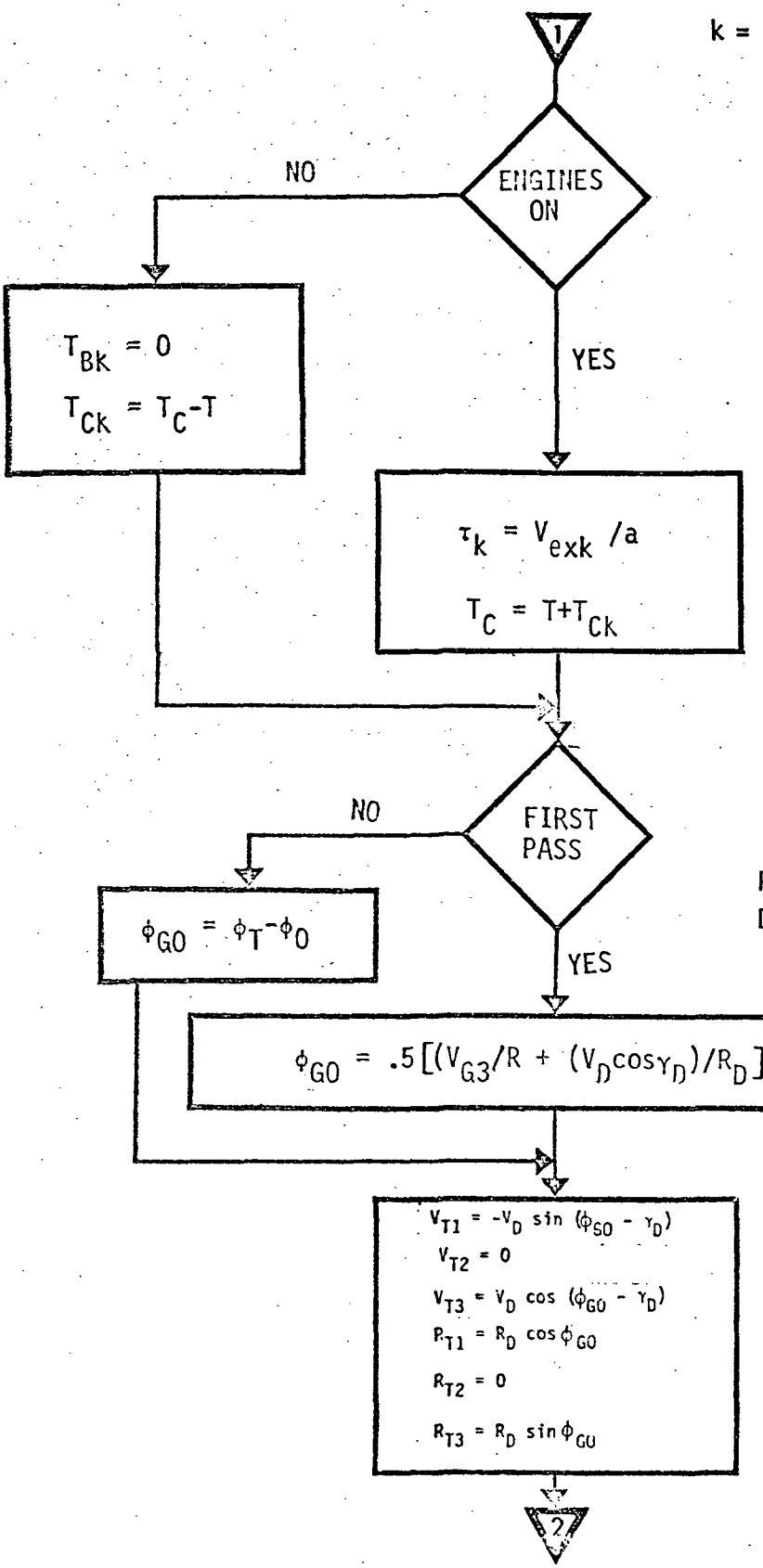

k = NO. OF PRESENT BURNING STAGE

RANGE ANGLE-TO-GO IN DESIRED ORBIT PLANE

TERMINAL VELOCITY AND RADIUS VECTORS IN LOCAL GUIDANCE FRAME

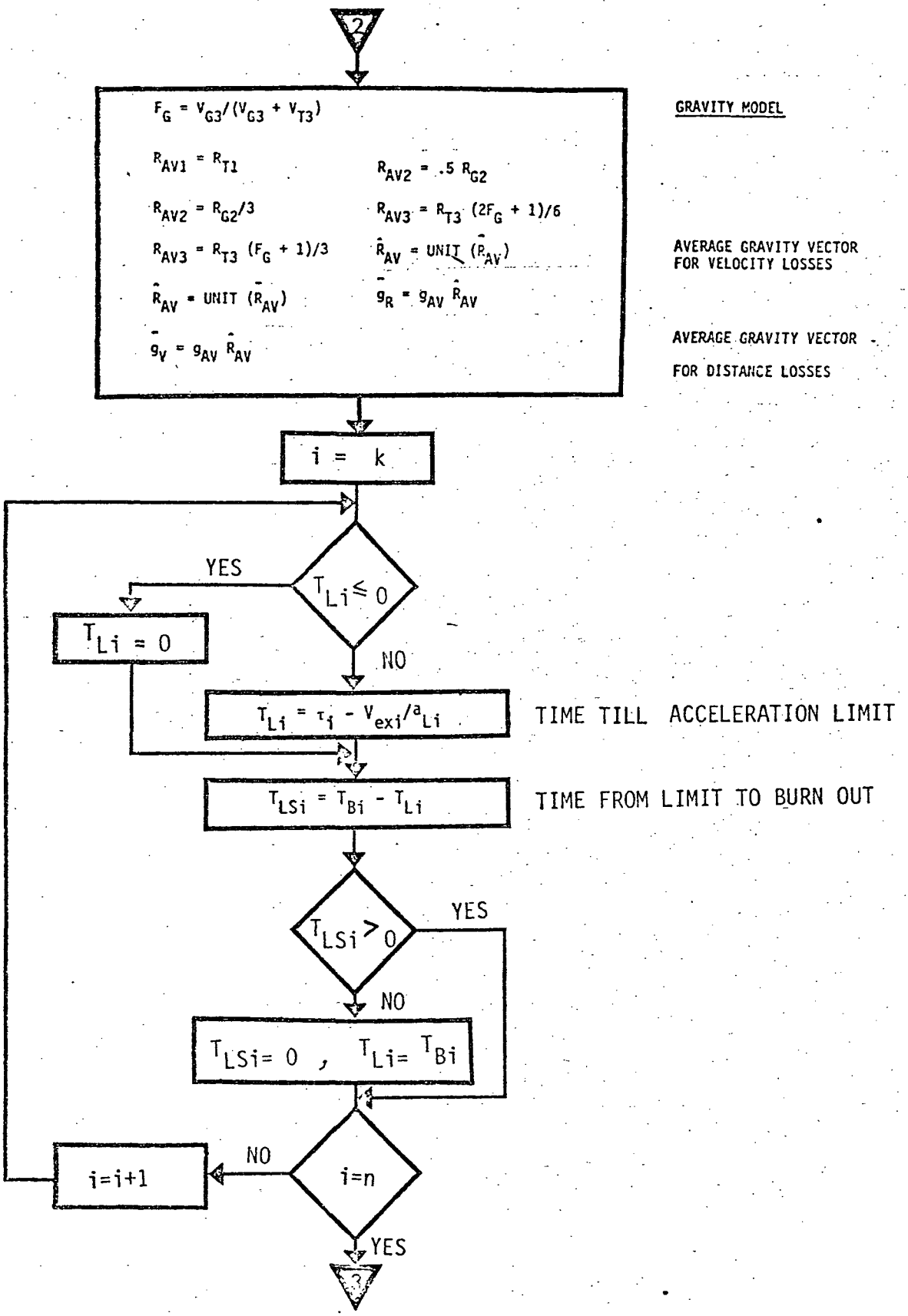
2
$F_G = V_{G3}/(V_{G3} + V_{T3})$
$R_{AV1} = R_{T1}$
$R_{AV2} = .5\ R_{G2}$
$R_{AV2} = R_{G2}/3$
$R_{AV3} = R_{T3}\ (2F_G + 1)/6$
$R_{AV3} = R_{T3}\ (F_G + 1)/3$
$\hat{R}_{AV} = \text{UNIT}\ (\bar{R}_{AV})$
$\bar{g}_R = g_{AV}\ \hat{R}_{AV}$
$\hat{R}_{AV} = \text{UNIT}\ (\bar{R}_{AV})$
$\bar{g}_V = g_{AV}\ \hat{R}_{AV}$
GRAVITY MODEL
AVERAGE GRAVITY VECTOR FOR VELOCITY LOSSES
AVERAGE GRAVITY VECTOR FOR DISTANCE LOSSES
i = k
$T_{Li} \leq 0$
YES
$T_{Li} = 0$
NO
$T_{Li} = \tau_i - V_{exi}/a_{Li}$
TIME TILL ACCELERATION LIMIT
$T_{LSi} = T_{Bi} - T_{Li}$
TIME FROM LIMIT TO BURN OUT
$T_{LSi} > 0$
YES
NO
$T_{LSi} = 0\ ,\ T_{Li} = T_{Bi}$
i=n
NO
i=i+1
YES
3

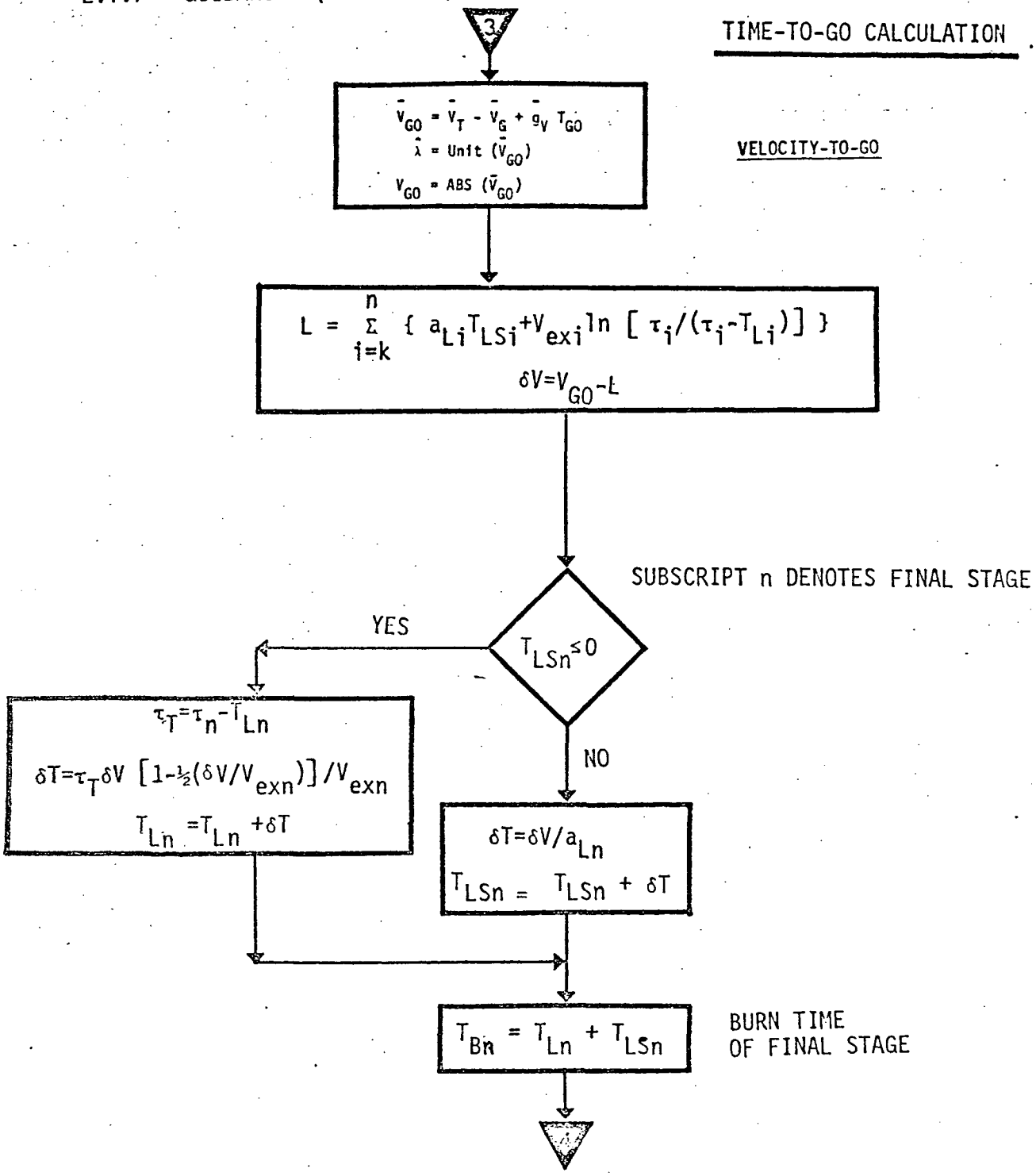
3
TIME-TO-GO CALCULATION
$\bar{V}_{GO} = \bar{V}_T - \bar{V}_G + \bar{g}_V T_{GO}$
$\hat{\lambda}$ = Unit ($\bar{V}_{GO}$)
V_{GO} = ABS ($\bar{V}_{GO}$)
VELOCITY-TO-GO
$L = \sum_{i=k}^{n} \{ a_{Li} T_{LSi} + V_{exi} \ln [\tau_i / (\tau_i - T_{Li})] \}$
$\delta V = V_{GO} - L$
SUBSCRIPT n DENOTES FINAL STAGE
$T_{LSn} \leq 0$
YES
NO
$\tau_T = \tau_n - T_{Ln}$
$\delta T = \tau_T \delta V [1 - \frac{1}{2}(\delta V / V_{exn})] / V_{exn}$
$T_{Ln} = T_{Ln} + \delta T$
$\delta T = \delta V / a_{Ln}$
$T_{LSn} = T_{LSn} + \delta T$
$T_{Bn} = T_{Ln} + T_{LSn}$
BURN TIME OF FINAL STAGE

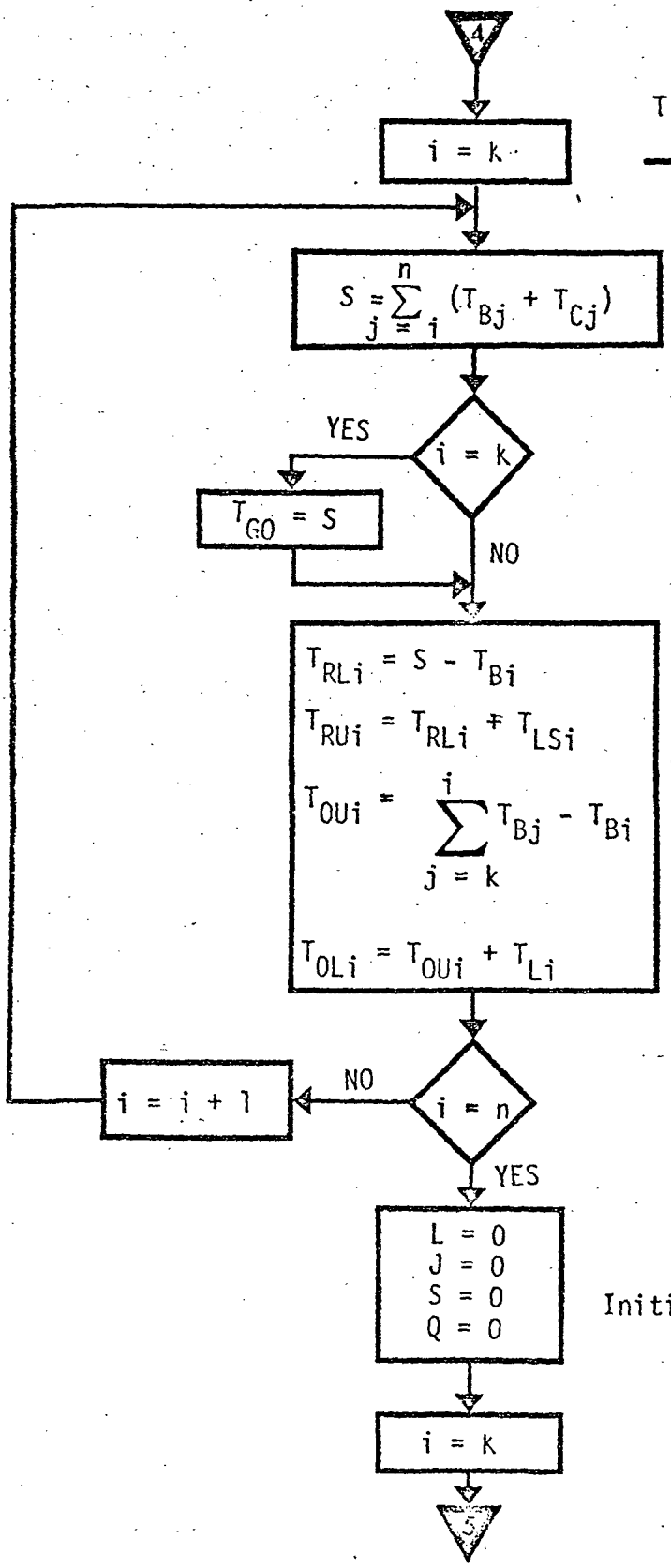

TIMES USED FOR MULTI-STAGE INTEGRALS

k = No. of present burning stage

n = No. of final stage

Time remaining after constant acceleration burn

Time remaining after constant thrust burn

Initial Time of constant thrust burn

Initial Time of constant acceleration burn

Initialize Summation Loop

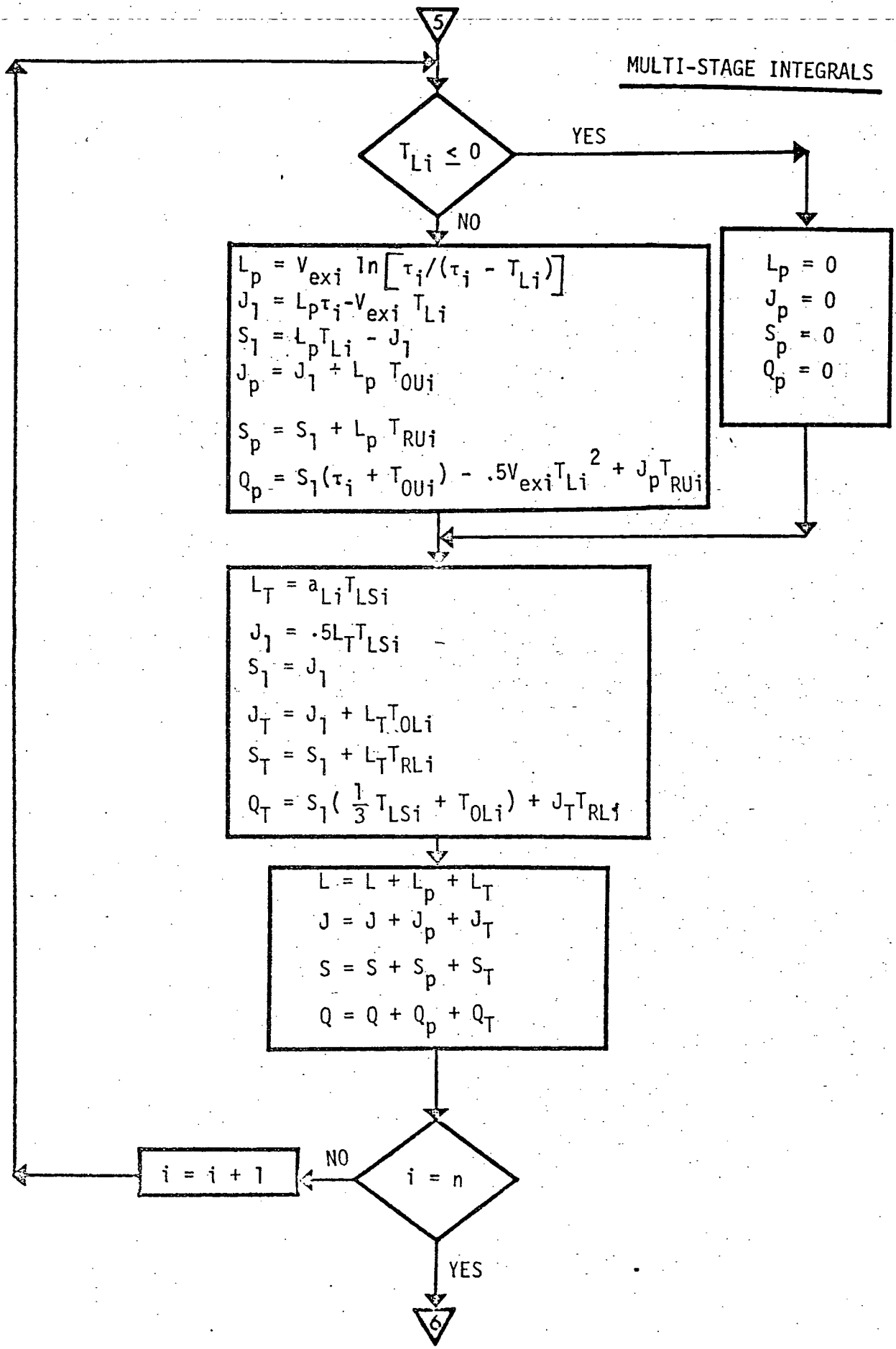
5
MULTI-STAGE INTEGRALS
$T_{Li} \leq 0$
YES
NO
$L_p = V_{exi} \ln[\tau_i/(\tau_i - T_{Li})]$
$J_1 = L_p\tau_i - V_{exi} T_{Li}$
$S_1 = L_p T_{Li} - J_1$
$J_p = J_1 + L_p T_{OUi}$
$S_p = S_1 + L_p T_{RUi}$
$Q_p = S_1(\tau_i + T_{OUi}) - .5V_{exi}T_{Li}^2 + J_p T_{RUi}$
$L_p = 0$
$J_p = 0$
$S_p = 0$
$Q_p = 0$
$L_T = a_{Li} T_{LSi}$
$J_1 = .5L_T T_{LSi}$
$S_1 = J_1$
$J_T = J_1 + L_T T_{OLi}$
$S_T = S_1 + L_T T_{RLi}$
$Q_T = S_1(\frac{1}{3} T_{LSi} + T_{OLi}) + J_T T_{RLi}$
$L = L + L_p + L_T$
$J = J + J_p + J_T$
$S = S + S_p + S_T$
$Q = Q + Q_p + Q_T$
$i = n$
NO
$i = i + 1$
YES
6

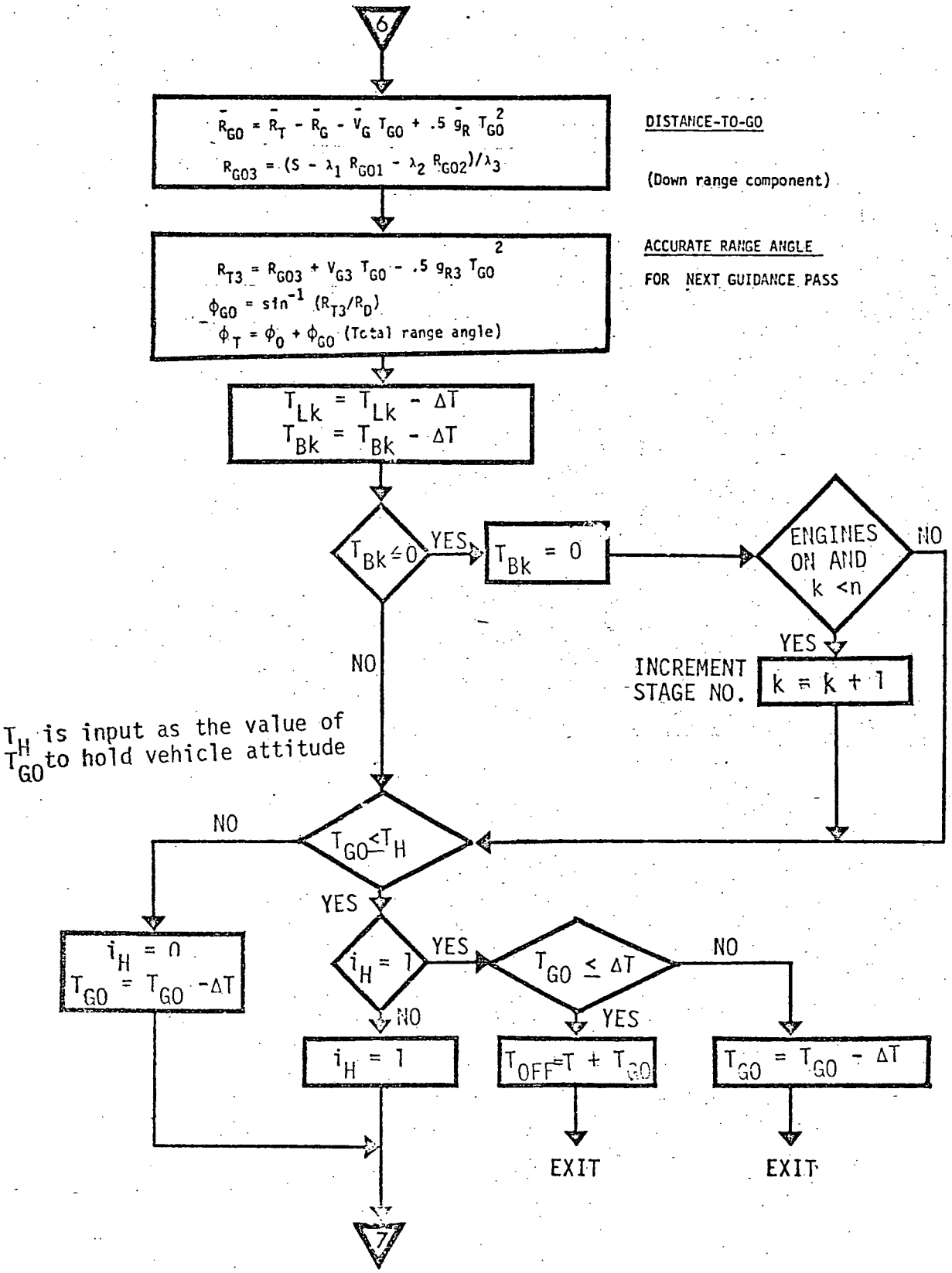
6
$\bar{R}_{GO} = \bar{R}_T - \bar{R}_G - \bar{V}_G T_{GO} + .5 \bar{g}_R T_{GO}^2$
$R_{GO3} = (S - \lambda_1 R_{GO1} - \lambda_2 R_{GO2})/\lambda_3$
DISTANCE-TO-GO
(Down range component)
$R_{T3} = R_{GO3} + V_{G3} T_{GO} - .5 g_{R3} T_{GO}^2$
$\phi_{GO} = \sin^{-1}(R_{T3}/R_D)$
$\phi_T = \phi_0 + \phi_{GO}$ (Total range angle)
ACCURATE RANGE ANGLE
FOR NEXT GUIDANCE PASS
$T_{Lk} = T_{Lk} - \Delta T$
$T_{Bk} = T_{Bk} - \Delta T$
$T_{Bk} \leq 0$
YES
$T_{Bk} = 0$
ENGINES ON AND k <n
NO
YES
INCREMENT STAGE NO.
k = k + 1
NO
T_H is input as the value of T_{GO} to hold vehicle attitude
$T_{GO} \leq T_H$
NO
YES
$i_H = 0$
$T_{GO} = T_{GO} - \Delta T$
$i_H = 1$
YES
$T_{GO} \leq \Delta T$
NO
NO
YES
$i_H = 1$
$T_{OFF} = T + T_{GO}$
$T_{GO} = T_{GO} - \Delta T$
EXIT
EXIT
7

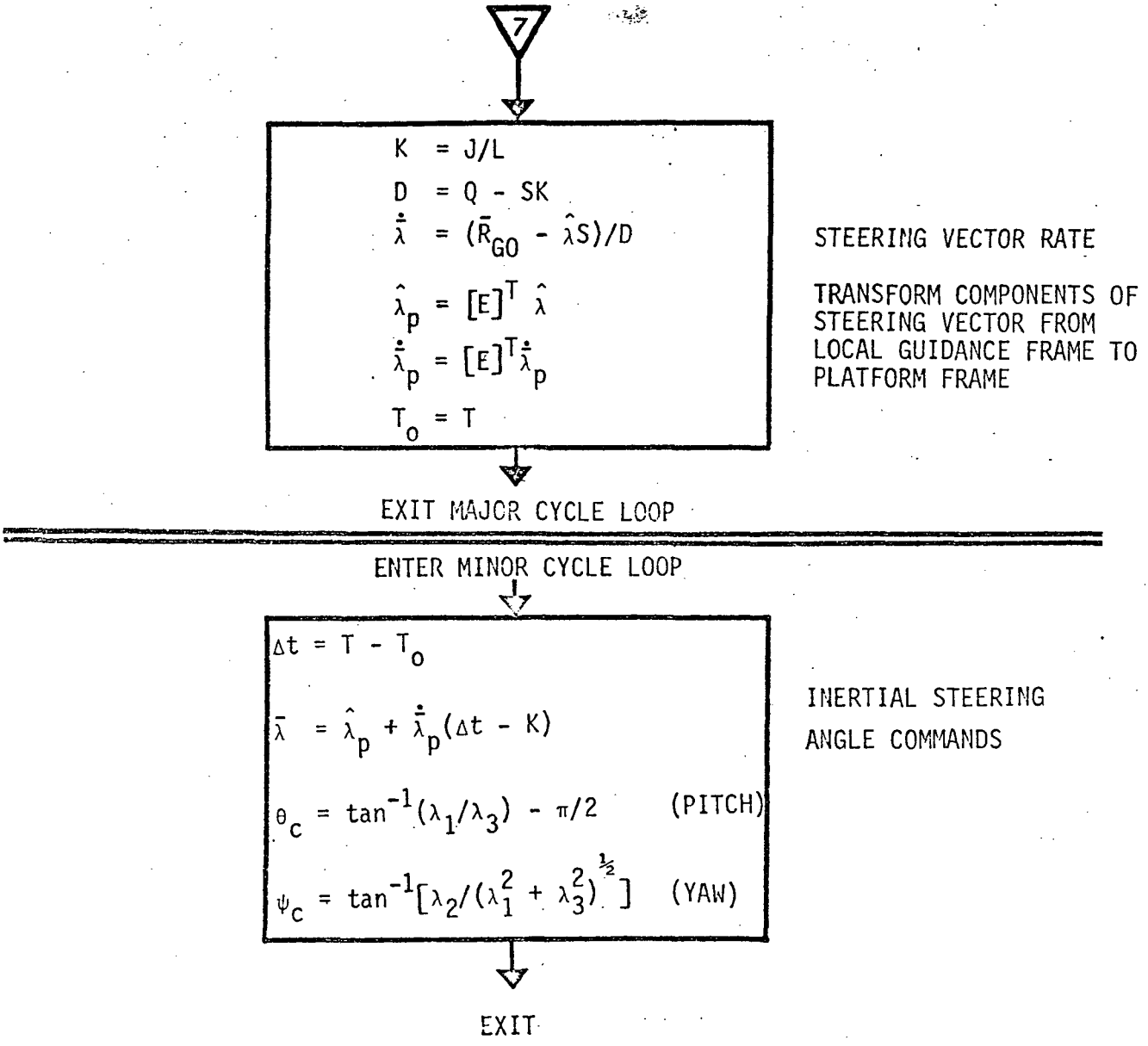
7
K = J/L
D = Q - SK
$\dot{\bar{\lambda}} = (\bar{R}_{GO} - \hat{\lambda}S)/D$
STEERING VECTOR RATE
$\hat{\lambda}_p = [E]^T \hat{\lambda}$
$\dot{\bar{\lambda}}_p = [E]^T \dot{\bar{\lambda}}_p$
TRANSFORM COMPONENTS OF STEERING VECTOR FROM LOCAL GUIDANCE FRAME TO PLATFORM FRAME
$T_o = T$
EXIT MAJOR CYCLE LOOP
ENTER MINOR CYCLE LOOP
$\Delta t = T - T_o$
$\bar{\lambda} = \hat{\lambda}_p + \dot{\bar{\lambda}}_p(\Delta t - K)$
INERTIAL STEERING ANGLE COMMANDS
$\theta_c = \tan^{-1}(\lambda_1/\lambda_3) - \pi/2$ (PITCH)
$\psi_c = \tan^{-1}[\lambda_2/(\lambda_1^2 + \lambda_3^2)^{\frac{1}{2}}]$ (YAW)
EXIT

2.1.7.4 INPUT-OUTPUT

The targeting program provides $\vec{U}_Q$, R, Y, $\dot{R}$, $\dot{Y}$, and $\dot{Z}$. The EOM program provides $\vec{R}_P$, $\vec{V}_P$ and $\vec{A}_T$. The gravity program provides $\vec{A}_{GRAV}$. The resulting quantities calculated by the model are θ_D, ψ_D, and ϕ_D. No flight software commands are accepted by this model. The EOM, Targeting, and Gravity programs must be present to provide inputs to the model.

2.1.7.5 COORDINATE SYSTEMS

The three systems used by this model are the Guidance, Platform, and Body systems. The center of the guidance system is at the earth center of mass. The R axis points from the center of the earth to the vehicle, the Y axis is perpendicular to the orbit plan pointing to the pilot's right, and the Z axis completes the right-handed triad. The body system is fixed with respect to the vehicle with the X axis forward through the main propellant tank centerline, the Z axis in the engine gimbal pivot plane and pointing down, and the Y axis points toward the pilot's right completing the right-handed triad. The platform system origin is at the earth's center of mass and is fixed in inertial space at the time of launch. The X axis is parallel to but opposite in sense to the launch pad gravity vector, the Z axis points downrange in the launch plane, and the Y axis points toward the pilot's right completing the right-handed triad.

$$[\theta] = \begin{bmatrix} \cos\theta & 0 & \sin\theta \\ 0 & 1 & 0 \\ -\sin\theta & 0 & \cos\theta \end{bmatrix}$$

$$[\psi] = \begin{bmatrix} \cos\psi & -\sin\psi & 0 \\ \sin\psi & \cos\psi & 0 \\ 0 & 0 & 1 \end{bmatrix}$$

$$[\phi] = \begin{bmatrix} 1 & 0 & 0 \\ 0 & \cos\phi & -\sin\phi \\ 0 & \sin\phi & \cos\phi \end{bmatrix}$$

$$\begin{bmatrix} X_P \\ Y_P \\ Z_P \end{bmatrix} = [\theta][\psi][\phi] \begin{bmatrix} X_B \\ Y_B \\ Z_B \end{bmatrix}$$

where X_P, Y_P, Z_P = platform coordinate vector

X_B, Y_B, Z_B = body coordinate vector

2.1.8 HINGE (HINGE MOMENT CALCULATION)

2.1.8.1 PROGRAM DESCRIPTION

This program returns the rudder hinge moment coefficient as a function of rudder deflection, angle of attack, sideslip angle, and Mach number. This is achieved by a table lookup for hinge moment coefficients due to sideslip (Ch_β) and hinge moment coefficient due to rudder deflection angle (Ch_{δ_R}), each as a function of angle of attack and Mach number. Tables of CH_β (M) and Ch_{δ_R} (M) for $\alpha = 0^\circ$, 5°, and 10° are used. If the angle of attack is greater than 10°, 10° is used for lookup; if angle of attack is less than 0°, 0° is used. A double linear interpolation is then used for CH_β and Ch_{δ_R} as a function of angle of attack and Mach number.

2.1.8.2 MATH MODEL

DATA / $Ch_\beta (M)_\alpha = 0$ /
DATA / $Ch_\beta (M)_\alpha = 5$ /
DATA / $Ch_\beta (M)_\alpha = 10$ /
DATA / $Ch_{\delta_R}(M)_\alpha = 0$ /
DATA / $Ch_{\delta_R}(M)_\alpha = 5$ /
DATA / $Ch_{\delta_R}(M)_\alpha = 10$ /
IF $\alpha > 10^\circ$ ------ $\alpha = 10^\circ$
IF $\alpha < 0^\circ$ ------ $\alpha = 0^\circ$
TABLE LOOPUP AND INTERPOLATION FOR,
$Ch_\beta = Ch_\beta (M, \alpha)$
$Ch_{\delta_R} = Ch_{\delta_R} (M, \alpha)$
$Ch = Ch_\beta * R_\beta + Ch_{\delta_R} * \delta_R$

2.1.8.3 INPUT/OUTPUT

Formal parameters in the call to HINGE are 1) rudder deflection angle (degrees), 2) angle of attack (degrees), 3) sideslip angle (degrees), 4) Mach number, 5) hinge moment coefficient to be returned, and 6) KDATA, a provision for using the routine for different aero surface coefficients, KDATA = 1 for rudder.

2.1.9 MASPRO (Mass Properties)

2.1.9.1 PROGRAM DESCRIPTION

This model provides the mass properties, which consist of center of gravity travel, moments of inertia as a function of weight and total mass calculation.

2.1.9.2 MATH MODEL

$$\dot{W} = \text{table lookup } F(H, P)$$

$$M = M - \dot{W}\,\Delta T/gc$$

$$\text{IF } M1 \geq M > M2,\ M = M - (M1 - M2)$$

$$W = Mg_c$$

$$CG_x = \text{table lookup } F(W)$$

$$CG_z = \text{table lookup } F(W)$$

$$I_{xx} = \text{table lookup } F(W)$$

$$I_{yy} = \text{table lookup } F(W)$$

$$I_{zz} = \text{table lookup } F(W)$$

$$I_{xz} = \text{table lookup } F(W)$$

Where:

W = total vehicle weight

M = total vehicle mass

$M1$ = mass prior to abort SRM jettison

$M2$ = mass after abort SRM jettison

$\dot{W}$ = weight flow rate

g_c = mass to weight conversion constant

ΔT = computational time increment

CG_X = X center of gravity location from vehicle reference

CG_Z = Z center of gravity location from vehicle reference

I_{XX} = Mass moment of inertia about X axis

I_{YY} = Mass moment of inertia about Y axis

I_{ZZ} = X - Z cross product of inertia

H = Altitude

P = Fractional throttle setting

2.1.9.3 INPUT/OUTPUT

Input g_c and initialize M and H from cards

Read $\dot{W}$, CG and Moments of Inertia from tables.

Output M, CG's and I's.

2.1.10 MAXMIN (Maximum and Minimum Values Printout)

2.1.10.1 PROGRAM DESCRIPTION

The MAXMIN program is used to printout the maximum and minimum values of several flight parameters at any time that it is scheduled. At any time that MAXMIN is called, the maximum-minimum values accumulated until that time is printed. The program may be called as often as desired.

2.1.10.2 MATH MODEL

In MAXMIN, all that is done is a series of WRITE statements. The actual saving of the desired maximum-minimum values and the times they occur is done in BLCONT. This is done in the form:

$$\text{If } X \geq |A| \text{ , } \begin{cases} A = X \cdot (F_k) \\ T = t \end{cases}$$

where X is the present value of the variable in question, A is the maximum value of the variable, T is the time that the maximum occurred, and t is present time. Although this is done in BLCONT, these values could be saved in any routine that is called every program cycle.

2.1.10.3 INPUT/OUTPUT

All of the variables which are output by MAXMIN are transferred from BLCONT in common blocks A_{MAX} and T_{MAX}. The following quantities are output:

q = dynamic pressure

α = angle-of-attack

β = sideslip angle

$q\text{-}\alpha$ = Q-Alpha

$q\text{-}\beta$ = Q-Beta

p = roll (inertial)

$\dot{p}$ = roll rate

δ_a = aileron deflection

$\dot{\delta}_a$ = aileron deflection rate

δ_r = rudder deflection

$\dot{\delta}_r$ = rudder deflection rate

δ_e = engine deflections

R_{HM} = rudder hinge moment

A_{HM} = aileron hinge moment

R_{HP} = rudder horsepower hours

F_k = Foonman's Constant (equals 1.0)

2.1.11 ORBITI (Orbit Parameters)

2.1.11.1 PROGRAM DESCRIPTION

This math model calculates the parameters of the trajectory achieved at insertion from knowledge of the state vector in polar equatorial coordinates at the time of orbiter engine shutdown. The program calculates node, inclination angle, orbit phase angle, eccentricity, orbit parameter, true anomaly, apogee altitude, and perigee altitude.

2.1.11.2 MATH MODEL

$$\eta = \text{Arctan}\left(\frac{-V_{YPE}\,R_{ZPE} + V_{ZPE}\,R_{YPE}}{-V_{XPE}\,R_{ZPE} + V_{ZPE}\,R_{XPE}}\right)$$

$$\zeta = \text{Arctan}\left(\frac{V_{ZPE}}{-V_{XPE}\sin\eta + V_{YPE}\cos\eta}\right)$$

$$\nu = \text{Arctan}\left(\frac{-V_{XPE}\cos\eta - V_{YPE}\sin\eta}{\cos\zeta(-V_{XPE}\sin\eta + V_{YPE}\cos\eta) + V_{ZPE}\sin\zeta}\right)$$

$$R = \sqrt{R_{XPE}^{2} + R_{TPE}^{2} + R_{ZPE}^{2}}$$

$$V = \sqrt{V_{XPE}^{2} + V_{YPE}^{2} + V_{ZPE}^{2}}$$

$$P = \frac{|R \times V|^2}{K}$$

$$SMA = \frac{K}{\frac{2K}{R} - V^2}$$

$$\varepsilon = \sqrt{1 - \frac{P}{SMA}}$$

$$FP = \frac{R \cdot V}{\sqrt{R^2V^2 - |R \cdot V|^2}}$$

$$TA = \text{Arctan} \frac{(P)(FP)}{P-R}$$

$$R_p = SMA\ (1-E) - R_r$$

$$R_a = 2 \cdot SMA - R_p - 2\ R_e$$

2.1.11.3 SYMBOL DEFINITIONS

V_{XPE}, V_{YPE}, V_{ZPE} = Velocity in polar-inertial coordinates

R_{XPE}, R_{YPE}, R_{ZPE} = Position in polar-inertial coordinates

η = Longitude of the ascending node

ζ = Inclination angle

ϵ = Eccentricity

K = Gravitational constant = 1.407654×10^{16} ft^3/sec^2

ν = Orbit phase angle (angle between equator and perigee)

P = Orbit parameter

SMA = Semi-major axis

FP = Tangent of flight path angle

TA = True anomaly

R_p = Altitude at perigee

R_a = Altitude at apogee

R_e = Mean radius of the earth

2.1.11.4 INPUT/OUTPUT

The ORBITI math model requires the vehicle state vector in platform equatorial coordinates as input. As output the model prints out ascending node, inclination angle, orbit phase angle, eccentricity, orbit parameter, true anomaly, apogee altitude, and perigee altitude.

2.1.12 ORBITR (3D EQUATIONS OF MOTION)

2.1.12.1 PROGRAM DESCRIPTION

This Math Model calculates vehicle acceleration from active guidance commands and integrates to get velocity and position in platform coordinates. Polar-Equatorial and Local Vertical coordinates systems are erected to calculate latitude, longitude, and flight path angle. Logic is included for acceleration limiting, integration cycle time rectification, and velocity cutoff.

2.1.12.2 MATH MODEL

$$Q_{PT} = \sum_{I=1}^{N} \frac{T_V}{M_V} (I)$$

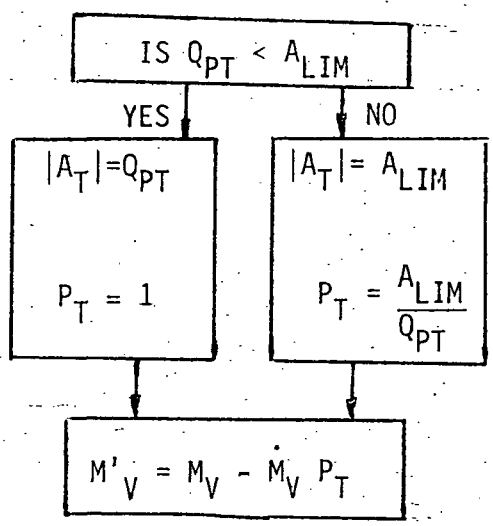

$$\vec{Q}_{AP} = \frac{\vec{A}_P}{|A_P|}$$

$$\vec{A}_{PT}' = Q_{PT} P_T \vec{Q}_{AP} + \vec{A}_{GRAV}$$

$$\vec{V}_P' = \int_t \vec{A}_{PT}\, dt + \vec{V}_P$$

$$\vec{R}_P' = \int_t \vec{V}_P\, dt + \vec{R}_P$$

$$\vec{R}_F = [\alpha]^T \vec{R}_P'$$

$$\lambda_V = \text{Arcsin}\left(\frac{R_F(3)}{|R_F|}\right)$$

$$\phi = \text{Arctan}\left(\frac{R_F(2)}{R_F(1)}\right) - \omega_e (t_L + t)$$

$$\vec{V}_{LV} = [\delta]^T [\alpha]^T \vec{V}'_P$$

$$\gamma = \text{Arcsin}\left(\frac{V_{LV}(1)}{|V_{LV}|}\right)$$

Integration Cycle Time Rectification

Acceleration limiting will most likely occur between integration time points. Therefore the integration for this interval must be done in two parts.

Velocity Cutoff

The program will be terminated either when $|V_P|$ exceeds $\dot{Z}$ or when M_V is less than M_{VO}, whichever occurs first.

2.1.12.3 SYMBOL DEFINITIONS

Q_{PT} = Thrust acceleration at full throttle

N = Number of engines

T_V = Maximum vacuum thrust of main engine

M'_V = Current vehicle mass

A_{LIM} = Maximum allowed vehicle acceleration

$|A_T|$ = Magnitude of acceleration due to thrust

P_T = Throttle setting

$\dot{M}_V$ = Total mass flow rate for all engines at full throttle

$\vec{A}_P$ = Acceleration command from guidance in platform coordinates

$\vec{Q}_{AP}$ = Unit vector acceleration command

$\vec{A}_{PT}'$ = Current total vehicle acceleration in platform coordinates

$\vec{A}_{GRAV}$ = Acceleration due to gravity in platform coordinates

$\vec{V}_P$ = Velocity of vehicle in platform coordinates on last pass

$\vec{V}_P'$ = Current vehicle velocity

$\vec{R}_P$ = Position of vehicle in platform coordinates on last pass

$\vec{R}_P'$ = Current vehicle position

$\vec{R}_F$ = Position of vehicle in polar equatorial coordinates

λ_L^* = Geodetic latitude of launch site

ϕ_L^* = Longitude of launch site

ω_e = Rotation rate of earth

T_L = Time of launch

t = Elasped time since launch

M_V = Mass of vehicle on last pass

A_L = Launch azimuth

λ_V = Present vehicle latitude

ϕ' = Temporary variable

$[\alpha]$ = Transformation from polar equatorial to platform coordinates

$[\delta]$ = Transformation from local vertical to polar equatorial coordinates

ϕ = Present vehicle longitude

γ = Flight path angle

$\vec{V}_{LV}$ = Velocity in local vertical coordinates

$\dot{Z}$ = Target velocity in guidance coordinates

M_{VO} = Mass of empty orbiter

2.1.12.4 INPUT/OUTPUT

The targeting program provides $\dot{Z}$. The Active Guidance program provides $\vec{A}_P$. The gravity program provides $\vec{A}_{GRAV}$. The resulting quantities calculated by this model are λ_V, ϕ, γ, V_P, R_P, A_{PT}, M_V, and $\vec{V}_{LV}$. Flight software commands accepted by this model are $\vec{A}_P$. The Active Guidance, Targeting, and Gravity programs must be present to provide inputs to the model.

The three systems used by this model are the Platform, Polar Equatorial, and Local Vertical systems. The platform system origin is at the earth's center of mass and is fixed in inertial space at the time of launch. The X axis is parallel to but opposite in sense to the launch pad gravity vector, the Z axis points downrange in the launch plane, and the Y axis points toward the pilot's right completing the right-handed triad. The polar equatorial system origin is at the earth's center of mass and is fixed in inertial space at the time of launch. The X axis is in the equatorial plane pointing toward a reference meridian, the Z axis points through the north pole, and the Y axis completes the right handed triad. The local vertical system origin is at the earth center of mass. The X axis points from the earth center to the vehicle, the Z axis is in the plane containing the earth's rotation axis and the X_{LV} axis. The Z axis is perperdicular to the X axis and points toward the north pole. The Y axis completes the right handed triad.

$$\vec{R}_P = [\alpha]\,\vec{R}_F$$

$$[\alpha] = \begin{bmatrix} a_{11} & a_{12} & a_{13} \\ a_{21} & a_{22} & a_{23} \\ a_{31} & a_{32} & a_{33} \end{bmatrix}$$

$$a_{11} = \cos \lambda_L^* \cos (\phi_L^* + \omega_e t_L)$$

$$a_{12} = \cos \lambda_L^* \sin (\phi_L^* + \omega_e t_L)$$

$$a_{13} = \sin \lambda_L^*$$

$$a_{21} = \sin A_L \sin \lambda_L^* \cos (\omega_e t_L + \phi_L^*) - \cos A_L \sin (\omega_e t_L + \phi_L)$$

$$a_{22} = \sin A_L \sin \lambda_L^* \sin (\omega_e t_L + \phi_L^*) - \cos A_L \cos (\omega_e t_L + \phi_L^*)$$

$$a_{23} = -\sin A_L \cos \lambda_L^*$$

$$a_{31} = -\cos A_L \sin \lambda_L^* \cos (\omega_e t_L + \phi_L^*) - \sin A_L \sin (\omega_e t_L + \phi_L^*)$$

$$a_{32} = -\cos A_L \sin \lambda_L^* \sin (\omega_e t_L + \phi_L^*) + \sin A_L \cos (\omega_e t_L + \phi_L^*)$$

$$a_{33} = \cos A_L \cos \lambda_L^*$$

$$\vec{R}_F = [\delta] \vec{R}_{LV}$$

$$[\delta] = \begin{bmatrix} d_{11} & d_{12} & d_{13} \\ d_{21} & d_{22} & d_{23} \\ d_{31} & d_{32} & d_{33} \end{bmatrix}$$

$$\sin \lambda_V = R_F(3) / |R_F|$$

$$\cos \lambda_V = \sqrt{1 - \sin^2 \lambda_V}$$

$$\sin \phi' = R_F(2) / (|R_F| \cos \lambda_V)$$

$$\cos \phi' = R_F(1) / (|R_F| \cos \lambda_V)$$

$$d_{11} = \cos \lambda_V \cos \phi'$$

$$d_{12} = -\sin \phi'$$

$$d_{13} = -\sin \lambda_V \cos \phi'$$

$$d_{21} = \cos \lambda_V \sin \phi'$$

$d_{22} = \cos \phi'$

$d_{23} = -\sin \lambda_V \sin \phi'$

$d_{31} = \sin \lambda_V$

$d_{32} = 0$

$d_{33} = \cos \lambda_V$

2.1.13 ORBTAR (Boost Orbit Insertion Targeting Model)

2.1.13.1 PROGRAM DESCRIPTION

The Targeting program is used in the flight software to describe the orbit plane with respect to the launch pad. Position, velocity, and a unit vector normal to the orbit plane at perigee are calculated from a knowledge of perigee and apogee altitudes, location of the launch pad, orbit inclination, and an orbit parameter.

2.1.13.2 MATH MODEL

$$R_P = R_e + h_P$$

$$R_A = R_e + h_A$$

$$A = \frac{R_P + R_A}{2}$$

$$R = R_P$$

$$Y = 0$$

$$Z = \text{unconstrained}$$

$$\dot{R} = 0$$

$$\dot{Y} = 0$$

$$\dot{Z} = \sqrt{\mu \left(\frac{2}{R_P} - \frac{1}{A}\right)}$$

$$S_G = \sin(\lambda)\cos(\beta) + \cos(A_Z)\cos(\lambda)\sin(\beta)$$

$$C_L = \sin(A_Z)\cos(\lambda)$$

$$C_G = \sqrt{1 - S_G^2}$$

$$C_P = \frac{C_L}{C_G}$$

$$\alpha = \cos(\gamma)/C_G$$

$$\Delta = \text{Arcsin}(C_P) - \text{Arcsin}(\alpha)$$

$$U_Q(1) = -\sin(\beta)\sin(\Delta)$$

$$U_Q(2) = \cos(\Delta)$$

$$U_Q(3) = \cos(\beta)\sin(\Delta)$$

Where :

R_P = distance from earth center of mass to periapsis

R_A = distance from earth center of mass to apoapsis

h_P = altitude at periapsis

h_A = altitude at apoapsis

A = semi-major axis

ϵ = eccentricity

R_e = radius of earth

R = radial distance at insertion

Y = cross-range distance at insertion

Z = downrange distance at insertion

$\dot{R}$ = radial rate at insertion

$\dot{Y}$ = lateral velocity at insertion

$\dot{Z}$ = downrange velocity at insertion

S_G, C_L, C_G, C_P, α, Δ = temporary variables

λ = latitude of launch pad

μ = universal gravitational constant

β = orbit parameter

A_Z = launch azimuth

γ = orbit inclination angle

$\vec{U}_Q$ = unit vector normal to desired orbit plane in platform coordinates (see Section IV)

2.1.13.3 INPUT/OUTPUT

This model requires R_e, h_p, h_a, λ , β, A_Z, and γ as input and calculates R, Y, Z, $\dot{R}$, $\dot{Y}$, $\dot{Z}$, and $\vec{U}_Q$. The model needs to be called only once per simulation.

2.1.13.4 COORDINATE SYSTEMS

This model calculates a unit vector in platform coordinates. The platform system origin is at the earth's center of mass and is fixed in inertial space at the time of launch. The X axis is parallel but opposite in sense to the launch pad gravity vector, the Z-axis points downrange in the launch plane and the Y axis points toward the pilot's right completing the right-handed triad.

2.1.14 RCS (Reaction Control System)

2.1.14.1 PROGRAM DESCRIPTION

This program calculates the moments and linear accelerations applied to the vehicle due to RCS thrust commands from the flight software.

2.1.14.2 MATH MODEL

Thrust commands are conditioned according to the following limitations:

(1) A jet cannot be commanded to ignite unless the duration of ignition is some minimum value

(2) No jet can be ignited continuously longer than T_B seconds

(3) A jet cannot be commanded to ignite unless T_A seconds has elapsed since the previous ignition has ceased.

Figure 2-1 shows a logic diagram which can be used to implement these limitations.

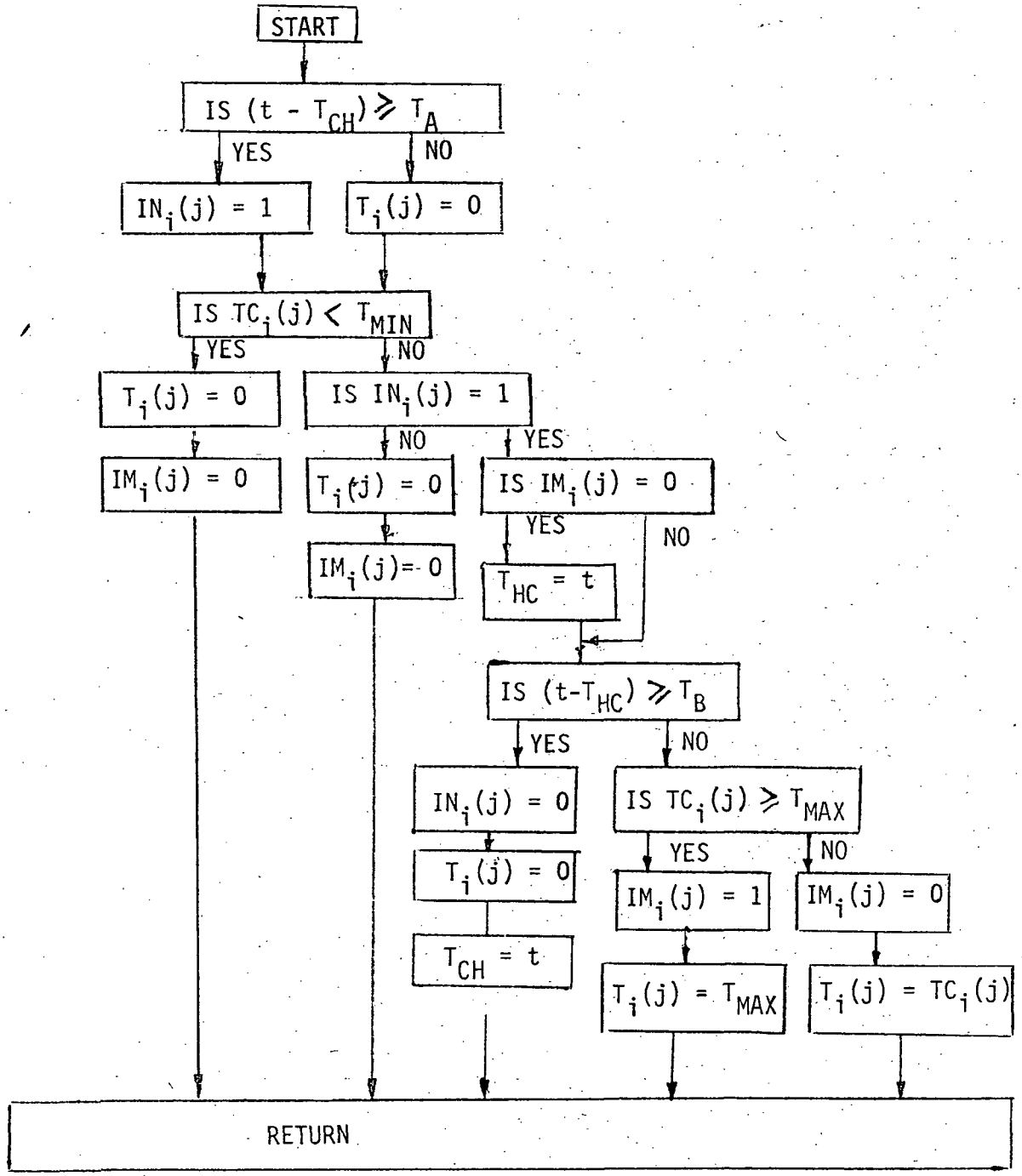

RCS LOGIC DIAGRAM

FIGURE 2-1

i = engine index

j = 1, 2, or 3 for x, y, or z respectively

T_{MAX} = thrust achieved with continuous ignition

T_{MIN} = average thrust for a computation cycle for minimum thrust duration

$TC_i(j)$ = commanded thrust

$T_i(j)$ = realized thrust

$IM_i(j)$ = indicator for continuous thrust for the previous pass (set equal to zero for restart)

$IN_i(j)$ = thrust enable flag (set equal to zero for restart)

T_{CH} = check time for T_A

T_{HC} = check time for T_B

t = current time at entry to RCS program

$$\vec{M}_i = \vec{P}_i \times \vec{T}_i \tag{1}$$

$$\begin{aligned} P_i(1) &= ELX_i - XCG \\ P_i(2) &= ELY_i - YCG \\ P_i(3) &= ELZ_i = ZCG \end{aligned} \tag{2}$$

$\vec{P}_i$ = engine position vector for the i^{th} jet; ELX_i, ELY_i, ELZ_i = X, Y, and Z locations, respectively, of the i^{th} RCS jet cluster; XCG, YCG, ZCG = X, Y, and Z locations, respectively of the vehicle center of mass

i = engine index

$\vec{M}_i$ = moment vector due to thrust from the i^{th} jet

$\vec{T}_i$ = thrust vector for the i^{th} jet

X = indicates vector cross product

$$\vec{MR} = \sum_{i=1}^{N} \vec{M}_i \qquad (3)$$

$\vec{MR}$ = total effective moment from all RCS jets

N = number of RCS jets

$$\vec{F} = \sum_{i=1}^{N} \vec{T}_i \qquad (4)$$

F = total effective linear force

$$A = R_j \sum_{j=1}^{3} \sum_{i=1}^{N} \left| T_i(j) \right|$$

A = reduction in mass of vehicle due to RCS fuel usage

R = RCS jet efficiency constant

2.1.14.3 INPUT/OUTPUT

The model requires ELX, ELY, ELZ, XCG, YCG, ZCG, $\vec{T}_c$, t, and M as input. The flight software command accepted is $\vec{T}_c$. The cross product, mass properties, and EOM subroutines must be present. The model provides $\vec{MR}$, A, and $\vec{F}$ as output.

2.1.14.4 COORDINATE SYSTEMS

The body coordinate system is used in this model. The RCS thrust axes are parallel to the body axes. Its X axis points toward the nose through the main propellant tank centerline, the Z axis points down in the engine gimbal pivot plane, and the Y axis points toward the pilot's right.

2.1.15 THRUST (Thrust Model)

2.1.15.1 PROGRAM DESCRIPTION

The inputs to the model are ambient atmospheric pressure, throttle setting, and engine gimbal angles and the outputs are forces and moments due to thrust from all engines in body coordinates.

2.1.15.2 MATH MODEL

$$ET_i = PT_i(T_{SLi} + A_i\ (PA-P)) \tag{1}$$

where:

ET_i = engine thrust

P_{Ti} = throttle setting

T_{SLi} = sea level thrust

A_i = engine area

PA = sea level atmospheric pressure

P = ambient atmospheric pressure

i = engine index, maximum value = 12

$$\begin{bmatrix} TBX_i \\ TBY_i \\ TBZ_i \end{bmatrix} = \begin{bmatrix} \cos\theta_P & 0 & -\sin\theta_P \\ 0 & 1 & 0 \\ -\sin\theta_P & 0 & \cos\theta_P \end{bmatrix} \begin{bmatrix} \cos\theta_Y & -\sin\theta_Y & 0 \\ -\sin\theta_Y & \cos\theta_Y & 0 \\ 0 & 0 & 1 \end{bmatrix} \begin{bmatrix} ET_i \\ 0 \\ 0 \end{bmatrix} \tag{2}$$

or:

$$\begin{aligned} T_{BXi} &= ET_i \cos\theta_P \cos\theta_Y \\ T_{BYi} &= -ET_i \sin\theta_Y \\ T_{BZi} &= -ET_i \sin\theta_P \cos\theta_Y \end{aligned} \tag{3}$$

$$F_{TBX} = \Sigma T_{BXi}$$
$$F_{TBY} = \Sigma T_{BYi} \qquad (4)$$
$$F_{TBZ} = \Sigma T_{BZi}$$

where

T_{BXi}, T_{BYi}, T_{BZi} = X, Y, and Z components, respectively, of forces due to engine thrust for engine number i

θY = yaw engine gimbal angle

θP = pitch engine gimbal angle

F_{TBX}, F_{TBY}, F_{TBZ} = X, Y, and Z components, respectively, of total thrust forces in body coordinates.

$$MTXB_i = TBZ_i\ (ELY_i - YCG) - TBY_i\ (ELZ_i - ZCG)$$
$$MTYB_i = TBX_i\ (ELZ_i - ZCG) - TBZ_i\ (ELX_i - XCG) \qquad (5)$$
$$MTZB_i = TBY_i\ (ELX_i - XCG) - TBX_i\ (ELY_i - YCG)$$

$MTXB_i$, $MTYB_i$, $MTZB_i$ = X, Y, and Z components, respectively, of moments due to engine number i. ELX_i, ELY_i, ELZ_i = X, Y, and Z components, respectively, of engine locations in body coordinates. XCG, YCG, ZCG = X, Y, and Z components of location of center of mass of the vehicle.

$$MTB(1) = \Sigma MTXB_i$$
$$MTB(2) = \Sigma MTYB_i \qquad (6)$$
$$MTB(3) = \Sigma MTZB_i$$

MTB(1), MTB(2), MTB(3) are X, Y, and Z components, respectively, of total moments due to engine thrust.

All of the models described in equations (1) through (6) are in body coordinates. Body coordinates are fixed with respect to the vehicle. The X axis normally points forward along the main propellant tank centerline, the Z axis points down in a plane containing the engine gimbal pivots, and the Y axis points toward the pilot's right forming a right-handed triad.

2.1.15.3 INPUT/OUTPUT

The parameters which must be supplied to the model as input are ELX_i, ELY_i, ELZ_i, PT_i, T_{SLi}, P, θ_P, θ_Y, XCG, YCG, and ZCG. The resulting quantities calculated by the model are FTB and MTB. The flight software command accepted by the model is PT_i. The model has no calling arguments and calls no subroutine while operating. The Maspro, Aero, Autopilot, and Initialization subroutines provide the model inputs and the EOM accepts the model outputs.

2.1.16 TSHAPE (Trajectory Shaping)

2.1.16.1 PROGRAM DESCRIPTION

The trajectory and control parameters which must be calculated to accomplish trajectory shaping are α_D, desired angle-of-attack; θ_C, desired pitch attitude angle; δ_D, desired engine deflection angle; and $\ddot{Z}_{DCG}$, desired body sensed acceleration. The values of θ_C, δ_D, and $\ddot{Z}_{DCG}$ are dependent on α_D. The boost flight is divided into three phases: vertical rise, tilt maneuver, and alpha policy. For each of these flight phases, α_D is calculated differently.

2.1.16.2 MATH MODEL

2.1.16.2.1 GENERAL CALCULATIONS

$$C_{Z^{\alpha_r}} = C_{Z^{\alpha}} \cdot \frac{\pi}{180}$$

$$N_o = q\ S\ C_{ZO}$$

$$N'_P = q\ S\ C_{Z^{\alpha_r}}$$

$$l_O = \bar{c}\ (C_{mo}/C_{zo}) + X_{CG} - X_R$$

$$l_{1P} = \bar{c}\ (C_{m^{\alpha}}/C_{z^{\alpha}}) + X_{CG} - X_R$$

$$D_Z = F_{ax}\ Z_{CG}$$

$$X_{lg} = X_{CG} - X_o$$

$$Z_{lg} = Z_{CG} - Z_o$$

$$L_o = (X_{lg}^{\ 2} + Z_{lg}^{\ 2})^{\frac{1}{2}}$$

$$L_B = \left[(X_B - X_{CG})^2 + (Z_B - Z_{CG})^2\right]^{1/2}$$

$$\delta_{CGB} = -\tan\left[\frac{Z_{CG} - Z_B}{X_{CG} - X_B}\right]$$

$$\delta_{CGO} = \tan\left[\frac{-Z_{1g}}{X_{1g}}\right]$$

2.1.16.2.2 ANGLE-OF-ATTACK CALCULATIONS

2.1.16.2.2.1 VERTICAL RISE

$$\delta_D = \delta_{CGO} - L_B F_B \left(\frac{\delta_B - \delta_{CGB}}{L_O F_O}\right)$$

$$\alpha_D = \tan^{-1}\left[\frac{F_O \cos \delta_D = F_B \cos \delta_B}{-F_O \sin \delta_D - F_B \sin \delta_B}\right]$$

$$\theta_C = \alpha_D$$

2.1.16.2.2.2 TILT MANEUVER (Parking Lot Tilt)

The maneuver modeled here is a modification of the tilt maneuver presented in the previous memo. Here, α_m is used as the value of angle-of-attack at a time half-way between the time to begin and end the tilt maneuver, T_T and T_D. Therefore, this procedure can fit any part of a parabola to the three points, depending on the value of α_m, and its relation to α_0 and α_D. This is illustrated in Figure 2-2.

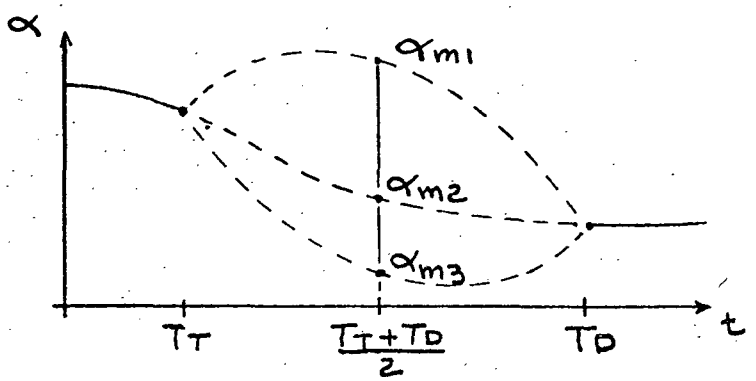

FIGURE 2-2

where α_{m1}, α_{m2}, and α_{m3} are three examples of values for α_m which cause a different shape curve to be fitted. The calculation for α_D during this maneuver is as follows:

$$\alpha_0 = \tan\left[\frac{V_{BZ}}{V_{BX}}\right], \text{ calculated only at } t = T_T$$

$$T_{OP} = \frac{T_T + T_D}{2}$$

$$A_1 = \frac{\alpha_D - \alpha_0}{2}$$

$$A_2 = \frac{(\alpha_D - \alpha_m) + (\alpha_D - \alpha_m)}{2}$$

$$Z = \frac{T - T_{OP}}{\frac{1}{2}(T_D - T_T)}$$

$$\alpha_D = \alpha_m + A_1 Z + A_2 Z^2$$

2.1.16.2.2.3 ALPHA POLICY

During this portion of flight a choice of several criterion for calculation of angle-of-attack can be made.

2.1.16.2.2.3.1 ZERO LIFT

$$\alpha_D = \frac{-C_{Z0}}{C_{Z\alpha}}$$

2.1.16.2.2.3.2 ZERO ANGLE-OF-ATTACK

$$\alpha_D = 0.$$

2.1.16.2.2.3.3 GRAVITY TURN

For this criterion, gravity turn is defined as no acceleration normal to flight path.

$$C_{2B} = \frac{L_B F_B}{I_{yy}} \sin(\delta_B - \delta_{CGB})$$

$$K_{3B} = \frac{F_B}{m} \sin \delta_B$$

$$C_{1P} = \frac{-l_{1P} N'_P}{I_{yy}}$$

$$C_{2P} = (X_{lg}^2 + Z_{lg}^2)^{\frac{1}{2}} \frac{F_0}{I_{yy}}$$

$$K_2 = \frac{-N'_P + F_T}{m}$$

$$K_3 = \frac{F_0}{m}$$

$$\ddot{\theta}_o = \frac{l_o N_o - F_{ax} (Z_{CG} - Z_R)}{I_{yy}}$$

$$\ddot{Z}_o = N_o/m$$

$$B_1 = C_{2P} \delta_{CGO} + \ddot{\theta} - C_{2B}$$

$$B_2 = \ddot{Z}_o - K_{3B}$$

$$\alpha_D = \frac{B_1 K_3 - B_2 C_{2P}}{C_{1P} K_3 - C_{2P} K_2}$$

2.1.16.2.2.3.4 AERODYNAMIC MOMENT CONTROL

$$\alpha_D = \frac{-l_o N_o + D_z}{l_{1P} N'_P}$$

2.1.16.2.3 REMAINING SHAPING AND CONTROL PARAMETERS

The following parameters are calculated after a value for α_D has been determined by some specified alpha policy.

$$\theta_R = \tan^{-1}\left[\frac{V_{RZ}}{V_{RX}}\right]$$

$$\theta c = \alpha_D - \theta_R$$

$$\ddot{\theta}_o = \frac{l_o N_o - F_{ax}\,(Z_{CG} - Z_R)}{I_{yy}}$$

$$C_{1P} = \frac{-l_{1P}\,N'_P}{I_{yy}}$$

$$\delta_D = \frac{(\ddot{\theta}_o - C_{1P}\,\alpha_D)\,I_{yy}}{L_o F_o} + \delta_{CGO}\,\frac{-L_B F_B(\delta_B - \delta_{CGB})}{L_o F_o}$$

$$\ddot{Z}_{DCG} = \frac{1}{m}\left[N_o + N'_P\,\alpha_D - F_o \sin\delta_D - F_B \sin\delta_B\right]$$

2.1.16.3 DEFINITION OF SYMBOLS

Variable	Definition
A_1, A_2	Temp. variables
B_1, B_2	Temp. variables
C_{1P}, C_{2P}, C_{2B}	Temp. variables
$\bar{c}$	Mean aerodynanic cord
C_{mo}, C_m	Aero. moment coefficients
C_{ZO}, $C_{Z\alpha}$	Aero. normal force coefficients (pitch)

Variable	Definition
D_Z	Drag moment due to CG offset
F_T	Total force acting on vehicle
F_{ax}	Aeoo. axial force
I	Moments of inertia
K_2, K_3, K_{3B}	Temp. variables
L_O, L_B	Moment arms from CG to orbiter and booster engines
m	Mass
N_o	Normal force at zero angle-of-attack
N'_P	Partial of normal
q	Dynamic pressure
S	Aerodynamic reference area
T	Present time
T_D	Time to end tilt maneuver (begin alpha policy)
T_{OP}	Mid point between T_D and T_T
T_T	Time to begin tilt maneuver (end vertical rise)
V_{BX}, V_{BZ}	Velocity components in body coordinates
V_{RX}, V_{RZ}	Inertial components of velocity relative to air
X_{CG}, Y_{CG}, Z_{CG}	Location of center of gravity
X_{lg}, Z_{lg}	Moment arm from CG to orbiter engines
X_o, Z_o	Average orbiter engine location
X_R, Z_R	Location of aerodynamic reference
X_a	Location of body fixed accelerometer
Z	Temp. variable
$\ddot{Z}_{DCG}$	Desired body sensed acceleration

Variable	Definition
α_D	Desired angle-of-attack
α_m	Value of angle-of-attack at T_{OP}
α_o	Angle-of-attack at T_T
δ_{CGB}, δ_{CGO}	Deflection for thrust through center of gravity at booster and orbiter engines
δ_D	Desired orbiter engine deflection angle
θ_c	Commanded pitch angle
$\ddot{\theta}_o$	Acceleration at zero angle-of-attack

2.1.16.4 INPUT-OUTPUT

The inputs necessary for TSHAPE are the aerodynamic constants, configuration constants, I, m, CG's, T, T_D, T_T, V_B, V_R, and α_m. The outputs of this program are α_D, θ_C, δ_D, $\ddot{Z}_{DG}$, δ_{CGB}, and δ_{CGO}.

2.1.17 TVC (Thrust Vector Control)

2.1.17.1 PROGRAM DESCRIPTION

This model describes the motions of massless engines with limits on deflection, deflection rate, and acceleration.

2.1.17.2 MATH MODEL

a. $\delta_{NEW} = \delta$ command

b. $\dot{\delta} = (\delta_{NEW} - \delta_{OLD}) / \Delta time$

c. Test and limit $\dot{\delta}$ to obtain $\dot{\delta}_{NEW}$

d. $\ddot{\delta} = (\dot{\delta}_{NEW} - \dot{\delta}_{OLD}) / \Delta time$

e. Test and limit $\ddot{\delta}$ to obtain $\ddot{\delta}_{NEW}$

f. $\dot{\delta}_{NEW} = \dot{\delta}_{OLD} + \ddot{\delta}_{NEW} \times \Delta time$

g. $\delta_{NEW} = \delta_{OLD} + \dot{\delta}_{NEW} \times \Delta time$

δ_{NEW} = Present engine deflection

δ_{OLD} = Previous engine deflection

$\dot{\delta}$ = Engine deflection rate

$\ddot{\delta}$ = Engine deflection acceleration

NOTE: δ_{OLD}, $\dot{\delta}_{OLD}$ are only reset at the end of a computation cycle

III. INPUT/OUTPUT

Inputs: Pitch and yaw deflection commands from the flight control system (for each engine), deflection rate, and acceleration limits.

Outputs: δ_{NEW}, $\dot{\delta}$, $\ddot{\delta}$

2.1.18 INITIAL POSITION MATH MODEL

2.1.18.1 PROGRAM DESCRIPTION

This program calculates the difference between geodetic and geocentric latitude and uses it to calculate the initial state vector. This calculation needs to be done once each time either the launch azimuth or latitude is changed.

2.1.18.2 MATH MODEL

$$\psi_L = \text{Arctan}\left[(1-f)^2 \tan \phi_L\right]$$

$$R_L = \frac{R_e\,(1-f)}{\sqrt{1-f\,(2-f)\cos^2 \psi_L}} + ho$$

$$\beta = \phi_L - \psi_L$$

$$R_X = R_L \cos \beta$$

$$R_Y = R_L \sin \beta \sin A_Z$$

$$R_Z = -R_L \sin \beta \cos A_Z$$

$$V_X = 0$$

$$V_Y = \omega R_L \cos A_Z \cos \psi_L$$

$$V_Z = \omega R_L \sin A_Z \cos \psi_L$$

Where:

ω = rotation rate of earth

ϕ_L = launch geodetic latitude

f = earth flattening constant

R_e = earth equatorial radius

A_Z = launch azimuth

ψ_L = launch geocentric latitude

R_L = magnitude of initial position vector

β = difference between geodetic & geocentric latitude

R_X, R_Y, R_Z = initial position vector in platform coordinate

V_X, V_Y, V_Z = initial velocity vector in platform coordinate

ho = altitude of vehicle CG above Fischer ellipse

2.1.18.3 INPUT/OUTPUT

The constants needed by this model are ω, ϕ_L, f, R_e, and A_Z. The output of the program is R_X, R_Y, R_Z, V_X, V_Y, and V_Z.

2.1.18.4 COORDINATE SYSTEM

Platform System - an orthogonal system with its origin at the center of the earth, X axis parallel to the launch site gravity vector and positive in the direction opposite to gravitational acceleration. The Z axis lies in the launch plane and points downrange and the Y axis completes the right handed triad.

2.2 Rigid Body Boost Simulation (RIBBS)

Between the time of the initial model development and when the SSFS first stage boost simulation became operational, boost dynamics and control analyses were performed using RIBBS. In the course of these analyses a number of improvements and modifications were incorporated into the RIBBS simulation. These improvements were subsequently incorporated in SSFS. Some of the improvements were trajectory shaping, control gain calculation and state vector calculation subroutines.

RIBBS was used extensively for analysis of the LOX-propane configuration which used liquid injection thrust vector control. For this study the thrust vector control scheme in RIBBS was revised to take out engine gimbals and add thrust vectoring by use of propane injection. The multi-stage guidance system described in Reference 15 was also initially originated and checked out in the RIBBS program. RIBBS was also modified to provide plotting and printout capabilities in case of any type of termination during a trajectory run, by means of a subroutine called RESTART.

2.3 POINT TIME STABILITY ANALYSIS USING MDELTA

The Boeing developed MDELTA program was used to perform point time stability analysis of pitch and lateral directional vehicle axes. The MDELTA program was modified to output Bode (magnitude and phase vs. frequency) plots and Nichols (magnitude vs. phase) plots. These plots are extremely helpful for quick analysis in determining stability characteristics of a system.

2.3.1 PITCH PLANE DYNAMICS

A derivation and discussion of the pitch axis dynamic model is found in Reference 16. Fig. 2- 3 shows the control diagram for the pitch axis, and the equations-of-motion are shown below.

$$\ddot{\theta} = C_{m^\alpha}\,\bar{c} + (X_{CG} - X_R)\,C_{Z^\alpha}\,\frac{\dot{Z}_q S}{I_y V} - \frac{F}{I_y}\,(X_{CG} - X_E)\,\delta_E$$

$$\ddot{Z} = \frac{q_s\,C_{Z^\alpha}}{m\,V}\,\dot{Z} + V\dot{\theta} - \frac{F}{m}\,\delta_E + (g \sin \theta_o)\,\theta$$

A test case analysis of pitch plane dynamics was run using data from the Shuttle Delta-Delta configuration. These values are shown in Table 2-1. For the three time points selected (0, 80, and 200 sec.). The resulting Bode and Nichols plots are shown in Figures 2-4 through 2- 9

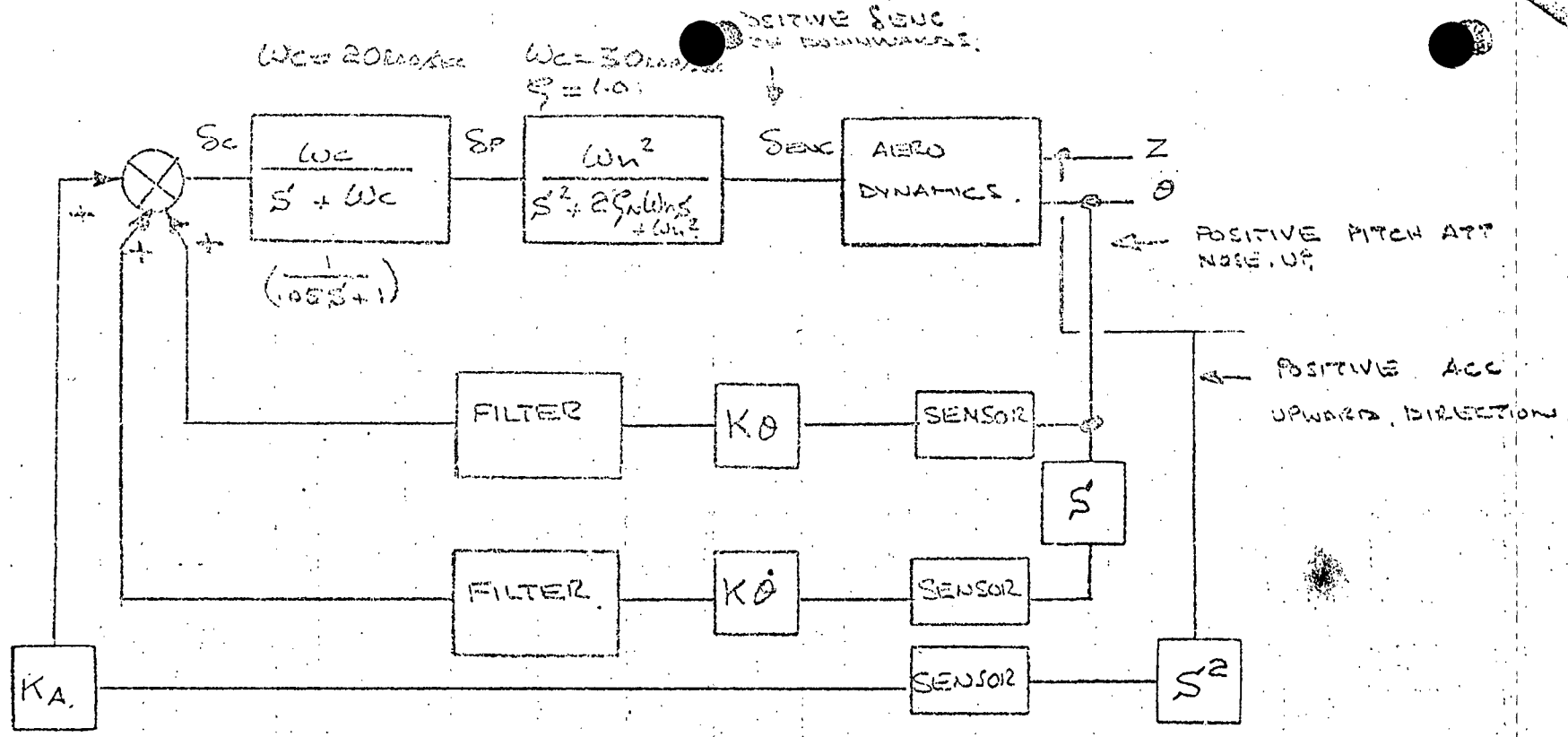

$$\frac{\delta P}{\delta c} = \frac{\omega_c}{s + \omega_c} \quad \therefore \quad \delta P(s + \omega_c) = \omega_c \delta c \quad \therefore \quad \delta P(s + \omega_c) - \omega_c \delta c = 0. \quad \text{—— (1)}$$

$$\frac{\delta_{ENC}}{\delta P} = \frac{\omega_n^2}{s^2 + 2\xi_n \omega_n s + \omega_n^2} \qquad \delta_{ENC}(s^2 + 2\xi_n \omega_n s + \omega_n^2) - \omega_n^2 \delta P = 0. \quad \text{—— (2)}$$

$$\delta c = + (K\theta + K\dot{\theta} s)\theta + K_A(A_s) \qquad \delta c - (K\theta + K\dot{\theta}.s)\theta - (K_A s^2)z \quad \text{—— (3)}$$

$\hookrightarrow z s^2$

FIGURE 2-3 RIGID BODY PITCH PLANE MODEL

TABLE 2-1

VARIABLE	MDELTA NAME	0 SEC.	80 SEC.	200 SEC.
X_{CG}	XCG	144.73	129.94	103.54
X_R	XR	235.	235.	235.
$C_{z\alpha}$	CZA	-.062	-.0548	-.0221
$C_{m\alpha}$	CMA	-.1149	-.1125	-.04283
$\bar{c}$	CBAR	74.	74.	74.
q	QUE	0.	579.18	9.71
s	AREA	8308.	8303.	8308.
I_y	IY	482136000.	439268000.	309800000.
U	V	0.	1470.735	10099.187
F	F	6480000.	6996500.	2315700.
X_E	XE	0.	0.	0.
m	MASS	149948.1	109467.5	53119.9
G	G	32.2118	32.0787	31.5253
θ_o	THETO	-.0354	-.70404	-1.679966
K_θ	KTHET	.5	.2	.4973
$K_\theta^\bullet$	KTDOT	.7	.7612	.6972
K_A	KA	0.	.007	0.
ζ_n	SIGN	1.	1.	1.
ω_n	WN	30.	30.	30.
ω_c	WC	20.	20.	20.

PITCH PLANE DYNAMICS DATA

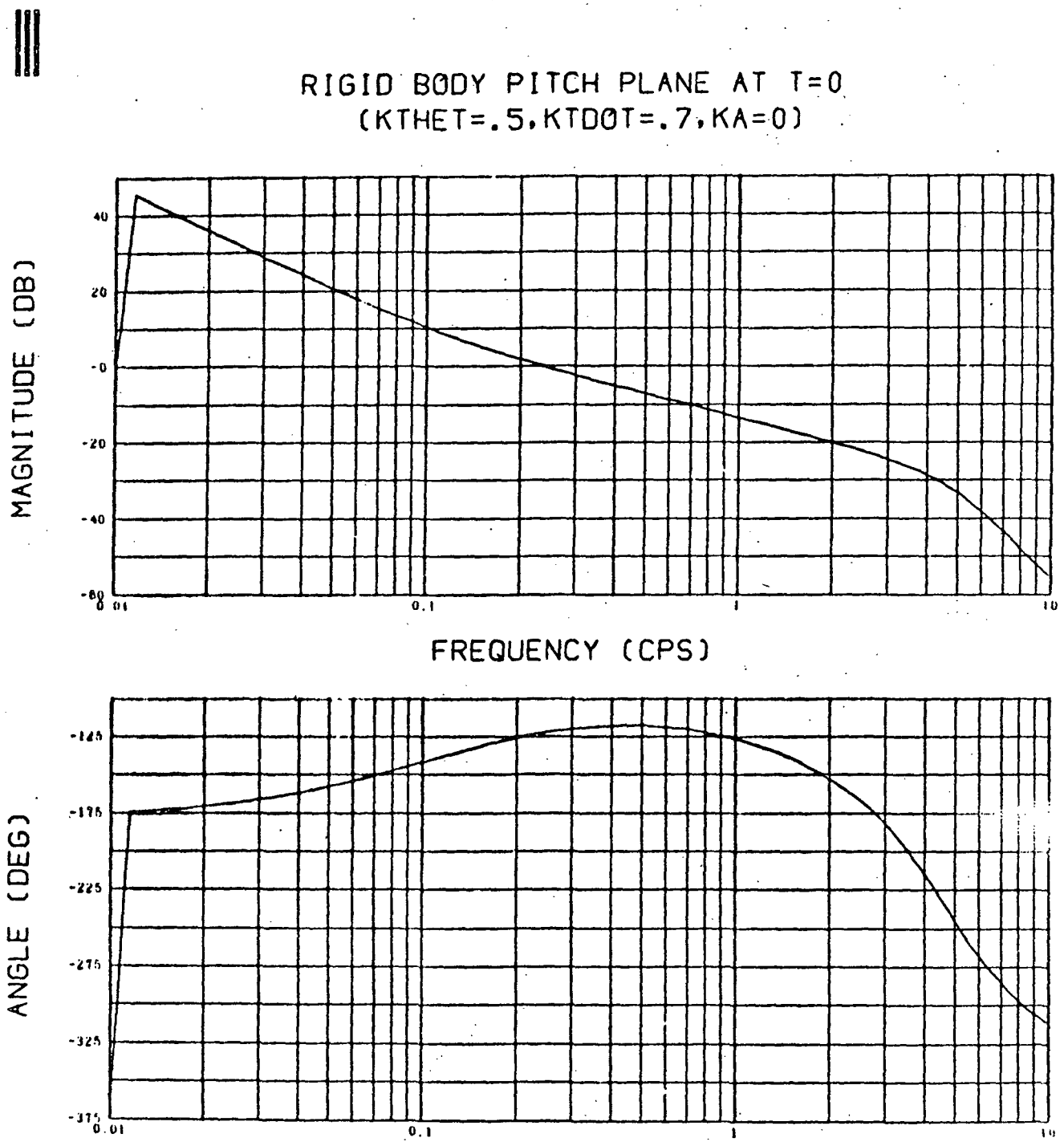
RIGID BODY PITCH PLANE AT T=0
(KTHET=.5,KTDOT=.7,KA=0)
MAGNITUDE (DB)
40
20
-0
-20
-40
-60
0.01
0.1
1
10
FREQUENCY (CPS)
ANGLE (DEG)
-125
-175
-225
-275
-325
-375
0.01
0.1
1
10

FIGURE 2-4

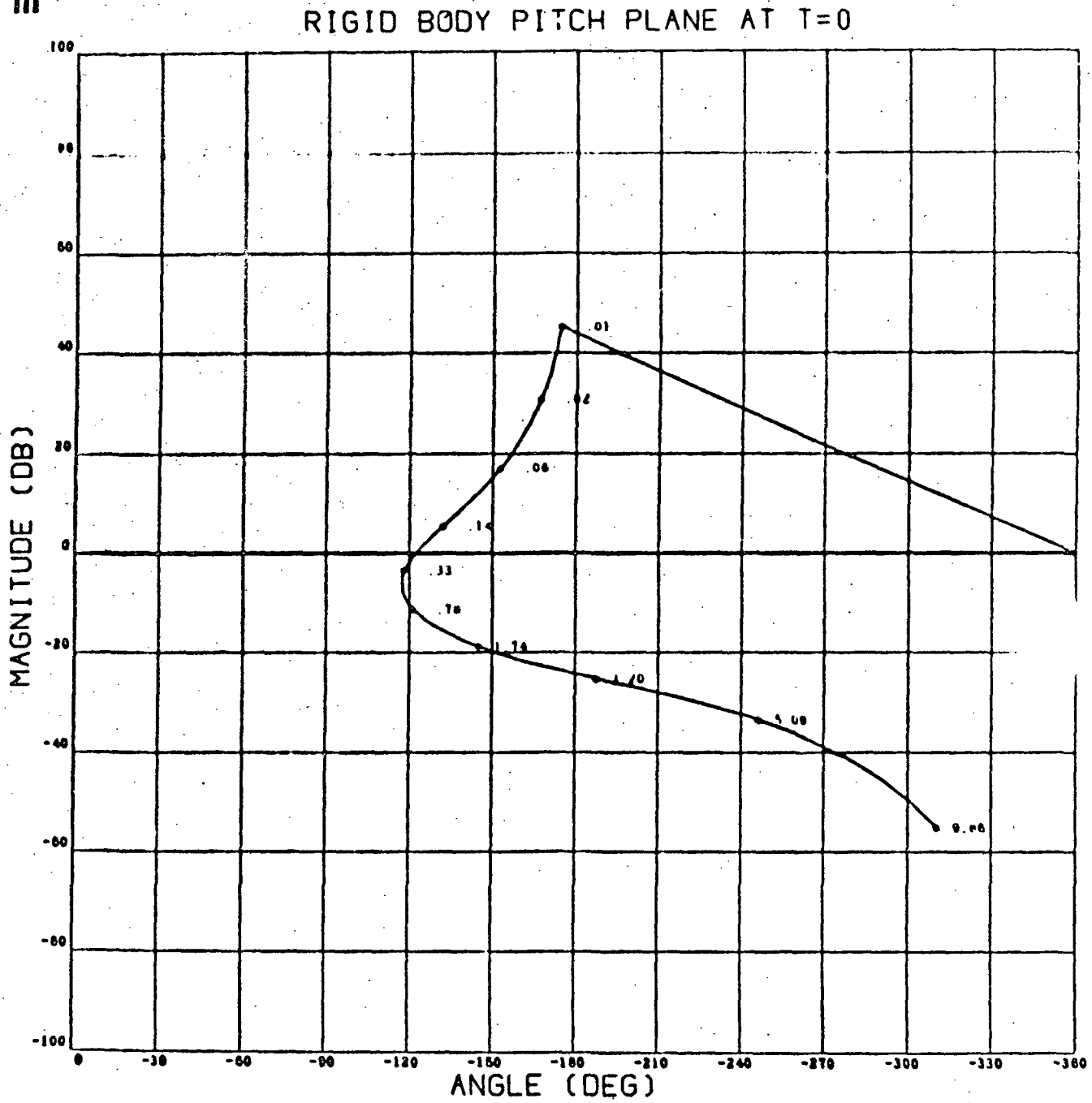
RIGID BODY PITCH PLANE AT T=0
MAGNITUDE (DB)
ANGLE (DEG)
100
80
60
40
20
0
-20
-40
-60
-80
-100
0
-30
-60
-90
-120
-150
-180
-210
-240
-270
-300
-330
-360
.01
.02
.06
.14
.33
.78
1.84
4.30
10.00
23.46

FIGURE 2-5

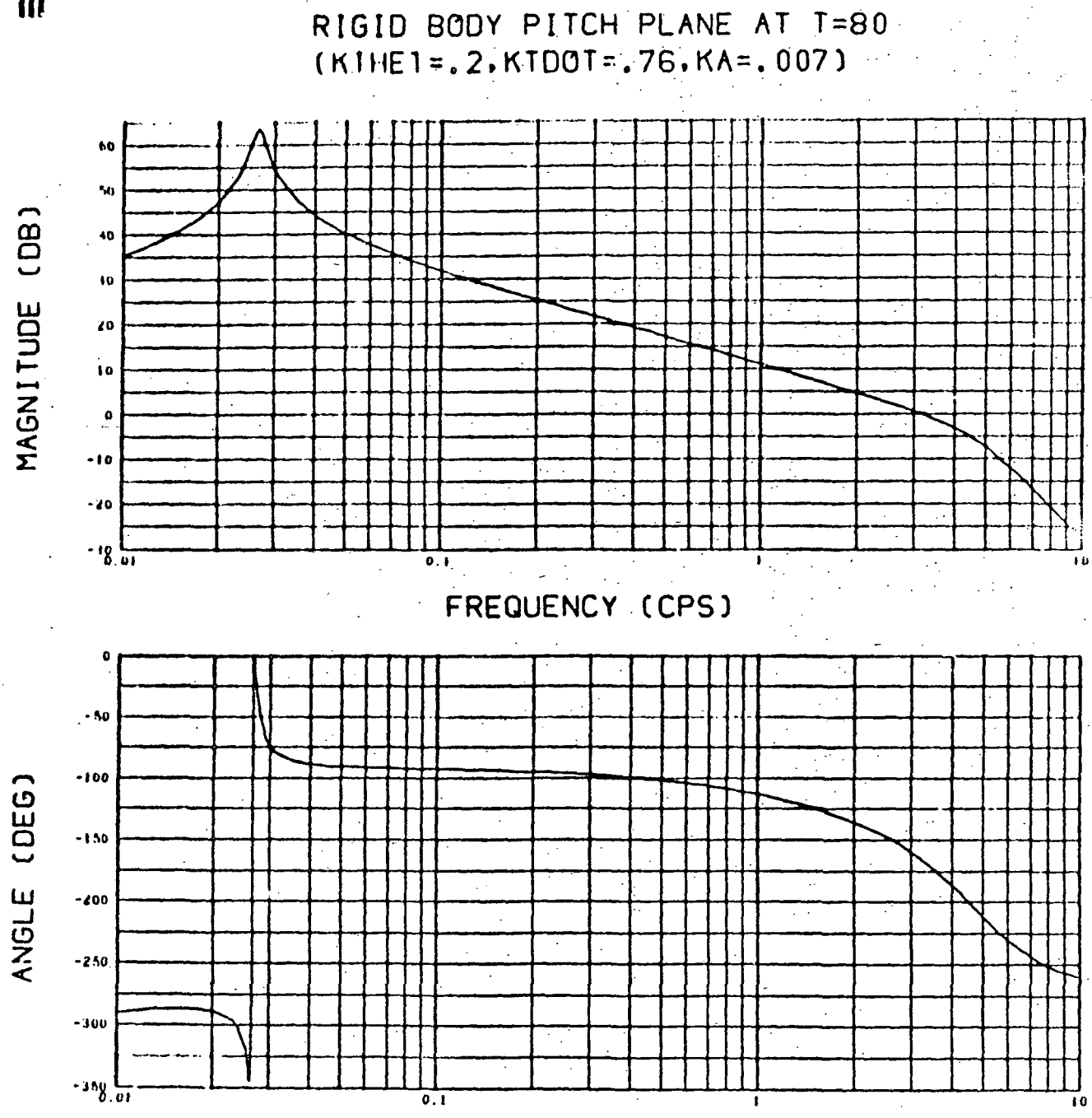
RIGID BODY PITCH PLANE AT T=80
(KTHE1=.2,KTDOT=.76,KA=.007)
MAGNITUDE (DB)
60
50
40
30
20
10
0
-10
-20
-30
0.01
0.1
1
10
FREQUENCY (CPS)
ANGLE (DEG)
0
-50
-100
-150
-200
-250
-300
-350
0.01
0.1
1
10

FIGURE 2-6

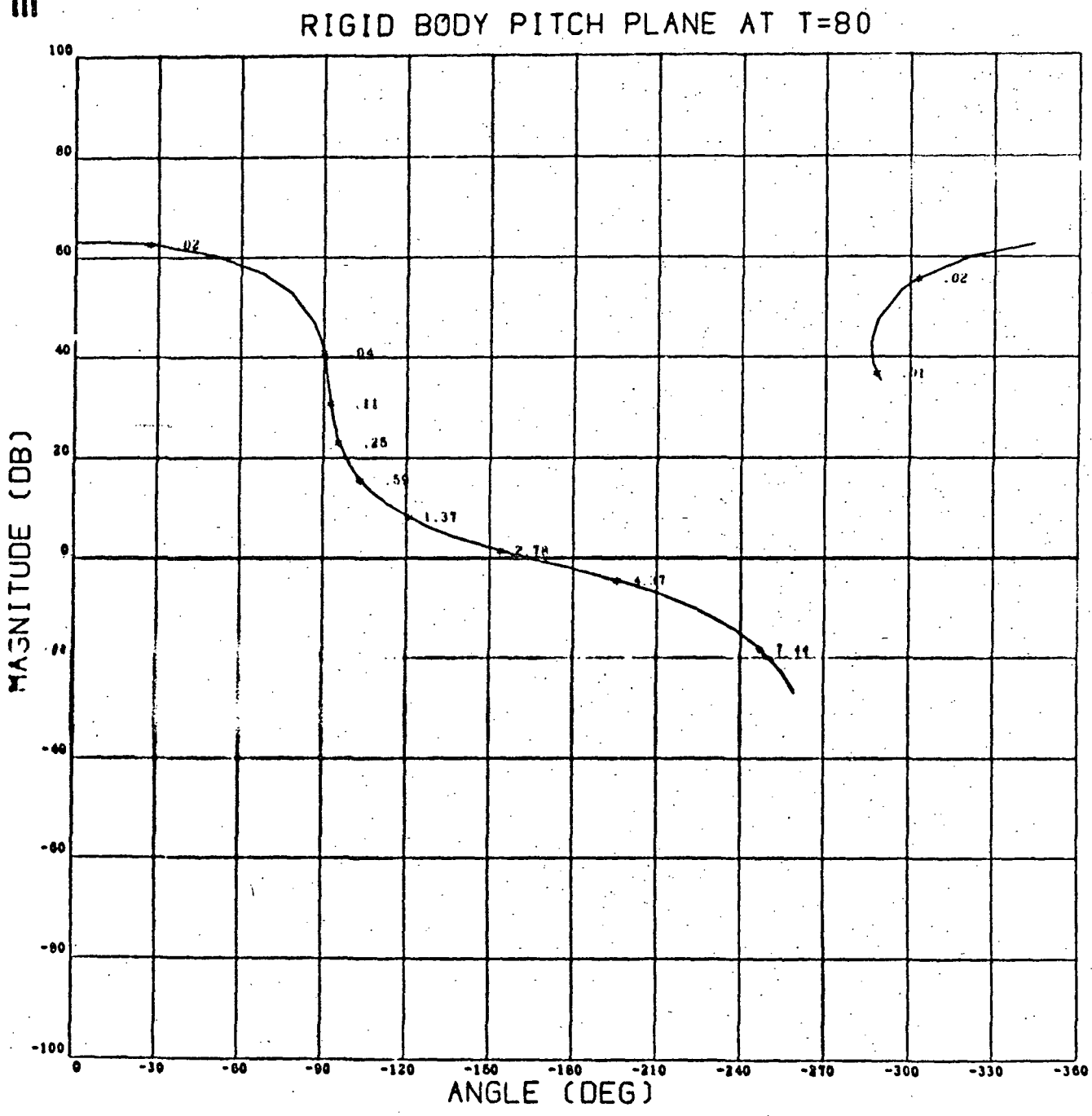
RIGID BODY PITCH PLANE AT T=80
MAGNITUDE (DB)
ANGLE (DEG)
100
80
60
40
20
0
-40
-60
-80
-100
0
-30
-60
-90
-120
-150
-180
-210
-240
-270
-300
-330
-360
.02
.04
.11
.25
.59
1.31
2.78
4.17
7.11
.02
.01

FIGURE 2-7

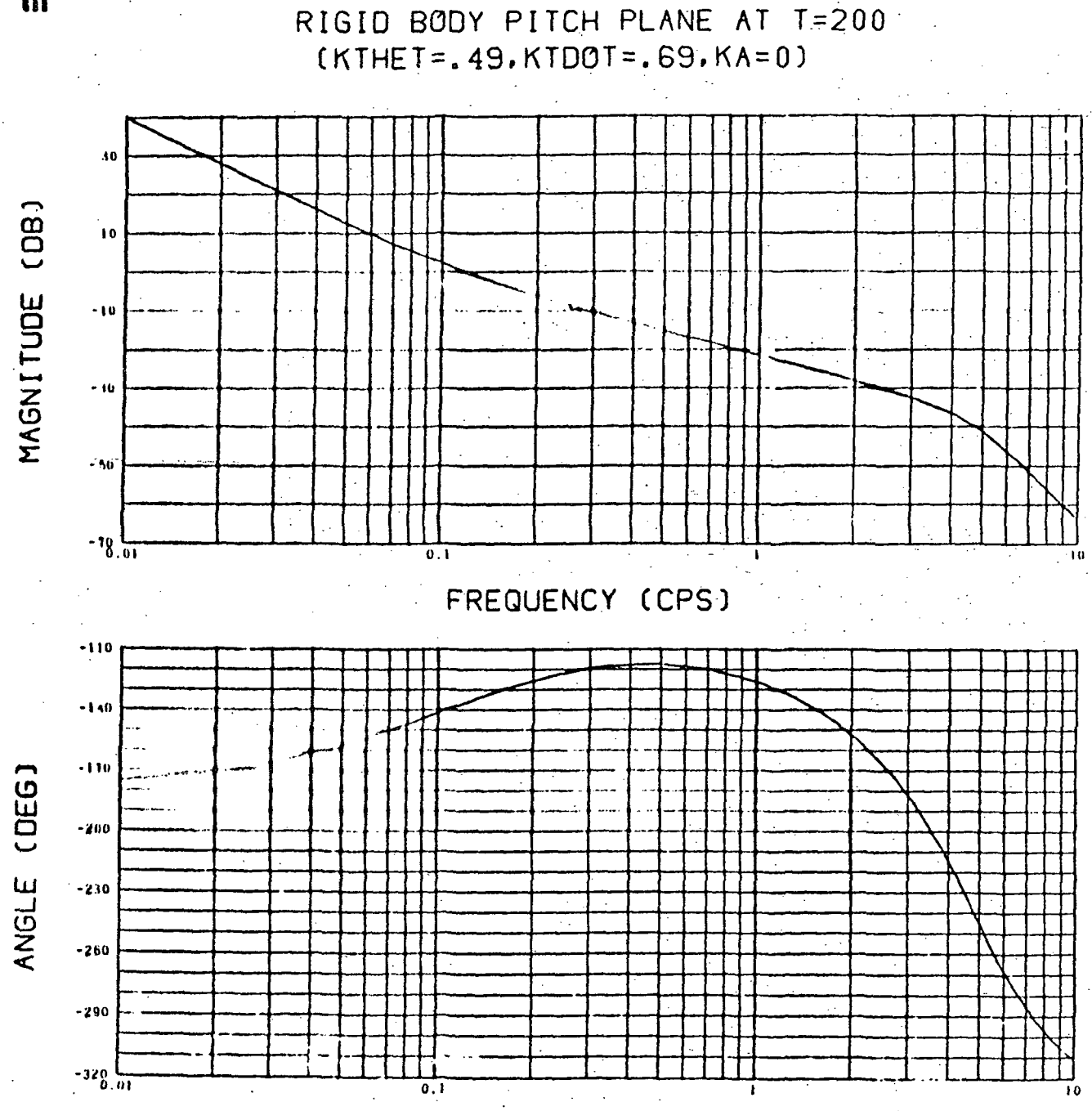
RIGID BODY PITCH PLANE AT T=200
(KTHET=.49,KTDOT=.69,KA=0)
MAGNITUDE (DB)
30
10
-10
-30
-50
-70
0.01
0.1
1
10
FREQUENCY (CPS)
ANGLE (DEG)
-110
-140
-170
-200
-230
-260
-290
-320
0.01
0.1
1
10

FIGURE 2-8

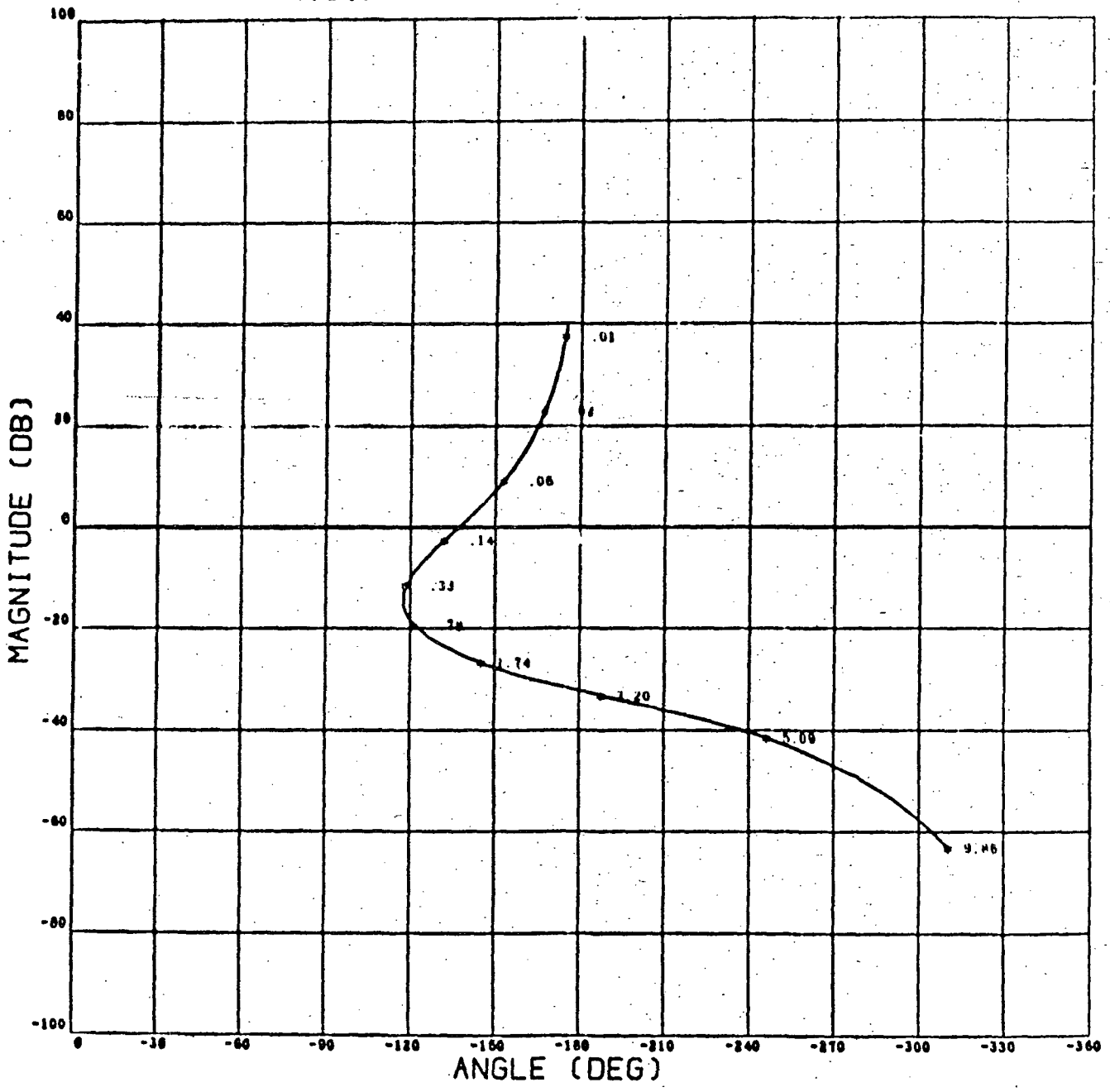
RIGID BODY PITCH PLANE AT T=200
MAGNITUDE (DB)
ANGLE (DEG)
100
80
60
40
20
0
-20
-40
-60
-80
-100
0
-30
-60
-90
-120
-150
-180
-210
-240
-270
-300
-330
-360
.01
.06
.14
.33
.74
1.20
5.00
9.46

FIGURE 2-9

2.3.2 LATERAL DIRECTIONAL DYNAMICS

The Lateral directional equations-of-motion and lateral control system were developed in Reference 17 but never used because of time allowance in scheduling of the tasks to be done under this contract. The Lateral-Directional control system is shown in Figure 2-10, and the vehicle dynamic equations are as follows:

$$T\delta_y = mV\dot{\beta} - \delta q\, C_{y\beta}\,\beta - (\sin\alpha)\, mV\, P + (\cos\alpha) mV\, r - (gm)\,\Phi$$

$$\frac{T\left(X_e^2 + Z_e^2\right)}{Sqb}\,\delta_r = (C_{l_\beta})\,\beta - \frac{I_{xx}}{sqb}\,\dot{P} + C_{lP}\frac{b}{2V}\,P + C_{lr}\frac{b}{2V}\,r + \frac{P_{XZ}}{Sqb}\,\dot{r} + (C_{l_{\delta_a}})\,\delta_a$$

$$T\frac{X_{CG}}{Sqb}\,\delta_y = (C_{n_\beta})\,\beta + C_{nP}\frac{b}{2V}\,P + \frac{P_{XZ}}{sqb}\,\dot{P} - \frac{I_{ZZ}}{sqb}\,\dot{r} + C_{nr}\frac{b}{2V}\,r + C_{n_{\delta_a}}\,\delta_a$$

$$0 = (\cos\theta_o)\, P + (\sin\theta_o)\, r$$

$$\dot{\psi} = \frac{\cos\phi}{\cos\theta_o}\, r$$

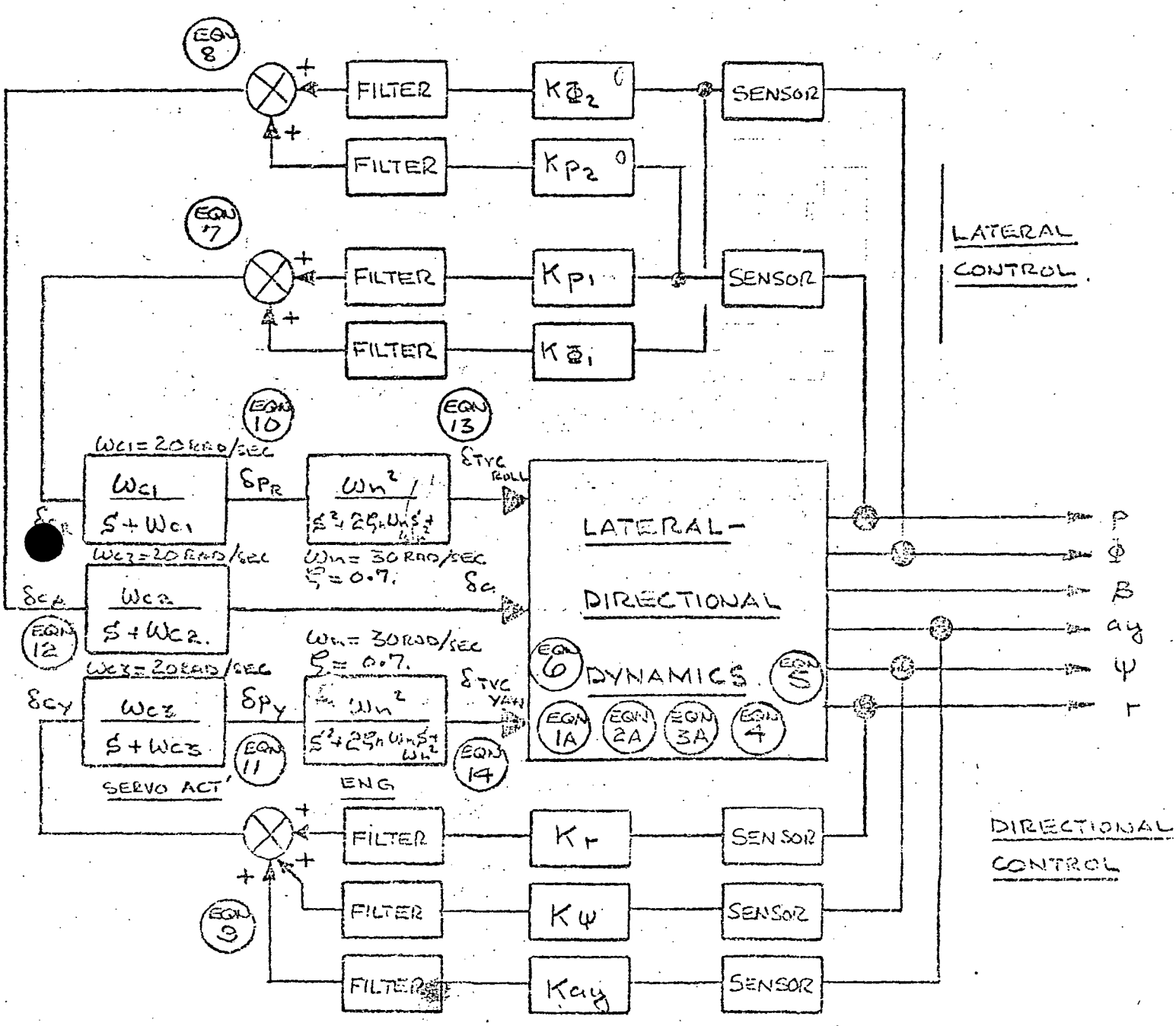

DEF: (EQN XX) IDENTIFIES THE CORRESPONDING EQUATION USED TO DEFINE THE TRANSFER FUNCTIONS

FIG 2-10
BLOCK DIAGRAM OF THE LATERAL-DIRECTIONAL CONTROL SYSTEM FOR THE SSV BOOSTER

2.4 LINEAR TANGENT GUIDANCE LAW (LTG) DEVELOPMENT

The explicit guidance law presented in this section (LTG) is very similar to the Saturn Iterative Guidance Mode (IGM) of Reference 53. Anyone familiar with the IGM can follow through the development term by term and see that LTG could be considered as an improved and somewhat simplified IGM. It can also be shown that E Guidance, the Apollo lunar ascent guidance, is a special case of the generalized derivation presented in Section 2.4.1. The guidance law presented in Section 9.4.2 of Reference 54 is a modified form of Apollo E Guidance.

LTG is characterized by its utilization of the linear tangent steering law resulting from application of classical optimization theory. The derivation of LTG is presented in this Section. The generalized form of the steering commands is shown in Section 2.4.1 without defining the specific form of the terminal position and velocity vectors and the gravity model. (The major difference between IGM and E Guidance is the difference in the form of the terminal position and velocity vectors and the gravity model.) A simple second order gravity model is derived in Section 2.4.1. Implementation of the gravity model is incorporated in the equation flow chart os Section 2.1.7. In order to desmonstrate the flexibility of LTG to applications other than boost, it is also shown in Section 2.4.1 how to use the scheme to provide a throttle command for rendezvous.

A computational flow of multi-stage guidance equations, as implemented in RIBBS (Boeing RIgid Body Boost Simulation Program), is shown in Section 2.1.7. Multi-stage guidance was implemented for two reasons: (1) to accommodate a constant acceleration phase as well as a constant thrust phase in the orbiter and (2) to enable active guidance turn on during booster flight. Linear tangent IGM type guidance was implemented in RIBBS rather than E Guidance because E Guidance, as implemented in the MSC/GCD Space Shuttle Functional Simulator, was derived for a one stage vehicle and, therefore, cannot tolerate a discontinuity in acceleration. The main simplifying

assumption of E Guidance is that the effective gravity (gravity plus centrifugal acceleration) can be represented as the product of thrust acceleration and a linear function of burn time. Effective gravity is continuous with time and decreases with the square of the velocity. Therefore, the E Guidance effective gravity assumption is not very accurate for a constant acceleration burn, since this means that effective gravity is approximated by a linear function of time (whereas it is actually a higher order function). However, E Guidance is quite accurate for a one-stage constant thrust burn, since the acceleration has a higher order shape. LTG, as shown in Section 2.1.7, eliminates these restricting assumptions.

2.4.1 DERIVATION OF GUIDANCE LAW

We will consider vacuum flight equations of motion of a one-stage vehicle in developing the basic LTG equations. In a general derivation it is not necessary to specify the form of (F/m), the thrust acceleration (e.g., F/m can be constant or thrust and mass flow rate can be constant). It is only necessary to assume that F/m is a time function that can be integrated in closed form. Also, it will be seen that implementing multi-stage guidance is simply a matter of expanding the closed form integrals of F/m. It is also sufficient to assume that the gravity vector can be approximated by a time function that can be integrated in closed form.

2.4.1 DERIVATION OF GUIDANCE LAW (Continued)

The following definitions are used in the analysis of this section.

$\ddot{\bar{R}}$	Total inertial acceleration vector
(F/m)	Thrust to mass ratio
$\bar{g}$	Gravitational acceleration vector
$\hat{\lambda}_F$ *	Unit vector of Euler-Lagrange multipliers defining thrust direction
$\bar{V}$	Inertial velocity vector
$\bar{V}_T$	Desired terminal velocity vector
$\bar{V}_{GO}$	Velocity-to-go (to be gained by thrust)
$\bar{R}$	Inertial radius vector
$\bar{R}_T$	Desired terminal radius vector
$\bar{R}_{GO}$	Distance-to-go (to be gained by thrust)
T_{GO}	Time-to-go (burn time plus coast time)
θ_c	Commanded inertial pitch angle
ψ_c	Commanded inertial yaw angle

The following integrals are defined assuming that T_{GO} is given. It is sufficient here to assume that closed form integrals exist for these quantities. The expressions for the integrals are given in Section 2.1.7.

* In the following analysis "^" is used to denote a unit vector.

$$L \equiv \int_0^{T_{GO}} (F/m)dt \quad , \quad S \equiv \int_0^{T_{GO}} \left[\int_0^t (F/m)ds \right] dt$$

$$J \equiv \int_0^{T_{GO}} (F/m)t\, dt \quad , \quad Q \equiv \int_0^{T_{GO}} \left[\int_0^t (F/m)\, s\, ds \right] dt$$

$$\Delta\bar{V}_g \equiv \int_0^{T_{GO}} \bar{g}\, dt \quad , \quad \Delta\bar{R}_g \equiv \int_0^{T_{GO}} \left[\int_0^t \bar{g} ds \right] dt$$

2.4.1.1 Steering Commands

The vacuum equations of motion can be written according to the above definitions as:

1) $\ddot{\bar{R}} = \frac{F}{m} \hat{\lambda}_F - \bar{g}.$ (i.e. $\bar{g} \equiv -\bar{g}$)

It is desirable to determine the thrust direction ($\hat{\lambda}_F$) time history that satisfies the terminal velocity ($\bar{V}_T$) and radius ($\bar{R}_T$) and simultaneously minimizes burn time.

According to classical optimization theory the direction cosines of the unit thrust vector are defined by linear functions of time where the six coefficients are constant Euler-Lagrange multipliers (i.e., for a flat earth assumption or expressed in a spherical earth local horizontal

coordinate system rotating with the vehicle)*. Also, the value of one of the six coefficients is arbitrary due to homogeneity of the equations. Therefore the reference thrust vector can be expressed as a unit vector, since three of the coefficients define the thrust vector and the remaining three define the rate of change. The solution for the coefficients is made simple by defining the thrust vector as an expansion about a reference unit vector, of the form:

$$2)\quad \bar{\lambda}_F = \hat{\lambda} + \dot{\bar{\lambda}}\,(t-K), \text{ where}$$

K is a constant time about which the linear expansion (equation 2) is made. $\hat{\lambda}$ is a unit vector and $\dot{\bar{\lambda}}$ is the time rate of change of $\bar{\lambda}_F$. In general, the downrange component of terminal position ($\bar{R}_T$) is unspecified. It will later be shown that this leads to the fact that $\dot{\bar{\lambda}}$ is normal to $\hat{\lambda}$, or expressed as a vector dot product,

$$3)\quad \hat{\lambda} \cdot \dot{\bar{\lambda}} = 0.$$

The unit thrust vector can be written as:

$$4)\quad \hat{\lambda}_F = \frac{\hat{\lambda} + \dot{\bar{\lambda}}\,(t-K)}{\sqrt{1 + \dot{\bar{\lambda}} \cdot \dot{\bar{\lambda}}\,(t-K)^2}},$$

since $\hat{\lambda}$ is a unit vector and $\hat{\lambda} \cdot \dot{\bar{\lambda}} = 0$. Equation 4 is the key to the simplicity and accuracy of this guidance algorithm.

If θ is defined as the angle between $\hat{\lambda}_F$ and $\hat{\lambda}$, then by definition of the vector dot product $\hat{\lambda}_F \cdot \hat{\lambda} = \cos\theta$, since both vectors are unit vectors. Making use of equations 3 and 4:

* In application LTG is piece wise linear with time, somewhat approximating the Euler-Lagrange equations of a spherical earth in an inertial coordinate system.

$$5)\quad \hat{\lambda}_F \cdot \hat{\lambda} = \frac{1}{\sqrt{1 + \dot{\lambda}^2(t-K)^2}} = \cos\theta$$

where $\dot{\lambda}^2 \equiv \dot{\bar{\lambda}} \cdot \dot{\bar{\lambda}}$. Therefore, $\dot{\lambda}^2(t-K)^2 = \tan^2\theta$ since $\cos\theta = \frac{1}{\sqrt{\sec^2\theta}} = \frac{1}{\sqrt{1 + \tan^2\theta}}$.

It will be seen later that K is approximately equal $.5T_{GO}$. From equation 5 it is seen that when $t = K \approx .5T_{GO}$, $\cos\theta = 1$, or $\theta = 0$. ("$\approx$" denotes "is approximately equal to"). Experience has shown that it is a very good assumption in the derivation of the guidance equations to assume that:

$$6)\quad \cos\theta = \frac{1}{\sqrt{1 + \dot{\lambda}^2(t-K)^2}} \approx 1.$$

The above approximation is compensated for in the manner that it affects the calculated value of T_{GO} and the integrals. The net effect of the assumption yields more accuracy than a small angle approximation.

Substituting equations 4 and 6 into equation 1 and rearranging, the approximate equation of motion becomes:

$$7)\quad \frac{F}{m}\left[\hat{\lambda} + \dot{\bar{\lambda}}\,(t-K)\right] = \ddot{\bar{R}} + \bar{g}.$$

2.4.1.1 Steering Commands (Continued)

Specifying the form of $\hat{\lambda}_F$ in equation 7 reduces the guidance problem to determining values of $\hat{\lambda}$, $\dot{\overline{\lambda}}$, and K that satisfy $\overline{V}_T$ and $\overline{R}_T$, specified terminal conditions. Integration of equation 7 according to the above definitions yields:

$$8)\quad L\hat{\lambda} + \dot{\overline{\lambda}}(J - LK) = \overline{V}_T - \overline{V} + \Delta\overline{V}_g \equiv \overline{V}_{GO} \quad \text{and}$$

$$9)\quad S\hat{\lambda} + \dot{\overline{\lambda}}(Q - SK) = \overline{R}_T - \overline{R} - \overline{V}T_{GO} + \Delta\overline{R}_g \equiv \overline{R}_{GO},$$

The downrange component of terminal position (let us call this the Z component, or R_{T3}) is unspecified in equation 9; therefore in component form there are six equations in eight unknowns (λ_1, λ_2, λ_3, $\dot{\lambda}_1$, $\dot{\lambda}_2$, $\dot{\lambda}_3$, R_{T3}, and K). The solution for $\hat{\lambda}$ and K is found by setting J - LK = 0 in equation 8, from which:

$$10)\quad K = J/L \text{ and } L\hat{\lambda} = \overline{V}_{GO} \text{ or}$$

$$11)\quad \hat{\lambda} = \overline{V}_{GO}/L \text{ and}$$

$$12)\quad L = \text{ABS}(\overline{V}_{GO}) \equiv V_{GO}$$

Time-to-go is determined from equation 12 as shown in Section 2.1.7. As mentioned earlier $K \approx .5T_{GO}$. This can be seen by inspecting equation 10 and

$$K = J/L = \left[\int_0^{T_{GO}} (F/m)t\ dt\right] \Big/ \left[\int_0^{T_{GO}} (F/m)\ dt\right] \approx \frac{.5(F/m)T_{GO}^2}{(F/m)T_{GO}} = .5T_{GO}.$$

(i.e. F/m = (F/m) average)

If the acceleration (F/m) is constant then K is exactly $.5T_{GO}$. Equation 11 shows that the average thrust direction is in the velocity-to-go direction.

An additional scalar equation is obtained by performing the vector dot product of $\hat{\lambda}$ and equation 9, from which:

13) $\hat{\lambda} \cdot \bar{R}_{GO} = S + \hat{\lambda} \cdot \dot{\bar{\lambda}}\ (Q-SK)$ and

14) $R_{GO3} = (S - \lambda_1 R_{GO1} - \lambda_2 R_{GO2})/\lambda_3 + \hat{\lambda} \cdot \dot{\bar{\lambda}}\ (Q-SK)/\lambda_3$.

The quantity $\hat{\lambda} \cdot \bar{R}_{GO}$ is unspecified since it contains R_{T3} which is unspecified; therefore, there should be no component of $\dot{\bar{\lambda}}$ in the $\hat{\lambda}$ direction, which means that $\dot{\bar{\lambda}}$ is normal to $\hat{\lambda}$ as expressed in equation 3;

3) $\hat{\lambda} \cdot \dot{\bar{\lambda}} = 0.$

Equation 3 could be called a transversality condition in the classical optimization sense.

2.4.1.1 Steering Commands (Continued)

From equation 5 it was shown that if $\hat{\lambda} \cdot \dot{\bar{\lambda}} = 0$

$$\tan^2 \theta = \dot{\lambda}^2 (t-K)^2 \text{ or}$$

$$\tan \theta = \pm \dot{\lambda}(t-K) = \pm (-\dot{\lambda}K + \dot{\lambda}t) \equiv a + bt.$$

(In the inertial coordinate system:

$$\tan \chi = \frac{\lambda_1 + \dot{\lambda}_1(t-K)}{\lambda_3 + \dot{\lambda}_3(t-K)} \equiv \frac{A + Bt}{C + Dt}$$, a bi-linear tangent

law, however, in the coordinate system defined by $\hat{\lambda}$ and $\bar{R}_{GO} - \hat{\lambda}(\hat{\lambda} \cdot \bar{R}_{GO})$, $\tan \theta = a + bt$, a linear tangent law.)

Applying equation 3, equations 13 and 14 become:

13) $\hat{\lambda} \cdot \bar{R}_{GO} = S$ and

14) $R_{GO3} = (S - \lambda_1 R_{GO1} - \lambda_2 R_{GO2})/\lambda_3$.

Rearranging the Z component of equation 9,

15) $R_{T3} - R_3 = R_{GO3} + V_3 T_{GO} - \Delta R_{g3}$.

Equation 15 is used to compute the range angle-to-go in Section 2.2.

2.4.1.1 Steering Commands (Continued)

$\hat{\lambda}$ and $\overline{R}_{GO}$ are now defined in equation 9, therefore the solution for $\dot{\overline{\lambda}}$ becomes

$$16) \quad \dot{\overline{\lambda}} = \frac{\overline{R}_{GO} - S\hat{\lambda}}{Q - SK} \quad .$$

This completes the solution for K, $\hat{\lambda}$, and $\dot{\overline{\lambda}}$. The thrust direction is defined by:

$$\hat{\lambda}_F = \frac{\hat{\lambda} + \dot{\overline{\lambda}}(\Delta T - K)}{\sqrt{1 + \dot{\lambda}^2(\Delta T - K)^2}} \quad \text{or}$$

$$17) \quad \overline{U}_F \equiv \hat{\lambda} + \dot{\overline{\lambda}}(\Delta T - K), \text{ where}$$

$\Delta T = T - T_o$ (T is present time and T_o is time when K, $\hat{\lambda}$, and $\dot{\overline{\lambda}}$ were computed). The steering commands are:

$$18) \quad \theta_c = \tan^{-1}(U_{F1}/U_{F3}) - \pi/2 \text{ and}$$

$$19) \quad \psi_c = \tan^{-1}\left[U_{F2}/(U^2_{F1} + U^2_{F3})^{\frac{1}{2}}\right]$$

A summary of the equations in the order of calculations is now given.

2.4.1.1. Steering Commands (Continued)

$$\bar{V}_{GO} = \bar{V}_T - \bar{V} + \Delta\bar{V}_g$$

$$V_{GO} = \text{ABS}\ (\bar{V}_{GO})$$

$$\hat{\lambda} = \bar{V}_{GO}/V_{GO}$$

$$R_{GOi} = R_{Ti} - R_i - V_i\ T_{GO} + \Delta R_{gi}\ (i = 1,\ldots,2)$$

$$R_{GO3} = (S - \lambda_1\ R_{GO1} - \lambda_2\ R_{GO2})/\lambda_3$$

$$K = J/L$$

$$\dot{\bar{\lambda}} = (\bar{R}_{GO} - S\hat{\lambda})/\ (Q - SK)$$

$$\Delta T = T - T_o$$

$$\bar{U}_F = \hat{\lambda} + \dot{\bar{\lambda}}(\Delta T - K)$$

$$\theta_c = \tan^{-1}\ (U_{F1}/U_{F3}) - \pi/2$$

$$\psi_c = \tan^{-1}\left[U_{F2}/(U^2_{F1} + U^2_{F3})^{\frac{1}{2}}\right]$$

2.4.1.2 Gravity Model

The Saturn guidance law, Iterative Guidance Mode (IGM), of Reference 1 has demonstrated that a sophisticated gravity model is unnecessary. In the IGM, gravity is approximated as having a constant, average direction and magnitude, i.e.

$$\bar{g}_{AV} = .5\left(\bar{g}_T + \bar{g}\right) \text{ , where}$$

$\bar{g}_{AV}$ = average gravity vector,

$\bar{g}_T$ = terminal gravity vector, and

$\bar{g}$ = present gravity vector.

Then the velocity and position terms due to gravity are expressed as:

$$20) \quad \overline{\Delta V}_g \equiv \int_0^{T_{GO}} \bar{g}\, dt = \bar{g}_{AV}\, T_{GO}, \text{ and}$$

$$21) \quad \overline{\Delta R}_g \equiv \int_0^{T_{GO}} \left[\int_0^{t} \bar{g} ds \right] dt = .5\, \bar{g}_{AV}\, T_{GO}^2 .$$

However, a more accurate, yet simple, gravity model has been implemented in this scheme (as shown in Section 2.2) in order to be consistent with the accuracy of the steering commands. Referring to equations 7, 8, and 9 of Section 2.4.1.1, it is seen that the steering parameters ($\hat{\lambda}$ and $\dot{\bar{\tau}}$) are on the left hand side and the gravity terms are on the right hand side. Section 2.4.1.1 showed the solution of the left hand side of the equation. The purpose of this gravity model is to make the accuracy of the right side consistent with that of the left.

2.4.1.2 Gravity Model (Continued)

The gravity magnitude is defined as the average value

$$22)\quad g_{AV} = .5g\left[1 + \left(\frac{R}{R_D}\right)^2\right], \text{where}$$

g = present gravity magnitude,

R = present radius magnitude, and

R_D = desired terminal radius magnitude.

At insertion $R = R_D$, therefore, $g_{AV} = g$.

The average downrange and crossrange components of position are determined by assuming second order expansions of downrange and crossrange position. This will be illustrated by considering the downrange component of position (Z),

$$23)\quad Z(t) = Z_0 + \dot{Z}t + .5\,\ddot{Z}t^2$$

The coordinate system in Section 2.2 is such that $Z_0 = 0$. It is assumed that:

$$\ddot{Z} = \ddot{Z}_{average} = \frac{\dot{Z}_T - \dot{Z}}{T_{GO}}\ , \text{where}$$

$\dot{Z}_T$ is terminal value of $\dot{Z}$. Equation 23 becomes:

$$24)\quad Z(t) = \dot{Z}t + .5\,\frac{(\dot{Z}_T - \dot{Z})\,t^2}{T_{GO}}\ .$$

2.4.1.2 Gravity Model (Continued)

Spherical gravity is assumed in the form:

25) $g_Z = g_{AV} \frac{Z}{R_{AV}}$ or substituting equation 24 in equation 25:

26) $g_Z = \frac{g_{AV}}{R_{AV}} \left[\dot{Z}t + .5 \frac{(\dot{Z}_T - \dot{Z})t^2}{T_{GO}} \right]$, where

R_{AV} is average radius magnitude, to be defined later. The gravity velocity and position terms are defined by equations 20 and 21. Integrating equation 26 twice from 0 to T_{GO} yields:

$$\Delta\dot{Z}_g = \frac{g_{AV}}{R_{AV}} \left[(1/2)\, \dot{Z}\, T_{GO}^2 + (1/6) \left(\frac{\dot{Z}_T - \dot{Z}}{T_{GO}} \right) T_{GO}^3 \right] \text{ and}$$

$$\Delta Z_g = \frac{g_{AV}}{R_{AV}} \left[(1/6)\dot{Z}\, T_{GO}^3 + (1/24) \left(\frac{\dot{Z}_T - \dot{Z}}{T_{GO}} \right) T_{GO}^4 \right], \text{ or}$$

27) $\Delta\dot{Z}_g = \frac{g_{AV}}{R_{AV}} (2\dot{Z} + \dot{Z}_T) \frac{T_{GO}^2}{6}$ and

28) $\Delta Z_g = \frac{g_{AV}}{R_{AV}} (3\dot{Z} + \dot{Z}_T) \frac{T_{GO}^3}{24}$.

Substituting T_{GO} into equation 24 yields:

29) $Z(T_{GO}) = Z_T = .5\, (\dot{Z} + \dot{Z}_T)\, T_{GO}$, the terminal value of Z.

Multiplying equations 27 and 28 by the left side of 29, and dividing by the right side gives:

2.4.1.2 Gravity Model (Continued)

$$\dot{\Delta Z}_g = \frac{g_{AV}}{R_{AV}} \quad (2\dot{Z} + \dot{Z}_T) \quad \frac{T_{GO}^2}{6} \left[\frac{Z_T}{.5\ (\dot{Z} + \dot{Z}_T)\ T_{GO}} \right] \quad \text{and}$$

$$\Delta Z_g = \frac{g_{AV}}{R_{AV}} \quad (3\dot{Z} + \dot{Z}_T) \quad \frac{T_{GO}^3}{24} \left[\frac{Z_T}{.5\ (\dot{Z} + \dot{Z}_T)\ T_{GO}} \right] .$$

By manipulation the above equations become:

30) $\dot{\Delta Z}_g = (g_{AV}\ T_{GO}) \left[Z_T \quad (F_G + 1)/3 \right] /R_{AV}$ and

31) $\Delta Z_g = (.5\ g_{AV}\ T_{GO}^2) \left[Z_T\ (2F_G + 1)/6 \right] /R_{AV}$,

where

32) $F_G \equiv \dot{Z}/(\dot{Z} + \dot{Z}_T)$.

The crossrange or y components of these quantities can be obtained by inspection of equations 30, 31, and 32, since the derivation is analogous. In the y direction F_G (equation 32) is:

$$F_G = \dot{y}/(\dot{y} + \dot{y}_T)$$

Consider a local coordinate system where the local radius vector defines the X direction, Z is parallel to the desired orbit plane, and y is orthgonal. In this system $\dot{y}_T = 0$ and $y_0 = 0$, therefore:

$$F_G = 1$$

$$y_T\ (F_G + 1)/3 = (2/3)y_T$$

$$y_T\ (2F_G + 1)/6 = (1/2)y_T.$$

2.4.1.2 Gravity Model (Continued)

So the average y position for gravity velocity losses is 2/3 of the way from local position to the desired orbital plane and the average for distance losses is halfway. However, the X and Z axis of the guidance coordinate system implemented in Section 2.2 lie in the desired orbital plane. Therefore, the average y for gravity velocity losses is 1/3 of the way from the desired orbital plane to local position. In the orbital coordinate system $y_T = 0$, so y_0 is used instead of y_T. X_T is used for the average radial distance.

In summary, the gravity model is constructed by defining the average radius vector for velocity losses and the average radius vector for distance losses in terms of the terminal radius vector. As implemented in Section 2.1.7, the actual terminal radius vector is used instead of using approximations such as equation 29. Equation 29 is used only to derive the factors 1/3, $(F_G + 1)/3$, 1/2, and $(2F_G + 1)/6$ as shown in Section 2.1.7.

Inspection of $F_G = \dot{Z}/(\dot{Z} + \dot{Z}_T)$ shows that F_G ranges from 0 to 1/2 as $\dot{Z}$ ranges from 0 to $\dot{Z}_T$. Therefore, the above factors range as follows:

1/3, crossrange velocity factor, is constant.

$(F_G + 1)/3$, downrange velocity factor, ranges from 1/3 to 1/2.

1/2, crossrange position factor, is constant.

$(2F_G + 1)/6$, downrange position factor, ranges from 1/6 to 1/3.

So, at orbital insertion the factors are 1/3, 1/2, 1/2, and 1/3.

If these factors were all constant and equal to 1/2, this gravity model would be almost identical to the gravity model of the Saturn IGM of Reference 1.

2.4.1.3 Throttle Command for Rendezvous

Although there is presently no requirement for rendezvous capability in the SSV boost-to-orbit, this section is presented to illustrate the flexibility of this guidance scheme.

In general, rendezvous implies that all components of the desired terminal position and velocity are specified. However, if rendezvous with a target vehicle is being performed, the position and velocity of the target are functions of the burn time of the vehicle performing rendezvous, and an iteration is involved. But for simplicity the example given here can be thought of as lunar descent to a hover point over a given landing site. In this case the desired terminal position is a given altitude over the landing site and the desired terminal velocity magnitude is zero with respect to the landing site.

We will assume that the vehicle propulsion system has a constant specific impulse (or exhaust velocity) and that when closed-loop throttling begins a constant thrust level is desired for achieving the terminal conditions. (It is even easier to compute a constant acceleration command).

Equations 12 and 13 are used to compute the time-to-go and throttle command, i.e.,

12) $L = V_{GO}$ and

13) $S = \hat{\lambda} \cdot \bar{R}_{GO}$.

The quantities in the above equations are functions of T_{GO}; however, it will be assumed that the equations are recycled through until T_{GO} stops changing (as in the range free mode shown in Section 2.1.7). The expressions for the integrals, L and S, are given in Section 2.1.7. One stage constant thrust is assumed.

2.4.1.3 Throttle Command for Rendezvous (Continued)

33) $L = V_{ex} \ln \left[\tau/(\tau - T_{GO}) \right] = V_{GO}$

$S = L\, T_{GO} - J = L\, T_{GO} - L\tau + V_{ex}\, T_{GO}$ or

34) $S = L\,(T_{GO} - \tau) + V_{ex}\, T_{GO} = \hat{\lambda} \cdot \bar{R}_{GO}$

Define $\Delta R \equiv \hat{\lambda} \cdot \bar{R}_{GO}$.

Rearranging equation 33:

35) $T_{GO} = \tau(1-e^{-V_{GO}/V_{ex}})$.

Defining $e' \equiv 1-e^{-V_{GO}/V_{ex}}$,

36) $T_{GO} = \tau e'$.

Substituting into equation 34:

$V_{GO}\,(\tau e' - \tau) + V_{ex}\,\tau e' = \Delta R$, from which

37) $\tau = \Delta R/\left[V_{GO}(e'-1) + V_{ex}e' \right]$.

Remembering that $\tau = V_{ex}/(F/m)$ it follows that the throttle command is

38) $(F/m)_c = V_{ex}/\tau$, where τ is computed from equation 37.

Time-to-go is now computed by substituting the above value of τ into equation 35. The steering angles are computed as in Section 2.4.1.1.

2.4.2 COMPARISON OF IGM WITH LTG

In order to compare IGM with LTG the vector derivation of LTG is converted to an angular derivation and the linear tangent law is introduced.

2.4.2.1 Steering Parameters

Referring to Reference 1, the form of the steering angles is

$$\chi_p = \bar{\chi}_p - K_1 + K_2 t \equiv \bar{\chi}_p + K_2(t-K) \text{ (where } K \equiv J/L)$$
$$\chi_y = \bar{\chi}_y - K_3 + K_4 t \equiv \bar{\chi}_y + K_4(t-K)$$

or

1) $\chi_p - \bar{\chi}_p = K_2(t-K)$ and

2) $\chi_y - \bar{\chi}_y = K_4(t-k)$

however, the linear tangent form is:

3) $\tan(\chi_p - \bar{\chi}_p) = K_2(t-K)$

4) $\tan(\chi_y - \bar{\chi}_y) = K_4(t-K)$.

Differentiation of Equations 3 and 4 yields

5) $\dot{\chi}_p \sec^2(\chi_p - \bar{\chi}_p) = K_2$ and

6) $\dot{\chi}_y \sec^2(\chi_y - \bar{\chi}_y) = K_4$.

Inspection of Equations 3, 4, 5, and 6 shows that when $t = k$, $\chi_p = \bar{\chi}_p$, $\chi_y = \bar{\chi}_y$, $\dot{\chi}_p = K_2$, and $\dot{\chi}_y = K_4$.

The relationship between vector and angles is:

7) $$\hat{\lambda}_F = \frac{\hat{\lambda} + \dot{\hat{\lambda}}(t-K)}{\left[1 + \dot{\lambda}^2(t-K)^2\right]^{\frac{1}{2}}} = \begin{bmatrix} \sin\chi_p \cos\chi_y \\ \sin\chi_y \\ \cos\chi_p \cos\chi_y \end{bmatrix}$$

Differentiation of the above equation yields:

$$8)\quad \dot{\bar{\lambda}}/u - \dot{\lambda}^2(t-K)\bar{u} = \begin{bmatrix} \dot{x}_p\cos x_p\cos x_y - \dot{x}_y\sin x_p\sin x_y \\ \dot{x}_y\cos x_y \\ -\dot{x}_p\sin x_p\cos x_y - \dot{x}_y\cos x_p\sin x_y \end{bmatrix}$$

where $\bar{u} \equiv \hat{\lambda} + \dot{\bar{\lambda}}(t-K)$ and $u \equiv \mathrm{ABS}(\bar{u}) = [1 + \dot{\lambda}^2(t-K)^2]^{\frac{1}{2}}$

Inspection of Equations 3, 4, 5, 6, 7 and 8 (for t = K) shows that:

$$9)\quad \hat{\lambda} = \begin{bmatrix} \sin\bar{x}_p\cos\bar{x}_y \\ \sin\bar{x}_y \\ \cos\bar{x}_p\cos\bar{x}_y \end{bmatrix} \qquad \text{and}$$

$$12)\quad \dot{\bar{\lambda}} = \begin{bmatrix} K_2\cos\bar{x}_p\cos\bar{x}_y - K_4\sin\bar{x}_p\sin\bar{x}_y \\ K_4\cos\bar{x}_y \\ -K_2\sin\bar{x}_p\cos\bar{x}_y - K_4\cos\bar{x}_p\sin\bar{x}_y \end{bmatrix}$$

From the above equations

$$\dot{\bar{\lambda}}\cdot\dot{\bar{\lambda}} \equiv \dot{\lambda}^2 = K_2^2\cos^2\bar{x}_y + K_4^2.$$

The first order approximation of LTG and IGM could be thought of as an average value approximation:

$$\frac{1}{T_{GO}}\int_0^{T_{GO}} \left[1/\sqrt{1 + (K_2^2\cos^2\bar{x}_y + K_4^2)(t-K)^2}\right] dt \approx 1,$$

which turns out better than a small angle approximation, by the way that it is compensated for in other calculations.

2.4.2.1 Steering Parameters (Continued)

The IGM steering parameters, $\bar{\chi}_p$, $\bar{\chi}_y$, K_1, K_2, K_3 and K_4, are obtained from Equations 9 through 13. It was shown in Section 2.4.1.1 that

15) $\hat{\lambda} = \text{Unit}(\bar{V}_{GO})$ and

16) $\dot{\bar{\lambda}} = \dfrac{\bar{R}_{GO} - S\hat{\lambda}}{Q - SK}$

From Equations 9, 10, 11 and 15 it follows that

17) $\bar{\chi}_p = \tan^{-1}(V_{GO1}/V_{GO3})$ and

18) $\bar{\chi}_y = \tan^{-1}\left[V_{GO2}/(V_{GO1}^2 + V_{GO3}^2)^{\frac{1}{2}}\right]$

From the definition $K_3 \equiv K_4 K$ and Equations 10, 13, 15 and 16

19) $K_3 = \dfrac{(R_{GO2} - S\sin\bar{\chi}_y)K}{\cos\bar{\chi}_y(Q - SK)}$

From the definition $K_1 = K_2 K$ and Equations 9, 12, 15 and 16

20) $K_1 = \dfrac{R_{GO1} - S\sin\bar{\chi}_p\cos\bar{\chi}_y}{\cos\bar{\chi}_p\cos\bar{\chi}_y(Q - SK)} + K_3\tan\bar{\chi}_p\tan\bar{\chi}_y$ and

$K_2 = K_1/K$

A direct comparison can now be made between the steering parameters of LTG and IGM. The above equations for $\bar{\chi}_p$, $\bar{\chi}_y$, K_3 and K_4 are identical to those on pages 38 and 39 of Reference 1. However, the equation for K_1 on page 40 omits the term $K_3\tan\bar{\chi}_p\tan\bar{\chi}_y$ of Equation 20. This equation *should be*

21) $K_1 = K_1 + K_3\tan\bar{\chi}_p\tan\bar{\chi}_y$.

2.4.2.1 Steering Parameters (Continued)

The equations

$$x_p = \bar{x}_p - K_1 + K_2\Delta t \qquad \text{and}$$
$$x_y = \bar{x}_y - K_3 + K_4\Delta t$$

should be

22) $x_p = \bar{x}_p + \tan^{-1}(-K_1 + K_2\Delta t)$ and

23) $x_y = \bar{x}_y + \tan^{-1}(-K_3 + K_4\Delta t)$.

2.4.2.2 Range Angle

An IGM range angle is implemented slightly differently than that in Section 2.2 due to the difference in the implementation of the guidance coordinate system. A local coordinate system is implemented in Section 2.2, whereas a terminal coordinate system is in Reference 1. Also opposite signs are on the gravity vector. An IGM, LTG type range angle calculation should be (employing the notation of Reference 53):

24) $V_{GO} = (\Delta\dot{X}^2 + \Delta\dot{Y}^2 + \Delta\dot{Z}^2)^{\frac{1}{2}}$

$$Z_{GO} = \left(S - \frac{\Delta\dot{X}}{V_{GO}} R_{GO1} - \frac{\Delta\dot{Y}}{V_{GO}} R_{GO2}\right) \frac{V_{GO}}{\Delta\dot{Z}}$$

$$\Delta Z = Z_{GO} + \dot{Z}T_{GO} + .5g_{Rz}T_{GO}^2$$

25) $\phi_{GO} = \tan^{-1}(\Delta Z/X)$

26) $\phi = \tan^{-1}(Z''''/X'''') + \phi_{GO}$

The range angle calculation on page 36 of Reference 53 is adequate for a first pass estimate.

2.4.2.3 Gravity Model

A second order IGM gravity model is implemented differently than in Section 2.1.7 due to the difference in the coordinate systems. A second order gravity model is recommended for the sake of convergence and terminal accuracy (i.e., chi tilde steering is unnecessary). The notation of Reference 1 is used in the following equations. Using the IGM coordinate system, the factors $(F_G + 1)/3$ and $(2F_G + 1)/6$ of Section 2.1.7 should be $1 - (F_G + 1)/3$ and $1 - (2F_G + 1)/6$, where $F_G = \dot{Z}/(\dot{Z} + \dot{Z}_T)$. The equations are as follows:

$$g = -(\ddot{X}_g^2 + \ddot{Y}_g^2 + \ddot{Z}_g^2)^{\frac{1}{2}}_{pL}$$

$$g_{AV} = .5g\left[1 + (R/R_{BO})^2\right]$$

27) $$g_{DR} = g_{AV}/\sqrt{X^2 + (Y/3)^2 + [Z(2 - F_G)/3]^2}$$

28) $$g_{VX} = g_{DR}X$$

29) $$g_{VY} = g_{DR}(Y/3)$$

30) $$g_{VZ} = g_{DR}Z(2 - F_G)/3$$

31) $$g_{DR} = g_{AV}/\sqrt{X^2 + (Y/2)^2 + [Z(5 - 2F_G)/6]^2}$$

32) $$g_{RX} = g_{DR}X$$

33) $$g_{RY} = g_{DR}(Y/2)$$

34) $$g_{RZ} = g_{DR}Z(5 - 2F_G)/6$$

2.4.2.4 Time-to-Go

Time-to-go correction comes from the equation

35) $$L = V_{GO}.$$

2.4.2.4 Time-to-Go (Continued)

Define: $\delta V = V_{GO} - L.$

A time-to-go correction is

$$\delta T_n = \tau_T(1 - e^{-\delta V/V_{exn}})$$

Assuming that $\delta V/V_{exn}$ is small and using the first two terms of the exponential expansion, $e^{-x} \simeq 1 - x$, the above equation becomes

$$36) \quad \delta T_n = \tau_T \delta V/V_{exn}$$

$\tau_T = \tau_n - T_n'$ or V_{exn}/a_{max_n} depending on whether the insertion burn is constant thrust or constant acceleration. The present IGM time-to-go correction employs a square root algorithm

$$V_{GO} \simeq \tfrac{1}{2}\left(\frac{\Delta\dot{X}^2 + \Delta\dot{Y}^2 + \Delta\dot{Z}^2}{L_T} + L_T\right)$$

instead of

$$V_{GO} = (\Delta\dot{X}^2 + \Delta\dot{Y}^2 + \Delta\dot{Z}^2)^{\frac{1}{2}}.$$

2.4.3 COMPARISON OF E GUIDANCE WITH LTG

The form of E Guidance that is discussed here is that presented in Section 9.4.2 of Reference 54. It is a modified form of Apollo lunar ascent guidance. E Guidance can be derived as in Section 2.4.1.1. It is characterized by employing a local coordinate system rotating with the vehicle, such that centrifugal acceleration ($\omega^2 R$) appears in the equations of motion. The vector equation of motion is

1) $\ddot{\bar{R}} = a\hat{\lambda}_F - (\frac{u}{R^2} - \omega^2 R)\underline{i}_r$ (spherical earth)

where

a = thrust acceleration

$\hat{\lambda}_F$ = unit vector in thrust direction

$g = -(\frac{u}{R^2} - \omega^2 R)$ = effective gravity, and

$\underline{i}_r$ = unit vector in radial direction.

The simplifying approximations are

2) $\hat{\lambda}_F \approx \bar{u} + \dot{\bar{u}}t$ (linear function of time) and

3) $g \approx a(g_o + \dot{g}t)$ (product of thrust acceleration and a linear function of time).

The approximate vector equation of motion is

4) $\ddot{\bar{R}} = a(\bar{u} + \dot{\bar{u}}t) + \frac{a}{a_o}(g_o + \dot{g}t)\underline{i}_r$.

This equation can be written in the form

5) $\ddot{\bar{R}} = a[\hat{\lambda} + \dot{\hat{\lambda}}(t-K)] + \frac{a}{a_o}[\bar{g}_{AV} + \dot{\bar{g}}(t-K)]$

where

$K \equiv J/L \equiv A_{12}/A_{11}$ (Reference 2)

$\bar{g}_{AV} = (g_o + \dot{g}K)\underline{i}_r$, and

$\dot{\bar{g}} = \dot{g}\underline{i}_r$

The following definitions are made:

$$g_o = -u/R_o^2 + \omega_o^2 R_o$$

$$g_F = -u/R_D^2 + \left(\frac{\dot{Z}_D}{R_D}\right)^2 R_D$$

a_F = final predicted value of thrust acceleration

$$\dot{g} = \frac{1}{T_{GO}}\left(g_F \frac{a_o}{a_F} - g_o\right)$$

$$\bar{c}_o = (g_o/a_o)\underline{i}_r$$

$$\dot{\bar{c}} = (\dot{g}/a_o)\underline{i}_r, \text{ and}$$

$$\bar{c}_{AV} = \bar{c}_o + \dot{\bar{c}}K.$$

Equation 5 is now written in the form

$$6)\quad a\left[\hat{\lambda} + \bar{c}_{AV} + (\dot{\hat{\lambda}} + \dot{\bar{c}})(t - K)\right] = \ddot{\bar{R}}.$$

Differentiation of Equation 6 as in Section 2.1.1 yields

$$7)\quad L(\hat{\lambda} + \bar{c}_{AV}) + (\dot{\hat{\lambda}} + \dot{\bar{c}})(J - LK) = \bar{V}_T - \bar{V} \equiv \overline{\Delta V}$$

$$8)\quad S(\hat{\lambda} + \bar{c}_{AV}) + (\dot{\hat{\lambda}} + \dot{\bar{c}})(Q - SK) = \bar{R}_T - \bar{R} - \bar{V}T_{GO} \equiv \overline{\Delta R}.$$

Since $K = J/L$ or $J - LK = 0$

$$9)\quad \hat{\lambda} = (\overline{\Delta V} - L\bar{c}_{AV})/L$$

$$10)\quad \bar{V}_{GO} = \overline{\Delta V} - L\bar{c}_{AV},$$

$$11)\quad V_{GO} = ABS(\bar{V}_{GO}), \text{ and}$$

$$12)\quad L = V_{GO}$$

From Equations 7, 8 and 9

$$13)\quad \dot{\bar{\lambda}} = (\overline{\Delta R} - S\overline{\Delta V}/L)/(Q - SK) - \dot{\bar{c}} \equiv \bar{B} - \dot{\bar{c}}$$

Inspection of Equations 4 and 5 shows that

$$14)\quad \bar{u} \equiv \hat{\lambda} - \dot{\bar{\lambda}}K \qquad \text{and}$$

$$\dot{\bar{u}} \equiv \dot{\bar{\lambda}}$$

from which

$$15)\quad \bar{u} = \frac{\Delta V}{L} - \bar{c}_{AV} - \bar{B}K + \dot{\bar{c}}K = \frac{\overline{\Delta V}}{L} - \bar{B}K - \bar{c}_o$$

The third or downrange component of $\bar{R}_T$ is generally unspecified; however, in Section 2.1.1 it is shown that

$$16)\quad \hat{\lambda}\cdot\dot{\bar{\lambda}} = 0 \qquad \text{and}$$

$$17)\quad \hat{\lambda}\cdot\bar{u} = 1$$

from which the third components of Equations 13 and 15 are derived:

$$18)\quad \dot{\lambda}_3 = -(\lambda_1\dot{\lambda}_1 + \lambda_2\dot{\lambda}_3)/\lambda_3 \equiv \dot{u}_3 \qquad \text{and}$$

$$19)\quad u_3 = (1 - \lambda_1 u_1 - \lambda_2 u_2)/\lambda_3.$$

The desired thrust vector is now defined as

$$20)\quad \bar{u}_T = \bar{u} + \dot{\bar{u}}(t - t_o)$$

$$21)\quad \bar{a}_T = a_o\bar{u}_T$$

$$22)\quad \underline{i}_D = \text{Unit}\ (\bar{a}_T)$$

From Equations 17 and 21 it is seen that

$$23)\quad \hat{\lambda}\cdot\bar{a}_T = a_o$$

2.4.3 COMPARISON OF E GUIDANCE WITH LTG (Continued)

Equations 13 and 15 can now be converted to component form and compared with the equations in Section 9.4.2 of Reference 54. The following definitions are made:

$$a_T \equiv a_o$$

$$g_{eff} \equiv g_o$$

$$A \equiv \Delta V_1/L - B_1 K, \quad B \equiv B_1$$

$$C \equiv \Delta V_2/L - B_2 K, \quad D \equiv B_2$$

These coefficients are identical to those in Reference 54. From the above coefficients and Equations 13, 15, 20 and 21, referring to the definitions of $g_{eff} = g_o$ and $\dot{g}$:

24) $$a_{Tr} = a_T \left[A + B(t' - t_o) \right] - g_{eff} - \dot{g}(t - t_o)$$

25) $$a_{Ty} = a_T \left[C + D(t - t_o) \right]$$

26) $$\bar{V}_{GO} = \bar{V}_T - \bar{V} - A_{11} C_{AV} \underline{i}_r \quad \text{(Equation 46)}$$

$$\hat{\lambda} = \text{Unit } (\bar{V}_{GO}) \quad \text{and}$$

27) $$a_{Tz} = (a_T - \lambda_1 a_{Tr} - \lambda_2 a_{Ty})/\lambda_3 \quad \text{(Equation 59).}$$

The desired unit thrust vector is

28) $$\underline{i}_D = \begin{bmatrix} a_{TR} \\ a_{Ty} \\ a_{Tz} \end{bmatrix} \frac{1}{(a_{TR}^2 + a_{Ty}^2 + a_{Tz}^2)^{\frac{1}{2}}} .$$

Equations 24 through 28 are in a linear tangent form, whereas the equations in Reference 54 are in a linear sine form. The above equations are

made identical to those in Reference 54 if the following approximations are made:

29) $\dot{g} \simeq 0$ (Equation 24)

30) $A_{11}C_{AV} \simeq (1/2)T_{GO}g_{eff}$ (Equation 26) and

31) $a_{TZ} \simeq (a_T^2 - a_{TR}^2 - a_{Ty}^2)^{\frac{1}{2}}$ sign $(\dot{Z}_D - \dot{Z})$ (Equation 27)

Equation 30 is not a good approximation in the early part of boost flight. A much better approximation is

$$A_{11}C_{AV} \simeq \left(\frac{1}{2a_T}\right) ABS(\bar{V}_T - \bar{V})\, g_{eff}.$$

This approximation or a more exact form should be used in the time-to-go calculation. Equation 27 yields more accurate results than Equation 31 and is simpler to implement since it eliminates logic.

The form of E Guidance in Reference 54 and in this section is limited to one-stage guidance due to the gravity model. Effective gravity is approximated as a product of thrust acceleration and a linear function of time; therefore, guidance cannot handle a discontinuity in thrust. Also, it is not a good approximation for a constant acceleration burn. A simple gravity model that eliminates these restrictions is shown in the next section. An alternate derivation of E Guidance is as follows:

$$\bar{a} = \ddot{\bar{R}} + a\left[g_{AV} + g(t - K)\right]\underline{i}_R$$

$$\bar{V}_{GO} = \bar{V}_T - \bar{V} + Lg_{AV}\underline{i}_R, \quad K = J/L$$

$$\hat{\lambda} = \text{Unit}\,(\bar{V}_{GO}), \quad \hat{\lambda}\cdot\dot{\hat{\lambda}} \simeq 0, \quad S = \hat{\lambda}\cdot\bar{R}_{GO}$$

$$\bar{R}_{GO} = \bar{R}_T - \bar{R} - \bar{V}T_{GO} + \left[Sg_{AV} + \dot{g}(Q - SK)\right]\underline{i}_R$$

$$R_{GO3} = (S - \lambda_1 R_{GO1} - \lambda_2 R_{GO3})/\lambda_3$$

$$\dot{\bar{\lambda}} = (\bar{R}_{GO} - S\hat{\lambda})/(Q - SK), \quad \dot{\lambda}^2 = \dot{\bar{\lambda}} \cdot \dot{\bar{\lambda}}$$

$$\underline{i}_D = \left[\hat{\lambda} + \dot{\bar{\lambda}}(t - t_o - K)\right] / \left[1 + \dot{\lambda}^2 (t - t_o - K)^2\right]^{\frac{1}{2}}$$

Inspection of the above equations shows that the magnitude of $\dot{\bar{\lambda}}(t - t_o - K)$ is the tangent of the angle between $\hat{\lambda}$ and $\hat{\lambda} + \dot{\bar{\lambda}}(t - t_o - K)$, and the magnitude of the latter quantity is the secant of the angle, since the magnitude of $\hat{\lambda}$ is unity.

3.0 TASK II - RIGID BODY DYNAMICS AND CONTROL ANALYSIS

Trajectory shaping techniques were developed as described in Reference 18. Drift minimum and loads minimum control laws were derived and continuously variable control gains were calculated using the methods reported in Reference 19. Design winds were synthesized using the techniques described in NASA Terrestrial Environment documents (1969 and 1971), References 20 and 21, respectively. The differences between these references were found to be insignificant to the studies as discussed in Reference 22. The NR-GD 161B/B9T Delta Wing Booster/Delta Wing Orbiter and the MSC 036B/280 inch SRM series burn configuration were analyzed during the first half of the contract period and reported in the semi-annual report (Reference 23). Since the semi-annual report, the MSC 040A/LOX propane liquid injectant TVC configuration and the parallel burn dual SRM configurations MSC 040 and MSC 049 have been analyzed. These studies are summarized in the following paragraphs.

161B/B9T

A series of studies (reported in References 24 through 35) were performed to determine the control requirements of a Delta Wing Booster/Delta Wing Orbiter, typified by the NR-GD 161B/B9T. The unsymmetrical aerodynamic and mass characteristics of this type of piggyback configuration necessitated development of analytical techniques for trajectory shaping and control gain calculations. Because thrust vector control is inadequate to prevent large roll errors, several roll control techniques were investigated, including: limiting roll engine commands to permit large roll angles without loss of pitch and yaw control; aerodynamic roll control; and yawing to decrease the aerodynamic rolling moment.

In the pitch plane, wind response studies revealed that drift minimum control can reduce trajectory dispersions about 65% as compared with a fixed gain attitude control law. The aerodynamic forces and moments were 10% higher using drift minimum but the force was still 1/3 less than the booster would experience during a 5g entry. The engine deflection

3.0 Continued

requirement was approximately ±7.5 degrees, about half of which is due to winds and the other half required to control cg travel and no wind aerodynamics. For crosswind control, ailerons were used during the high dynamic pressure region with thrust vector control only near lift-off and after 100 seconds of flight. Yawing away from the wind may also be useful for this configuration though the method of implementation would require additional study. Yawing into the wind tended to increase rather than decrease control requirements.

036B/280 SRM

The 036B/280 inch SRM booster series burn launch configuration was analyzed very briefly and found to be easily controlled in winds. Roll control used the orbiter rudder. Reference 36 contains the results of this analysis.

040A/LOX Propane

In February, 1972, the 040A/LOX propane liquid injectant TVC configuration was loaded into the SSFS Program as documented in Reference 37. A brief wind response study was performed, and it was determined (References 38 and 39) that liquid injectant requirements could be reduced from 135,000 pounds to 60,000 pounds by incorporating aerodynamic roll control. An additional study of load relief control was performed (Reference 40), and it was shown that additional injectant savings are possible by adjusting the slopes of the transition ramps from attitude control to load relief and back to attitude control.

3.1 SRM/040C CONFIGURATION ANALYSIS

The SRM/040C configuration defined in Reference 41 was loaded into the SSFS, and both lift-off and inflight analyses were conducted. The lift-off investigation is described in Reference 42. The results of 135 flight simulations were reported together with the conclusions obtained from the investigation. Two modifications of the standard vehicle were considered using equations presented in Reference 43. The first involved tilting the SRM engines while the second translated and tilted the SRM engines. The results showed that all three configurations were flyable with reasonable values of thrust misalignment and unbalance. However, with an orbiter engine failure, only the configuration with the SRM's relocated to pass their thrust through the cg at lift-off was flyable during lift-off.

The inflight analysis contained in Reference 44 included two parts: 1) control law development including an active sideslip feedback roll control system; and 2) inflight studies where the vehicle's response to wind distrubances, SRM engine misalignments, thrust unbalance and engine failure were investigated.

The control law development covered the following items:

- Reviewing the available control moment authority in the maximum dynamic pressure regime.
- Selecting an engine deflection logic to maximize control authority without excessive roll-yaw coupling.
- Modifying the basic SSFS control law to incorporate the use of rudder yaw control and rudder/aileron roll control.
- Calculating attitude control gains
- Initial design of a roll command sideslip feedback control scheme.

3.1 Continued

The inflight analysis produced several broad conclusions:

- "Simple" pitch plane load relief is inadequate for use with the sideslip control scheme - the control scheme itself minimizes $q\alpha$ and qB but positive attitude control is required to prevent excessive trajectory dispersions.

- The "back to the wind" sideslip control scheme was promising but it needed further development.

- The vehicle was satisfactorily controlled when flow in jimsphere winds. However, the more severe 95% synthetic design wind profiles sometimes produced unsatisfactory results.

- The vehicle was not successfully flown with an engine out because dynamic pressure became excessive. An engine out guidance modification would be required.

3.2 SRM/049 PARALLEL BURN CONFIGURATION ANALYSIS

In May, 1972, the SRM-049 configuration data was loaded into the SSFS program as reported in Reference 45. This vehicle was extensively analyzed both in lift-off phases of flight and in full boost to oribt dynamics and control studies as reported in References 45 through 51. In addition to the standard configuration with fixed SRM's, studies were initiated in July to investigate the use of vectorable SRM trim control.

3.2.1 Lift-Off Analysis - Nonvectorable SRM's

Results of investigations of the control capability and lift-off dynamic characteristics of the 049 launch configuration without vectorable SRM trim control have been documented in Reference 46. Lift-offs were flown in the presence of ground winds using various combinations of SRM angular misalignments and SRM thrust unbalances. Typical SRM thrust misalignments and the definition of the RMS roll yaw misalignment combination method is shown in Figure 3-1.

Results indicated that the most demanding control problems occurred with SRM misalignments that produced vehicle perturbations of -roll and -yaw with a right crosswind. Plots of roll error, pitch error, and yaw error for the right crosswind case with 0.5 degree RMS SRM misalignments in -roll and -yaw are shown in Figure 3-2.

Initially it was believed that with a right crosswind the most severe combination of roll yaw misalignments would be one with polarities of -roll/+yaw, which would be "in phase" with the wind disturbances. However, as demonstrated in Reference 46, the -roll/-yaw combination produces the more uncontrollable configuration. The reason for this is the "orientation" of the available TVC roll/yaw control torques. The -roll/-yaw combination places the control system nearer or outside the limits of control authority than does the -roll/+yaw combination. Likewise, due to symmetry, the +roll/-yaw combination is similar to the -roll/+yaw and the +roll/+yaw produces perturbations equivalent to the -roll/-yaw misalignment combination.

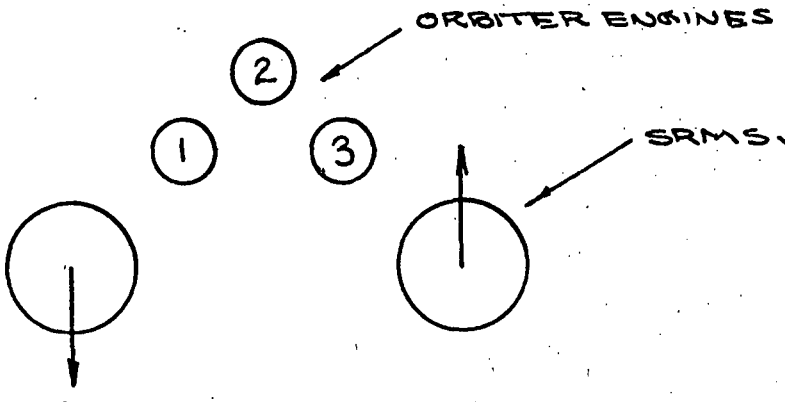

REAR VIEW OF VEHICLE SHOWING SRM MISALIGNMENTS TO PRODUCE VEHICLE PERTURBATIONS OF + ROLL

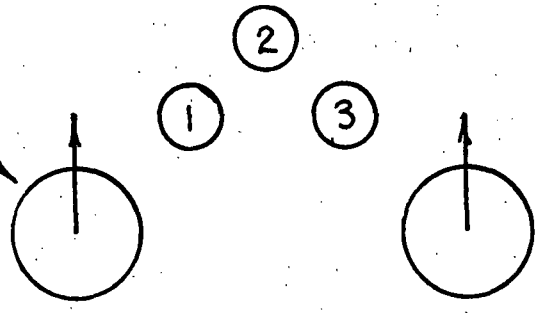

REAR VIEW OF VEHICLE SHOWING SRM MISALIGNMENTS TO PRODUCE VEHICLE PERTURBATIONS OF + PITCH

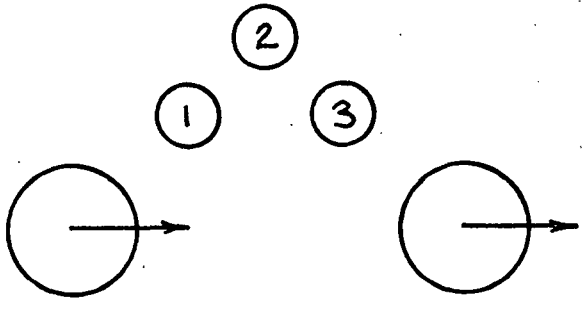

REAR VIEW OF VEHICLE SHOWING SRM MISALIGNMENTS TO PRODUCE VEHICLE PERTURBATIONS OF + YAW

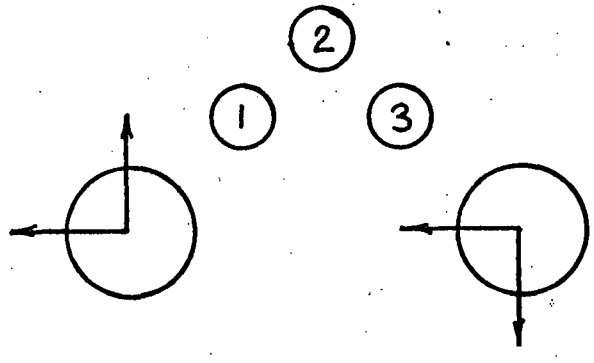

REAR VIEW OF VEHICLE SHOWING SRM MISALIGNMENTS TO PRODUCE VEHICLE PERTURBATIONS OF
1° RMS - ROLL - YAW COMBINATION
$\delta_p = 1°/\sqrt{2} = .707°$
$\delta_y = 1°/\sqrt{2} = .707°$

FIGURE 3-1 – TYPICAL SRM THRUST MISALIGNMENTS

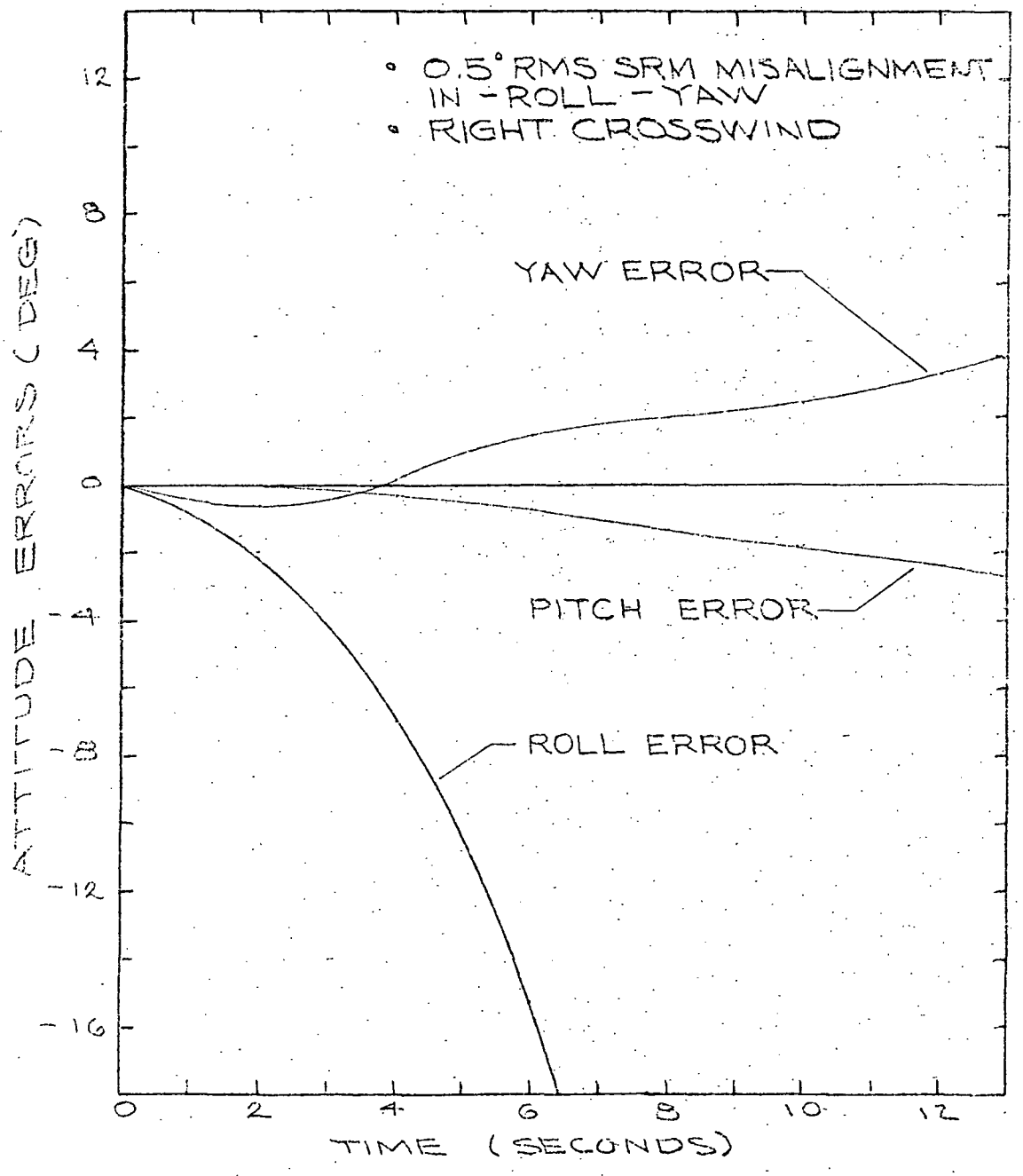

FIGURE 3-2 LIFTOFF RESULTS - 0.5° MISALIGNMENT - ATTITUDE ERRORS

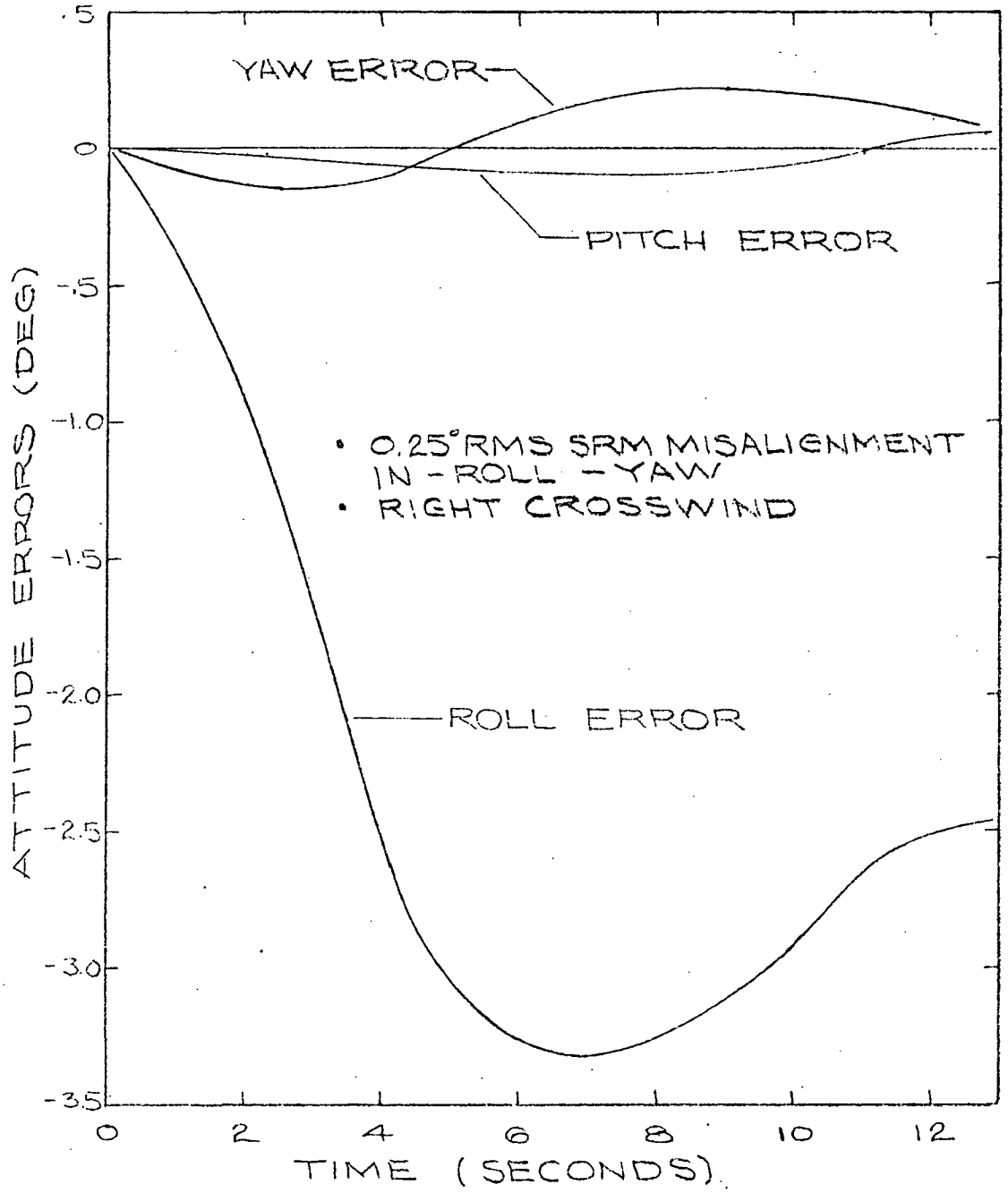

FIGURE 3-3 **LIFTOFF RESULTS - 0.25° MISALIGNMENT - ATTITUDE ERRORS**

3.2.1 Continued

Results of simulations flown with 0.25° RMS SRM misaligments were observed to produce no uncontrollable characteristics. Roll and yaw attitude errors for the +roll/-yaw and -roll/+yaw combinations of misalignments for all winds were found to be of the damped oscillatory form. Maximum engine deflections were on the order of 2 degrees, with maximum attitude errors of approximately 1 degree for these misalignments.

For those simulations performed with -roll/-yaw combinations of 0.25° RMS SRM misalignments, it was observed that the engines would momentarily hit their limits in pitch, but as control was regained, engine deflections were reduced. An example of these types of misalignments, attitude errors for the crosswind simulation with -roll/-yaw combinations of 0.25° RMS SRM misalignments are shown in Figure 3-3. As illustrated in this plot after approximately 6 seconds, control is regained and engine deflections and attitude errors begin to decrease.

Drift distances at tower clearnace for the simulations performed were found to be of acceptable magnitude, i.e., on the order of 2 to 3 feet. Exceptions to this were those flights with thrust unbalance; these cases produced crossrange drift distances approximately twice that of similar simulations without thrust unbalance. However, these were still felt to be within acceptable limits.

3.2.2 Inflight Response - Nonvectorable SRM's

Inflight response of the SRM/049 configuration to SRM misalignments, winds, and control system modifications has been documented in References 47 and 48. The SRM-049 vehicle simulation was "flown" from lift-off to orbital insertion using a wind matrix composed of winds shearing to gusts at 10K, 20K, and 40K feet. Eastern test range 95 percentile winds were used as tailwinds and crosswinds; they reach a maximum velocity of 75 meters per second. However, the maximum 95 percentile headwind velocity

3.2.2 Continued

for the eastern test range is only 28 meters per second. Hence, the 42-meter per second Vandenberg Air Force Base wind was used for headwinds.

In addition to the six wind velocity profiles investigated, consideration was given to inflight changes of wind direction or azimuth. Wind azimuth change profiles were prepared as directed by MSC/G&C Division. The wind matrix thus consisted of: fixed azimuth head, tail and crosswinds; winds that started as head, tail and crosswinds and then sheared away from these azimuths as the gust was approached; and winds that started an appropriate distance away from the nominal azimuth (both clockwise and counterclockwise) and then sheared to the nominal direction at the gust. In all cases the wind azimuth remained constant both below and above the 2KM change region. Wind velocity and azimuth change profiles used are tabulated in Tables 3-1 through 3-7.

Drift minimum control using accelerometer feedback as described in Reference 21 was employed in both pitch and yaw. The control gains were varied continuously to maintain a natural frequency of one radian per second and a damping ratio of one-half. This provided a resonant frequency of about 0.14 Hz which should be low enough to minimize control interaction with structural bending and propellant slosh. No load relief methods were used in pitch or yaw in these studies.

Four roll control techniques were investigated. The first was a simple attitude and attitude rate damping system. The second system added proportional and integral sideslip feedback to the roll attitude channel in order to roll the vehicle tail into the wind and decrease sideslip. The third technique was the same as the second except a higher natural control frequency was investigated. The fourth scheme was the same as the second except the proportional sideslip signal was fed to the roll rate channel. The fourth control scheme was selected as a new baseline for

VANDENBERG WESTERN TEST RANGE 10K SHEAR GUST WITH AZIMUTH SHEAR				
ALTITUDE (M)	VELOCITY (M/S)	HEADWIND AT LIFTOFF (CLOCKWISE SHEAR) (DEG)	HEADWIND AT MAX Q (CLOCKWISE SHEAR) (DEG)	HEADWIND AT MAX Q (COUNTER CW SHEAR) (DEG)
0	0	38.3	-36.7	113.3
1000	2.9	38.3	-36.7	113.3
1650	4.7	73.3	-1.7	78.3
2050	5.9	85.3	10.3	66.3
2650	12.1	102.3	27.3	49.3
3050	19.0	113.3	38.3	38.3
3080	25.5	113.3	38.3	38.3
3280	25.5	113.3	38.3	38.3
3310	20.2	113.3	38.3	38.3
4000	23.	113.3	38.3	38.3
5000	27.	113.3	38.3	38.3
6000	31.	113.3	38.3	38.3
10000	42.	113.3	38.3	38.3
14000	42.	113.3	38.3	38.3
20000	7.	113.3	38.3	38.3
23000	7.	113.3	38.3	38.3
50 000	60.	113.3	38.3	38.3
60 000	60.	113.3	38.3	38.3
75 000	32.	113.3	38.3	38.3
80 000	32.	113.3	38.3	38.3

TABLE 3-1

HEADWIND PROFILES - 10K VANDENBERG,
WESTERN TEST RANGE

VANDENBERG WESTERN TEST RANGE
28K SHEAR GUST WITH AZIMUTH SHEAR

ALTITUDE (M)	VELOCITY (M/S)	HEADWIND AT LIFTOFF (CLOCKWISE SHEAR) (DEG)	HEADWIND AT MAX Q (CLOCKWISE SHEAR) (DEG)	HEADWIND AT MAX Q (COUNTER CW SHEAR) (DEG)
0	0.	38.3	-1.7	79.3
6540	11.2	38.3	-1.7	79.3
6940	12.5	56.3	15.3	61.3
7340	14.0	64.8	23.8	52.8
7540	14.4	68.3	27.3	49.3
7940	21.4	73.1	32.1	44.5
8140	25.6	75.3	34.3	42.3
8440	33.3	78.3	37.3	39.3
8540	38.0	79.3	38.3	38.3
8570	44.5	79.3	38.3	38.3
8770	44.5	79.3	38.3	38.3
8800	38.5	79.3	38.3	38.3
10000	42.	79.3	38.3	38.3
14000	42.	79.3	38.3	38.3
20000	7.	79.3	38.3	38.3
23000	7.	79.3	38.3	38.3
50000	60.	79.3	38.3	38.3
60000	60.	79.3	38.3	38.3
75000	32.	79.3	38.3	38.3
80000	32.	79.3	38.3	38.3

HEADWIND PROFILES - 28K VANDENBERG,
WESTERN TEST RANGE

TABLE 3-2

VANDENBERG WESTERN TEST RANGE
40K SHEAR GUST WITH AZIMUTH SHEAR

ALTITUDE (M)	VELOCITY (M/S)	HEADWIND AT LIFTOFF (CLOCKWISE SHEAR) (DEG)	HEADWIND AT MAXQ (CLOCKWISE SHEAR) (DEG)	HEADWIND AT MAXQ (COUNTERCW SHEAR) (DEG)
0	0	38.3	1.9	74.7
2000	3.	38.3	1.9	74.7
5000	7.5	38.3	1.9	74.7
10200	15.2	38.3	1.9	74.7
10600	16.3	54.3	17.9	58.7
11000	17.5	62.3	25.9	50.7
11200	18.4	65.1	28.7	47.9
11600	25.4	69.3	32.9	43.7
12000	34.4	73.3	36.9	39.7
12200	42.0	74.7	38.3	38.3
12230	48.5	74.7	38.3	38.3
12430	48.5	74.7	38.3	38.3
12460	42.	74.7	38.3	38.3
14000	42.	74.7	38.3	38.3
20000	7.	74.7	38.3	38.3
23000	7.	74.7	38.3	38.3
50000	60.	74.7	38.3	38.3
60000	60.	74.7	38.3	38.3
75000	32.	74.7	38.3	38.3
80000	32.	74.7	38.3	38.3

HEADWIND PROFILES - 40K VANDENBERG,
WESTERN TEST RANGE

TABLE 3-3

EASTERN TEST RANGE
10 K SHEAR GUST WITH AZIMUTH SHEAR

ALTITUDE (M)	VELOCITY (M/S)	RIGHT XWD AT MAX Q (CLOCKWISE SHEAR) (DEG)	RIGHT XWD AT MAX Q (COUNTER CW SHEAR) (DEG)	LEFT XWD AT MAX Q (CLOCKWISE SHEAR) (DEG)	LEFT XWD AT MAX Q (COUNTER CW SHEAR) (DEG)	TAILWIND AT MAX Q (CLOCKWISE SHEAR) (DEG)	TAILWIND AT MAX Q (COUNTER C SHEAR) (DEG)
0	0.	80.3	176.3	260.3	356.3	170.3	266.3
1050	8.0	80.3	176.3	260.3	356.3	170.3	266.3
1250	9.5	91.2	165.4	271.2	345.4	181.3	255.3
1650	12.5	105.9	150.7	285.9	330.7	195.9	240.7
2050	15.6	114.5	142.1	294.5	322.1	204.5	232.1
2450	21.0	119.8	136.8	299.8	316.8	209.8	226.8
2850	27.8	125.6	131.0	305.6	311.0	215.6	221.0
2950	29.8	126.9	129.7	306.9	309.7	216.9	219.7
3050	33.3	128.3	128.3	308.3	308.3	218.3	218.3
3380	39.8	128.3	128.3	308.3	308.3	218.3	218.3
3580	39.8	128.3	128.3	308.3	308.3	218.3	218.3
3610	35.0	128.3	128.3	308.3	308.3	218.3	218.3
10000	75.0	128.3	128.3	308.3	308.3	218.3	218.3
14000	75.0	128.3	128.3	308.3	308.3	218.3	218.3
20000	25.0	128.3	128.3	308.3	308.3	218.3	218.3
23000	25.0	128.3	128.3	308.3	308.3	218.3	218.3
50000	120.0	128.3	128.3	308.3	308.3	218.3	218.3
60000	120.0	128.3	128.3	308.3	308.3	218.3	218.3
75000	90.0	128.3	128.3	308.3	308.3	218.3	218.3
80000	90.0	128.3	128.3	308.3	308.3	218.3	218.3

CROSS AND TAILWIND PROFILES-
10K EASTERN TEST RANGE

TABLE 3-4

EASTERN TEST RANGE
28K SHEAR GUST WITH AZIMUTH SHEAR

ALTITUDE (M)	VELOCITY (M/S)	RIGHT XWD AT MAX Q (CLOCKWISE SHEAR) (DEG)	RIGHT XWD AT MAX Q (COUNTER CW SHEAR) (DEG)	LEFT XWD AT MAX Q (CLOCKWISE SHEAR) (DEG)	LEFT XWD AT MAX Q (COUNTER CW SHEAR) (DEG)	TAILWIND AT MAX Q (CLOCKWISE SHEAR) (DEG)	TAILWIND AT MAX Q (COUNTER CW SHEAR) (DEG)
0	0	109.3	147.3	289.3	327.3	199.3	237.3
5540	28.4	109.3	147.3	289.3	327.3	199.3	237.3
6540	33.5	109.3	147.3	289.3	327.3	199.3	237.3
6740	35.0	114.2	142.4	294.2	322.4	204.2	232.4
7140	37.9	116.8	139.8	296.8	319.8	206.8	229.8
7540	40.8	118.8	137.8	298.8	317.8	208.8	227.8
7940	48.3	122.4	134.2	302.4	314.2	212.4	224.2
8340	58.0	124.8	131.8	1304.8	311.8	214.8	221.8
8540	66.3	125.9	130.7	305.9	310.7	215.9	220.7
8570	72.8	128.3	128.3	308.3	308.3	218.3	218.3
8770	72.8	128.3	128.3	308.3	308.3	218.3	218.3
8800	67.8	128.3	128.3	308.3	308.3	218.3	218.3
10 000	75.0	128.3	128.3	308.3	308.3	218.3	218.3
14 000	75.0	128.3	128.3	308.3	308.3	218.3	218.3
20 000	25.0	128.3	128.3	308.3	308.3	218.3	218.3
23000	25.0	128.3	128.3	308.3	308.3	218.3	218.3
50 000	120.0	128.3	128.3	308.3	308.3	218.3	218.3
60 000	120.0	128.3	128.3	308.3	308.3	218.3	218.3
75 000	90.0	128.3	128.3	308.3	308.3	218.3	218.3
80 000	90.0	128.3	128.3	308.3	308.3	218.3	218.3

CROSS AND TAILWIND PROFILES -
28K EASTERN TEST RANGE

TABLE 3-5

EASTERN TEST RANGE
40K SHEAR GUST WITH AZIMUTH SHEAR

ALTITUDE (M)	VELOCITY (M/S)	RIGHT XWD AT MAX Q (CLOCKWISE SHEAR) (DEG)	RGHT XWD AT MAX Q (COUNTER CW SHEAR) (DEG)	LEFT XWD AT MAX Q (CLOCKWISE SHEAR) (DEG)	LEFT XWD AT MAX Q (COUNTER CW SHEAR) (DEG)	TAILWIND AT MAX Q (CLOCKWISE SHEAR) (DEG)	TAILWIND AT MAX Q (COUNTER CW SHEAR) (DEG)
0	0	115.3	141.3	295.3	321.3	205.3	231.3
7200	27.4	115.3	141.3	295.3	321.3	205.3	231.3
9200	35.0	115.3	141.3	295.3	321.3	205.3	231.3
10200	40.6	115.3	141.3	295.3	321.3	205.3	231.3
10400	42.2	118.3	138.3	298.3	318.3	208.3	228.3
10800	45.3	122.3	134.3	302.3	314.3	212.3	224.3
11200	48.5	124.8	131.8	304.8	311.8	214.8	221.8
11600	56.5	125.9	130.7	305.9	310.7	215.9	220.7
12000	66.4	127.5	129.1	307.5	309.1	217.9	219.1
12200	75.0	128.3	128.3	308.3	308.3	218.3	218.3
12230	81.5	128.3	128.3	308.3	308.3	218.3	218.3
12430	81.5	128.3	128.3	308.3	308.3	218.3	218.3
12460	75.0	128.3	128.3	308.3	308.3	218.3	218.3
14000	75.0	128.3	128.3	308.3	308.3	218.3	218.3
20000	25.0	128.3	128.3	308.3	308.3	218.3	218.3
23000	25.0	128.3	128.3	308.3	308.3	218.3	218.3
50000	120.0	128.3	128.3	308.3	308.3	218.3	218.3
60000	120.0	128.3	128.3	308.3	308.3	218.3	218.3
75000	90.0	128.3	128.3	308.3	308.3	218.3	218.3
80000	90.0	128.3	128.3	308.3	308.3	218.3	218.3

CROSS AND TAILWIND PROFILES -
40K EASTERN TEST RANGE

TABLE 3-6

EASTERN TEST RANGE
10K SHEAR GUST WITH AZIMUTH SHEAR
(REDUCED VELOCITY PROFILE)

ALTITUDE (M)	VELOCITY (M/S)	RIGHT QUACTERING HEADWIND (CLOCKNISE SHEAR) (DEG)	LEFT QUARTERING HEADWIND (CLOCKWISE SHEAR) (DEG)	RIGHT QUART. HEADWIND (COUNTER CW SHEAR) (DEG)	LEFT QUART. HEADWIND (COUNTER CW SHEAR) (DEG)
0	0	35.3	-54.7	131.3	41.3
1050	6.9	35.3	-54.7	131.3	41.3
1250	8.2	46.2	-43.8	120.4	30.4
1650	10.8	60.9	-29.1	105.7	15.7
2050	13.5	69.5	-20.5	97.1	7.1
2450	18.2	74.8	-15.2	91.8	1.8
2850	24.1	80.6	-9.4	86.0	-4.0
2950	25.8	81.9	-8.1	84.7	-5.3
3050	28.9	83.3	-6.7	83.3	-6.7
3380	36.5	83.3	-6.7	83.3	-6.7
3580	36.5	83.3	-6.7	83.3	-6.7
3610	30.4	83.3	-6.7	83.3	-6.7
10 000	65.0	83.3	-6.7	83.3	-6.7
14 000	65.0	83.3	-6.7	83.3	-6.7
20 000	21.7	83.3	-6.7	83.3	-6.7
23000	21.7	83.3	-6.7	83.3	-6.7
50000	104.0	83.3	-6.7	83.3	-6.7
60000	104.0	83.3	-6.7	83.3	-6.7
75000	78.0	83.3	-6.7	83.3	-6.7
80000	78.0	83.3	-6.7	83.3	-6.7

QUARTERING HEADWIND PROFILES

TABLE 3-7

3.2.2 Continued

additional studies. These four control techniques and related parameters are summarized below.

	ROLL CONTROL TECHNIQUES				
	ω_n	ζ	Proportional Feedback	Integral Feedback	Proportional Feedback As Roll Rate Command
1	0.5	0.5	NO	No	No
2	0.5	0.5	Yes $K = 4$	Yes $K_I = .4\ T$	No
3	1.0	0.5	Yes $K = 4$	Yes $K_I = .4\ T$	No
4	0.5	0.5	No	Yes $K_I = .4\ T$	Yes $K = 4$

The baseline roll, yaw and pitch flight control techniques used are illustrated schematically in Figure 3-4. Notice that the rudder is used for roll control; it uses the same gains as for thrust vector control. The engines and the rudder were limited to ±10 degrees deflection.

With simple attitude control of roll (no sideslip feedback) all cases flew to orbit. The injected weight varied from 351,000 pounds for a headwind to 354,000 pounds for a tailwind (no wind is 352,500 pounds).

Maximum dynamic pressure (q) and positive $q\alpha$ were observed for a constant azimuth 40,000 ft headwind where q reached 569 lbs/ft^2 and $q\alpha$ reached 3848 degree-lbs/ft^2. The time history of these variables is shown in Figures 3-5 and 3-6. (The machine plot miss the 3838 momentary peak.) The highest negative $q\alpha$ was -2964 (Figure 3-7) for the 28,000 foot constant azimuth tailwind. The engines just reach the 10° stops as shown in Figure 3-8. (The scalloped deflection curves reflect the linear interpolation of the pitch command table.) Since the maximum headwind deflection is only 8.5°, the engine bias could be shifted about 1° to -16°.

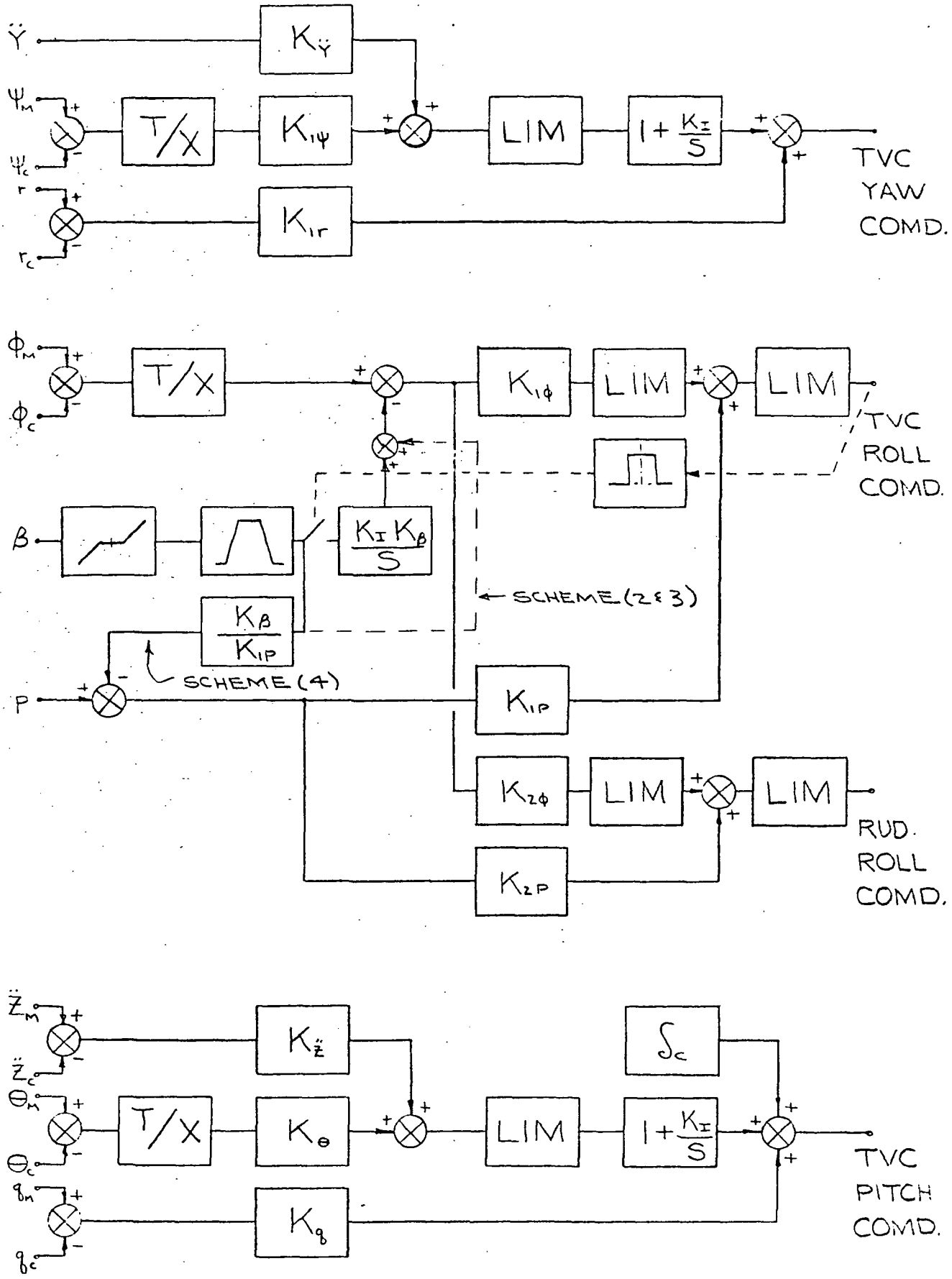

FIGURE 3-4

CONTROL SYSTEM SHOWING SEVERAL SIDESLIP ROLL COMMAND SCHEMES

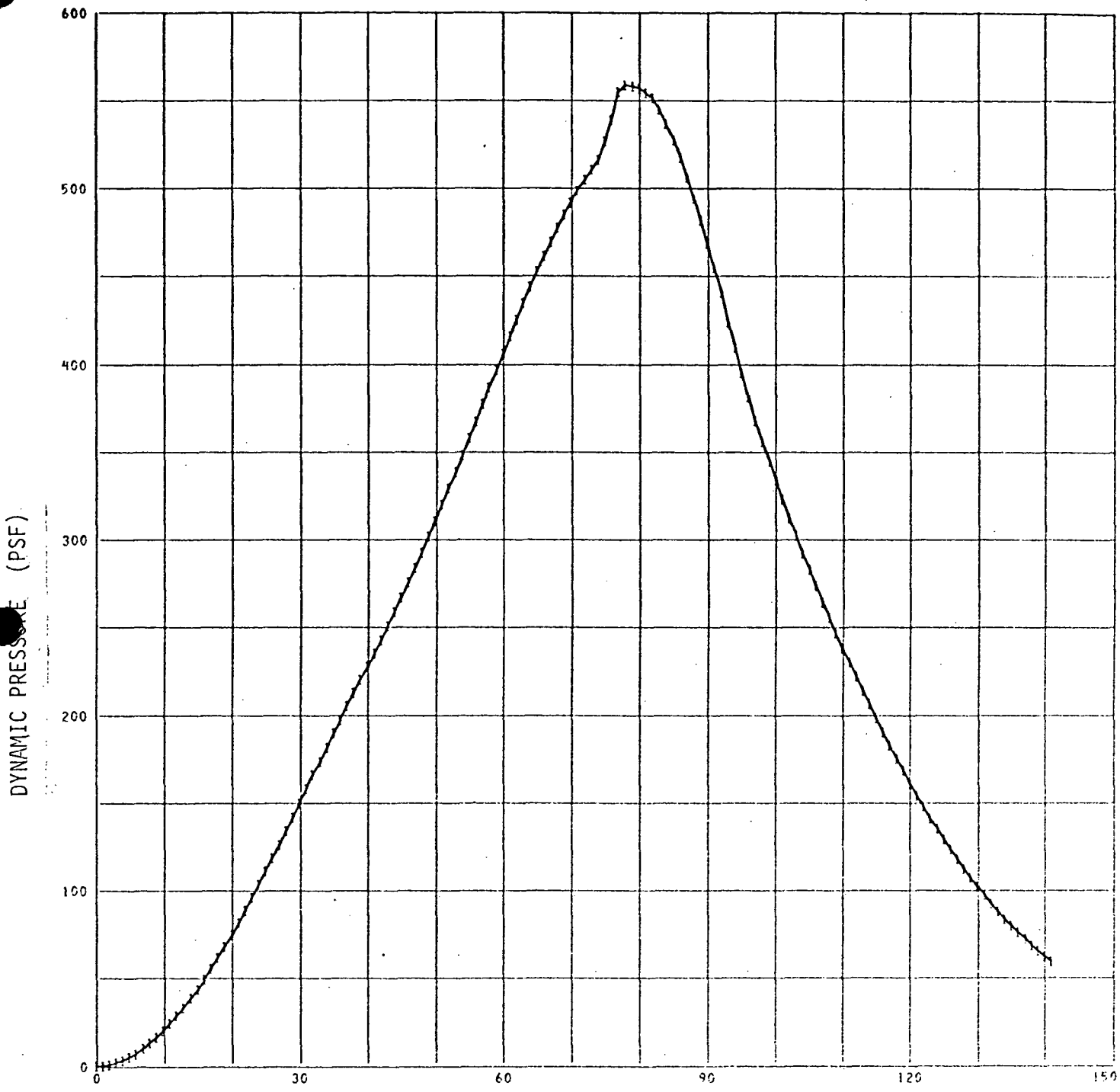

FIGURE 3-5

INFLIGHT RESULTS - NO SIDESLIP FEEDBACK 40K
HEADWIND - DYNAMIC PRESSURE

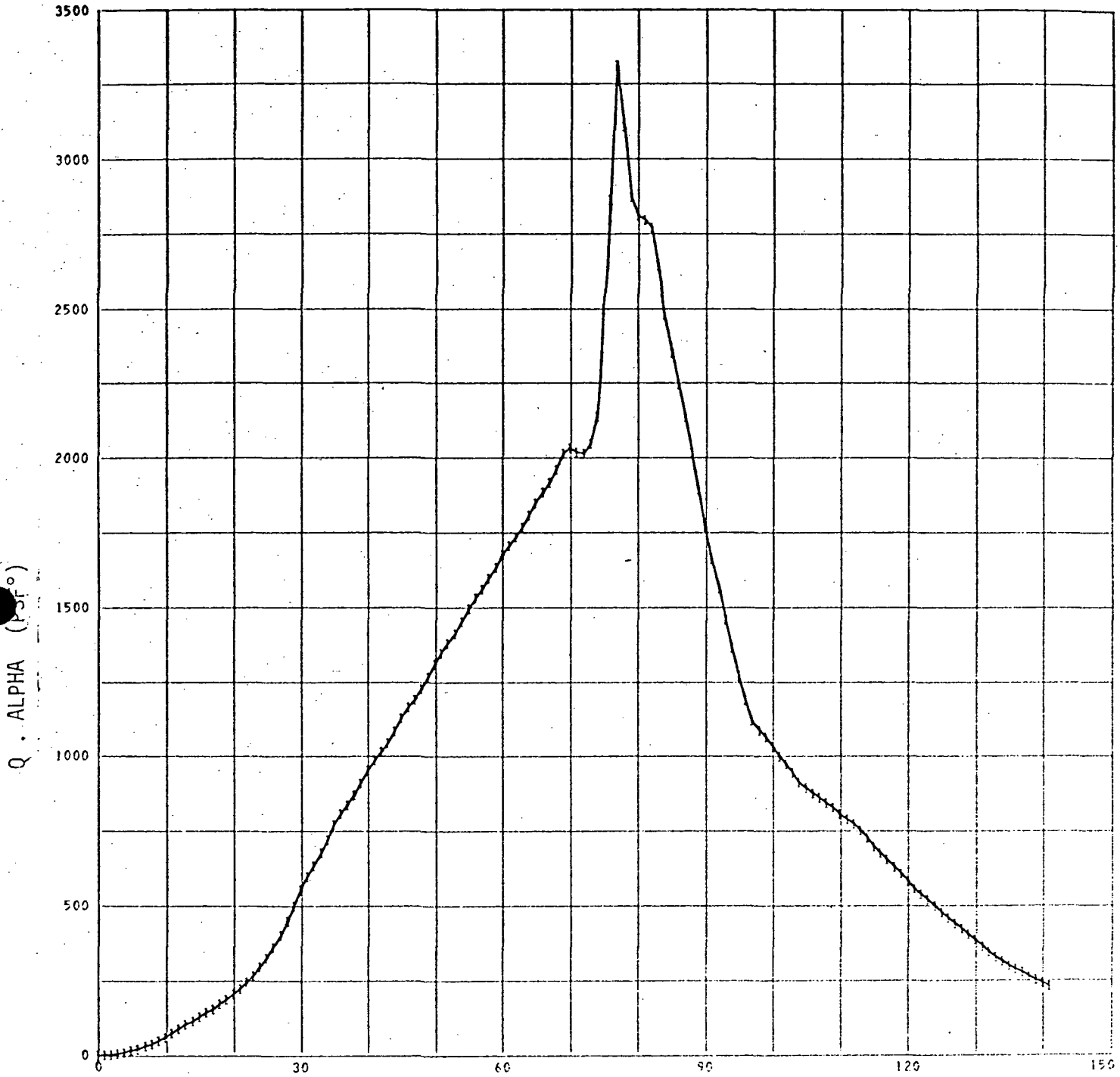

FIGURE 3-6

INFLIGHT RESULTS - NO SIDESLIP FEEDBACK -
40K HEADWIND - Q-ALPHA

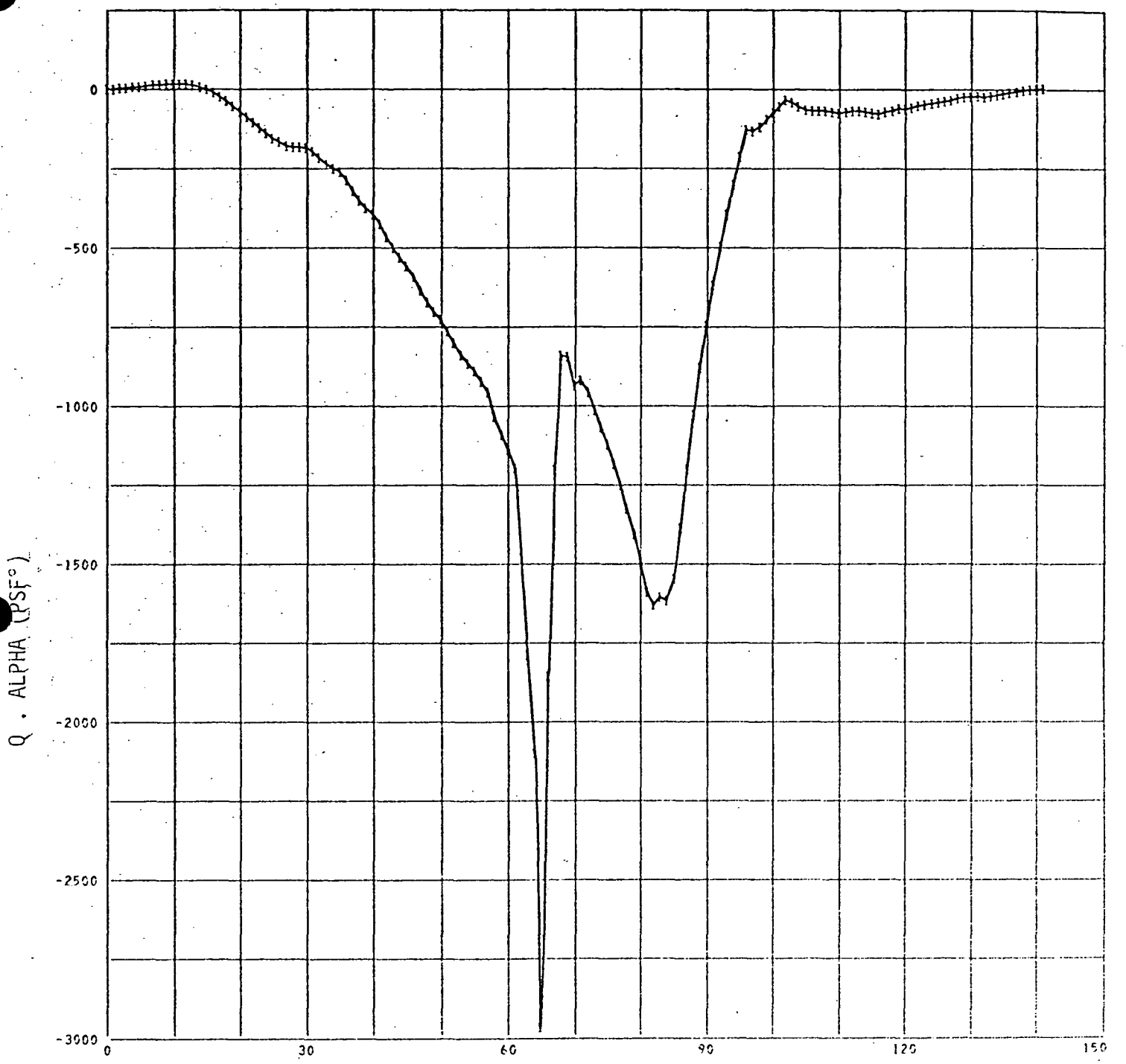

FIGURE 3-7

INFLIGHT RESULTS - NO SIDESLIP FEEDBACK - 28K TAILWIND - Q-ALPHA

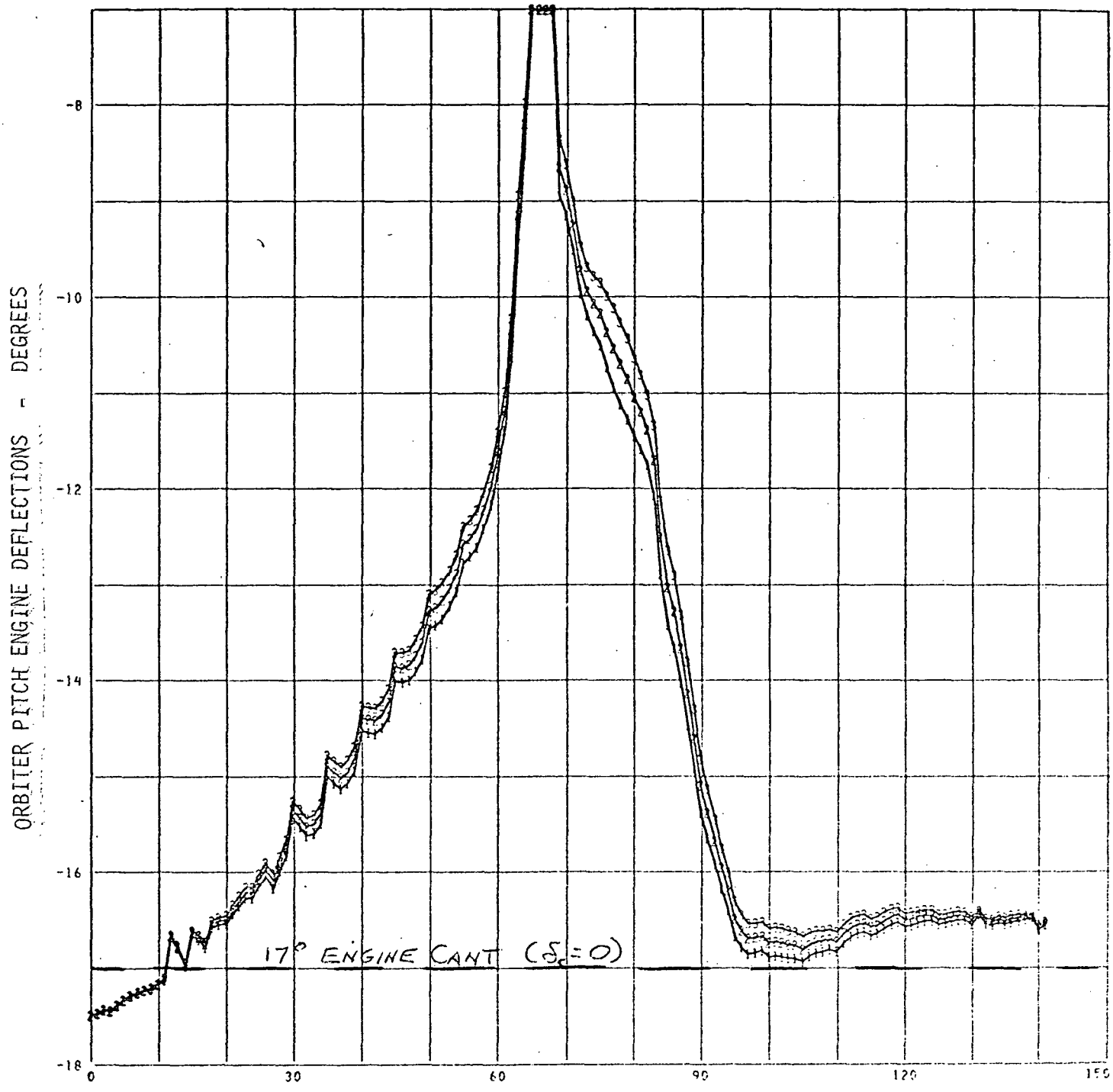

FIGURE 3-8

INFLIGHT RESULTS - NO SIDESLIP FEEDBACK -
28K TAILWIND - ORBITER PITCH ENGINE DEFLECTION

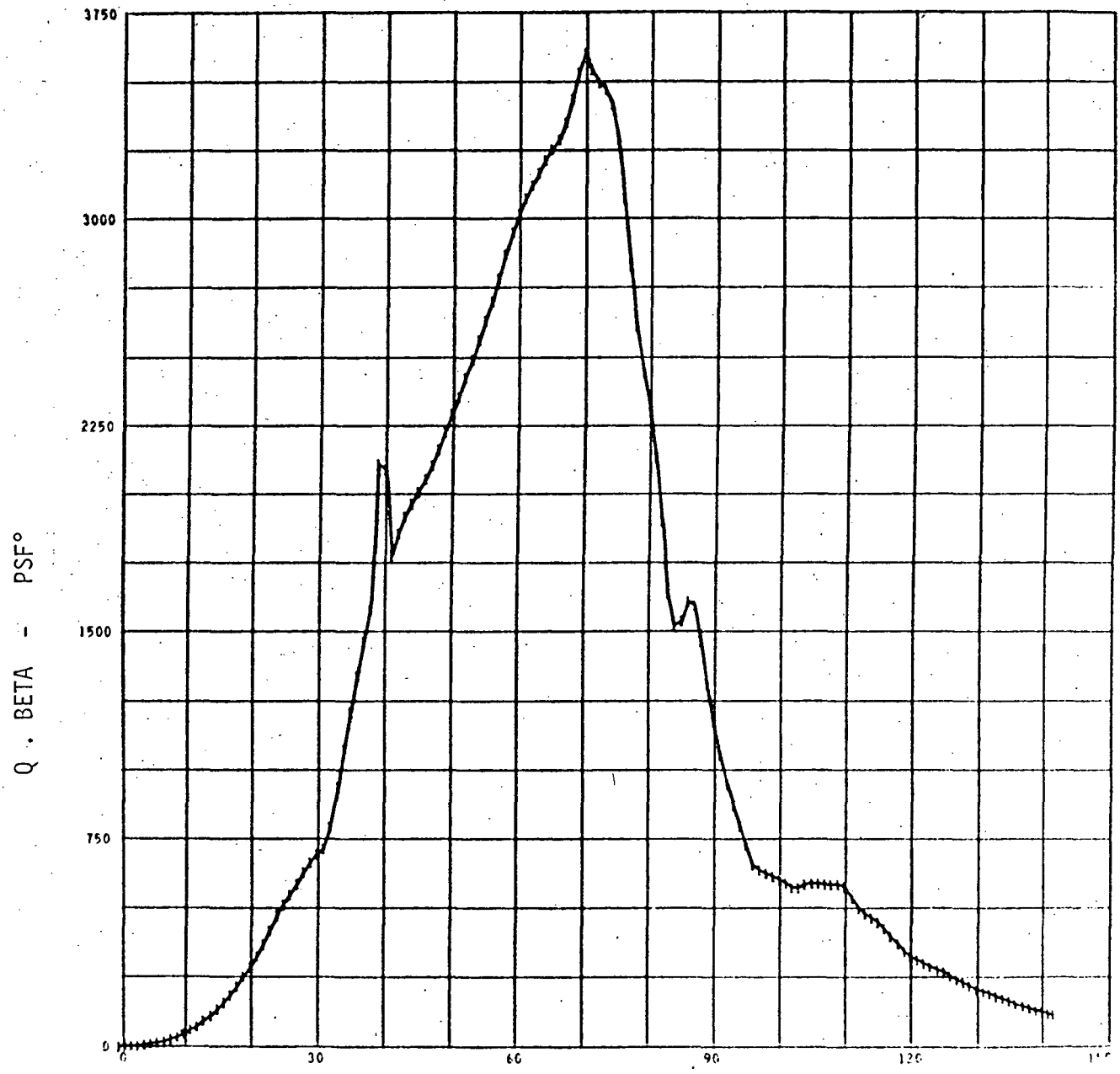

TIME - SECONDS

FIGURE 3-9

INFLIGHT RESULTS - NO SIDESLIP FEEDBACK -
10K CROSSWIND - Q-BETA

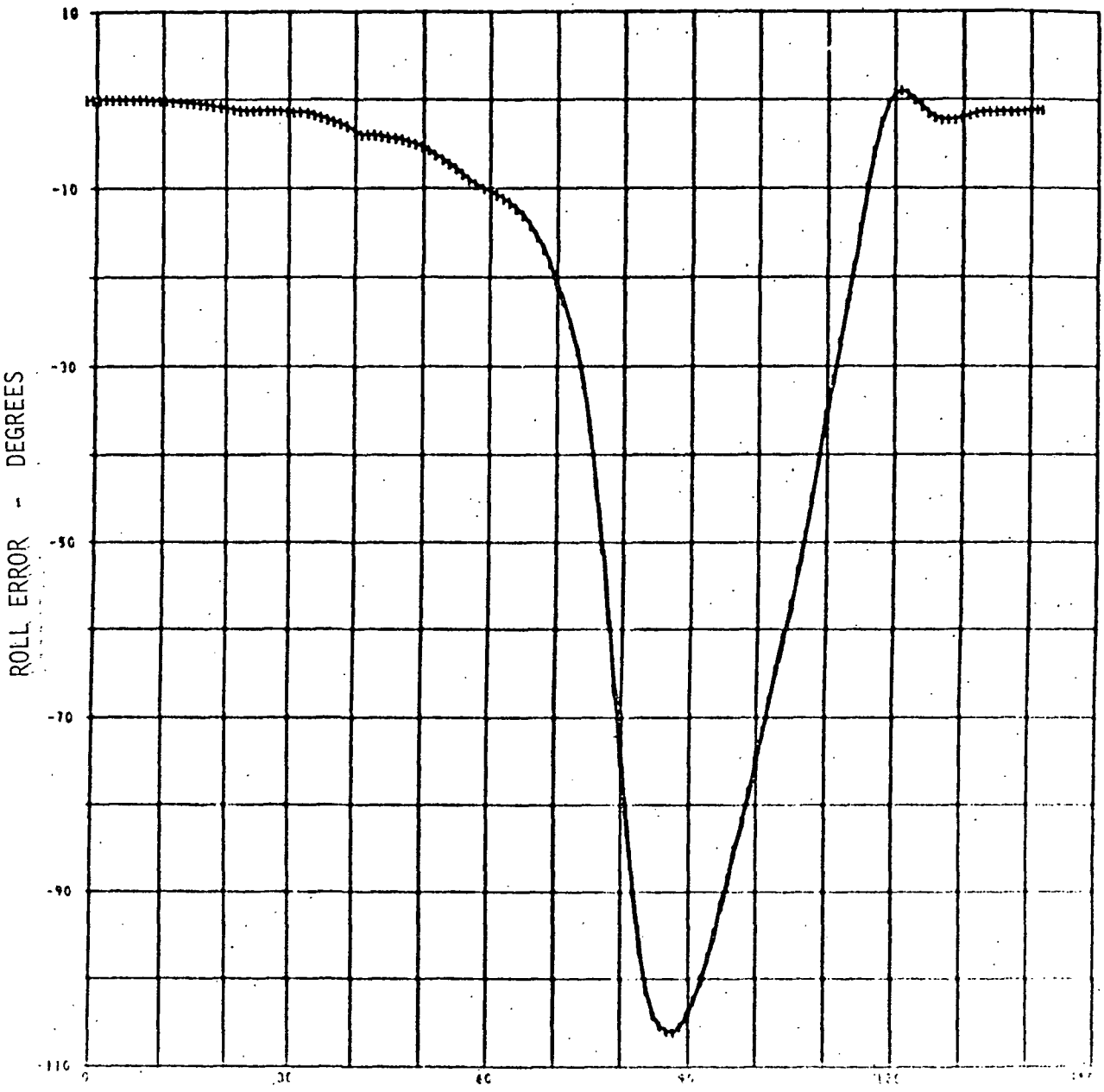

FIGURE 3-10

INFLIGHT RESULTS - NO SIDESLIP FEEDBACK - 10K CROSSWIND - ROLL ERROR

3.2.2 Continued

Maximum $q\beta$ went as high as 4806 for the 28,000 ft crosswind that swings around to approach a tailwind. Roll control authority even with rudder added is inadequate to hold $q\beta$ above about 3000 degree-lb/ft^2. Roll control was lost during the high q region for all crosswind cases and the lower altitude azimuth shear tailwinds which approach crosswinds after the shear. Figures 3-9 and 3-10 are $q\beta$ and roll error histories for the 10,000 foot shear crosswind.

Proportional plus integral sideslip feedback (control scheme 2) was added, as shown in Figure 3-4, to roll the vehicle to a tail into the wind orientation. (The input to the integrator is opened to prevent control saturation if the engine deflection command exceeds eight degrees.) This modification decreased the 28,000 ft $q\beta$ crosswind from 4806 to 910. The maximum $q\beta$ for this scheme was 2980 for a 40,000 foot crosswind.

Roll attitude errors remained as high as 54 degrees for control scheme 2 because of slow vehicle response. The natural frequency was then increased to 1.0 radian per second (control scheme 3). The result was to increase the roll attitude error (up to 83 degrees) because the scaled error signal reached the eight-degree limit and this combined with the increased rate gain limited the roll rate command capability to an even smaller value than previously.

The proportional part of the sideslip signal was then transferred to the rate channel as shown in Figure 3-4 (scheme 4). This eliminated the sluggish response and reduced roll attitude errors to less than 10 degrees.

Table 3-8 summarizes the results of these studies. This table lists all cases in which $q\alpha$ exceeded $\pm$3,000 degree-lbs/ft^2. All cases were below 4,000 and all were headwinds except for the 28K ft. crosswind without sideslip feedback. This case lost roll control in the high q region

3.2.2 Continued

because of the high sideforce and turned belly to the wind similar to the 10,000 ft case shown in Figures 3-9 and 3-10.

Table 3-8b lists all cases in which $q\beta$ exceeds ±3,000 degree-lbs/ft^2. The principal cases were the crosswinds without sideslip feedback. With sideslip feedback none of the cases exceeded 3000 except for the 28K shear from a headwind case with the rate command scheme. For this wind profile there is no sideslip until the wind azimuth started to chage at about 22,000 feet. For this case the vehicle rolled through a high sideslip angle region. The similar lower altitude cases had a lower dynamic pressure so $q\beta$ stayed lower, whereas at higher altitudes the wind velocity started to decrease soon enough to prevent β from reaching a large value so $q\beta$ remained below 3000. β also stayed lower for the cases without the rate command signal, although it is not clear why the slower response should have produced this result.

Table 3-8c contains those cases where the weight at orbit insertion differed from nominal by more than 1,000 pounds. Of the twelve cases listed four had weight gains resulting from tailwinds adding energy. Seven of the eight weight loss cases where headwinds and the most severe weight losses were headwind cases using sideslip feedback. Without sideslip feedback the headwind losses were less than 1500 pounds.

Table 3-8d lists the cases which had roll errors exceeding ten degrees. Large errors were experienced generally, until the proportional part of the sideslip signal was applied as a rate command. This control scheme improved vehicle response time sufficiently to keep the error less than ten degrees.

SRM perturbations considered were thrust misalignments and thrust unbalance. Lift-off studies had shown negligible problems with pitch misalignments of 0.25 degree so the inflight analysis was performed with combined

3.2.2 Continued

roll-yaw misalignments of 0.1768 degree in each direction. (0.1768 x 2 = 0.25). The thrust unbalance consisted of 2.5 percent increased thrust for one SRM and 2.5 percent decreased thrust for the other one.

The results are summarized in Table 3-9. None of the cases reached 4,000 degree-lbs/ft^2 for $q\alpha$ or $q\beta$ and most of those exceeding 3,000 were headwinds with sideslip feedback. The only crosswind cases with q exceeding 3,000 were those in which the misalignments and thrust unbalance tend to force the vehicle to roll and yaw away from the wind. These cases are marginal and misalignments much greater than 0.25 degree would result in loss of control.

Many cases showed weight losses exceeding 1,000 pounds. Only headwind cases exceeded 4,000 pounds weight loss and check cases of headwinds without sideslip feedback revealed no significant weight differences with and without roll-yaw misalignments.

A gain of 4 was originally selected for the feedback signal. Parameterization of these gains is shown in Figure 3-11. From this graph it is seen that these values were well chosen.

In summary, these studies demonstrated that, if SRM misalignments can be held to 0.25 degree or less and sideslip feedback is used when winds in the high q region are known to be more than 45 degrees away from headwinds, it appears that:

$q\alpha$ can be held below 4,000 degree-lbs/ft^2

$q\beta$ can be held below 3,500 degree-lbs/ft^2

weight to orbit can be held within 2500 lbs of nominal (for nominal thrust history).

TABLE 3-8 - CASES EXCEEDING CERTAIN VALUES - NOMINAL VEHICLE

3-8a. $q\alpha$ Greater than $\pm$3000 Degree-lb/ft^2

	$q\alpha$
No sideslip feedback ω = 0.5	
All headwinds - (Constant Azimuth are highest)	
10K Constant Azimuth Headwind	3572
28K Constant Azimuth Headwind	3742
40K Constant Azimuth Headwind	3848
28K Shear Clockwise from right crosswind	3072
Sideslip Feedback ω = 0.5	
Constant Azimuth Headwinds (same as above)	
40K Shear from headwind	3407
Sideslip Feedback ω = 1.0	
Constant Azimuth Headwinds (same as above)	
40K Shear from Headwind	3174
Sideslip Feedback Plus Rate Command ω=0.5	
Constant Azimuth Headwinds (Same as above)	
40K Shear from Headwind	3077
40K Shear to Headwind	3566

3-8b. $q\beta$ Greater than $\pm$3000 Degree-lb/ft^2

	$q\beta$
No sideslip feed back ω = 0.5	
10K Crosswind	3598
10K Shear from Tailwind	-3945
28K Shear Clockwise from Right crosswind	4806
40K Shear Clockwise from Right Crosswind	4333
Sideslip Feedback ω = 0.5, 1.0	
None	
Sideslip Feedback Plus Rate Command	
28K Shear from Headwind	3358

TABLE 3-8 (Continued)

3-8c. Delta Weight to Orbit Greater than 1000 lb.

No Sideslip Feedback	
10K Constant Azimuth Headwind	-1480 lb
10K Shear to Headwind	-1480
28K Constant Azimuth Headwind	-1420
28K Shear to Headwind	-1420
40K Constant Azimuth Tailwind	+2300
40K Shear from Tailwind	+1230
10K Constant Azimuth Tailwind	+1030
Sideslip Feedback ω = 0.5	
Constant Azimuth Winds (Same as above)	
Sideslip Feedback ω = 1.0	
Constant Azimuth Winds (Same as above)	
10K Shear from Tailwind	-1480
Sideslip Feedback + Rate Command ω = 0.5	
Constant Azimuth Winds (Same as above)	
10K Shear Clockwise from Right Crosswind	+1285
10K Shear to Headwind	-4550
28K Shear to Headwind	-3540
40K Shear to Headwind	-1870

3-8d. Roll Error Greater than Ten Degrees

No sideslip feedback ω = 0.5	
All Crosswinds	62 -106°
10K Shear from Tailwind	102°
28K Shear from Tailwind	24°
Sideslip Feedback ω = 0.5	
All Headwinds except Constant Azimuth	15 - 54°
10K Shear from Tailwind	19°
Sideslip Feedback ω = 1.0	
All Headwinds Except Constant Aximuth	14 - 83°
all Crosswinds	16 - 43°
10K Shear from Tailwind	67°
Sideslip Feedback Plus Rate Command ω = 0.5	
None	

TABLE 3-9 - CASES EXCEEDING CERTAIN VALUES - SRM PERTURBATIONS (SIDESLIP FEEDBACK PLUS RATE COMMAND, $\omega = 0.5$)

3-9a. $q\alpha$ greater than $\pm$ 3000 degree -lb/ft^2

28K Shear cw to headwind +Yaw, -Roll Misalign, +5% unbalance	3697
40K Shear cw to Headwind +Yaw, -Roll Misalign, +5% unbalance	3808
28K Shear ccw to Headwind - Yaw, -Roll misalign, -5% unbalance	3566
40K Shear ccw to Headwind - Yaw, -Roll Misalign, -5% unbalance	3627

(Headwinds without sideslip feedback $\sim$50 higher than no misalignments)

3-9b. $q\beta$ greater than $\pm$ 3000 degree -lb/ft^2

28K Shear cw from headwind + Yaw, -roll misalign, +5% unbalance	+3800
40K Shear cw from headwind + Yaw, -Roll Misalign, +5% Unbalance	+3545
28K Shear cw to Headwind -Yaw, -Roll Misalign, -5% Unbalance	-3586
40K Shear cw to Headwind -Yaw, -Roll Misalign, -5% Unbalance	-3243
10K Shear ccw to Headwind - Yaw, -Roll Misalign, -5% Unbalance	-3644
28K Shear ccw to Crosswind -Yaw, -Roll Misalign, -5% Unbalance	+3204
40K Shear ccw to Crosswind -Yaw, -Roll Misalign, -5% Unbalance	+3194

3-9c. Delta Weight to Orbit Greater than 1000 lb

10 K Shear cw from crosswind +Yaw, -Roll Misalign, +5% Unbalance	+1320
10K Shear cw from Tailwind +Yaw, -Roll Misalign, +5% Unbalance	-1125
10K Shear cw to Headwind +Yaw, -Roll Misalign, +5% Unbalance	-1160
10K Shear cw to Headwind -Yaw, -Roll Misalign, -5% Unbalance	-5480
10K Shear cw to Tailwind -Yaw, -Roll Misalign, -5% Unbalance	+1095
28K Shear cw to Headwind -Yaw, -Roll Misalign, -5% Unbalance	-4370
28K Shear cw to Tailwind -Yaw, -Roll Misalign, -5% Unbalance	+1060
40K Shear cw to Headwind -Yaw, -Roll Misalign, -5% Unbalance	-3020
40K Shear cw to Tailwind -Yaw, -Roll Misalign, -5% Unbalance	+1580
10K Shear cw to Left Crosswind -Yaw, -Roll Misalign, -5% Unbalance	-1900
28K Shear cw to Left Crosswind -Yaw, -Roll Misalign, -5% Unbalance	-2030
40K Shear cw to Left Crosswind -Yaw, -Roll Misalign, -5% Unbalance	-1830
10K Shear ccw to Headwind -Yaw, -Roll Misalign, -5% Unbalance	-3960
10K Shear ccw to Tailwind -Yaw, -Roll Misalign, -5% Unbalance	+1255

3-9c. (Continued)

28K Shear ccw to Headwind -Yaw, -Roll Misalign, -5% Unbalance	-2350
28K Shear ccw to Tailwind -Yaw, -Roll Misalign, -5% Unbalance	+1090
40K Shear ccw to Headwind -Yaw, -Roll Misalign, -5% Unbalance	-1250
40K Shear ccw to Tailwind -Yaw, -Roll Misalign, -5% Unbalance	+1510

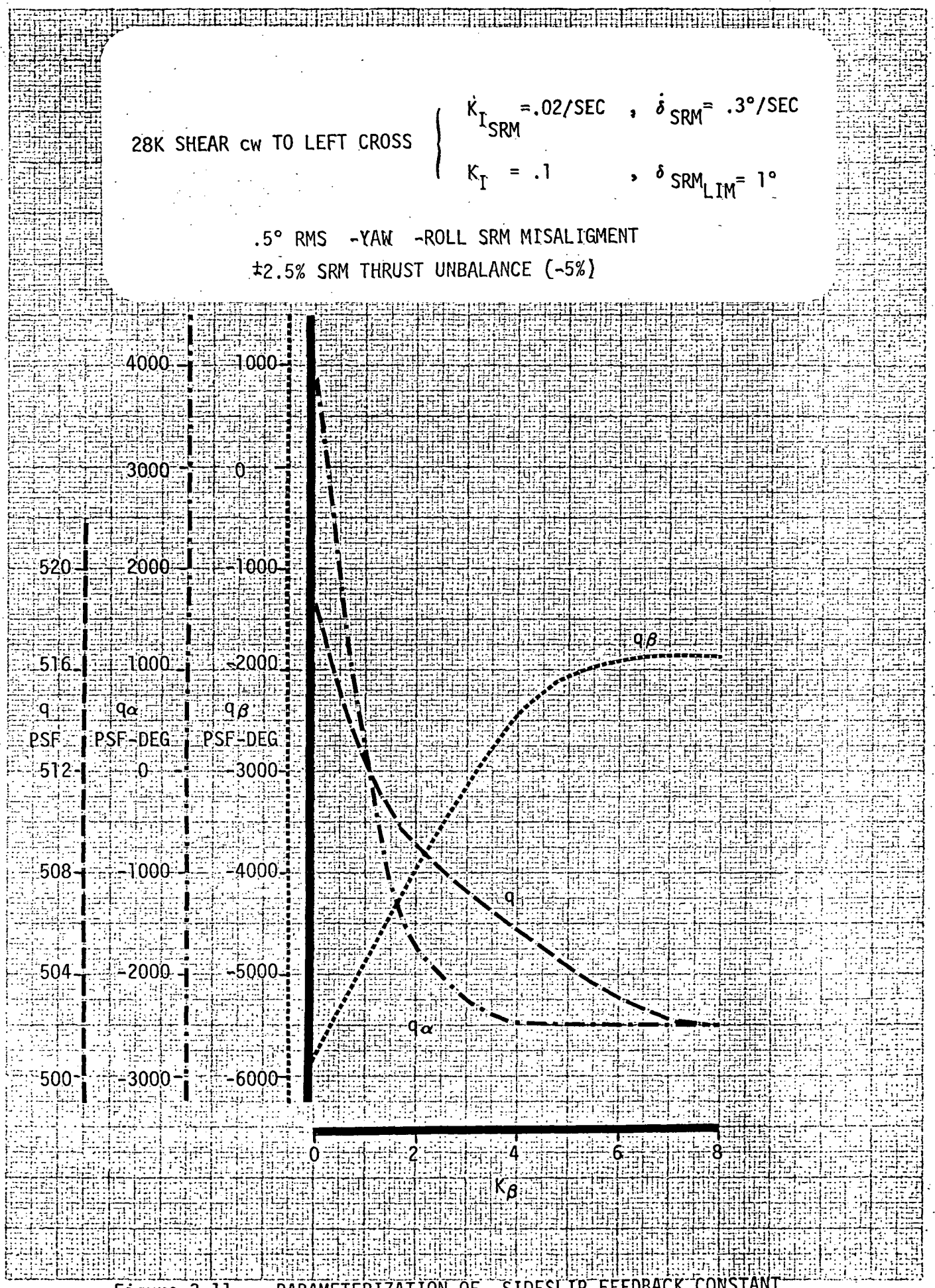

Figure 3-11 .- PARAMETERIZATION OF SIDESLIP FEEDBACK CONSTANT

3.2.3 Development of Vectorable SRM Control and Lift-off Analysis

Vectorable SRM trim control was investigated in an effort to be able to trim out SRM angular misalignments on the order of 0.5 degree and larger. In an effort to rapidly implement vectorable SRM trim control into the 049 SSV dynamics and control simulation, the basic orbiter TVC baseline control system was utilized as a source of scaled attitude errors and attitude rates. Since the SRM's would be used only as trim control and would be of low frequency, it was assumed that the control gains associated with the orbiter TVC system would still be applicable.

Lift-off boost dynamics and control studies on the 049 SSV utilizing several forms of SRM control logic, in addition to normal orbiter TVC, were performed as discussed in References 49 and 50. Five basic forms of control logic were investigated.

Initial efforts to include SRM trim TVC capability into the Space Shuttle Functional Simulator (SSFS) employed use of integral attitude error feedback. For each control axis the attitude error from the normal orbiter TVC system was scaled and integrated to provide trim control to the SRM's. Flight simulations were performed initially with no limits on the SRM integrators, but with one degree hardware limits on the SRM actuators. Flights were performed with 1 degree SRM misalignments in roll, with values of .02, .04 and .06 for the SRM integrator constant, and with values of .1, .3 and .5 for SRM actuator rate limits. Results indicated that loss of control occurred for the system due to "overcharging" of the SRM integrators. Since the actuators were limited to 1 degree and the SRM integrators were unlimited, this introduced excessive lag into the control system. Limits were then applied to the integrators. However, large roll errors still persisted.

Numerous intermediate control systems were investigated; however, final conclusions from the analysis (Reference 49) indicated that a control system using integral attitude error plus rate damping for roll and yaw and only integral attitude error in the pitch axis produced acceptable results.

3.2.3 Continued

Figures 3-12 and 3-13 summarize the data obtained for those runs made with this system. Peak roll and yaw errors are seen to decrease as actuator rate limit is increased. In order to minimize power requirements to drive the SRM's, it was desired to keep actuator rate limits as low as possible and still hold peak roll to a reasonable value. From these plots a compromise rate limit value of 0.3°/sec was chosen for a baseline system. This value along with an integrator constant of 0.02 were felt at this point to represent a satisfactory system. (An integrator constant of 0.04, although producing smaller roll errors, was found to lead to more "ringing" in the control system.)

As directed by MSC/G&C Division, this system was modified slightly such that all control axes were composed of the integral of attitude error and rate damping for vectorable SRM trim control. This control system is illustrated in Figure 3-14. This addition to the control system presented a more unified approach to SRM trim control. Comparison of the results of this system with those of the previous one without rate damping in pitch indicate insignificant differences.

Figures 3-15 through 3-18 present the results of simulated lift-offs of the 049 SSV configuration flown with 0.5° RMS -roll/-yaw combination SRM misalignments and ±2.5% SRM thrust unbalance. Shown in these plots are attitude errors, pitch and yaw orbiter engine traces, and SRM pitch gimbal traces. The same parameters are shown in Figures 3-19 through 3-22 for 1.0° RMS -roll/-yaw combination SRM misalignments and ±2.5% thrust unbalance.

3.2.4 Inflight Performance for Vectorable SRM System

Inflight results were presented in Reference 51 verifying the capability of the vectorable SRM trim control system under severe wind conditions. Simulations were performed in the presence of 28,000 ft. crosswinds and

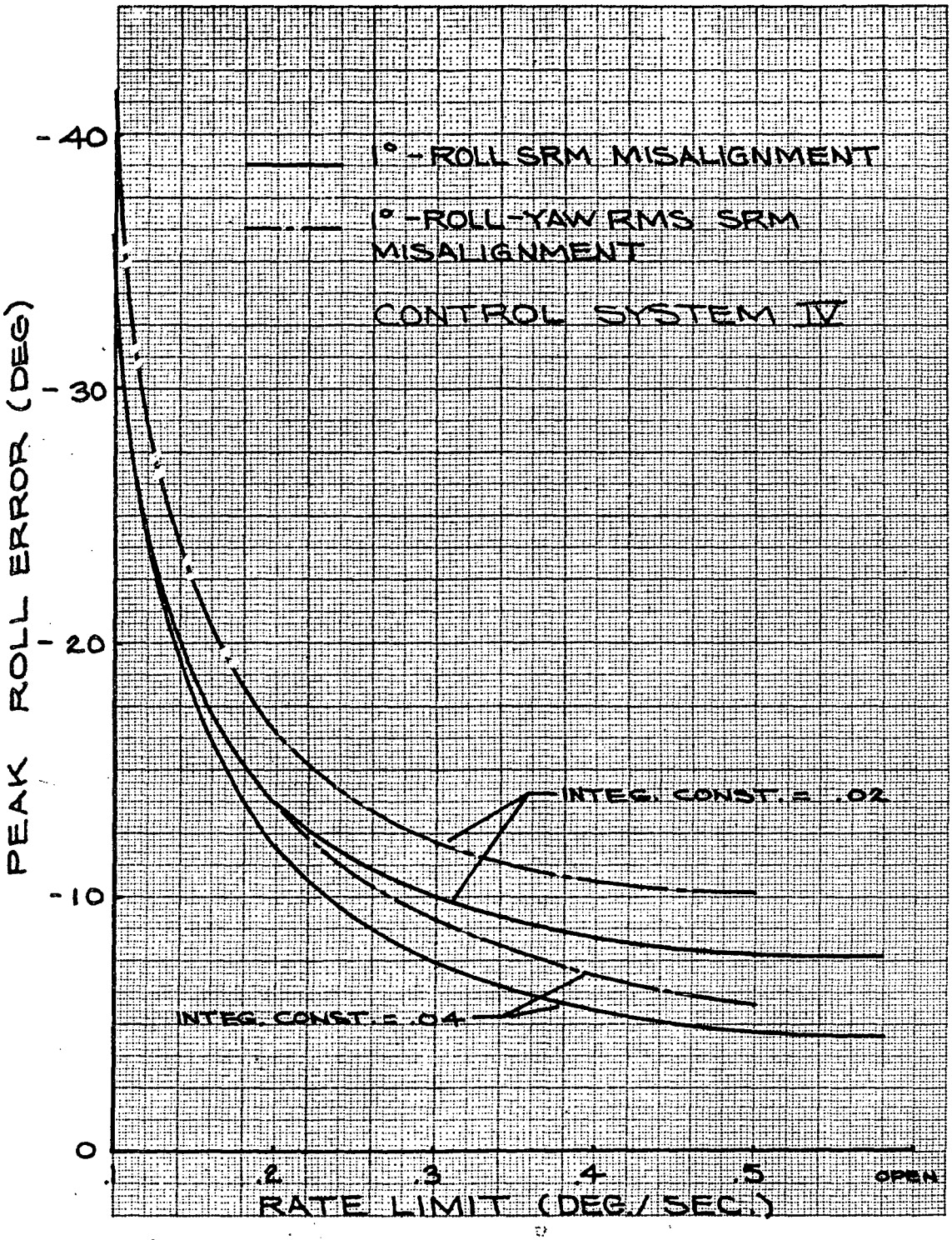

FIGURE 3-12

PEAK ROLL ERROR DURING LIFT OFF AS A FUNCTION OF RATE LIMIT

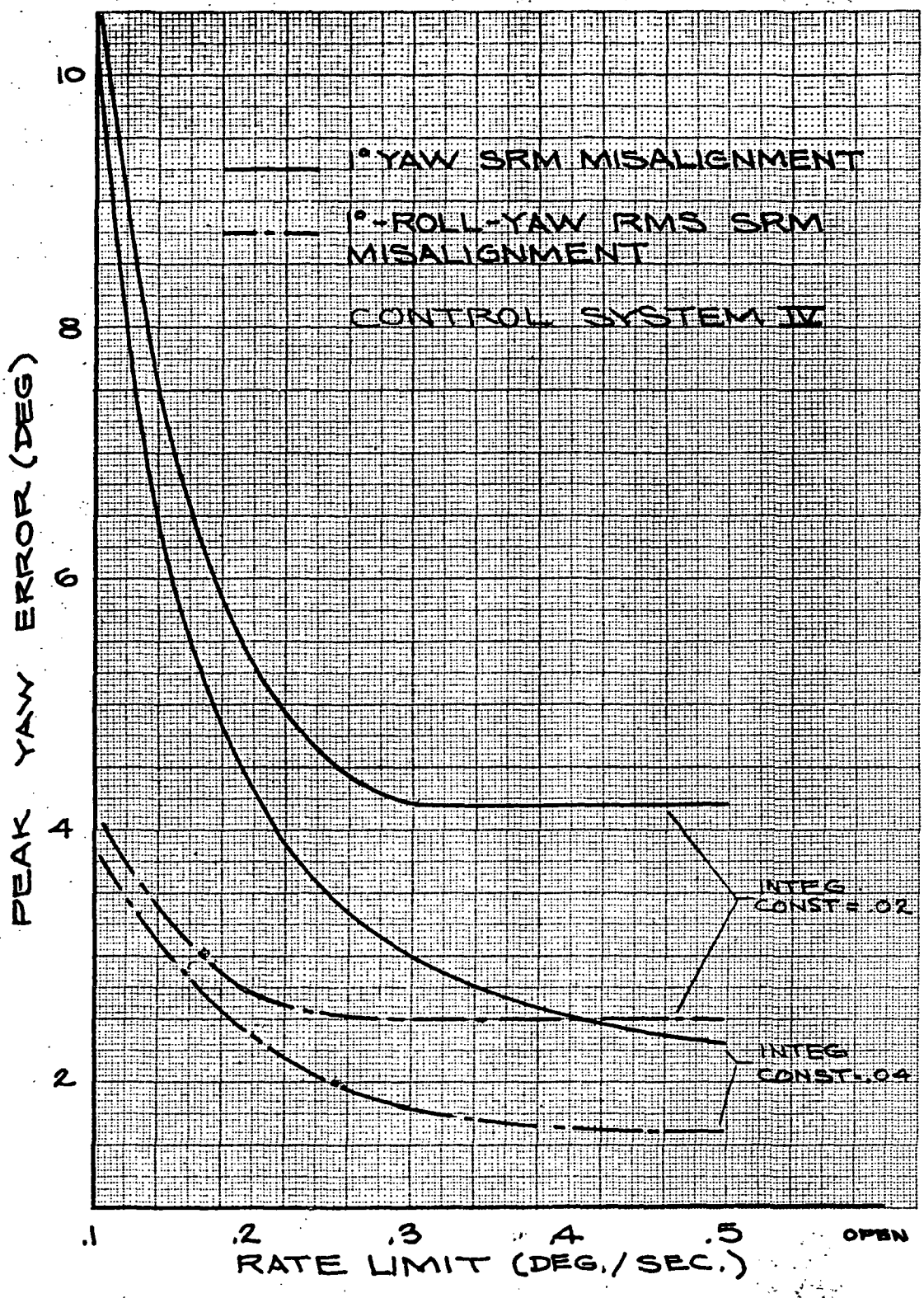

FIGURE 3-13

PEAK YAW ERROR AS A FUNCTION OF RATE LIMIT

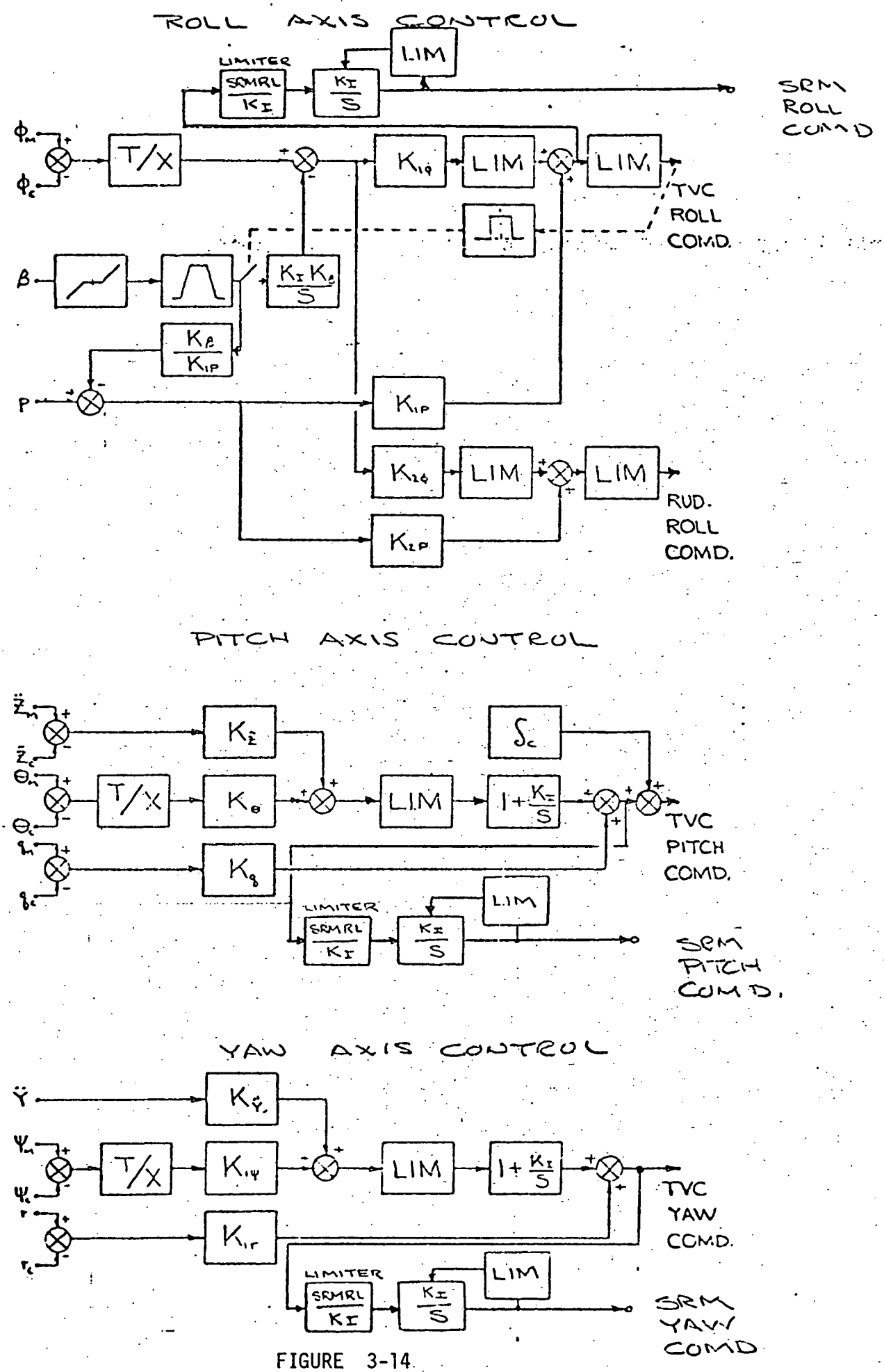

FIGURE 3-14

CONTROL SYSTEM WITH VECTORABLE SRM CONTROL

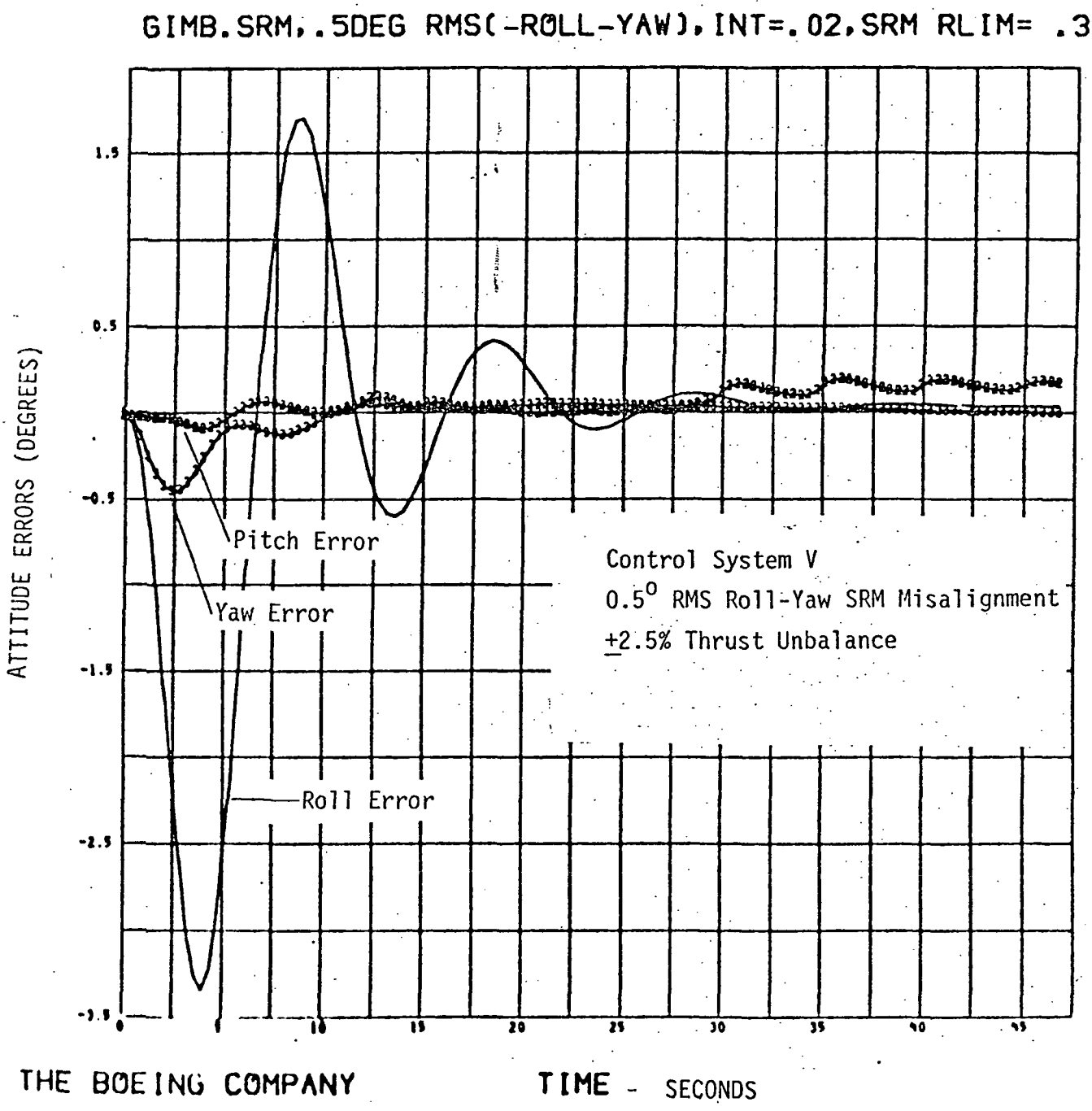

FIGURE 3-15

LIFTOFF RESULTS - VECTORABLE SRM - 0.5° SRM MISALIGNMENT - ATTITUDE ERRORS

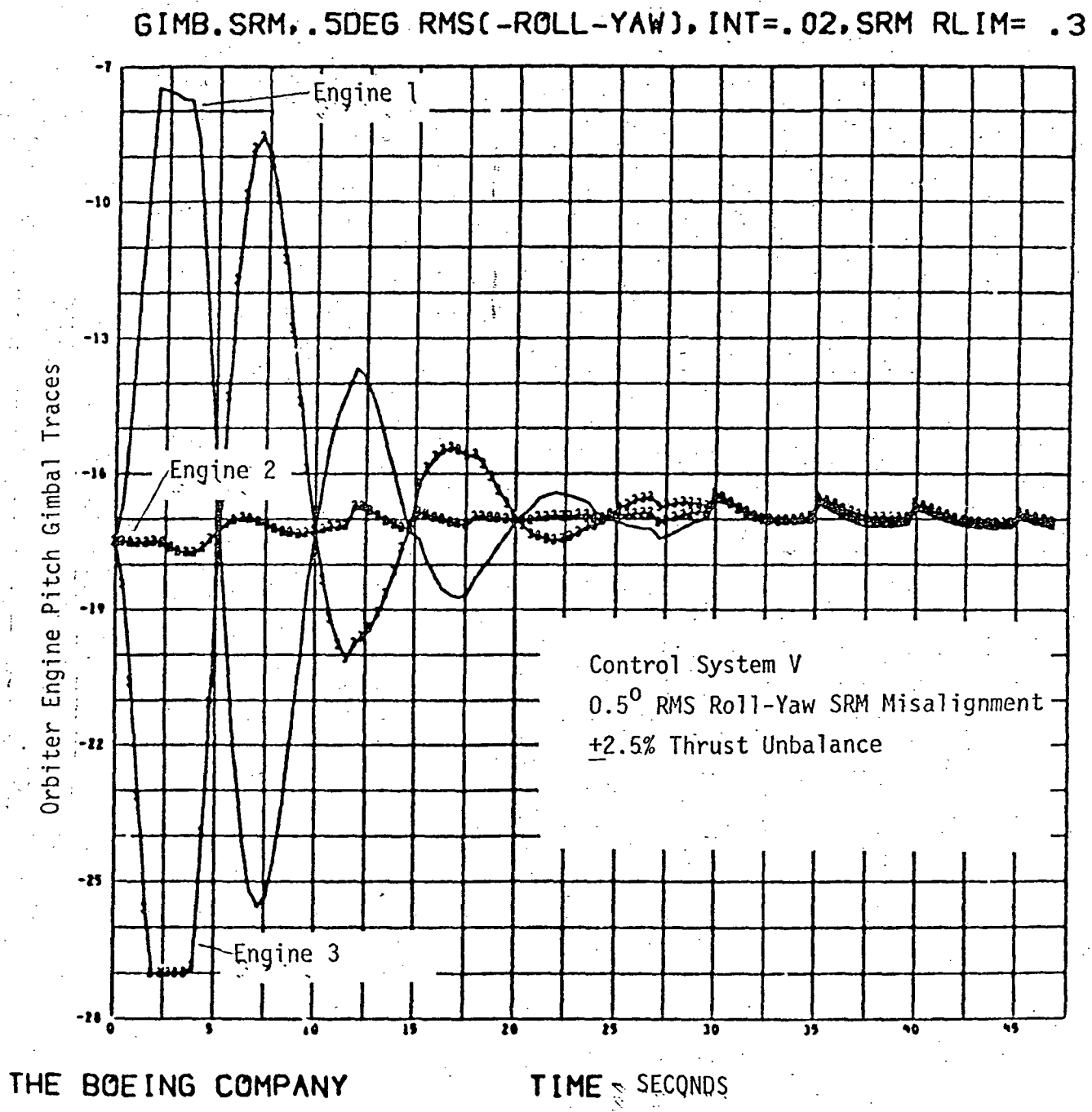

FIGURE 3-16

LIFTOFF RESULTS - VECTORABLE SRM - -5° SRM MISALIGNMENT - ORBITER PITCH ENGINE DEFLECTIONS

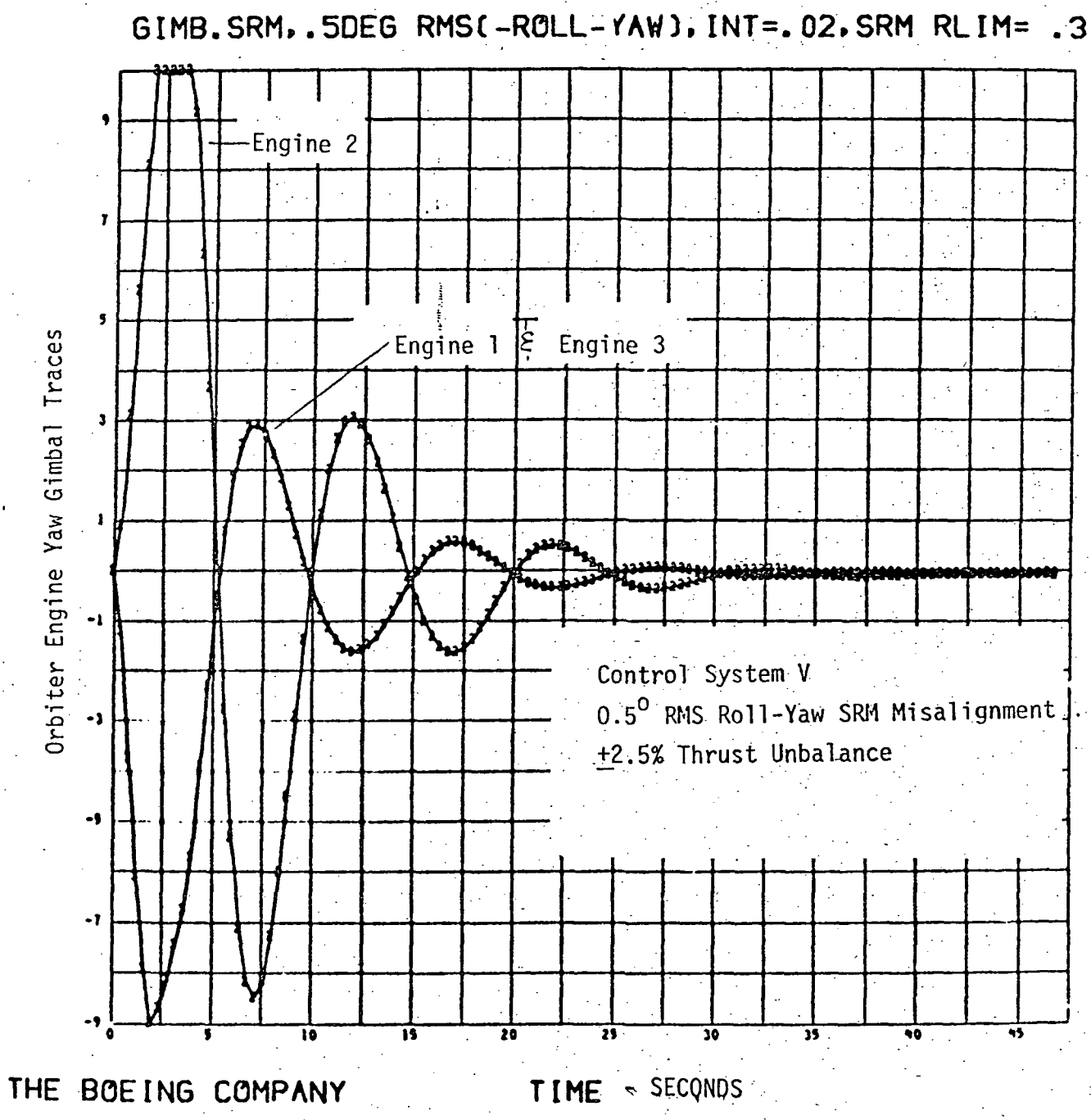

FIGURE 3-17

LIFTOFF RESULTS - VECTORABLE SRM - -0.5° SRM MISALIGNMENT - ORBITER YAW ENGINE DEFLECTIONS

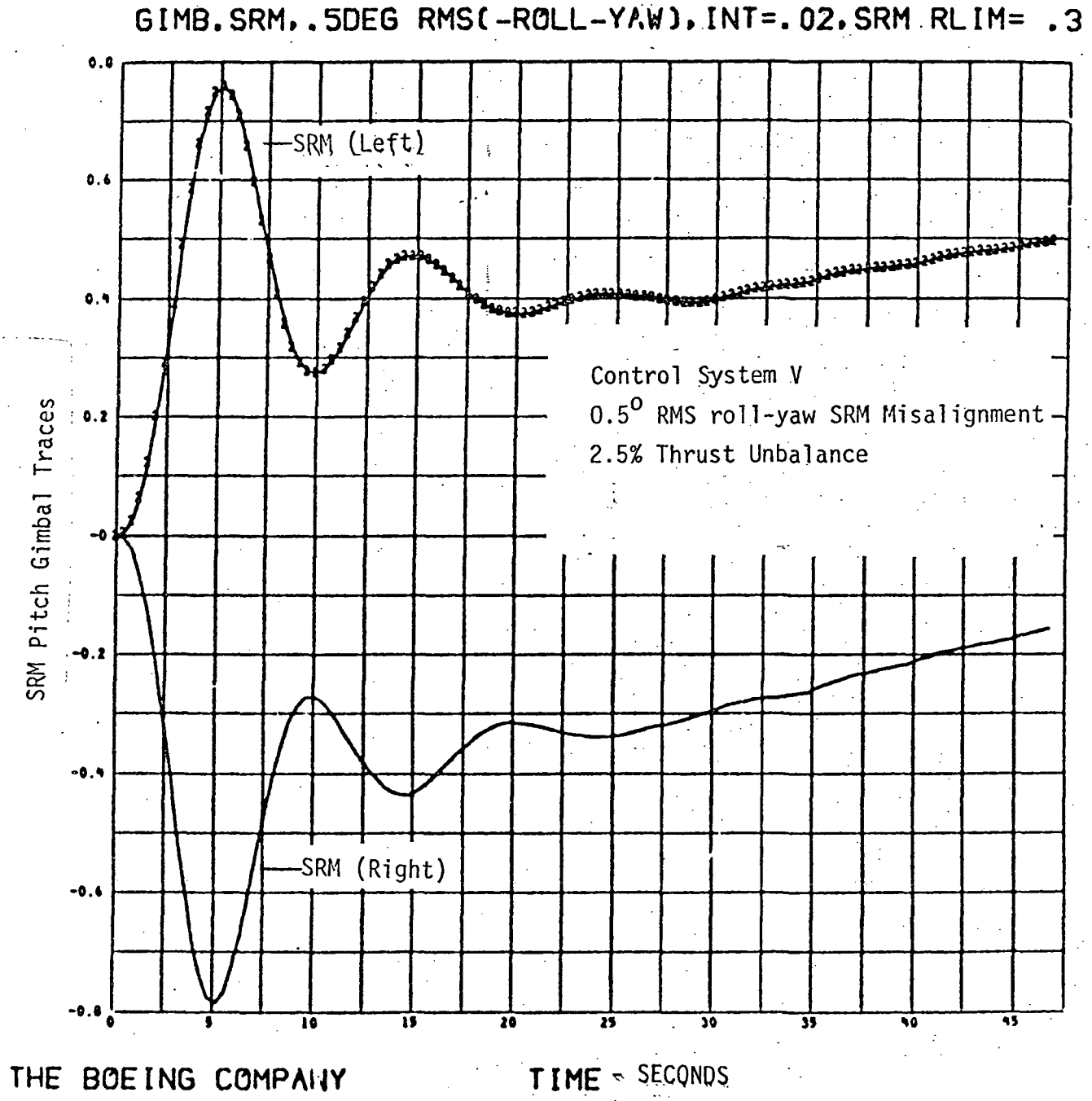

FIGURE 3-18

LIFTOFF RESULTS - VECTORABLE SRM - .-0.5° SRM MISALIGNMENT - SRM PITCH ENGINE DEFLECTIONS

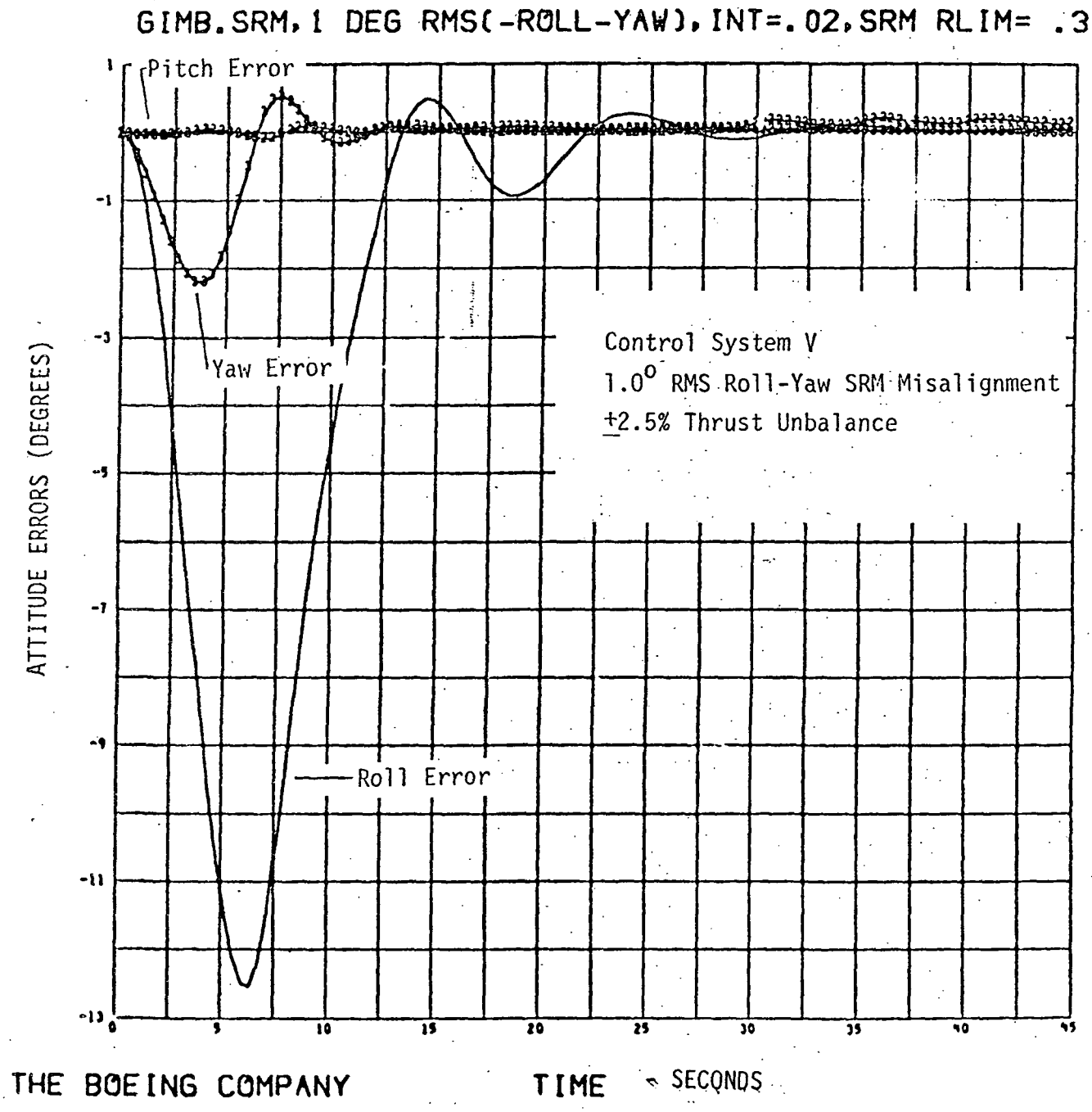

FIGURE 3-19

LIFTOFF RESULTS - VECTORABLE SRM - 1.0° SRM MISALIGNMENT - ATTITUDE ERRORS

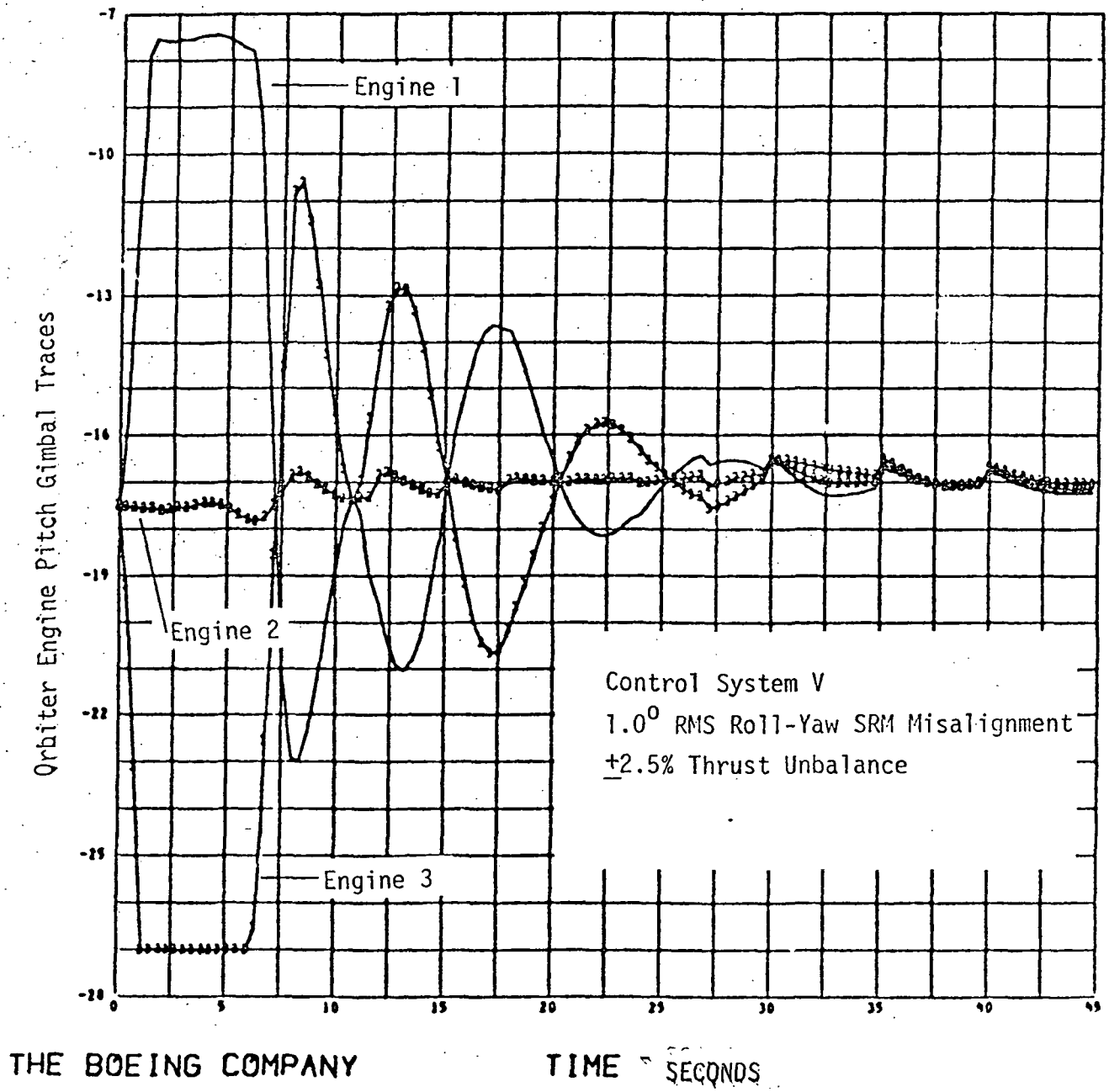

FIGURE 3-20

LIFTOFF RESULTS - VECTORABLE SRM - 1.0° SRM MISALIGNMENT - ORBITER PITCH ENGINE DEFLECTIONS

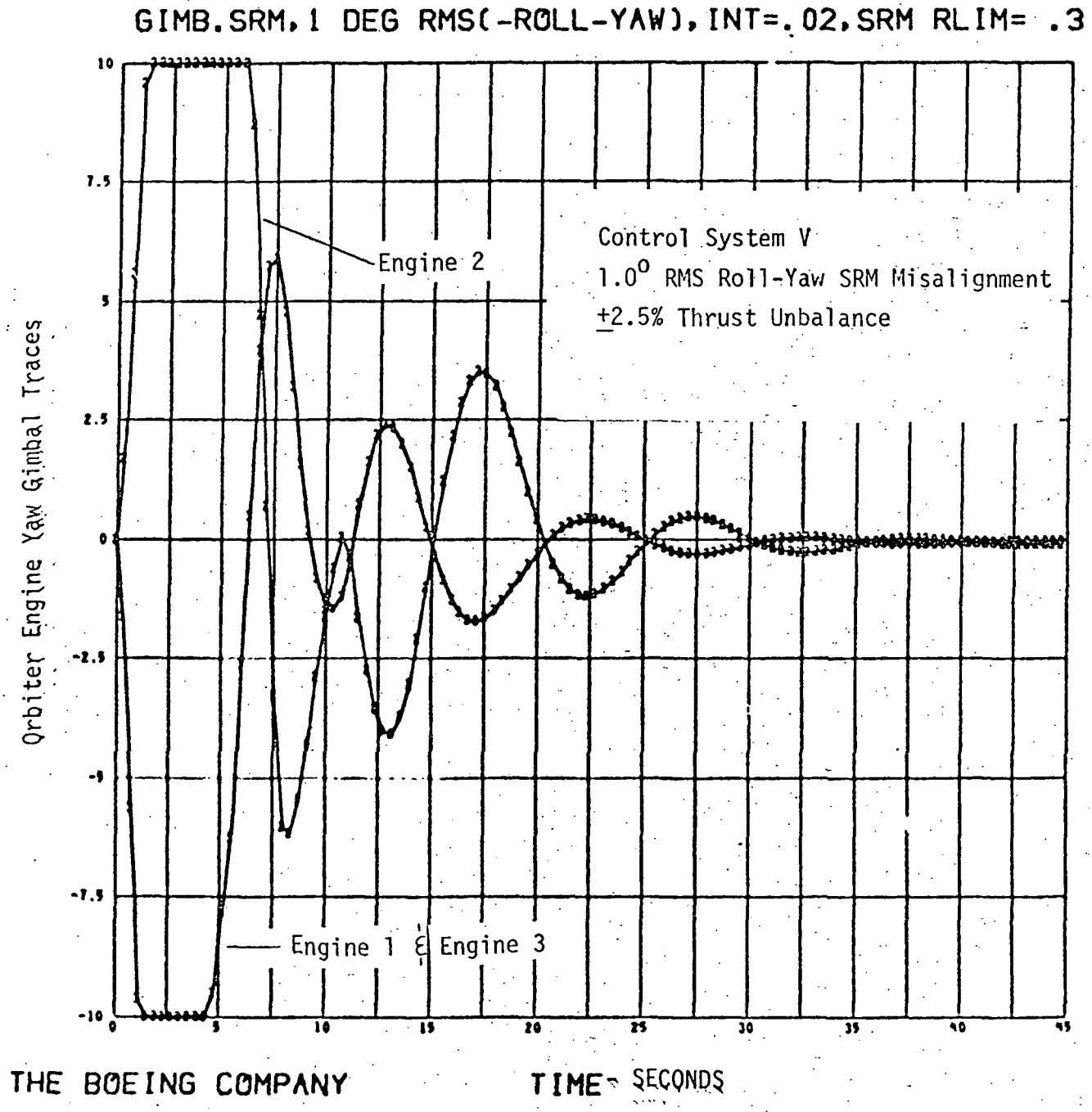

FIGURE 3-21

LIFTOFF RESULTS - VECTORABLE SRM 1.0° SRM MISALIGNMENT - ORBITER YAW ENGINE DEFLECTIONS

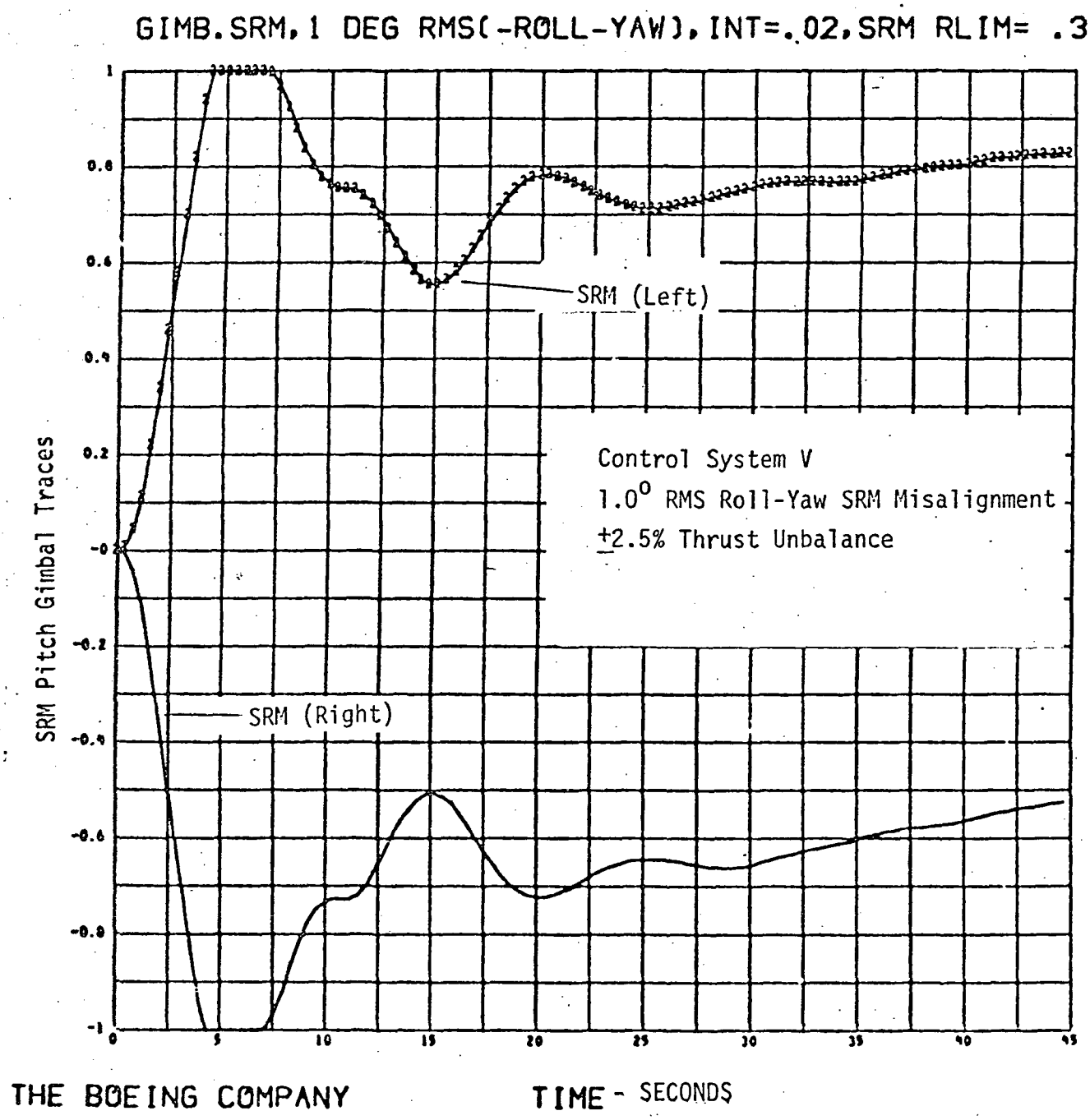

FIGURE 3-22

LIFTOFF RESULTS - VECTORABLE SRM 1.0° SRM MISALIGNMENT - SRM PITCH ENGINE DEFLECTIONS

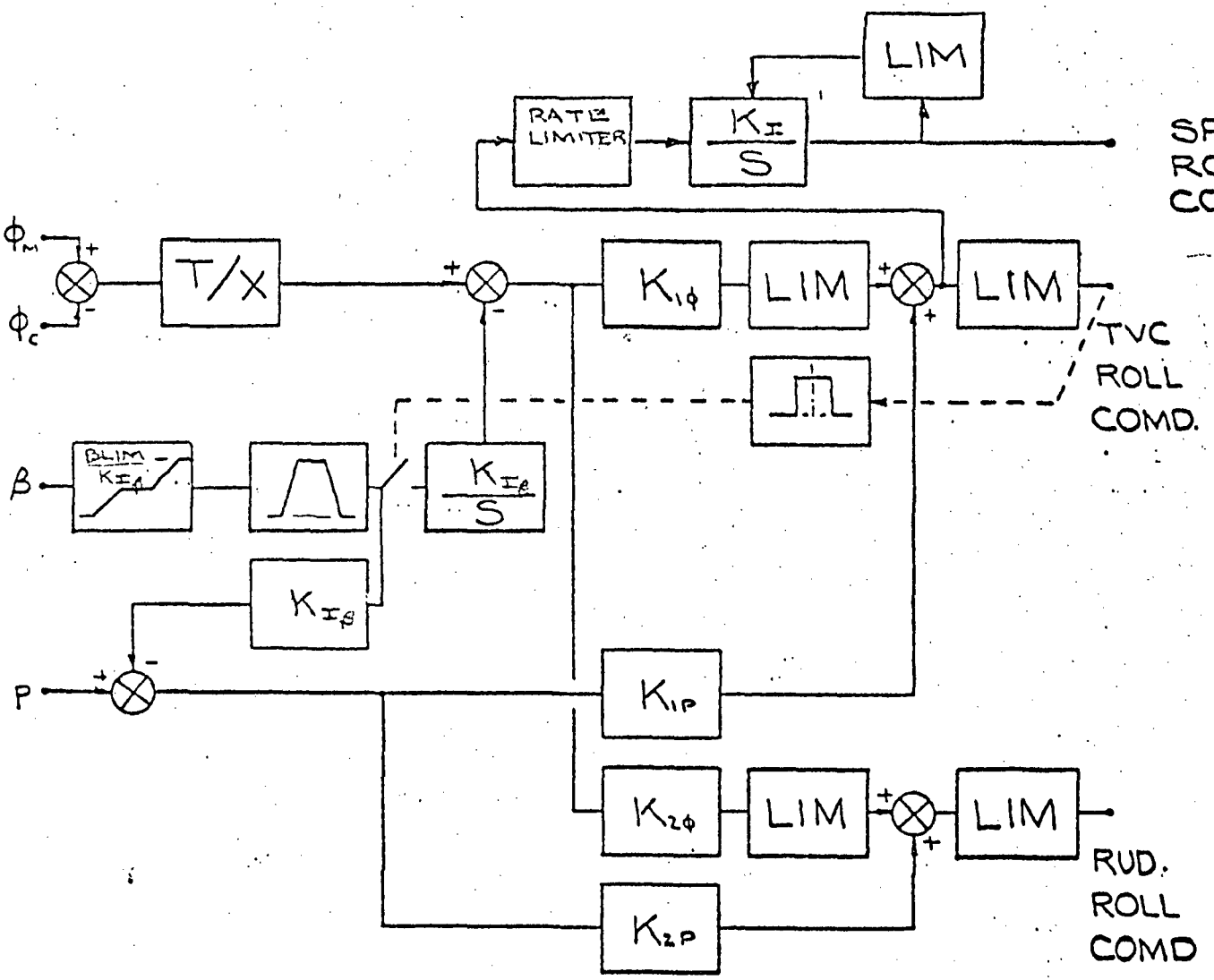

FIGURE 3-23 - Roll Axis Channel of Control System

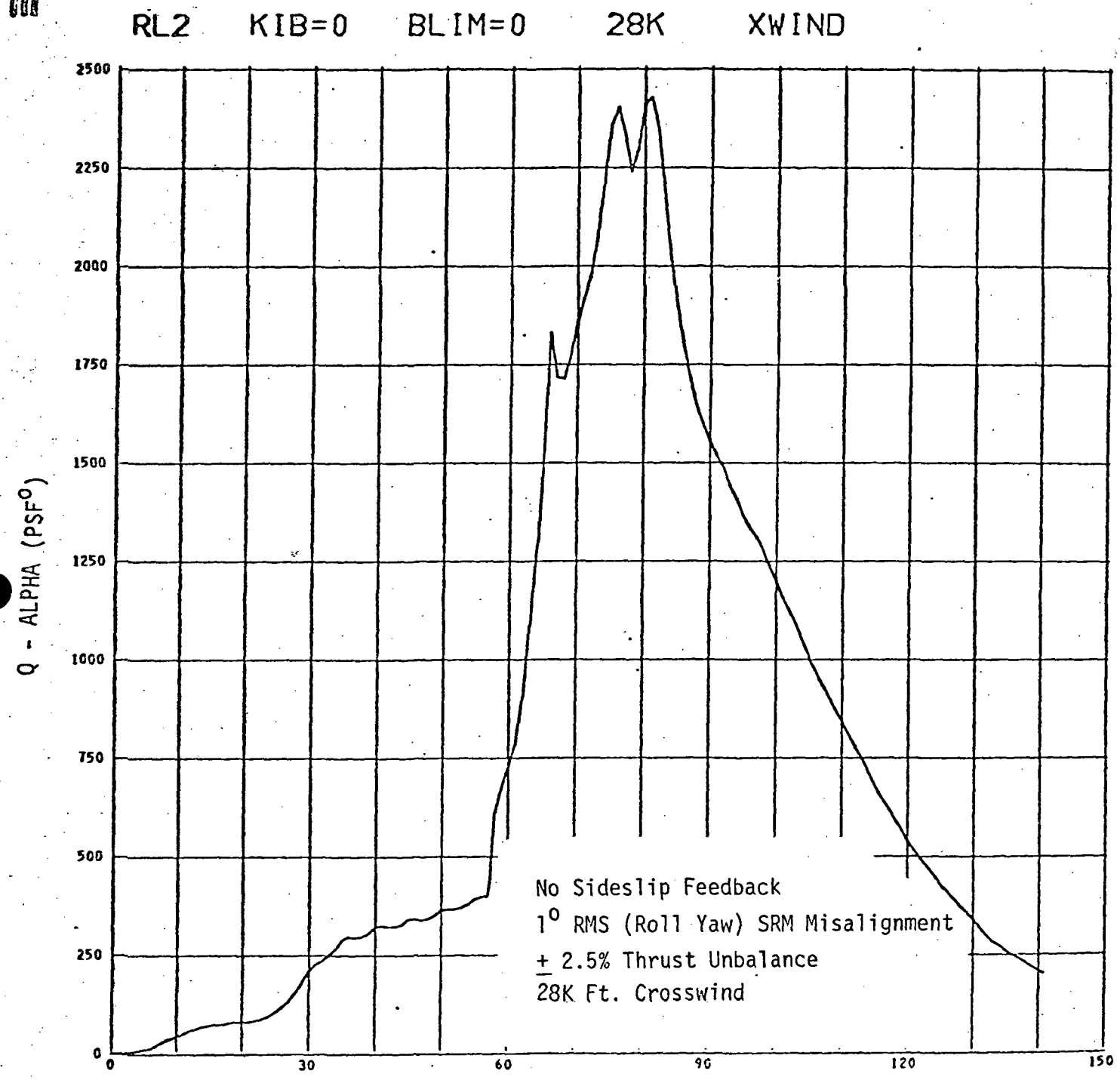

FIGURE 3-24

INFLIGHT RESULTS - NO SIDESLIP FEEDBACK -
VECTORABLE SRM - 1° SRM MISALIGNMENT - Q-ALPHA

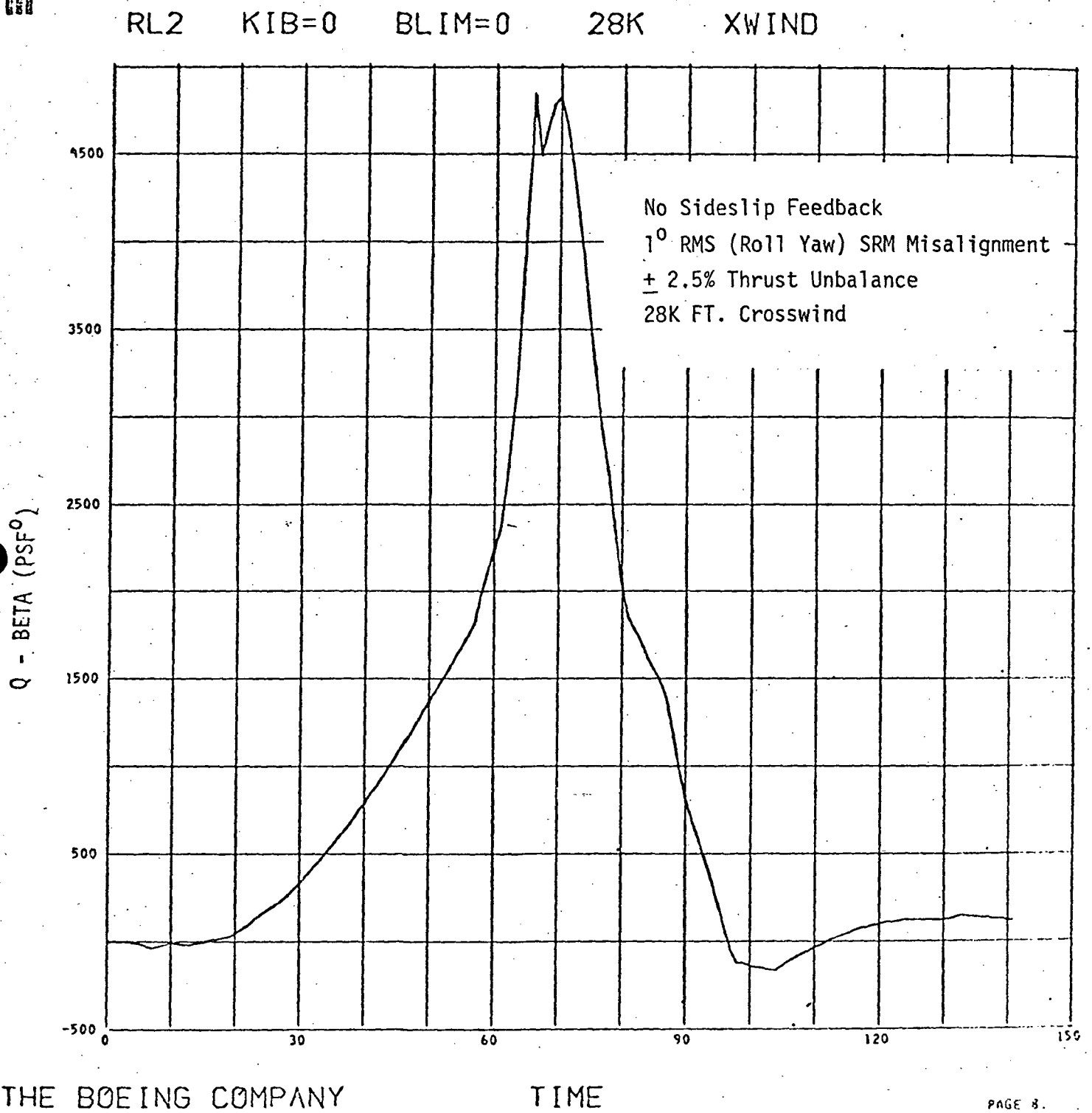

FIGURE 3-25

INFLIGHT RESULTS - NO SIDESLIP FEEDBACK - VECTORABLE SRM - 1.0° SRM MISALIGNMENT - Q-BETA

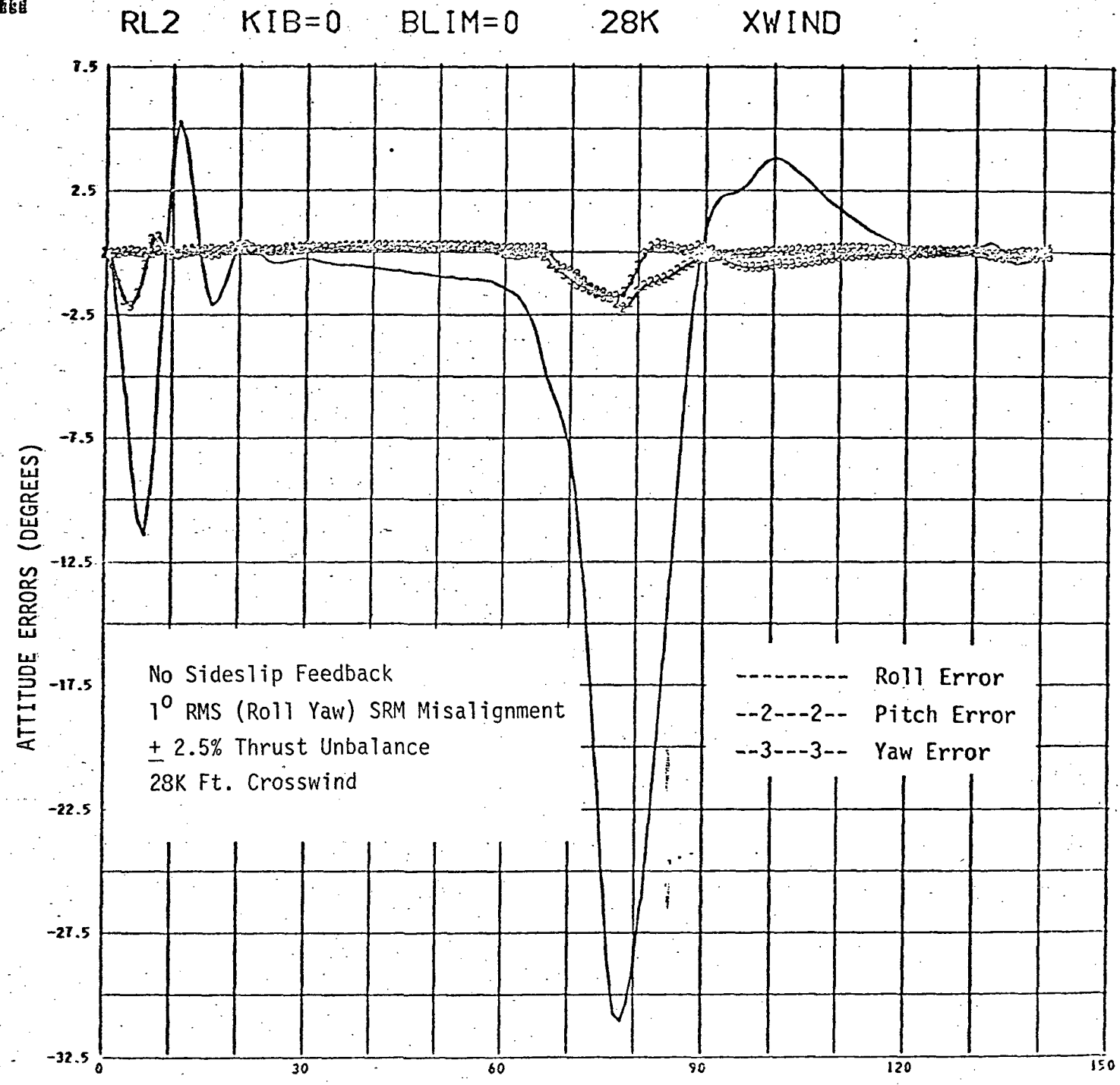

THE BOEING COMPANY

PAGE 19.

FIGURE 3-26

INFLIGHT RESULTS - NO SIDESLIP FEEDBACK - VECTORABLE SRM - 1.0° SRM MISALIGNMENT - ATTITUDE ERRORS

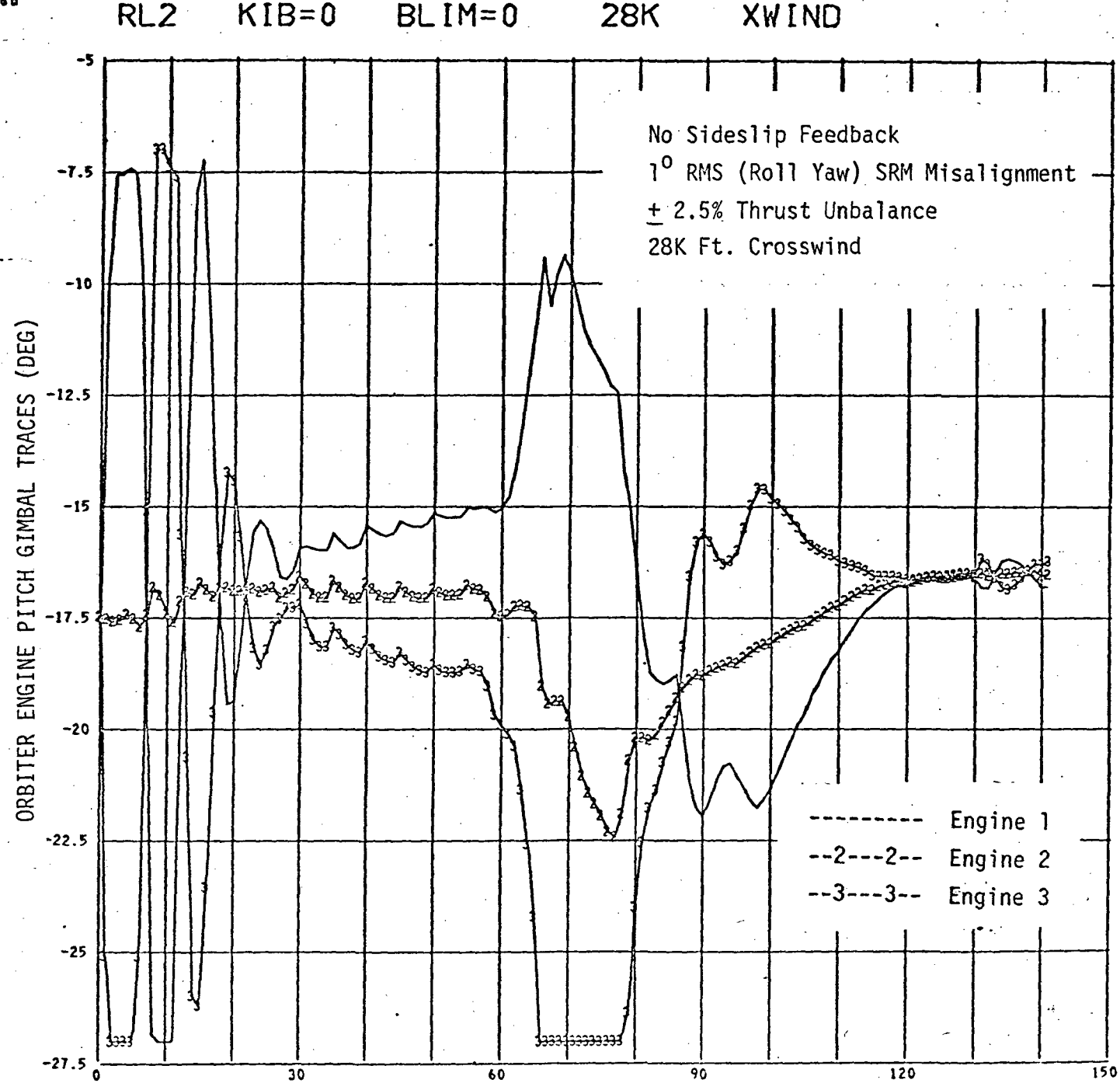

THE BOEING COMPANY

PAGE 22.

FIGURE 3-27

INFLIGHT RESULTS - NO SIDESLIP FEEDBACK - VECTORABLE SRM - 1.0° SRM MISALIGNMENT - ORBITER PITCH ENGINE DEFLECTIONS

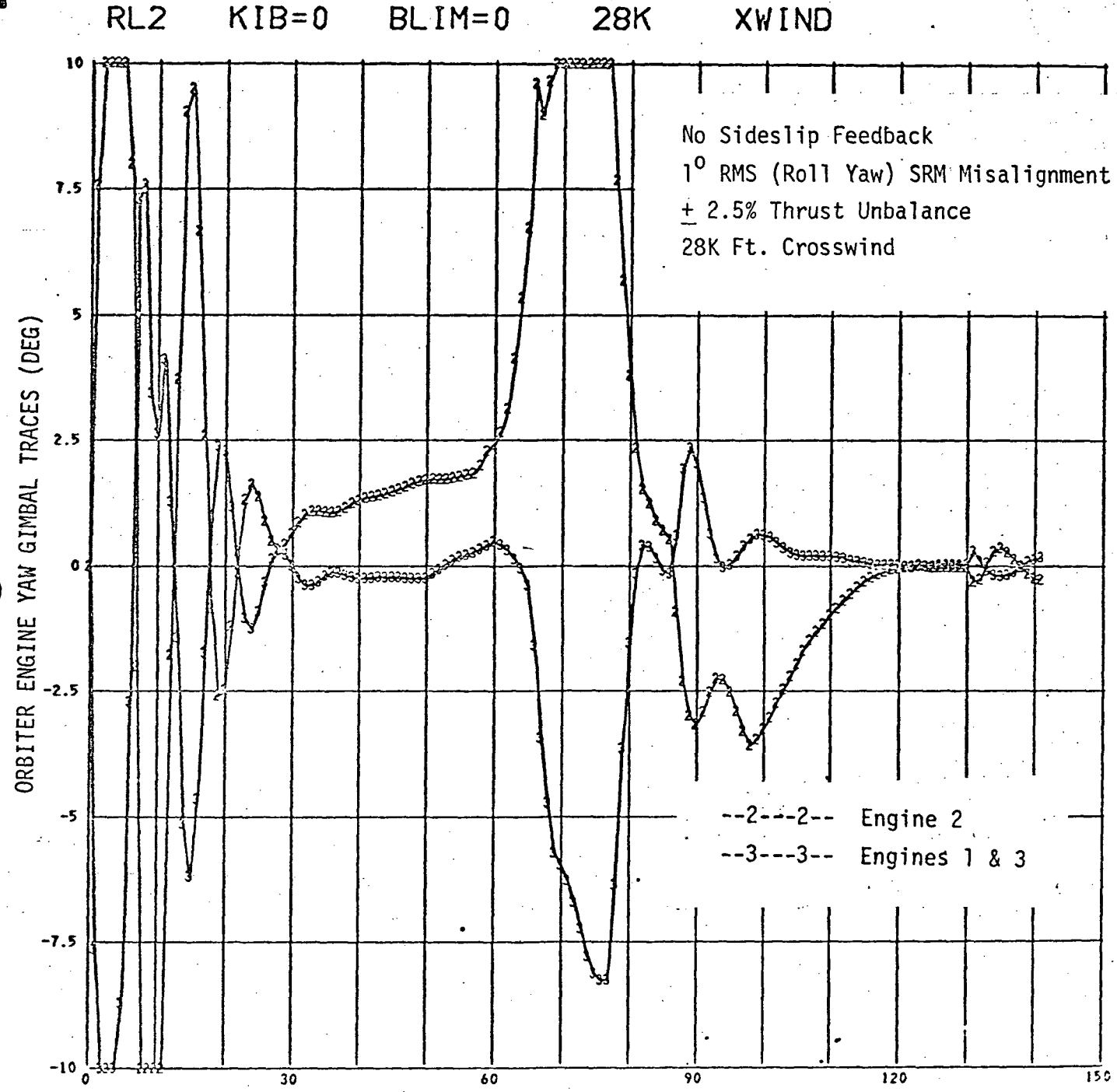

THE BOEING COMPANY

PAGE 23.

FIGURE 3-28

INFLIGHT RESULTS - NO SIDESLIP FEEDBACK - VECTORABLE SRM - 1.0° SRM MISALIGNMENT - ORBITER PITCH ENGINE DEFLECTIONS

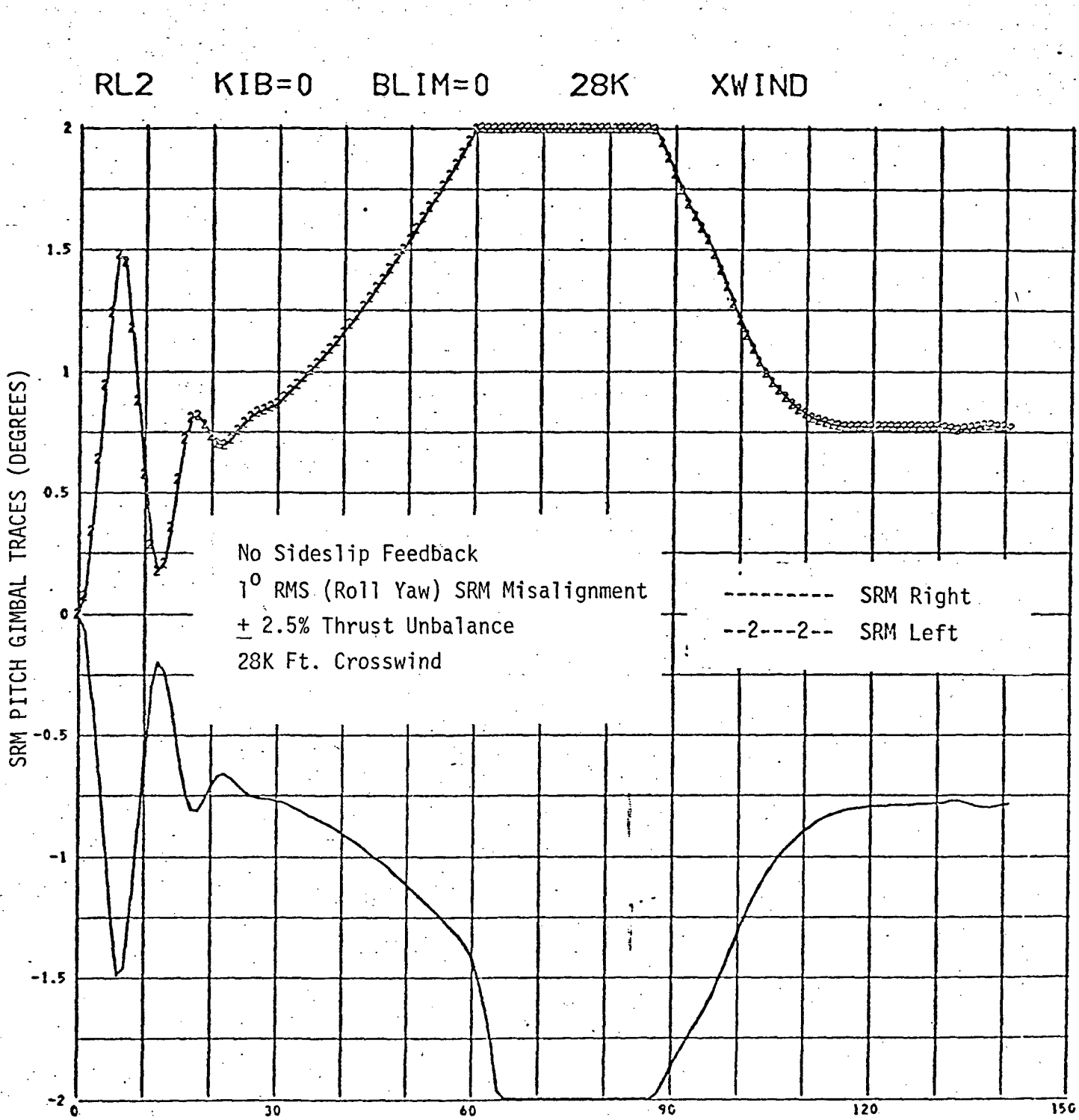

FIGURE 3-29

INFLIGHT RESULTS - NO SIDESLIP FEEDBACK - VECTORABLE SRM - 1.0° SRM MISALIGNMENT - SRM PITCH ENGINE DEFLECTIONS

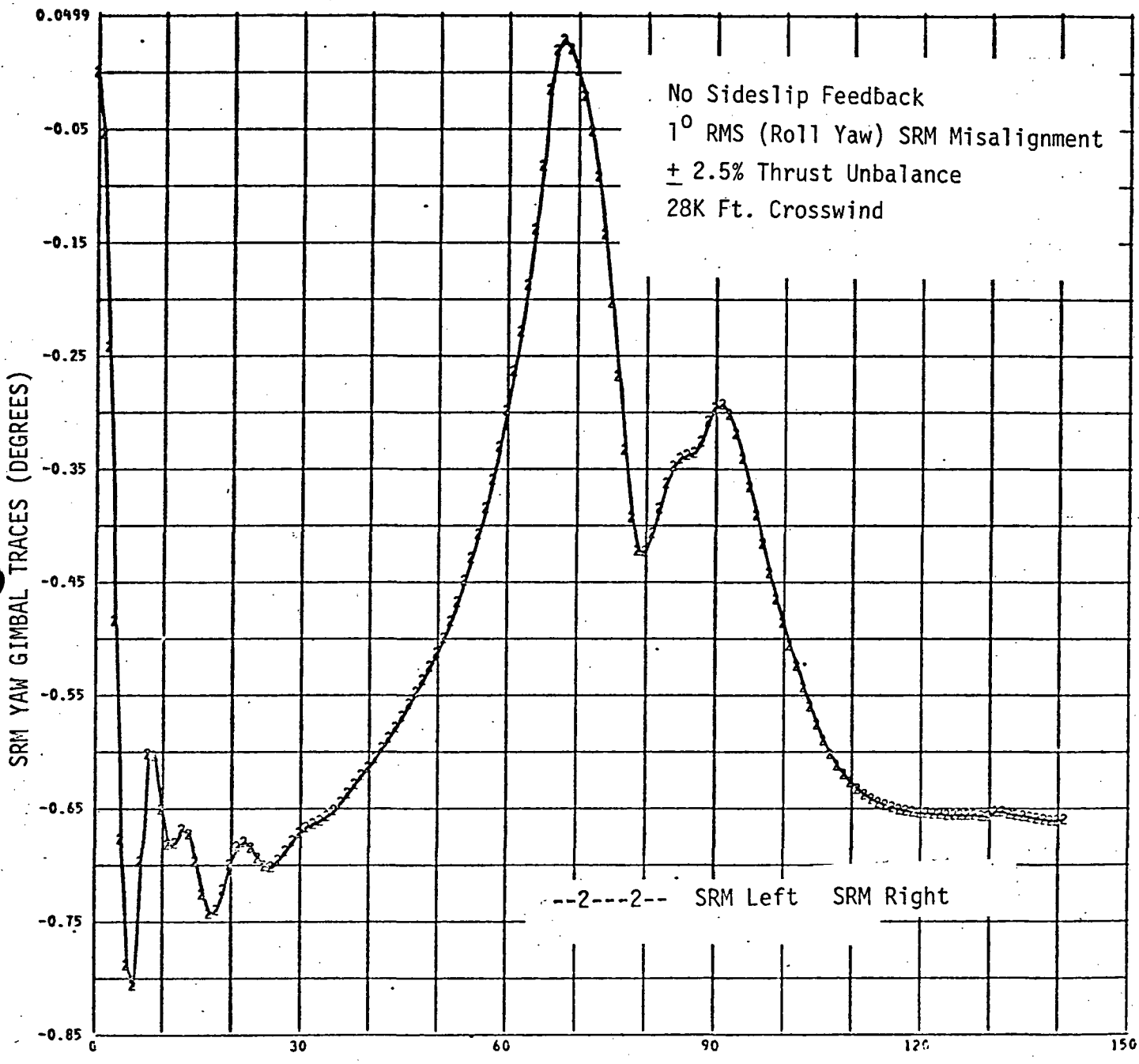

THE BOEING COMPANY

PAGE 25.

FIGURE 3-30

INFLIGHT RESULTS - NO SIDESLIP FEEDBACK - VECTORABLE SRM - 1.0° SRM MISALIGNMENT - SRM YAW ENGINE DEFLECTIONS

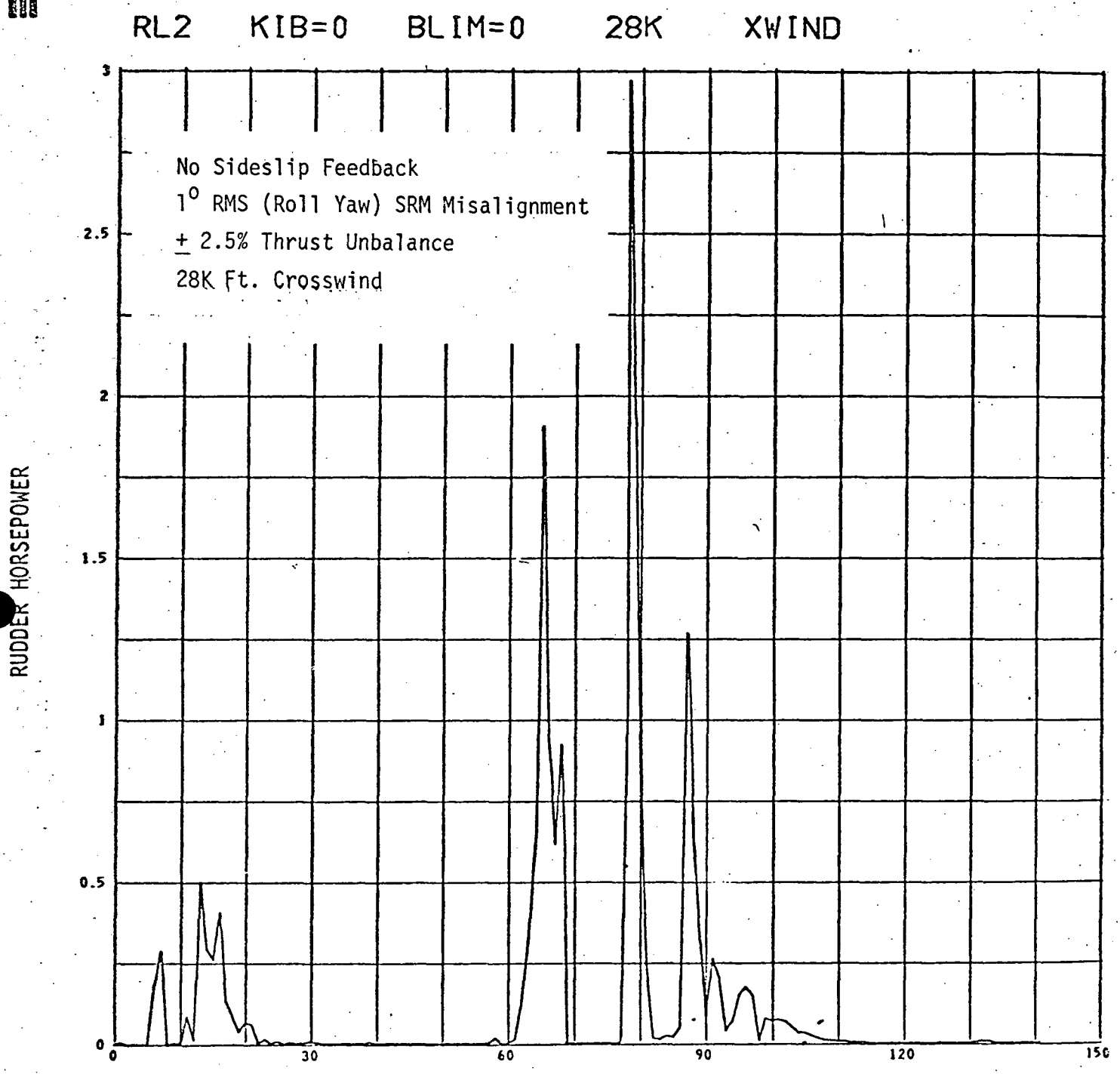

FIGURE 3-31

INFLIGHT RESULTS - NO SIDESLIP FEEDBACK - VECTORABLE SRM - 1.0° SRM MISALIGNMENT - RUDDER HORSEPOWER

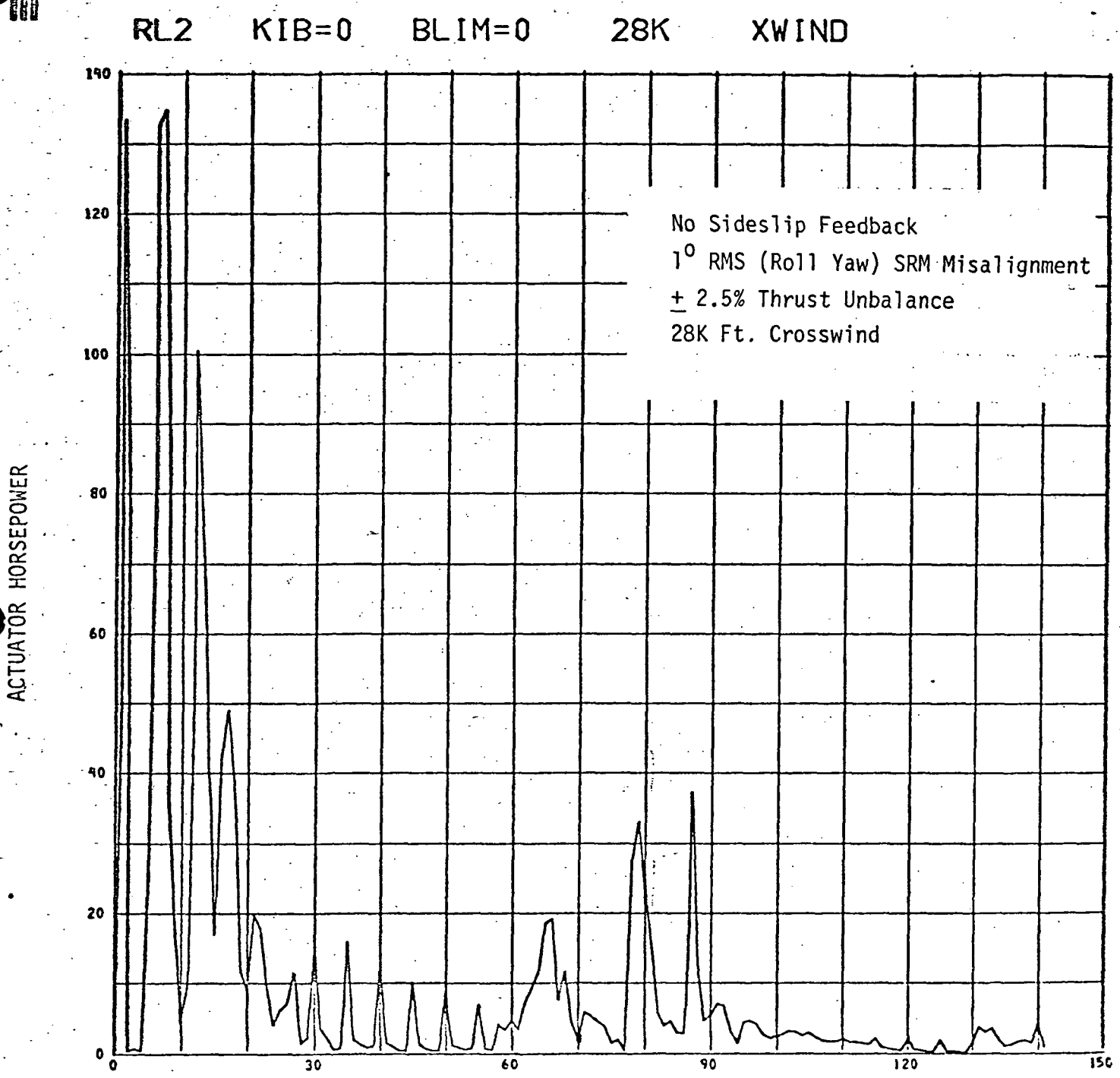

FIGURE 3-32

INFLIGHT RESULTS - NO SIDESLIP FEEDBACK - VECTORABLE SRM - 1.0° SRM MISALIGNMENT - ACTUATOR HORSEPOWER

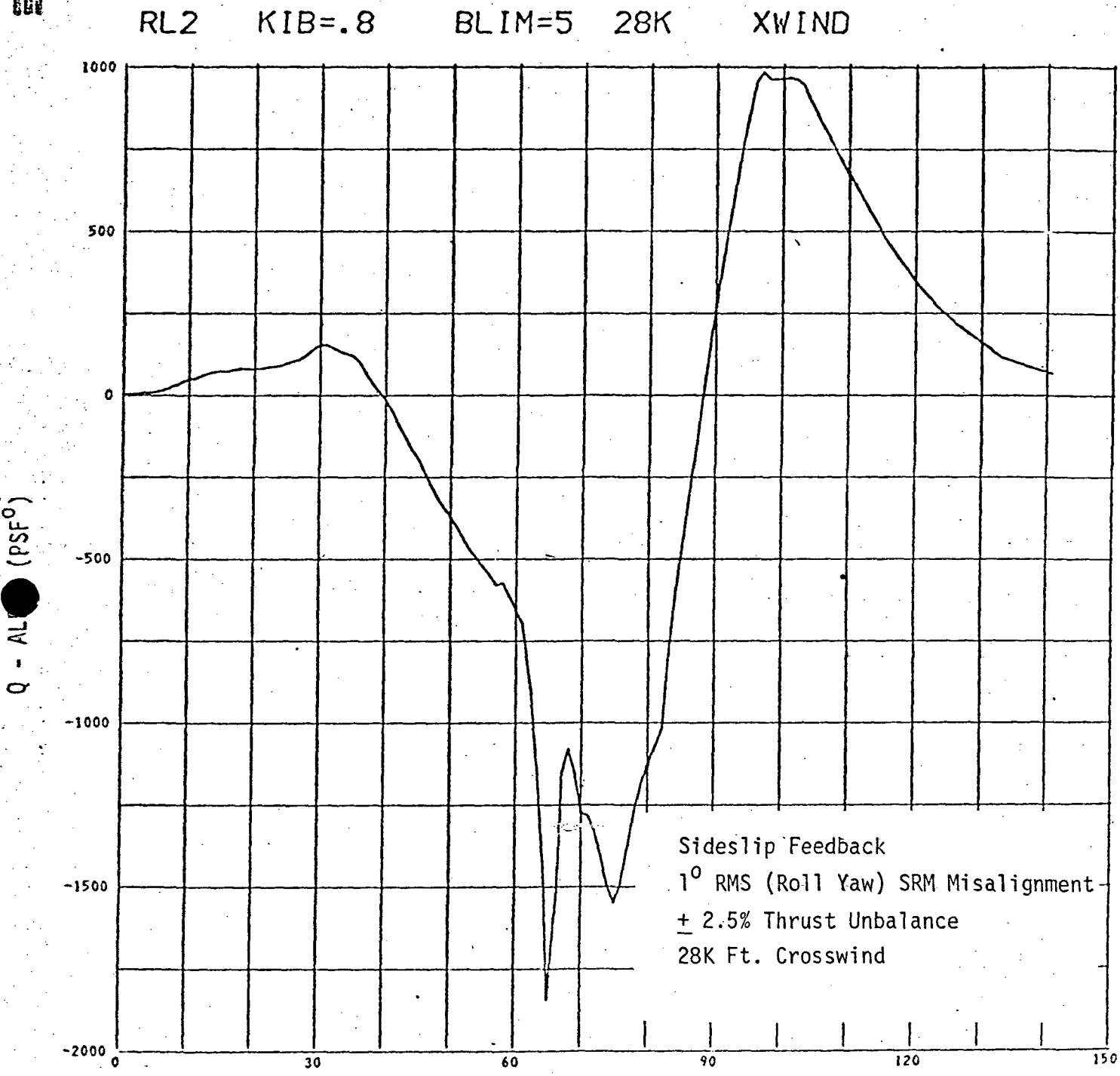

THE BOEING COMPANY

PAGE 88.

FIGURE 3-33

INFLIGHT RESULTS - SIDESLIP FEEDBACK VECTORABLE
SRM - 1.0° SRM MISALIGNMENT - Q-ALPHA

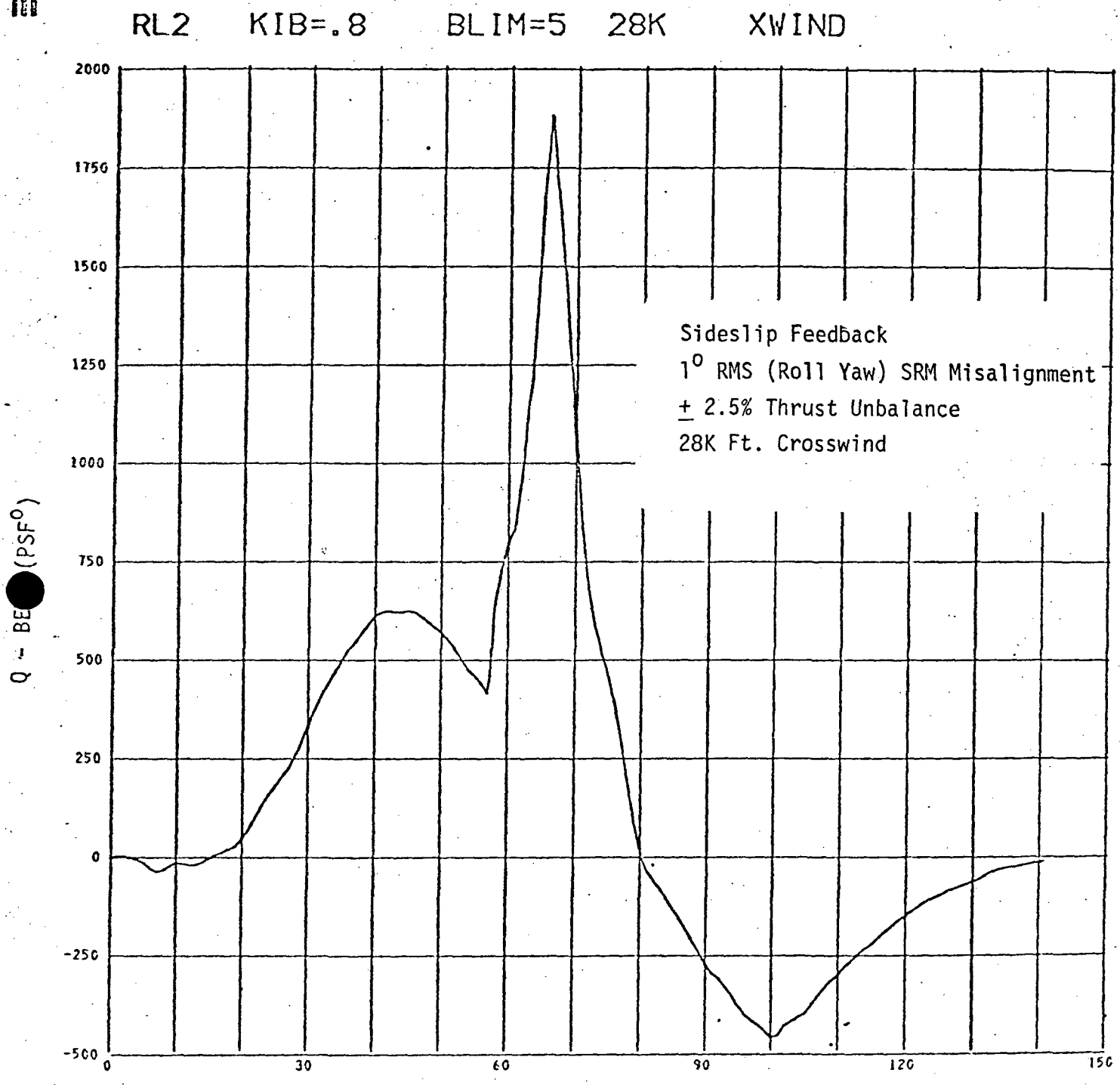

FIGURE 3-34

INFLIGHT RESULTS - SIDESLIP FEEDBACK - VECTORABLE SRM - 1.0° SRM MISALIGNMENT - Q-BETA

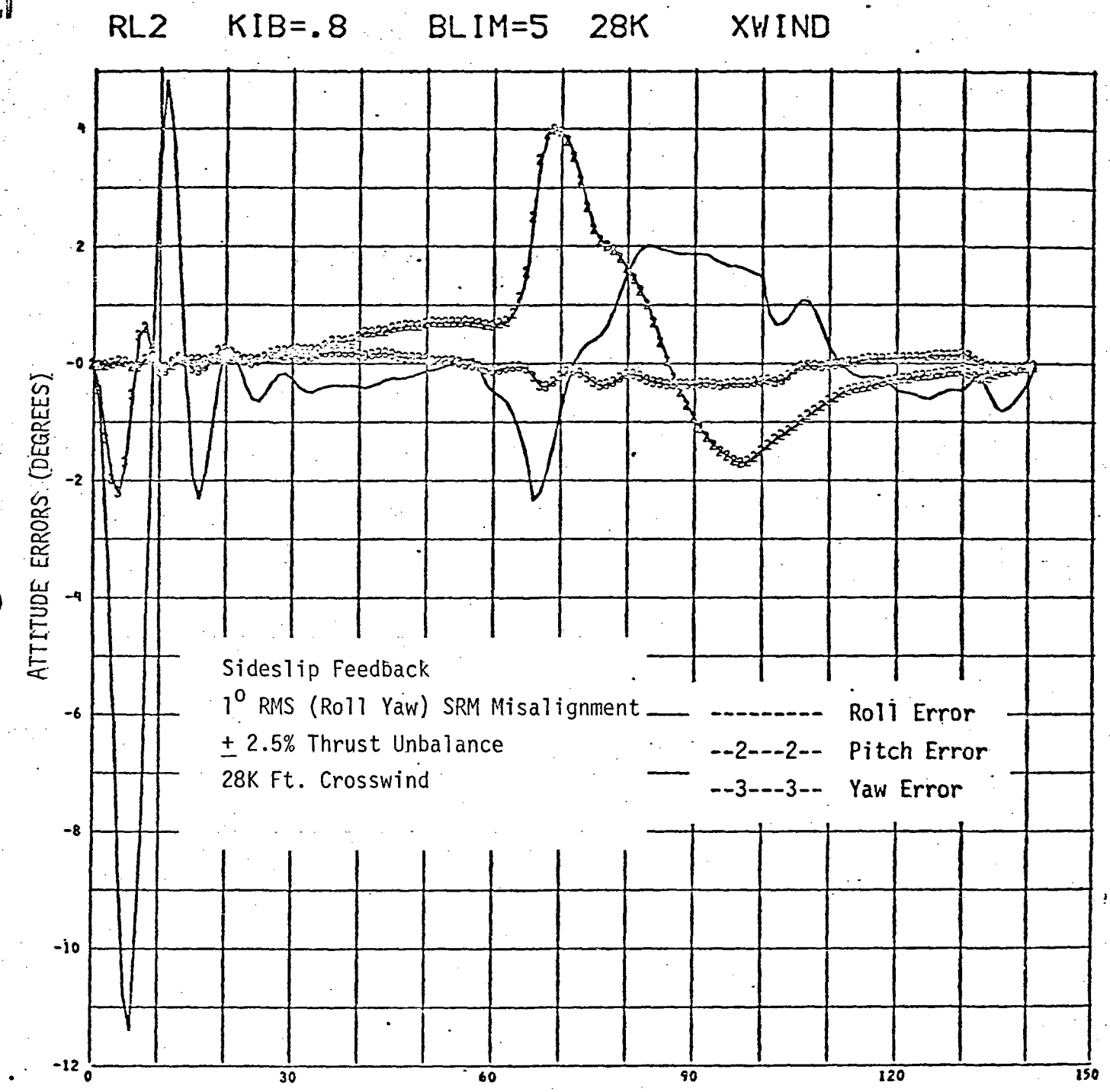

FIGURE 3-35

INFLIGHT RESULTS - SIDESLIP FEEDBACK - VECTORABLE SRM - 1.0° SRM MISALIGNMENT - ATTITUDE EERORS

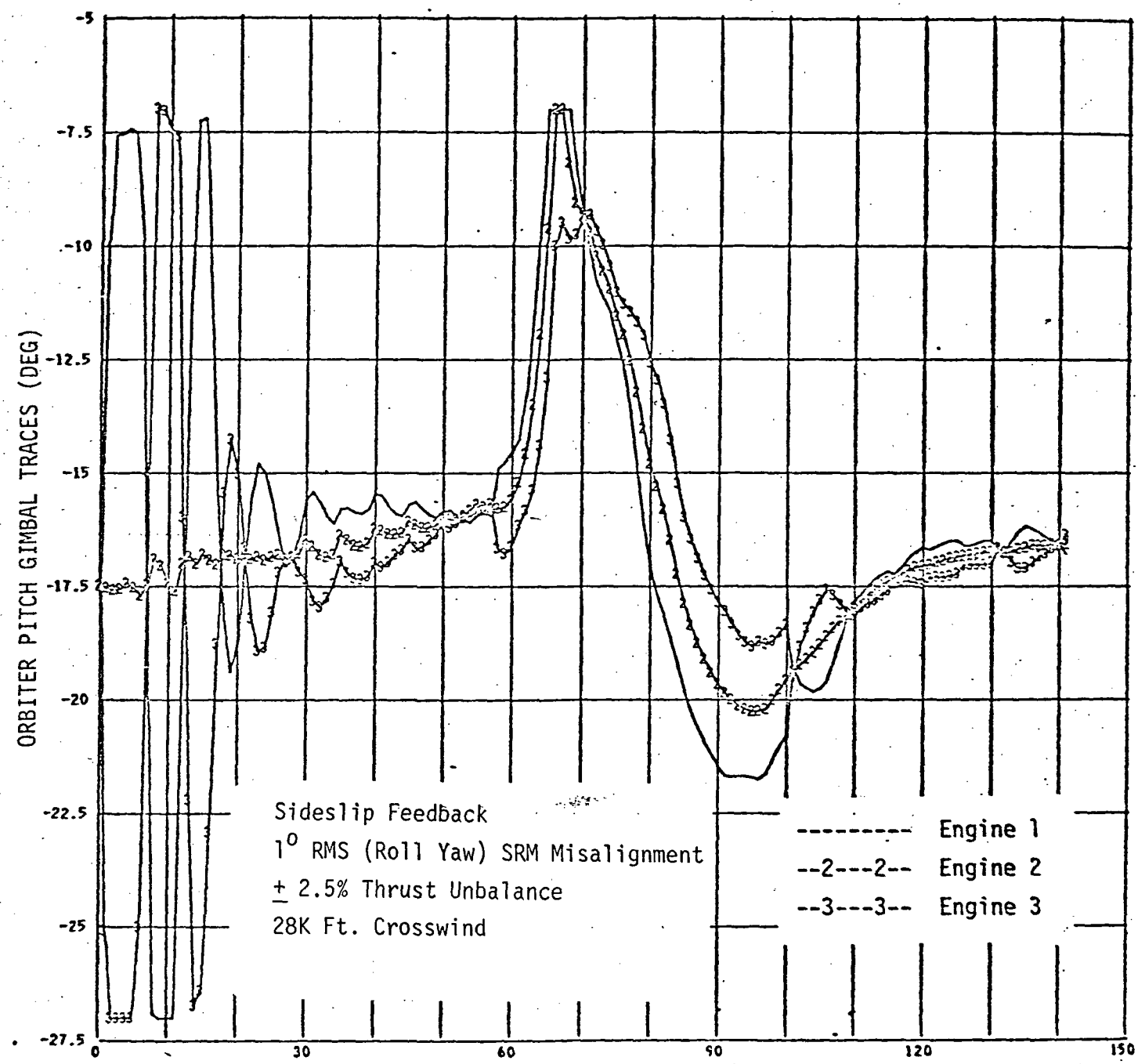

FIGURE 3-36

INFLIGHT RESULTS - SIDESLIP FEEDBACK - VECTORABLE SRM - 1.0° SRM MISALIGNMENT - ORBITER PITCH ENGINE DEFLECTIONS

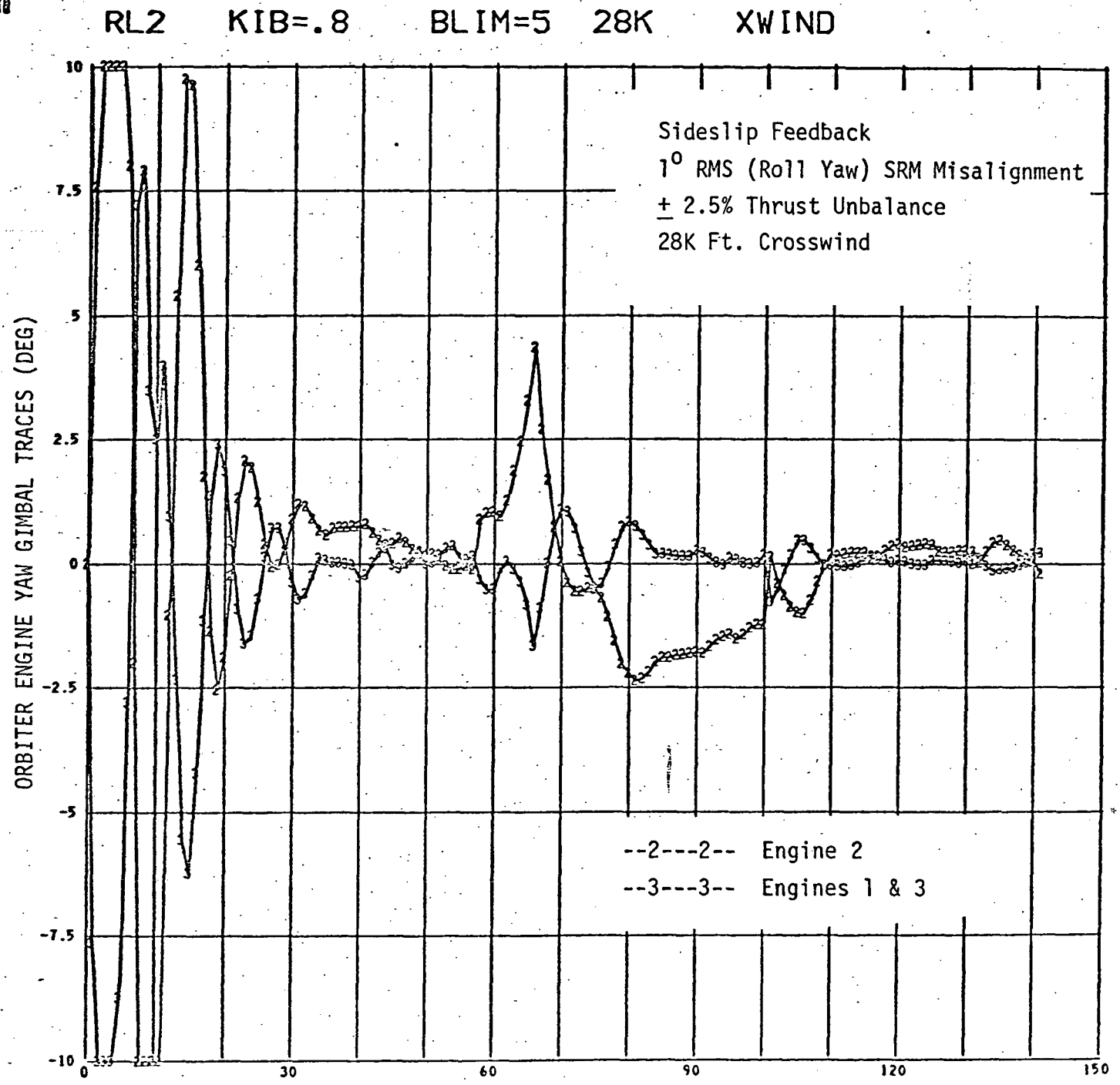

FIGURE 3-37

INFLIGHT RESUTLS - SIDESLIP FEEDBACK - VECTORABLE SRM - 1.0° SRM MISALIGNMENT - ORBITER YAW ENGINE DEFLECTIONS

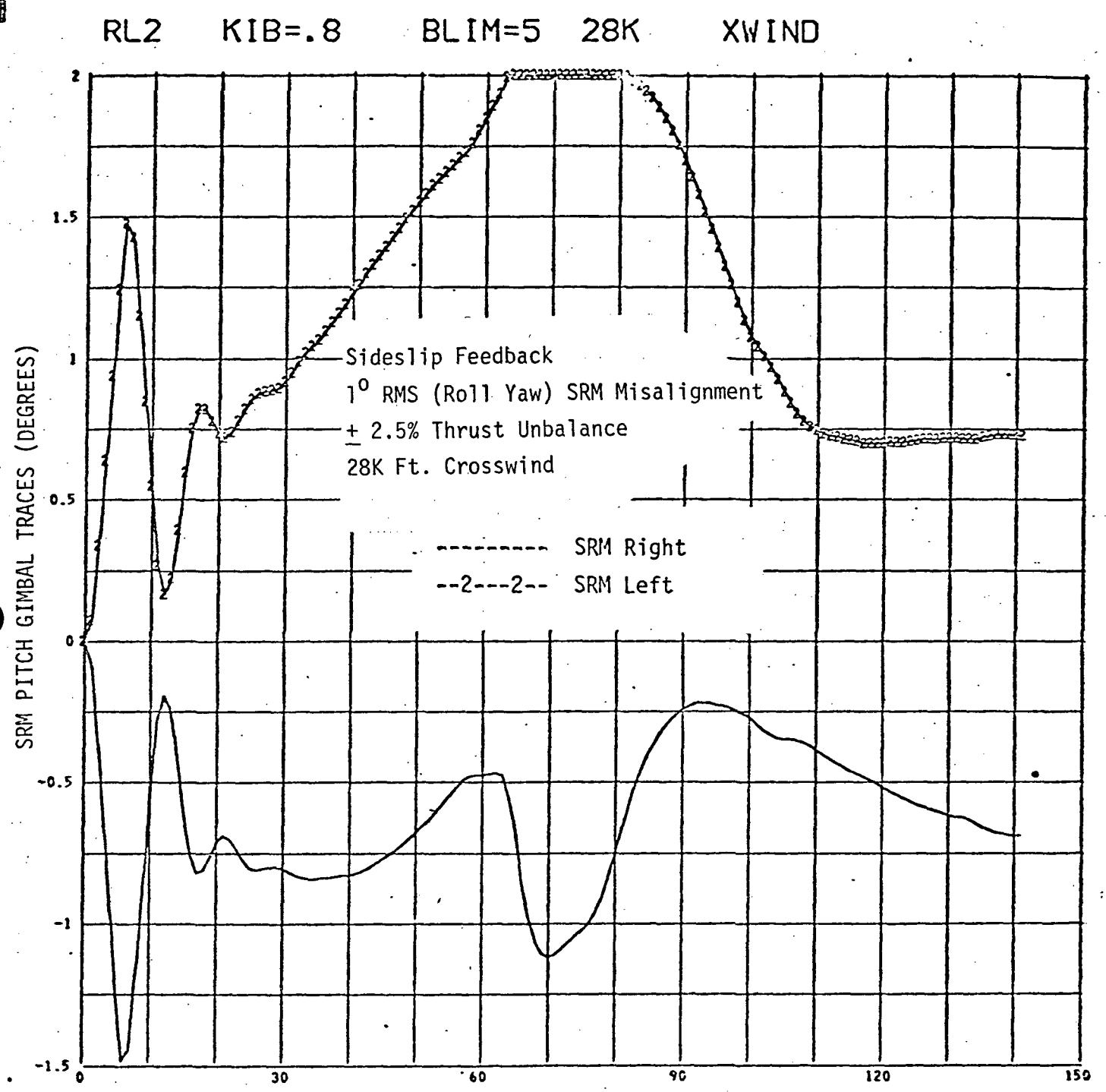

THE BOEING COMPANY

PAGE 105.

FIGURE 3-38

INFLIGHT RESULTS - SIDESLIP FEEDBACK - VECTORABLE SRM - 1.0° SRM MISALIGNMENT - SRM PITCH ENGINE DEFLECTIONS

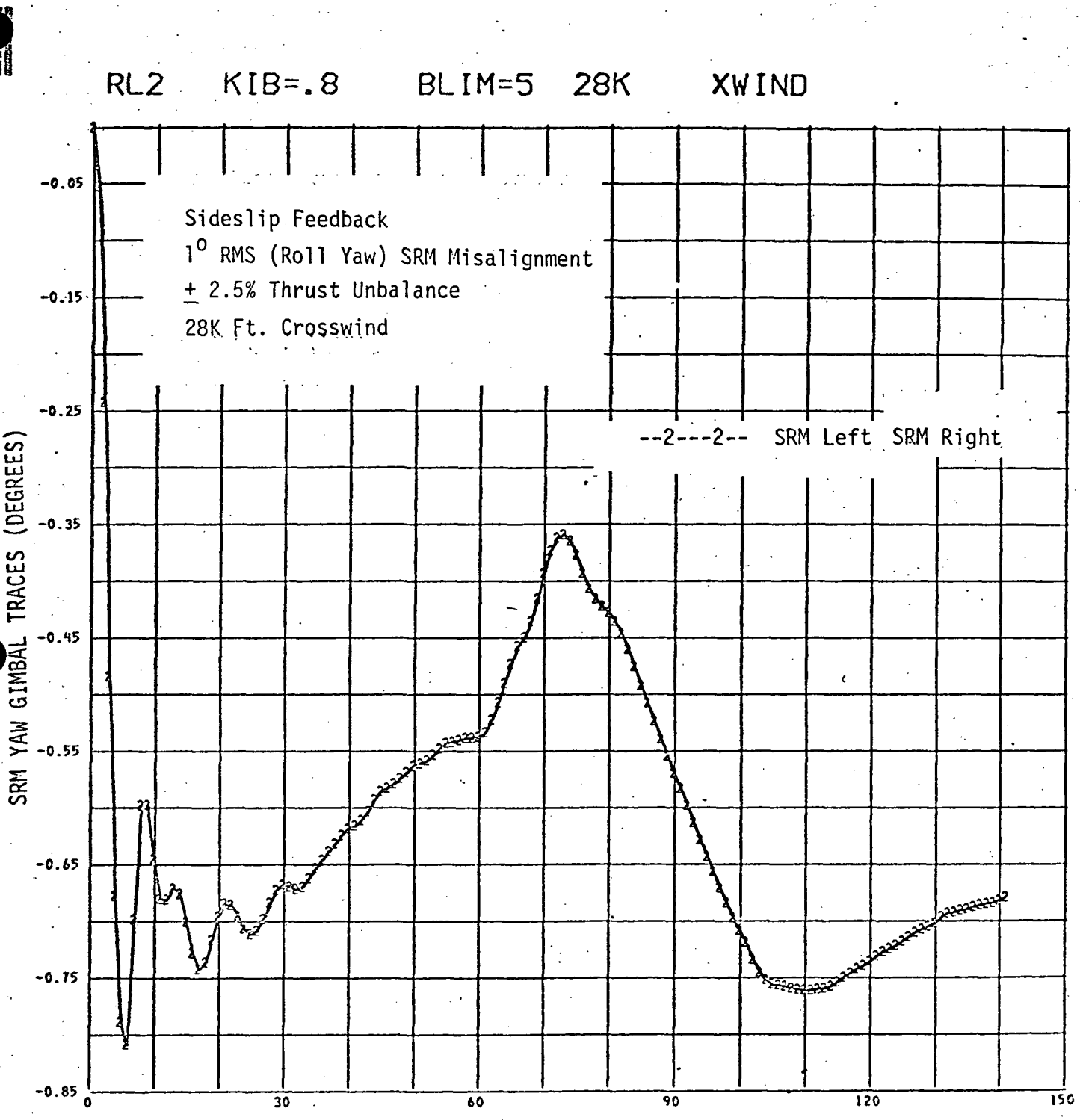

THE BOEING COMPANY

PAGE 106.

FIGURE 3-39

INFLIGHT RESULTS - SIDESLIP FEEDBACK - VECTORABLE SRM - 1.0° SRM MISALIGNMENT - SRM YAW ENGINE DEFLECTIONS

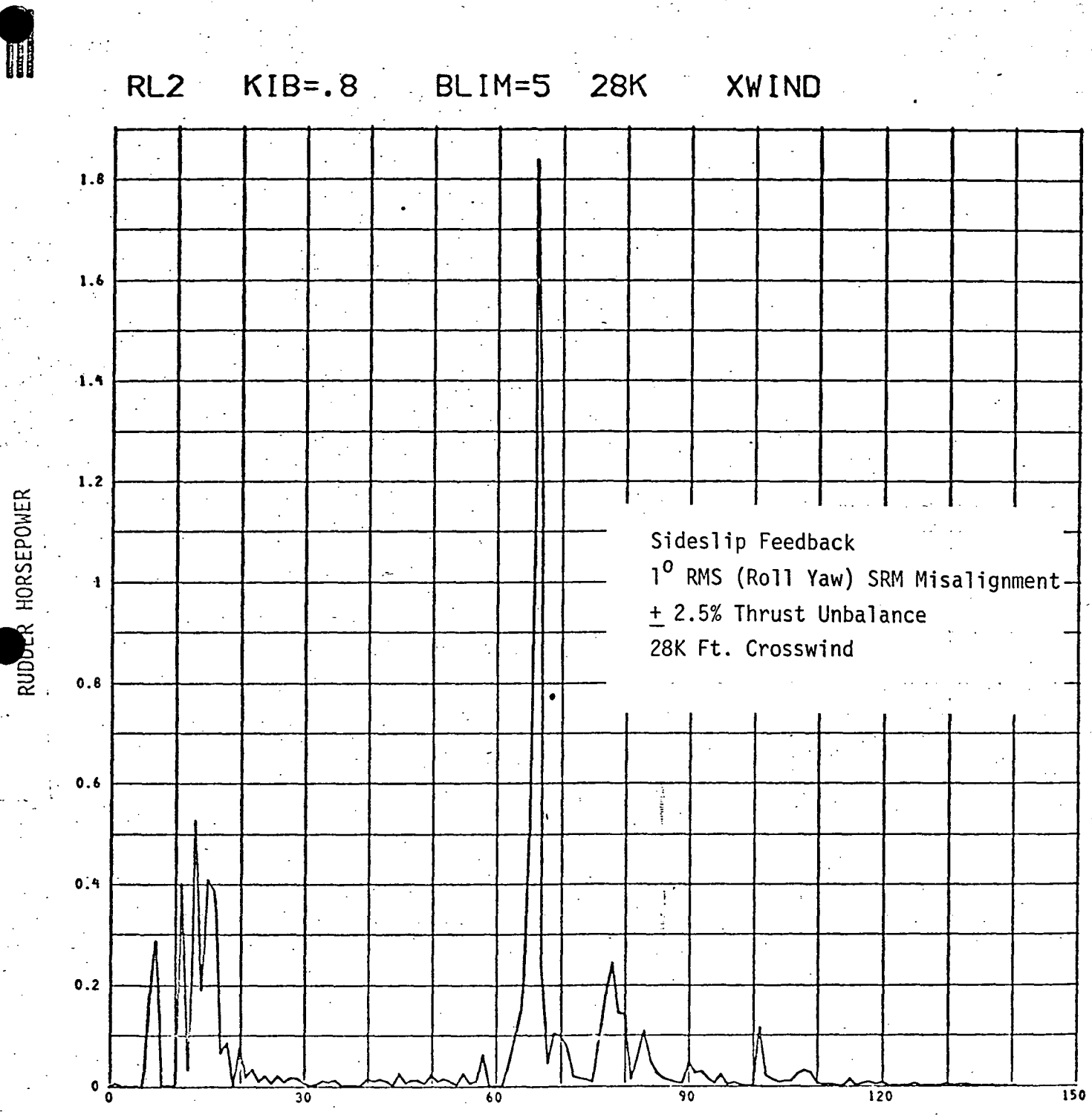

FIGURE 3-40

INFLIGHT RESULTS - SIDESLIP FEEDBACK - VECTORABLE SRM - 1.0° SRM MISALIGNMENT - RUDDER HORSEPOWER

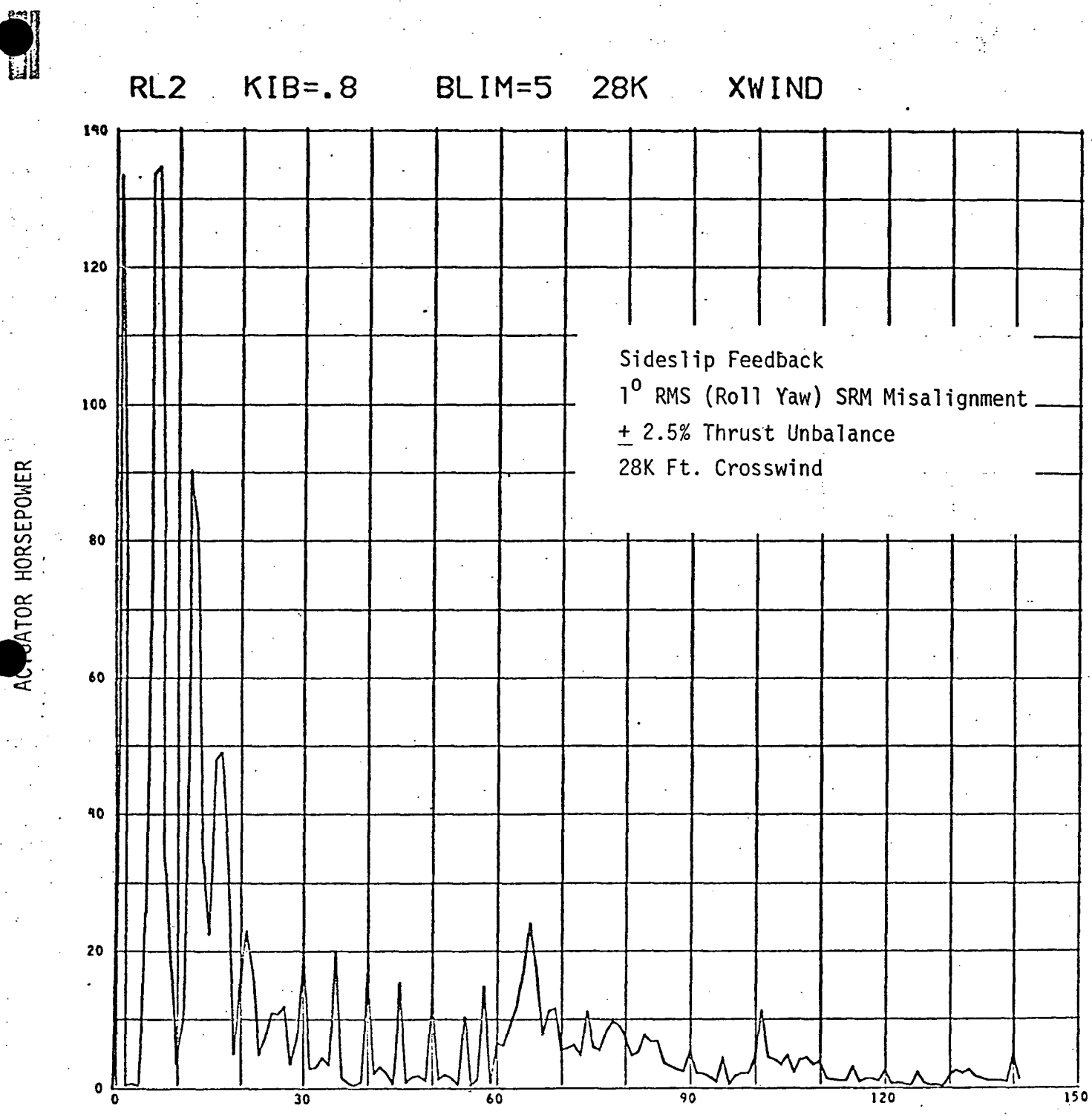

FIGURE 3-41

INFLIGHT RESULTS - SIDESLIP FEEDBACK - VECTORABLE SRM - 1.0° SRM MISALIGNMENT - ACTUATOR HORSEPOWER

TABLE 3-10

SIDESLIP FEEDBACK PARAMETERIZATION -
28K CROSSWIND - VECTORABLE SRM

28000 FT CROSSWIND 1° RMS ROLL YAW MISALIGMENT
± 2° SRM DEFLECTION LIMITS ± 2.5% THRUST UNBALANCE

SIDESLIP FEEDBACK GAIN	$q\alpha$ (PSF°)	$q\beta$ (PSF°)	ROLL ATTITUDE (DEG.)	WEIGHT TO ORBIT (POUNDS)	RUDDER HORSEPOWER HOURS	ACTUATOR HORSEPOWER HOURS
0	2432	4943	-31.0	352733	.0064	.3767
.4	-1381	3582	78.5	352179	.0034	.3669
.6	-1980	2683	85.5	352070	.0027	.3702
.8	-2287	2130	88.0	351936	.0025	.3834
1.0	-2382	1824	88.7	351873	.0028	.4042

TABLE 3-11

SIDESLIP FEEDBACK PARAMETERIZATION -
28K HEADWIND - VECTORABLE SRM

28000 FT HEADWIND 1° RMS ROLL YAW MISALIGMENT
±2° SRM DEFLECTION LIMITS ± 2.5 % THRUST UNBALANCE

SIDESLIP FEEDBACK GAIN	$q\alpha$ (PSF°)	$q\beta$ (PSF°)	ROLL ATTITUDE (DEG.)	WEIGHT TO ORBIT (POUNDS)	RUDDER HORSEPOWER HOURS	ACTUATOR HORSEPOWER HOURS
0	3845	-579	-11.5	345570	.0004	.3153
.4	3774	-1208	-34.1	344950	.0015	.3404
.6	3705	-1781	-69.8	344276	.0028	.3656
.8	3591	-2557	-119.0	343648	.0049	.3959
1.0	3401	-3229	-161.0	343516	.0070	.4267

3.2.4 Continued

headwinds because they had previously (Reference 48) been found to produce the most severe control requirements.

The roll axis channel of the baseline control system was modified slightly for inflight analysis to allow for limiting of the sideslip feedback signal. This modification is shown in Figure 3-23. Flights were simulated without sideslip feedback and with sideslip feedback gains (K_{I_β}) of 0.4, 0.6, 0.8, and 1.0 with a beta signal limit (BLIM) of 5°. Table 3-10 summarizes the crosswind results and Table 3-11 summarizes the headwind results. Several variables are shown, but the most interesting was $q\beta$. It is seen that, for the crosswind, $q\beta$ decreases as the feedback gain increases, while the opposite is true for the headwind. Based on these results, a feedback gain of 0.8 was selected as a baseline for future analysis.

Figures 3-24 through 3-41 show results of SRM gimbaling for the 28,000 ft crosswind simulations with 1 degree RMS misalignments. Figures 3-24 through 3-32 are without sideslip feedback, and Figures 3-33 through 3-41 are with sideslip feedback. They illustrate the smooth response using SRM gimbaling and the small demand on the orbiter main engine gimbaling in the high q region. Comparison with Reference 48 showed that, for the headwind case with sideslip feedback, $q\beta$ was reduced from 3566 PSF° to 2557 PSF° when SRM gimbaling is added. For the crosswind case $q\beta$ was reduced from 3194 PSF° to 2130 PSF°.

3.3 BASELINE CONTROL SYSTEM

The baseline launch configuration control system software described in this section satisfies the requirement to control the SRM parallel burn vehicle from lift-off through SRM engine cutoff and orbital insertion. This control system has evolved from the investigations of References 44, 48, 49, and 51. It is the result of efforts to provide active roll control for load alleviation and the option to vector SRM thrust such as to trim out SRM angular misaligments. Specific details presented in this section are for a nominal rigid body version of the MSC SRM-049 launch configuration. Compensation for bending and malfunctions can easily be incorporated.

The system is adaptable to various control laws, including attitude control (as in Saturn V), drift minimum control (with and without acceleraometer feedback), and/or load relief control. It also contains the option of using thrust vector control (TVC) on the SRM's as trim control to remove initial thrust misalignments. In addition, sideslip feedback may be employed during boost phases of flight to roll the vehicle into a tail to the wind attitude as a means of load alleviation.

The following paragraphs contain a description of the control systems with functional block diagrams of the pitch, yaw, and roll channels and a discussion of the configuration dependent variables.

3.3.1 Software Description

The baseline launch configuration control system is essentially a conventional booster control system. It is a digital autopilot receiving gimbal angles from a stable platform, body rates from body mounted rate gyros, and body Y and Z axes translational accelerations from body mounted accelerometers. It also receives prestored engine deflection and acceleration commands, and attitude commands either prestored or from a guidance system. From these inputs the control system determines and outputs deflection commands for the orbiter, SRM, and rudder actuators.

3.3.1 Continued

The prestored commands for attitude, acceleration, and orbiter engine deflections are the measured values taken from a reference trajectory. The baseline reference trajectory was shaped for gravity turn (zero resultant acceleration normal to the longitudinal stability axis) in order that roll maneuvers might be accomplished without deviation from the desired trajectory. Variable control gains are calculated to satisfy the selected control law and desired rigid body frequency and damping ratio. For current studies the drift minimum control law was employed with a natural frequency of one radian per second with a 0.7 damping ratio in both pitch and yaw. Roll control utilizes both thrust vector and rudder control at a natural frequency of 0.5 radian per second and a damping ratio of 0.5. It should be noted that gain calculations were made assuming no SRM thrust vector control. However, since the SRM's are used for trim control (low frequency), this assumption is valid for the rigid body analysis. Development of gain calculation equations is given in Reference 19.

A more detailed functional description of each channel of the control system is provided in the following paragraphs. Separate block diagrams for roll, pitch, and yaw channels are presented.

3.3.2 Roll Channel Description

Referring to Figure 3-42, the block in the lower right hand corner labeled "Vehicle and Subsystem Dynamics" represents actuator and sensor dynamics, prefiltering for the sensors, flight computer input and output registers and any A/D or D/A converters. Inputs to the control system from "Vehicle and Subsystem Dynamics" are the inertial platform outer gimbal angle and rate measurements from one or more body (or wing) mounted rate gyros. Outputs from the control system to the vehicle are orbiter engine, SRM engine, and rudder deflection commands.

BASELINE LAUNCH CONFIGURATION CONTROL SYSTEM SOFTWARE

ROLL CHANNEL

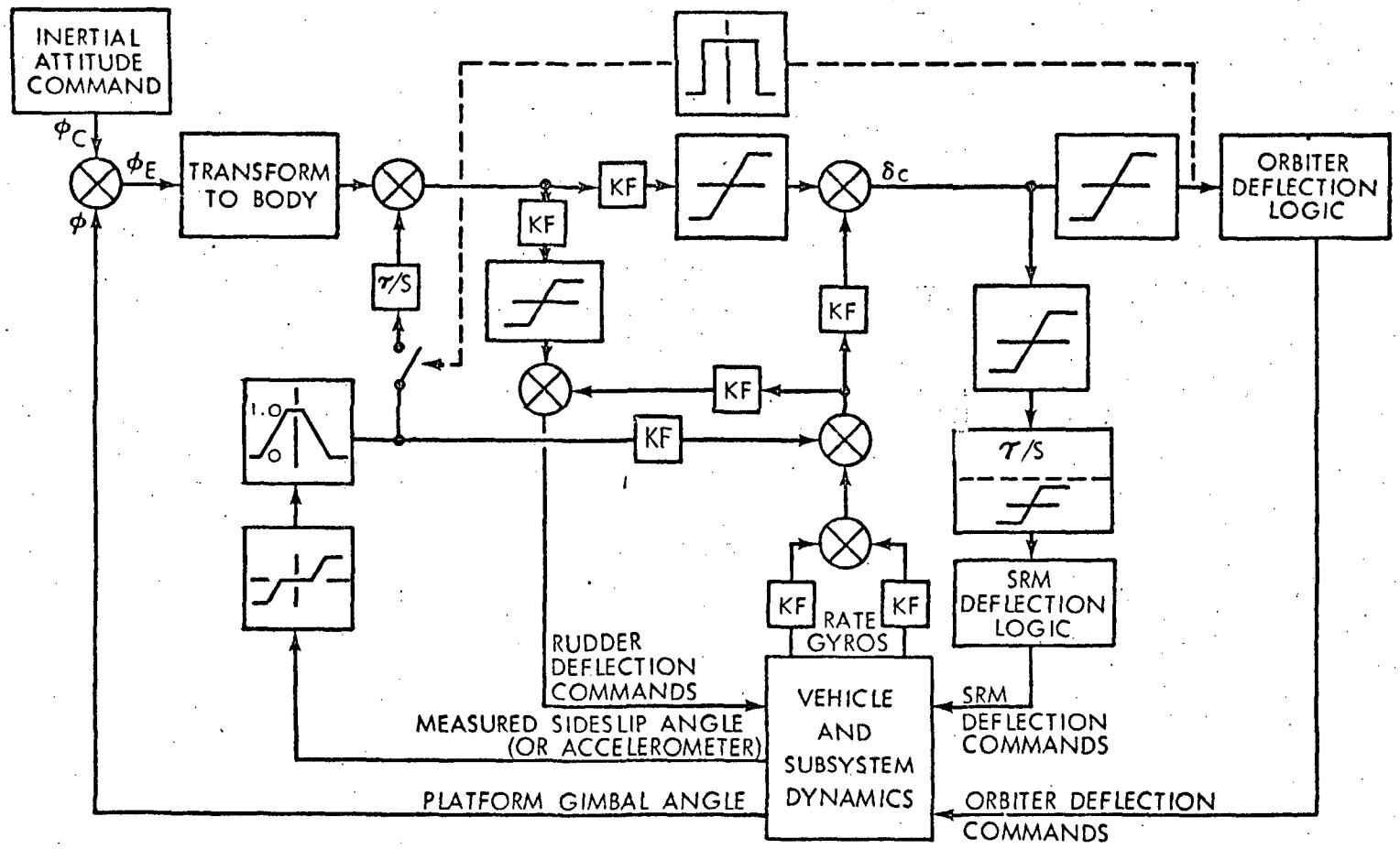

KF=SCALE AND/OR FILTER - f (τ) τ=INTEGRATOR GAIN-f (τ)

FIGURE 3-42

ROLL CHANNEL - NEW BASELINE CONTROL SYSTEM

3.3.2 Continued

Following the attitude loop in Figure 3-42, the platform gimbal angle (ϕ) is differenced with the inertial attitude command (ϕC) to produce the inertial attitude error (ϕE) which is transformed to a body roll error (ϕEB) by adding the inner gimbal angle error times the sine of the middle gimbal angle ($\phi EB = \phi EB + \phi EI \sin\psi$). At this point the body roll error signal is differenced with the signal from the sideslip feedback integrator.

The purpose of the sideslip feedback portion of the control system is to provide a means of alleviating large sideloads (qB) resulting from cross winds, by sensing the sideslip angle and producing appropriate control signals such as to roll the vehicle into a tail to the wind attitude. Referring to Figure 3-42, this is achieved by integrating the sideslip signal and subtracting it from the body roll error signal. In addition, the sideslip signal is scaled and differenced with the roll rate signal. It should be noted that the sideslip signal is passed through a 0.2° deadband and limited. Following this is a block which represents a "ramp-on" and "ramp-off" scheduling. This is to allow the sideslip roll to be initiated after tower clearance and be turned off after the wind effect has become negligible (after the high dynamic pressure region). The switch prior to the sideslip integrator is activated by the limited orbiter engine roll commands. When the roll command becomes greater than 8 degrees, the switch to the integrator is opened. This prevents the sideslip integrator from saturating the roll commands and reserves 2 degrees of roll control for rate damping commands. The body roll error signal, having been differenced with the sideslip integrator, is at this point split to supply commands to both the aerodynamic control and the thrust vector control. Referring to the roll channel block diagram, it should be noted that a limiter has been included in the attitude error loop. This limiter reserves some TVC authority for rate damping (even though the attitude error signal may be saturated) thus preventing oscillation and complete loss of control because of large signal instability.

3.3.2 Continued

Returning to the "Vehicle and Subsystem Dynamics" block in Figure 3-42, roll rate gyro signals are filtered and blended as required. The roll rate error is then scaled and filtered separately for the engine and aero channels and is mixed with the attitude error signals to produce total error signals. The rudder deflection signal is limited to avoid overdriving the servos and sent to the output registers of the rudder. In the engine TVC loop the combined roll signal (δC) is at this point split to provide signals for orbiter engine control and SRM trim control.

For SRM trim control, the combined roll signal is rate limited, integrated, and sent to the SRM deflection logic. The limiter associated with the SRM integrator limits the integrator and its output. As noted in Reference 49, it was found to be necessary to limit the integrator rather than just its output to prevent it from "overcharging" and inducing excessive lag into the system. The baseline SRM deflection logic is simple, equal and opposite SRM pitch actuator commands. Finally, the SRM engine deflection signals are limited to the hardware limits and stored in output registers.

In the orbiter engine TVC loop the combined roll signal (δC) is limited to the hardware limits and goes to the orbiter engine deflection logic. The orbiter engine deflection logic is complicated by the need to decouple yaw reaction from the roll command. Roll commands are sent to the appropriate orbiter engines actuators to produce the desired vehicle torque, i.e., equal and opposite pitch actuator deflections to the lower two orbiter engines and a yaw actuator command to the upper engine. In order to remove the yaw induced by the upper orbiter engine, the lower engines are commanded in yaw in a direction opposite to the upper engine and by an amount equal to one half of the yaw deflection of the upper engine. This deflection logic is illustrated in Figure 3-43.

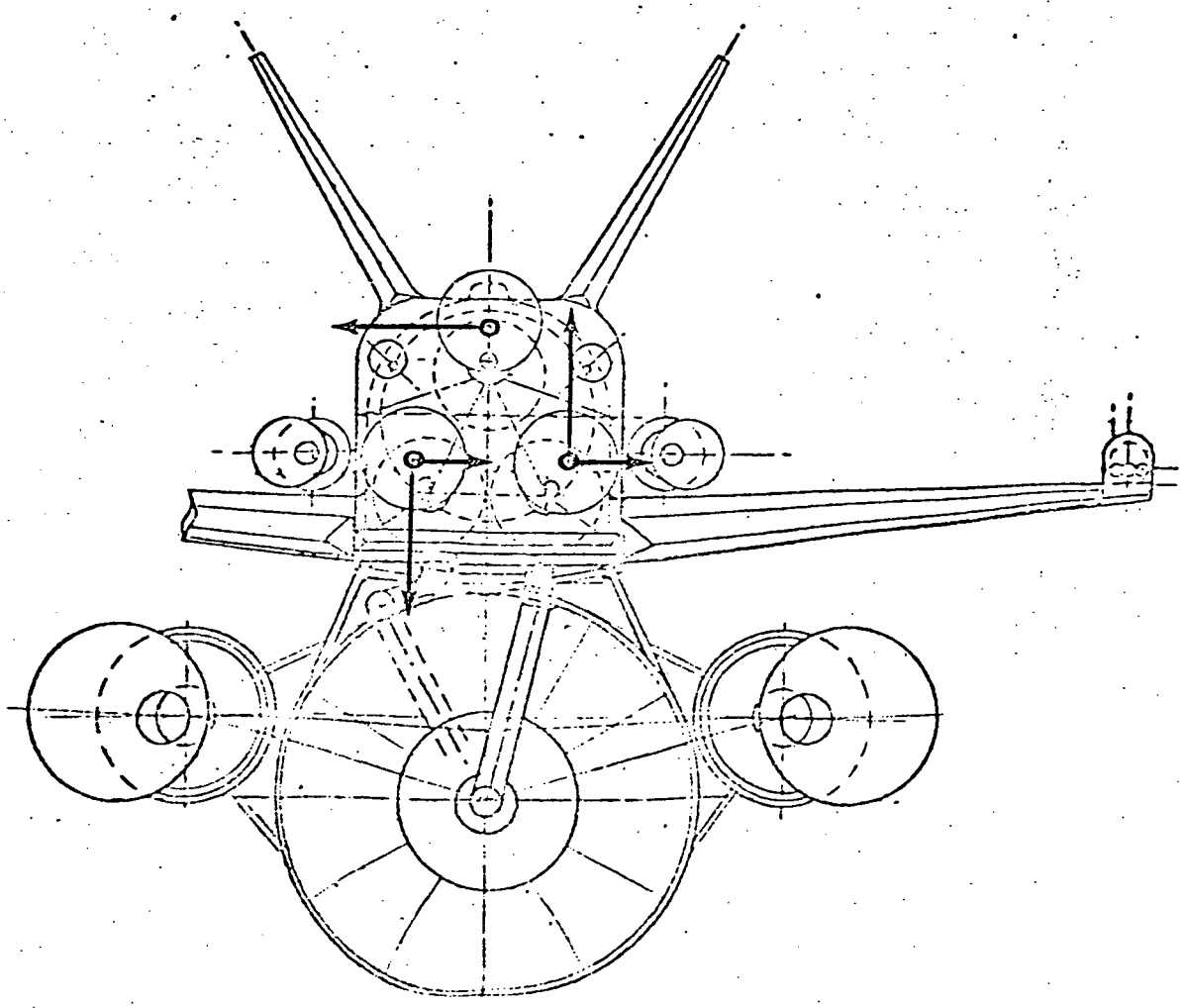

FIGURE 3-43

ORBITER ROLL CONTROL DEFLECTION LOGIC

3.3.3 Yaw Channel Description

The yaw channel block diagram in Figure 3-44 is laid out in the same manner as the roll channel with the "Vehicle and Subsystem Dynamics" block in the lower right hand corner, the "Inertial Attitude Command" in the upper left hand corner and the "Engine Deflection Logic" on the right. The aerodynamic control circuit is missing because there is adequate engine control authority to handle yaw plane torques.

Three features which were not included in the roll channel appear in the yaw channel. An accelerometer input has been added to the attitude loop, a forward loop integrator follows the limiter, and a rate command signal is differenced with the input from the rate gyros.

The platform gimbal angle (ψ) is differenced with the inertial attitude command (ψC), transformed to body attitude error ($\psi EB = \psi EI \cos\phi - \theta EI \sin\phi \cos\psi$) and scaled. The error signal is then modified by summing an acceleration error signal. The acceleration error is obtained by blending appropriately filtered signals from one or more body mounted accelerometers and then applying gain and filtering compensation according to the control law or bending requirements. For the baseline rigid body design, the gain is varied with time to meet the drift minimum requirements of Reference 19. After provision for additional filtering (not used in the rigid body baseline) and after limiting the combined error signal, the forward loop integrator trims out steady state errors resulting from biases or off-nominal conditions.

The rate command signal is introduced because the normal attitude command changes at a predictable rate. The rate command signal minimizes the tendency for the vehicle attitude to lag behind the attitude command due to rate feedback. If the vehicle rolls appreciably, the rate command must be applied partially to the yaw channel. In operation, the attitude command is differentiated, multiplied by the sine of ϕ, scaled the same as the rate feedback and differenced with the rate feedback signal. The

BASELINE LAUNCH CONFIGURATION CONTROL SYSTEM SOFTWARE

YAW CHANNEL

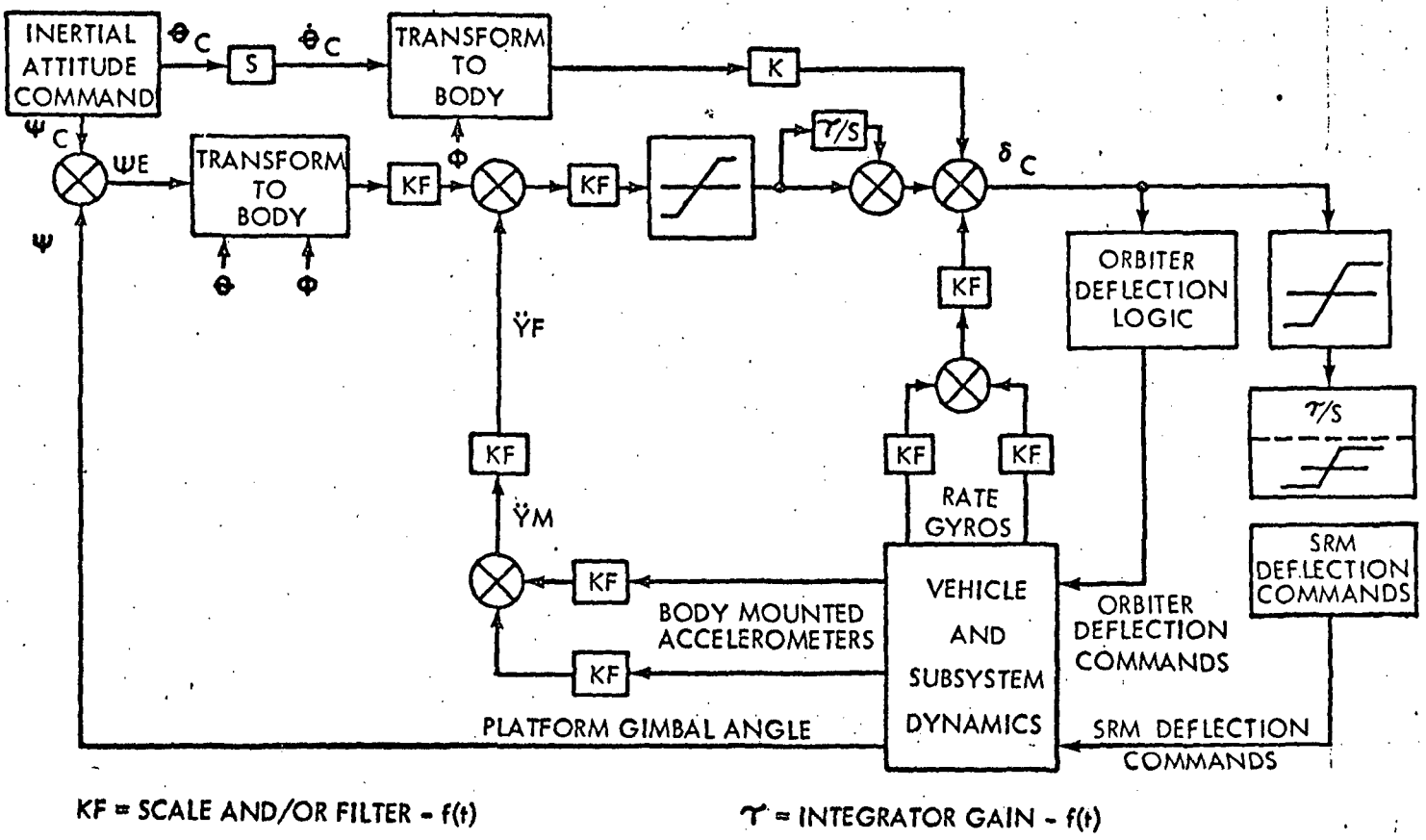

KF = SCALE AND/OR FILTER - f(t)

τ = INTEGRATOR GAIN - f(t)

FIGURE 3-44

YAW CHANNEL - NEW BASELINE CONTROL SYSTEM

3.3.3 Continued

rate error signal is then added to the attitude error signal and sent to the "orbiter engine deflection logic," where the lower two orbiter engines are commanded equally in yaw and also to the SRM trim control section. The SRM trim in yaw is the same as that previously described for roll. The command signal is rate limited, integrated and limited, and sent to the SRM deflection logic, where both SRM yaw actuators are commanded equally.

3.3.4 Pitch Channel Description

Comparison of Figure 3-45, which is the pitch channel block diagram, with Figure 3-44 (yaw channel) reveals that the only difference is the addition of prestored acceleration commands and prestored engine deflection commands. Both of these command schedules are the nominal values from a reference trajectory.

The prestored acceleration command is necessary because of the lack of vehicle symmetry, both in an offset center of gravity and in aerodynamic characteristics. The results of these asymmetries is that the nominal normal acceleration ($\ddot{Z}$) is typically non-zero. The addition of the prestored acceleration command permits use of accelerometer feedback with any feasible trajectory to modify the attitude error signal to conform to the desired control law (drift minimum for the baseline case).

The prestored engine deflection command schedule provides coarse control of the engine gimbal trim in the pitch plane. Center of gravity travel alone could be handled by the integrator. Aerodynamic pitching moment increases sharply in the vicinity of Mach one and decreases again thereafter. A high integrator gain would be required to follow these rapidly changing deflection requirements. Since a high integrator gain is undesirable in the high dynamic pressure region, the prestored commands are used to control the nominal part of this variation. For the baseline case the integrator gain (τ) is zero.

BASELINE LAUNCH CONFIGURATION CONTROL SYSTEM SOFTWARE

PITCH CHANNEL

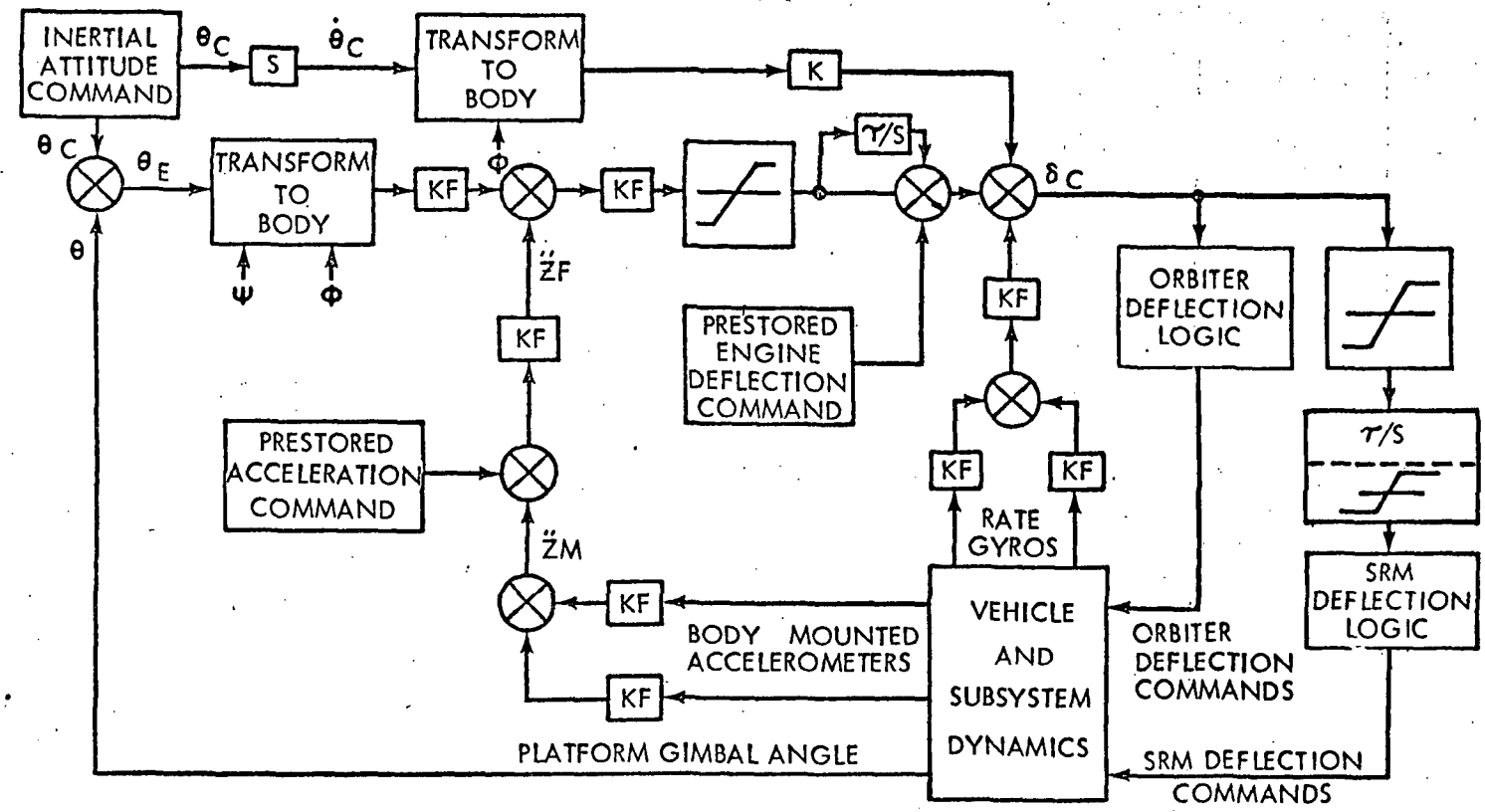

KF = SCALE AND/OR FILTER - f(t) τ = INTEGRATOR GAIN - f(t)

FIGURE 3-45

PITCH CHANNEL - NEW BASELINE CONTROL SYSTEM

3.3.4 Continued

For the orbiter engine deflection logic the pitch channel is the same as the yaw channel with the exception that all orbiter engines are deflected equally in pitch. For the SRM trim deflection logic the basic principles are the same as presented before for the roll and yaw channels. However, the pitch SRM deflection logic is slightly different. Since ample pitch control is available from the orbiter TVC system but limited orbiter TVC roll control is present, the SRM deflection logic has been devised such that roll control takes precedence over pitch commands. If the combined roll and pitch commands to either SRM produce a command signal rate greater than the limit, then the rate to the pitch integrator is the rate limit minus the roll rate command. Also, if the combined roll and pitch engine deflection command from the SRM integrators is greater than the limit, then the pitch deflection command is set equal to the limit minus the roll command. Thus full roll commands are preserved, and, if a reduction is necessary, it is taken from the pitch channel.

3.3.5 Configuration Dependency

The basic control system is designed for a dual SRM parallel burn configuration. The control gain and command schedules are, of course, configuration dependent. They will be affected by modifications to either the vehicle configuration or the reference trajectory. This will not impact the design, however, because all control gains and commands are continuously variable input functions of time. Some of them may subsequently be modified to functions of other trajectory variables, such as altitude and velocity, but this will involve only minor software modifications.

Filters have not been developed. They will be functions of the vibration and slosh characteristics of the launch configuration. The provision for incorporating filters at various points is intended to reduce the order of each filter.

4.0 TASK III FLEXIBLE BODY STABILITY AND CONTROL ANALYSIS

Frequent changes in vehicle configuration prevented performance of flexible body analysis. However mathematical models were developed for use in the SSFS. These models were programmed for a parallel burn solid rocket motor configuration such as the 049 configuration analyzed in Section 3. The flexible body version of SSFS is currently being checked out. The models as contained in Reference 52 are presented in the following paragraphs.

4.1 FLEXIBLE BODY PROGRAM DESCRIPTION

This program contains the bending and slosh models for the launch configuration during first stage boost. It uses a generalized modal approach to bending which represents the elastic response by standard normal modal equations with viscous damping. Included are models for aerodynamic forces and moment and thrust forces and moments to account for bending effects as well as the tail wags dog contribution to bending. The rigid body and elastic response equations provided here are uncoupled and are considered separately since the magnitude of the coupling is insignificant. The number of equations is very sensitive to the vehicle configuration and to the completeness of the bending analysis. Therefore, when data becomes available it is likely that only a small percentage of the general set provided here will actually be required for SSV analysis.

The model sums all the forces acting on each of the equivalent mass points and for a given mode numerically integrates the sum with a second order linear differential equation in modal displacement. The number of mass points at which aero forces and modal displacements are calculated will be less than 50. The number of modes at these points will be less than 10 each. The number of slosh masses will be less than 5 and the number of modes per slosh mass will be less than 5. The EOM, guidance atmosphere and control subroutine must be present to provide inputs for this model.

4.2 Vibration Equations

$$\sum_{j=1}^{N1} (F_{axj}\,\phi_{xij} + F_{ayj}\,\phi_{yij} + F_{azj}\,\phi_{zij})$$

$$+ \sum_{j=1}^{M1} (F_{txj}\,\phi_{xij} + F_{tyj}\,\phi_{yij} + F_{tzj}\,\phi_{zij})$$

$$+ \sum_{j=1}^{K1} (F_{sxj}\,\phi_{xij} + F_{syj}\,\phi_{yij} + F_{szj}\,\phi_{zij})$$

$$+ \sum_{j=1}^{N2} (M_{axj}\,\phi'_{xij} + M_{ayj}\,\phi'_{yij} + M_{azj}\,\phi'_{zij})$$

$$+ \sum_{j=1}^{M2} (M_{txj}\,\phi'_{xij} + M_{tyj}\,\phi'_{yij} + M_{tzj}\,\phi'_{zij})$$

$$+ \sum_{j=1}^{K2} (M_{sxj}\,\phi'_{xij} + M_{syj}\,\phi'_{yij} + M_{szj}\,\phi'_{zij})$$

$$= m_i\,(\ddot{q}_i + 2\,\zeta_i\,\omega_i\,\dot{q}_i + \omega_i^2\,q_i)$$

$$\dot{q}_i = \int \ddot{q}_i\,dt + \dot{q}_i$$

$$q_i = \int \dot{q}_i\,dt + q_i$$

4.2 Vibration Equations (Continued)

Where:

N1 = number of aero stations for aero forces

N2 = number of aero stations for aero moments

M1 = number of engines producing forces

M2 = number of engines producing moments

K1 = number of slosh stations for slosh forces

K2 = number of slosh stations for slosh moments

q_i = modal displacement due to bending mode i

ζ_i = damping coefficient for mode i

ω_i = frequency of mode i

m_i = normalized mass for mode i

F_{axj} = aero forces in X direction at station j

F_{ayj} = aero forces in Y direction at station j

F_{azj} = aero forces in Z direction at station J

F_{txj} = thrust forces in X direction for engine j

F_{tyj} = thrust forces in Y direction for engine j

F_{tzj} = thrust forces in Z direction for engine j

F_{sxj} = slosh forces in X direction at station j

F_{syj} = slosh forces in Y direction at station j

F_{szj} = slosh forces in Z direction at station j

M_{axj} = aero moments about X axis at station j

M_{ayj} = aero moments about y axis at station j

M_{azj} = aero moments about z axis at station j

4.2 Vibration Equations (Continued)

M_{txj} = thrust moments about X axis due to engine j

M_{tyj} = thrust moments about Y axis due to engine j

M_{tzj} = thrust moments about Z axis due to engine j

M_{sxj} = slosh moments about X axis at station j

M_{syj} = slosh moments about Y axis at station j

M_{szj} = slosh moments about Z axis at station j

ϕ_{xij} = mode shape translation in X direction for mode i at location j

ϕ_{yij} = mode shape translation in Y direction for mode i at location j

ϕ_{zij} = mode shape translation in Z direction for mode i at location j

ϕ'_{xij} = mode slope about X axis for mode i at location j

ϕ'_{yij} = mode slope about Y axis for mode i at location j

ϕ'_{zij} = mode slope about Z axis for mode i at location j

4.3 Aerodynamic Forces

$$\begin{bmatrix} V_{wxpj} \\ V_{wypj} \\ V_{wzpj} \end{bmatrix} = [\alpha] \quad [\delta] \quad \begin{bmatrix} 0 \\ -V_{w_j} \sin A_{zw_j} \\ -V_{w_j} \cos A_{zw_j} \end{bmatrix}$$

$$\begin{bmatrix} V'_{axbj} \\ V'_{aybj} \\ V'_{azbj} \end{bmatrix} = [\beta]^{-1} \left[\begin{bmatrix} V_{R_{X_p}} \\ V_{R_{X_p}} \\ V_{R_{X_p}} \end{bmatrix} - \begin{bmatrix} V_{wxpj} \\ V_{wypj} \\ V_{wzpj} \end{bmatrix} \right]$$

4.3 Aerodynamic Forces (Continued)

$$V''_{axbj} = Q\,(\bar{Z}_j - \bar{Z}_{cg}) - R\,(\bar{Y}_j - \bar{Y}_{cg})$$

$$V''_{aybj} = R\,(\bar{X}_j - \bar{X}_{cg}) - P\,(\bar{Z}_j - \bar{Z}_{cg})$$

$$V''_{azbj} = P\,(\bar{Y}_j - \bar{Y}_{cg}) - Q\,(\bar{X}_j - \bar{X}_{cg})$$

$$V''_{axbj} = \sum_{i=1}^{M3} \phi_{xij}\,\dot{q}_i$$

$$V''_{aybj} = \sum_{i=1}^{M3} \phi_{yij}\,\dot{q}_i$$

$$V'''_{azbj} = \sum_{i=1}^{M3} \phi_{zij}\,\dot{q}_i$$

$$V^{IV}_{axbj} = V_{aybj} \sum_{i=1}^{M3} \phi'_{zij}\,q_i - V_{azbj} \sum_{i=1}^{M3} \phi'_{yij}\,q_i$$

$$V^{IV}_{aybj} = V_{azbj} \sum_{i=1}^{M3} \phi'_{xij}\,q_i - V_{axbj} \sum_{i=1}^{M3} \phi'_{zij}\,q_i$$

$$V^{IV}_{azbj} = V_{axbj} \sum_{i=1}^{M3} \phi'_{yij}\,q_i - V_{aybj} \sum_{i=1}^{M3} \phi'_{xij}\,q_i$$

4.3 Aerodynamic Forces (Continued)

$$V_{axbj} = V_{axbj}' + V_{axbj}'' + V_{axbj}''' + V_{axbj}^{IV}$$

$$V_{aybj} = V_{aybj}' + V_{aybj}'' + V_{aybj}''' + V_{aybj}^{IV}$$

$$V_{azbj} = V_{azbj}' + V_{azbj}'' + V_{azbj}''' + V_{azbj}^{IV}$$

The previous 6 equations must be solved simultaneously for V_{axbj}, V_{aybj}, and V_{azbj}. The solution is as follows:

let

$$a_{11} = -1$$

$$a_{12} = \sum_{i=1}^{M3} \phi'_{zij}\, q_i$$

$$a_{13} = -\sum_{i=1}^{M3} \phi'_{yij}\, q_i$$

$$a_{21} = -\sum_{i=1}^{M3} \phi'_{zij}\, q_i$$

$$a_{22} = -1$$

$$A_{23} = +\sum_{i=1}^{M3} \phi'_{xij}\, q_i$$

4.3 Aerodynamic Forces (Continued)

$$a_{31} = \sum_{i=1}^{M3} \phi'_{yij}\, q_i$$

$$a_{32} = -\sum_{i=1}^{M3} \phi'_{xij}\, q_i$$

$$a_{33} = -1$$

$$[A] = \begin{bmatrix} a_{11} & a_{12} & a_{13} \\ a_{21} & a_{22} & a_{23} \\ a_{31} & a_{32} & a_{33} \end{bmatrix}$$

then:

$$\begin{bmatrix} V_{axbj} \\ V_{aybj} \\ V_{azbj} \end{bmatrix} = [A]^{-1} \begin{bmatrix} -V'_{axbj} - V''_{axbj} - V'''_{axbj} \\ -V'_{aybj} - V''_{aybj} - V'''_{aybj} \\ -V'_{azbj} - V''_{azbj} - V'''_{azbj} \end{bmatrix}$$

$$V_{aj} = \sqrt{V_{axbj}^2 + V_{aybj}^2 + V_{azbj}^2}$$

$$\beta_j = \text{Arcsin}\left(\frac{V_{aybj}}{V_{aj}}\right)$$

4.3 Aerodynamic Forces (Continued)

$$\alpha_j = \text{Arctan}\left(\frac{V_{azbj}}{V_{axbj}}\right)$$

$$M_j = \frac{V_{aj}}{a}$$

$$q_j = \tfrac{1}{2}\,\rho\, V_{aj}^{\,2}$$

$$F_{axj} = q_j\, S\, (C_{xoj} + C_{x\alpha j}\, \alpha_j)$$

$$F_{ayj} = q_j\, S\, C_{y\beta j}\, \beta_j + \frac{q_j\, Sb}{2\, V_{ax\beta j}}\, C_{ypj}\, P + q_j\, S\, C_{y\delta r}\, \delta_r$$

$$F_{azj} = q_j\, S\, (C_{zoj} + C_{z\alpha j}\, \alpha_j) + q_j\, S\, C_{z\delta e}\, \delta_e$$

Where:

V_{w_j} = magnitude of relative wind at Station j

A_{zw_j} = azimuth angle of relative wind at Station j

V_{wxpj}', V_{wypj}', V_{wzpj} = relative wind velocity at mass point j in platform coordinates

$[\alpha]$ = transformation described in "coordinate systems"

$[\beta]$ = transformation described in "coordinate systems"

$[\delta]$ = transformation described in "coordinate systems"

4.3 Aerodynamic Forces (Continued)

V'_{axbj}, V'_{aybj}, V'_{azbj} = components of air velocity in body coordinates at mass point j

P, Q, R = angular velocity about X, Y, and Z axes respectively

$\bar{X}_j, \bar{Y}_j, \bar{Z}_j$ = location of mass point j in body coordinates

$\bar{X}_{cg}, \bar{Y}_{cg}, \bar{Z}_{cg}$ = location of center of gravity in body coordinates

V''_{axbj}, V''_{aybj}, V''_{azbj} = component of velocity at mass point j due to rotation of mass point about c.g.

V'''_{axbj}, V'''_{aybj}, V'''_{azbj} = components of velocity of vibrating mass with respect to rigid body

V^{IV}_{axbj}, V^{IV}_{aybj}, V^{IV}_{azbj} = components of velocity due to perpendicular forces being rotated with respect to rigid body due to bending

M3 = number of bending modes

$V_{R_{X_P}}, V_{R_{Y_P}}, V_{R_{Z_P}}$ = velocity of vehicle relative to the earth in platform coordinate

V_{axbj}, V_{aybj}, V_{azbj} = components of velocity of mass point j with respect to air

4.3 Aerodynamic Forces (Continued)

α_j = angle of attack of mass point j

M_j = mach number of mass point j

V_{aj} = velocity of mass point j with respect to air

a = speed of sound

q_j = dynamic pressure at mass point j

ρ = mass density of air

S = aero reference area

δ_r = rudder deflection

δ_e = elevator deflection

C_{xoj}, $C_{x_{\alpha j}}$, $C_{y\beta j}$, C_{ypj}, $C_{y\delta r}$, C_{zoj}, $C_{z\alpha j}$, $C_{z\delta e}$ = aero coefficients for mass point j

β_j = sideslip angle for mass point j

4.4 Engine Forces

$$\theta_{yj} = \theta'_{yj} + \sum_{i=1}^{M3} \phi'_{zij}\, q_i$$

$$\theta_{pj} = \theta'_{pj} + \sum_{i=1}^{M3} \phi'_{yij}\, q_i$$

$$T_{bxj} = ET_j \cos \theta_{pj} \cos \theta_{yj}$$

$$T_{byj} = ET_j \sin \theta_{yj}$$

$$T_{bzj} = -ET_j \sin \theta_{pj} \cos \theta_{yj}$$

$$\dot{\hat{\theta}}_{pj} = \omega_a \left(\theta_{pcj} - \hat{\theta}_{pj}\right)$$

$$\dot{\hat{\theta}}_{yj} = \omega_a \left(\theta_{ycj} - \hat{\theta}_{yj}\right)$$

$$\hat{\theta}_{pj} = \int \dot{\hat{\theta}}_{pj}\, dt + \hat{\theta}_{pjo}$$

$$\hat{\theta}_{yj} = \int \dot{\hat{\theta}}_{yj}\, dt + \hat{\theta}_{yjo}$$

4.4 Engine Forces (Continued)

$$\ddot{\theta}'_{pj} + \dot{Q} + \sum_{i=1}^{M3} \phi'_{yij}\, \ddot{a}_i + 2\zeta_{ep}\, \omega_{ep}\, \dot{\theta}'_{pj} + \omega^2_{ep}\, \theta_{pj} =$$

$$\omega^2_{ep}\, \hat{\theta}_{pj} - \frac{F_{ezj}}{I_{yye}} (X_{ecgj} - X_{ej})$$

$$\ddot{\theta}'_{yj} + \dot{R} + \sum_{i=1}^{M3} \phi'_{zij}\, \ddot{q}_i + 2\,\zeta_{ej}\, \omega_{ey} \dot{\theta}'_{yj} + \omega^2_{ey}\, \theta'_{yj} =$$

$$\omega^2_{ey}\, \hat{\theta}_{yj} + \frac{F_{eyj}}{I_{zze}} (X_{ecgj} - X_{ej})$$

$$\dot{\theta}'_{pj} = \int \ddot{\theta}'_{pj}\, dt + \dot{\theta}'_{pjo}$$

$$\theta'_{pj} = \int \dot{\theta}'_{pj}\, dt + \theta'_{pjo}$$

$$\dot{\theta}'_{yj} = \int \dot{\theta}'_{yj}\, dt + \theta'_{yjo}$$

$$\dot{\theta}'_{yj} = \int \ddot{\theta}'_{yj}\, dt + \dot{\theta}_{yjo}$$

$$F_{txj}' = ET_j \cos \theta'_p, \cos \theta'_{yj}$$

$$F_{tyj}' = E_{tj} \sin \theta'_{yj}$$

$$F_{tzj}' = -E_{tj} \sin \theta'_{pj} \cos \theta'_{yj}$$

$$F_{exj} = -m_{ej} \left[A_x + \sum_{i=1}^{M3} \phi_{xij}\, \ddot{q}_i - (y_{ej} - y_{cg})\, \dot{R} + (Z_{cj} - Z_{cg})\, \dot{Q} \right]$$

$$F_{eyj} = -m_{ej} \left\{ A_y + (X_{ej} - X_{CG})\, \dot{R} - (Z_{ej} - Z_{CG})\, \dot{P} + \sum_{i=1}^{M3} \phi_{yij}\, \ddot{q}_i \right\}$$

$$- F_{exj} \sin \theta'_{yj}$$

4.4 Engine Forces (Continued)

$$F_{ezj} = -m_{ej}\left\{A_z - (X_{ej} - X_{cg})\,\dot{Q} + (y_{ej} - y_{cg})\,\dot{P} + \sum_{i=1}^{M3} \phi_{zij}\,\ddot{q}_i\right\}$$

$$-F_{exj} \sin \theta'_{pj}$$

$$F_{txj} = F'_{txj} + F_{exj}$$

$$F_{tyj} = F'_{tyj} + m_{ej}\,(X_{ej} - X_{ecg})\,\ddot{\theta}'_y + F_{eyj}$$

$$F_{tzj} = F'_{tzj} + m_{ej}\,(X_{ecg} - X_{ej})\,\ddot{\theta}'_p + F_{ezj}$$

Where:

θ'_{yj} = yaw engine gimbal angle with respect to the mounting surface for engine j

θ_{yj} = yaw engine gimbal angle with respect to rigid body coordinates for engine j

θ'_{pj} = pitch engine gimbal angle with respect to the mounting surface for engine j

θ_{pj} = pitch engine gimbal angle with respect to rigid body coordinates for engine j

$\left.\begin{matrix}-\\ X_{ej},\\ -\\ Y_{ej},\\ -\\ Z_{ej}\end{matrix}\right\}$ = location of engine j pivot point

4.4 Engine Forces (Continued)

$\bar{X}_{ecgj}$, $\bar{Y}_{ecgj}$, $\bar{Z}_{ecgj}$ = location of engine j center of mass

T_{bxj}, T_{byj}, T_{bzj} = thrust forces acting on vehicle

$\hat{\theta}_{pj}$ = pitch engine actuator angle

$\hat{\theta}_{yj}$ = yaw engine actuator angle

$\dot{\hat{\theta}}_{pj}$ = pitch engine actuator rate

I_{yye} = moment of inertia of engine bell about Y axis at engine gimbal point

I_{zze} = moment of inertia of engine bell about Z axis at engine gimbal point

$\dot{\hat{\theta}}_{yj}$ = yaw engine actuator rate

θ_{pcj} = pitch gimbal angle command

θ_{ycj} = yaw gimbal angle command

ζ_{ep} = damping factor for pitch engine dynamics

ζ_{ey} = damping factor for yaw engine dynamics

ω_e = frequency for engine dynamics

ω_a = frequency for actuator dynamics

$\dot{\theta}_p$ = present engine rate for pitch

$\dot{\theta}_y$ = present engine rate for yaw

$\ddot{\theta}_p$ = pitch engine angular acceleration

$\ddot{\theta}_y$ = yaw engine angular acceleration

4.4 Engine Forces (Continued)

M_{ej} = mass of engine j

A_x, A_y, A_z = linear acceleration of vehicle in body coordinates

$\bar{X}_{cg}$, $\bar{Y}_{cg}$, $\bar{Z}_{cg}$ = vehicle center of gravity

The characteristicsfrequencies associated with the engine dynamics are much higher than the vehicle characteristic frequencies. It is recommended that the engine dynamics be integrated separately with an integration cycle of 50 milliseconds.

4.5 Slosh Forces

$$\ddot{\lambda}_{xj} + 2\zeta_{sj}\,\omega_{sj}\,\dot{\lambda}_{xj} + \omega^2_{sj}\,\lambda_{xj} = -\sum_{i=1}^{M3} \phi_{xij}\,\ddot{q}_i - A_x - \dot{Q}\,(Z_{sj} - \bar{Z}_{cg}) + \dot{R}\,(\bar{Y}_{sj} - Y_{cg})$$

$$\ddot{\lambda}_{yj} + 2\zeta_{sj}\,\omega_{sj}\,\dot{\lambda}_{yj} + \omega^2_{sj}\,\lambda_{yj} = -\sum_{i=1}^{M3} \phi_{yij}\,\ddot{q}_i - A_y - \dot{R}\,(X_{sj} - \bar{X}_{cg}) + \dot{P}\,(Z_{sj} - \bar{Z}_{cg})$$

4.5 Slosh Forces (Continued)

$$\ddot{\lambda}_{zj} + 2\,\zeta_{sj}\,\omega_{sj}\,\dot{\lambda}_{zj} + \omega^2_{sj}\,\lambda_{zj} = -\sum_{i=1}^{M3} \phi_{zij}\,\ddot{q}_i - A_z - \dot{P}\,(Y_{sj} - \overline{Y}_{cg})$$

$$+ \dot{Q}\,(X_{sj} - \overline{X}_{cg})$$

$$F_{sxj} = -m_{sj}\,\ddot{\lambda}_{xj}$$

$$F_{xyj} = -m_{sj}\,\ddot{\lambda}_{yj}$$

$$F_{szj} = -m_{sj}\,\ddot{\lambda}_{zj}$$

$$\dot{\lambda}_{xj} = \int \ddot{\lambda}_{xj}$$

$$\dot{\lambda}_{yj} = \int \ddot{\lambda}_{yj}$$

$$\dot{\lambda}_{zj} = \int \ddot{\lambda}_{zj}$$

$$\lambda_{xj} = \int \dot{\lambda}_{xj}$$

$$\lambda_{yj} = \int \dot{\lambda}_{yj}$$

$$\lambda_{zj} = \int \dot{\lambda}_{zj}$$

Where:

$\lambda_{xj}, \lambda_{yj}, \lambda_{zj}$ = displacements of slosh mass j

$\dot{\lambda}_{xj}, \dot{\lambda}_{yj}, \dot{\lambda}_{zj}$ = velocities of slosh mass j

$\ddot{\lambda}_{xj}, \ddot{\lambda}_{yj}, \ddot{\lambda}_{zj}$ = acceleration of slosh mass j

4.5 Slosh Forces (Continued)

ζ_{sj} = damping factor for slosh mode j

ω_{sj} = characteristic frequency of slosh mode j

X_{sj},

Y_{sj}, = position of slosh mass j

Z_{sj}

m_{sj} = mass of sloshing fluid at mode j

4.6 Aerodynamic Moments

$$M'_{axj} = F_{ayj} (Z_{cg} - Z_{arj}) - F_{azj} (Y_{cg} - Y_{arj})$$

$$M'_{ayj} = F_{azj} (X_{cg} - X_{arj}) - F_{axj} (Z_{cg} - Z_{arj})$$

$$M'_{azj} = F_{axj} (Y_{cg} - Y_{arj}) - F_{ayj} (X_{cg} - X_{arj})$$

$$M''_{axj} = q_j S b (C_{l\beta j} \beta_j + C_{l\delta a} \delta a + C_{l\delta r} \delta r) + \frac{q_j s b^2}{2 V_{axbj}} (C_{lp} P + C_{lr} R)$$

$$M''_{ayj} = q_j S \bar{c} (C_{moj} + C_{m\alpha j} \alpha_j + C_{m\delta e} \delta_e + \frac{C_{mq} Q \bar{c}}{2 V_{a_{x_{b_j}}}})$$

4.6 Aerodynamic Moments (Continued)

$$M''_{azj} = q_j S b C_{n\beta j} + \frac{q_j S b^2}{2 V_{axbj}} C_{np} P + q_j S b_\beta (C_{n\delta a} \delta_a + C_{n\delta r} \delta r)$$

$$M_{axj} = M'_{axj} + M''_{axj}$$

$$M_{ayj} = M'_{ayj} + M''_{ayj}$$

$$M_{azj} + M'_{azj} + M''_{azj}$$

Where:

$C_{l\delta a}$, $C_{n\delta a}$, $C_{l\beta j}$, $C_{l\delta r}$, C_{lpj}, C_{lr}, C_{moj}, $C_{m\alpha j}$, b_j, $\bar{c}_j$, $C_{m\delta e}$, C_{mqj}, $C_{n\beta j}$,

C_{np}, $C_{n\delta r}$ = aero coefficients for station j

δ_a = aileron deflection

4.7 Engine Moments

$$M'_{txj} = -T_{ybj} (\bar{Z}_{ej} - \bar{Z}_{cg}) + T_{zbj} (\bar{Y}_{ej} - \bar{Y}_{cg})$$

$$M'_{tyj} = -T_{zbj} (\bar{X}_{ej} - \bar{X}_{cg}) + T_{xbj} (\bar{Z}_{ej} - \bar{Z}_{cg})$$

$$M'_{tzj} = -T_{xbj} (\bar{Y}_{ej} - Y_{cg}) + T_{ybj} (\bar{X}_{ej} - \bar{X}_{cg})$$

4.7 Engine Moments (Continued)

$$M''_{txj} = -T_{ybj} \sum_{i=1}^{M3} \phi_{zij}\, q_i + T_{zbj} \sum_{i=1}^{M3} \phi_{yij}\, q_i$$

$$M''_{tyj} = -T_{zbj} \sum_{i=1}^{M3} \phi_{xij}\, q_i + T_{xbj} \sum_{i=1}^{M3} \phi_{zij}\, q_i$$

$$M''_{tzj} = -T_{xbj} \sum_{i=1}^{M3} \phi_{yij}\, q_i + T_{ybj} \sum_{i=1}^{M3} \phi_{xij}\, q_i$$

$$M_{exj} = [\, F_{ezj} - m_{ej}(X_{ej} - X_{ecg})\ddot{\theta}'_{pj}\,](Y_{ej} - Y_{cg}) - [F_{eyj} + m_{ej}(X_{ej} - X_{ecgj})\ddot{\theta}'_{yj}](Z_{ej} - Z_{cg})$$

$$M_{eyj} = F_{exj}(Z_{ej} - Z_{ecgj}) - [F_{ezj} - m_{ej}(X_{ej} - X_{ecgj})\ddot{\theta}'_{pj}](X_{ej} - X_{cg})$$

$$M_{ezj} = [F_{eyj} + m_{ej}(X_{ej} - X_{ecgj})\ddot{\theta}'_{yj}](X_{ej} - X_{cg}) - F_{exj}(Y_{ej} - Y_{cg})$$

$$M_{txj} = M'_{txj} + M''_{txj} + M_{exj}$$

$$M_{tyj} = M'_{tyj} + M''_{tyj} + M_{eyj}$$

$$M_{tzj} = M'_{tzj} + M''_{tzj} + M_{ezj}$$

Where:

I_{ej} = moment of inertia of engine j

4.8 Slosh Moments

$$M'_{sxj} = A_y\, m_{sj}\, \lambda_{zj} - A_z\, m_{sj}\, \lambda_{yj}$$

$$M'_{syj} = A_z\, m_{sj}\, \lambda_{xj} - A_x\, m_{sj}\, \lambda_{zi}$$

$$M'_{szj} = A_x\, m_{sj}\, \lambda_{yj} - A_y\, m_{sj}\, \lambda_{xi}$$

$$M''_{sxj} = F_{syj}\,(\bar{Z}_{cg} - \bar{Z}_{sj}) - F_{szj}\,(\bar{Y}_{cg} - \bar{Y}_{sj})$$

$$M''_{syj} = F_{szj}\,(\bar{X}_{cg} - \bar{X}_{sj}) - F_{sxj}\,(\bar{Z}_{cg} - Z_{sj})$$

$$M''_{szj} = F_{sxj}\,(\bar{Y}_{cg} - \bar{Y}_{sj}) - F_{syj}\,(\bar{X}_{cg} - \bar{X}_{sj})$$

$$M_{sxj} = M'_{sxj} + M''_{sxj}$$

$$M_{syj} = M'_{syj} + M''_{syj}$$

$$M_{szj} = M'_{szj} + M''_{szj}$$

4.9 COORDINATE SYSTEMS

Inertial Polar-Equatorial - A right-handed orthogonal system with its origin at the center of the earth - X axis in the equatorial plane and positive through a reference meridian at the time of liftoff; the reference meridian is defined by the time of liftoff and the coordinate system used for gravity calculations. The Z axis is positive through the North Pole.

Inertial Plumbline - An orthogonal system with its origin at the center of the earth, X axis parallel to the launch site gravity vector and positive in the direction opposite to gravitational acceleration. The Z axis lies in the launch plane and points downrange and the Y axis completes a right-handed triad.

Local Vertical - An orthogonal system with its origin at the center of the earth, the X axis points from the earth center to the vehicle, the Z axis is in the plane containing the earth's rotation axis and the X_{LV} axis. The Z axis is perpendicular to the X axis and points towards the North Pole. The Y axis completes a right-handed triad.

Body - An orthogonal system with its origin at the engine gimbal pivot plane - X axis positive towards the nose of the vehicle along the main propellant tank centerline, Z axis positive "down", and the Y axis completes the right-handed system and is positive in the direction of the right wing.

Transformation matrix from polar-equatorial to plumbline coordinates:

$$[\alpha] = \begin{bmatrix} a_{11} & a_{12} & a_{13} \\ a_{21} & a_{22} & a_{23} \\ a_{31} & a_{32} & a_{33} \end{bmatrix}$$

$a_{11} = \cos \lambda_L^* \cos (\phi_L^* + \omega_e t_L)$

$a_{12} = \cos \lambda_L^* \sin (\phi_L^* + \omega_e t_L)$

$a_{13} = \sin \lambda_L^*$

$a_{21} = \sin A_L \sin \lambda_L^* \cos (\omega_e t_L + \phi_L^*) - \cos A_L \sin (\omega_e t_L + \phi_L^*)$

$a_{22} = \sin A_L \sin \lambda_L^* \sin (\omega_e t_L + \phi_L^*) - \cos A_L \cos (\omega_e t_L + \phi_L^*)$

$a_{23} = -\sin A_L \cos \lambda_L^*$

$a_{31} = -\cos A_L \sin \lambda_L^* \cos (\omega_e t_L + \phi_L^*) - \sin A_L \sin (\omega_e t_L + \phi_L^*)$

$a_{32} = -\cos A_L \sin \lambda_L^* \sin (\omega_e t_L + \phi_L^*) + \sin A_L \cos (\omega_e t_L + \phi_L^*)$

$a_{33} = \cos A_L \cos \lambda_L^*$

Where:

λ_L^* = geodetic latitude of launch site

ϕ_L^* = longitude of launch site

ω_e = angular rate of earth

T_L = time of launch (from epoch)

A_L = launch azimuth

Transformation matrix from body to inertial plumbline coordinates:

$$\left[\beta\right] = \begin{bmatrix} b_{11} & b_{12} & b_{13} \\ b_{21} & b_{22} & b_{23} \\ b_{31} & b_{32} & b_{33} \end{bmatrix}$$

$b_{11} = \cos\theta \cos\psi$

$b_{12} = \sin\theta \sin\phi - \cos\theta \sin\psi \cos\phi$

$b_{13} = \sin\theta \cos\phi + \cos\theta \sin\psi \sin\phi$

$b_{21} = \sin\psi$

$b_{22} = \cos\psi \cos\phi$

$b_{23} = -\cos\psi \sin\phi$

$b_{31} = -\sin\theta \cos\psi$

$b_{32} = \cos\theta \sin\phi + \sin\theta \sin\psi \cos\phi$

$b_{33} = \cos\theta \cos\phi - \sin\theta \sin\psi \sin\phi$

where the Euler angles θ, ψ and ϕ are calculated in EØM.

Transformation matrix from local vertical to polar-equatorial coordinates:

$$\left[\delta\right] = \begin{bmatrix} d_{11} & d_{12} & d_{13} \\ d_{21} & d_{22} & d_{23} \\ d_{31} & d_{32} & d_{33} \end{bmatrix}$$

$$d_{11} = \cos \lambda_V \cos \phi'$$

$$d_{12} = -\sin \phi'$$

$$d_{13} = -\sin \lambda_V \cos \phi'$$

$$d_{21} = \cos \lambda_V \sin \phi'$$

$$d_{22} = \cos \phi'$$

$$d_{23} = -\sin \lambda_V \sin \phi'$$

$$d_{31} = \sin \lambda_V$$

$$d_{32} = 0$$

$$d_{33} = \cos \lambda_V$$

Where:

$$\sin \lambda_V = Z_F/R$$

$$\cos \lambda_V = \sqrt{1 - \sin^2 \lambda_V}$$

$$\sin \phi' = Y_F/R \cos \lambda_V$$

$$\cos \phi' = X_F/R \cos \lambda_V$$

5.0 REFERENCES

1. Boeing Memorandum 5-2950-1-HOU-265, March 30, 1971, "SSFS Math Models"

2. Boeing Memorandum 5-2950-1-HOU-271, April 21, 1971, "SSFS Math Models"

3. Boeing Memorandum 5-2950-1-HOU-362, September 23, 1971, "Comparison of SSFS and RIBBS"

4. Boeing Memorandum 5-2950-1-HOU-391, November 1, 1971, "Comparison of SSFS and RIBBS Results (Boost through a 28K Shear and Gust Wind Profile)"

5. Boeing Memorandum 5-2950-1-HOU-299, June 15, 1971, "SSFS Math Models"

6. Boeing Memorandum 5-2950-1-HOU-305, June 22, 1971, "SSFS Math Models"

7. Boeing Memorandum 5-2950-1-HOU-321, July 21, 1971, "SSFS Math Models"

8. Boeing Memorandum 5-2950-1-HOU-330, July 30, 1971, "SSFS Math Models"

9. Boeing Memorandum 5-2950-1-HOU-377, October 8, 1971, "Equations for Calculation of Closed-Loop Control Gains and Trajectory Shaping for the SSFS"

10. Boeing Memorandum 5-2950-1-HOU-389, October 28, 1971, "Baseline Booster Control System Model for the SSFS"

11. Boeing Memorandum 5-2950-1-HOU-395, November 3, 1971, "SSFS Initial State Vector Math Model"

12. Boeing Memorandum 5-2581-HOU-011, December 17, 1971, "Checkout of Control Gains Calculations in SSFS"

13. Boeing Memorandum 5-2581-HOU-025, January 10, 1972, "Checkout of Trajectory Shaping Technique in SSFS"

14. Boeing Report 5-2950-1-HOU-387, October 27, 1971, "Baseline Launch Configuration Control System Software"

15. Boeing Report 5-2581-HOU-003, December 9, 1971, "A Multi-Stage Linear Tangent Guidance Law (LTG) Applied to Space Shuttle Vehicle (SSV) Boost Performance Analysis"

16. Boeing Memorandum 5-2581-HOU-005, December 6, 1971, "Preliminary Pitch-Axis Linearized Equations of Motion and Control Equations for SSV Point Time Stability Analysis"

17. Boeing Memorandum 5-2950-1-HOU-401, November 18, 1971, "Preliminary Lateral-Directional Linearized Equations of Motion and Control Equations for SSV Point Time Stability Analysis"

18. Boeing Report 5-2950-1-HOU-296, June 18, 1971, "Closed-Loop Trajectory Shaping Technique for Dynamics and Control Studies"

5.0 REFERENCES (Continued)

19. Boeing Memorandum 5-2950-1-HOU-278, May 12, 1971, "Derivation of a Drift Minimum/Loads Minimum Control Law for Booster, Atmospheric Flight"

20. NASA Technical Memorandum TMX-53872, "Terrestrial Environment (Climatic) Criteria Guidelines for Use in Space Vehicle Development," 1969 Revision

21. NASA Technical Memorandum TMX-64589, "Terrestrial Environment (Climatic) Criteria Guidelines for Use in Space Vehicle Development," 1971 Revision

22. Boeing Memorandum 5-2950-1-HOU-353, September 13, 1971, "Influence of New Wind Profiles on NAR-GD / Configuration (B9T/161B) Performance"

23. Boeing Memorandum 5-2581-HOU-028, January 17, 1972, "Boost Dynamics and Control Analysis - Semi-Annual Report"

24. Boeing Memorandum 5-2950-1-HOU-274, April 16, 1971, "Baseline Rigid Body Boost Simulation of the NAR-GD Delta Booster/Delta Orbiter Launch Configuration"

25. Boeing Memorandum 5-2950-1-HOU-280, May 5, 1971, "Drift Minimum Gains (No Wind) Trajectory for the NAR-GD Delta Booster/Delta Orbiter Launch Configuration"

26. Boeing Memorandum 5-2950-1-HOU-373, October 5, 1971, "Comparison of Drift Minimum Control Law With and Without Accelerometer Feedback During Boost"

27. Space Shuttle Guidance, Navigation and Control Phase B Final Report, May 1, 1971 (Honeywell)

28. Boeing Memorandum 5-2950-1-HOU-286, May 14, 1971, "Response of the NAR/GD / Launch Configuration to Steady State Winds"

29. Boeing Memorandum 5-2950-1-HOU-297, June 15, 1971, "Dynamic Response of the NAR-GD Delta Booster/Delta Orbiter Launch Configuration to Wind Disturbances at a 28,000 Foot Altitude"

30. Boeing Memorandum 5-2950-1-HOU-350, August 27, 1971, "Variation in Pitch Plane Flight Characteristics of the NAR-GD Delta Booster/Delta Orbiter Launch Configuration Due to Wind Gust (B9T/161B)"

31. Boeing Memorandum 5-2950-1-HOU-316, June 30, 1971, "Limiting Roll Attitude Control to Decrease Engine Deflections - Initial Results for B9T/161B Launch Configuration"

32. Boeing Memorandum 5-2950-1-HOU-333, August 4, 1971, "Addition of Aerodynamic Roll Attitude Control to the NAR-GD Delta Booster/Delta Orbiter Launch Configuration"

33. Boeing Memorandum 5-2950-1-HOU-375, October 7, 1971, "Lateral Control System Comparison when Subjected to 95% Steady State Crosswinds"

5.0 REFERENCES (Continued)

34. Boeing Memorandum 5-2581-HOU-016, December 20, 1971, "Study on the Effect of Yawing the SSV in the Presence of Design Crosswinds (B9T/161B Launch Configuration"

35. Boeing Memorandum 5-2950-1-HOU-393, November 1, 1971, "Critique of Phase B SSV Launch Configuration Boost Guidance and Control Analysis"

36. Boeing Memorandum 5-2950-1-HOU-347, August 24, 1971, "SRM 6 DOF Flight Simulation Results"

37. Boeing Memorandum 5-2581-HOU-041, February 2, 1972, "Converting SSFS to Accommodate the 040A/LOX Propane Launch Configuration"

38. Boeing Memorandum 5-2581-HOU-043, February 7, 1972, "Preliminary Roll Aerodynamic Control Studies (040A/LOX-Propane, Fins-Off Configuration)

39. Boeing Memorandum 5-2581-HOU-050, February 22, 1972, "Pure LITVC and Blended LITVC/Aerodynamic Roll Control Comparisons (040A/LOX-Propane Vehicle)"

40. Boeing Memorandum 5-2581-HOU-047, February 16, 1972, "Effect of Load Relief "Ramp-On Time" on Flight Parameters"

41. Boeing Memorandum 5-2581-HOU-045, February 15, 1972, "Converting SSFS to Accommodate the Dual SRM-040A Shuttle Launch Configuration"

42. Boeing Memorandum 5-2581-HOU-075, May 8, 1972, "Investigation of Liftoff Characteristics of the 040C-2 Launch Vehicle Configuration"

43. Boeing Memorandum 5-2581-HOU-067, April 25, 1972, "Realignment of SRM's on 040C-2 Launch Vehicle"

44. Boeing Memorandum 5-2581-HOU-069, April 28, 1972, "Inflight Control System Investigations for the SRM SSV Configuration (040C-2)"

45. Boeing Memorandum 5-2581-HOU-079, May 23, 1972, "SRM-049 Configuration Data"

46. Boeing Memorandum 5-2581-HOU-094, July 11, 1972, "Investigation of the Liftoff Characteristics of the 049 Launch Vehicle Configuration"

47. Boeing Memorandum 5-2581-HOU-083, May 31, 1972, "Preliminary Trajectory and Performance Results for the SRM-049 Shuttle Configuration"

48. Boeing Memorandum 5-2581-HOU-096, July 26, 1972, "SRM-049 Dynamics and Control Analysis - Inflight Wind Response"

49. Boeing Memorandum 5-2581-HOU-098, August 22, 1972, "Development of Vecturable SRM Control System"

50. Boeing Memorandum 5-2581-HOU-099, August 29, 1972, "Pitch Channel Modification to Vecturable SRM Control System"

5.0 REFERENCES (Continued)

51. Boeing Memorandum 5-2581-HOU-100, September 1, 1972, "Inflight Performance of Vecturable SRM Control System"

52. Boeing Memorandum 5-2581-HOU-001, December 6, 1971, "SSFS Flexible Body Math Models"

53. MSC Internal Note No. 71-FM-137, "Revision 1 to the Proposed Iterative Guidance Mode (IGM) Equations for the Shuttle Launch Guidance," May 3, 1971

54. MSC-04217, Revision B, "Project/Space Shuttle, Space Shuttle Guidance, Navigation and Control Design Equations Volume II, Preflight through Orbit Insertion," Revised December 1, 1971